TARGETING CELL METABOLISM IN CHRONIC LYMPHOCYTIC LEUKAEMIA (CLL) THROUGH THE INHIBITION OF MONOCARBOXYLATE TRANSPORTERS (MCT) -1 AND -4.

Thesis submitted in accordance with the requirements of the University of Liverpool for the degree of Doctor in Philosophy

by

Chloe Elizabeth Clapham

November 2014

TABLE OF CONTENTS

I. ABSTRACT

Chronic lymphocytic leukaemia (CLL) is a lymphoid malignancy which despite advances in the treatment options available is still incurable. Characterised by the gradual accumulation of CD5+ B cells, the paradigm that this is due to failed apoptosis has been challenged and a significant proliferative component has been identified. However, despite the crosstalk between pathways which regulate metabolism and proliferation the metabolic characteristics of these cells are not fully understood. Furthermore, there is a renewed interest in the field of cancer cell metabolism because of the Warburg effect, a hallmark of malignancy whereby cells preferentially switch to aerobic glycolysis and rapidly consume glucose. This has led to the development of new drugs such as AZD3965 an inhibitor of monocarboxylate transporter 1 (MCT1), which along with MCT4 mediates the export of lactate, a toxic bi-product of glycolysis, out of the cell. The aim of this project was to assess whether therapeutically targeting MCT -1 and -4 would be a viable approach for CLL. Chapter 2 of this thesis examines expression of MCT -1 and -4 as well as a specific chaperone protein needed for the surface expression of these proteins, CD147. This chapter confirms the presence of both MCT -1 and -4 and CD147 in normal B cells as well as demonstrating for the first time that these transporters are expressed in CLL cells using Western blotting and qRT-PCR to assess the MCTs and flow cytometry to measure CD147. The levels of both MCTs and CD147 are demonstrated to be significantly reduced in CLL cells in comparison normal B cells likely due to the adoption of a quiescent phenotype to aid cell survival. The following chapter investigates this further by assessing whether there are any changes in expression under the influence of microenvironmental stimuli, specifically CD40 ligand (CD40L). In this chapter it is demonstrated for the first time that MCT4 is upregulated in CLL cells in response to CD40L. Analysis of gene expression using a Fluidigm Biomark™ array suggests this is due to the induction of glycolysis and that CLL cells may promote fatty acid synthesis as well as instigating changes in the metabolism of the tumour stroma possibly to provide substrates. Finally, chapter 4 evaluates the sensitivity of CLL cell lines to AZD3965 using cell death and cell viability assays. Both MEC-1 and HG3 CLL cell lines are shown to be resistant to MCT1 inhibition using AZD3965 and silencing of MCT4 using siRNA cells also has no effect on the viability of MEC-1 cells. That MCT4 can compensate for MCT1 inhibition is shown by the transient expression of MCT4 in a Raji cell line where only MCT1 is expressed. Taken together, the data presented in this study indicates that while the inhibition of MCT1 is likely to be ineffective dual inhibition of both MCT -1 and -4 may be a viable strategy for the localised inhibition of CLL in the secondary tissues. Furthermore, MCT inhibition in this disease may have the potential to negate mechanisms of resistance and protection from oxidative stress mediated by CD40L.

II. ACKNOWLEDGEMENTS

I would like to thank my supervisors Dr Joseph Slupsky and Professor Andrew Pettitt for their support throughout my PhD (Institute of Translational medicine, University of Liverpool, UK). Thanks are due to all those who assisted or advised me during the project from the Department of Molecular and Clinical Cancer Medicine (Institute of Translational medicine, University of Liverpool, UK). Special mentions are due to Dr Jane Armstrong (Pancreas Biomedical Research Unit, Institute of Translational medicine, University of Liverpool, UK) for her expertise with the SeahorseXF24 and Dr Hayley Campbell who assisted with the Fluidigm Biomark™ qRT-PCR (AstraZeneca, Manchester, UK). Furthermore, special thanks are due to those who made this project possible including AstraZeneca (Manchester, UK) for funding the work and of course the University of Liverpool. I would also like to thank Dr Paul Smith and Dr Susan Critchlow (AstraZeneca, Manchester, UK) for their guidance.

III. DECLARATION

The work presented in this thesis is my own.

IV. LIST OF FIGURES

CHAPTER 1:

CHAPTER 2:

CHAPTER 3:

CHAPTER 4:

APPENDIX

V. LIST OF TABLES

CHAPTER 3:

APPENDIX:

VI. ABBREVIATIONS

µL Microlitre (10^{-6} litre)

µg Microgram (10^{-6} gram)

µm Micrometer (10^{-3} meter)

ACACA Acetyl-CoA carboxylase alpha

ACACB Acetyl-CoA carboxylase beta

ACSS2 Acyl-CoA synthetase short-chain family member 2

ACLY ATP citrate lyase

ADCC Antibody-dependent cell-mediated-cytotoxicity

ADP Adenosine diphosphate

ALL Acute lymphocytic leukaemia

ANOVA Analysis of variance

APC Allophycocyanin

APAAP Alkaline phosphatase

APS Ammonium per sulphate

ATF4 Activating transcription factor 4

ATP Adenosine triphosphate

BCR B cell receptor

BLAST Basic Local Alignment Search Tool

BSA Bovine serum albumin

Btk Bruton's tyrosine kinase

CAMKK2 Calcium/calmodulin-dependent protein kinase kinase 2

CD40L CD40 ligand

cDNA Complementary DNA

CLL Chronic lymphocytic leukaemia

CLP Common lymphoid progenitor

cm Centimeter

CMV Cytomegalovirus

COPI Coatamer protein complex-I

COPII Coatamer protein complex-II

CPT1A Carnitine palmitoyltransferase 1 A

CPT1B Carnitine palmitoyltransferase 1 B

D Diversity

DGAT1 Diacylglycerol acyltransferase-1

$DiOC_6$ 3,3'-dihexyloxacarbocyanine Iodide

DMEM Dulbecco's modified eagle medium

DMSO Dimethyl sulfoxide

DNA Deoxyribonucleic acid

dNTP Deoxynucleotide triphosphates

EBV Epstein-Barr virus

ECAR Extracellular acidification rate

EDTA Ethylenediaminetetraacetic acid

ELOVL5 Elongation of long-chain fatty acids family member 5

ELOVL6 Elongation of long-chain fatty acids family member 6

FACS Fluorescence assisted cell sorting

FAD Flavin adenine dinucleotide

FAM 6-carboxyfluorescein

FAS Fatty acid synthesis

FASN Fatty acid synthase

FBC Full blood count

FCCP Trifluoromethoxy carbonyl cyanide phenylhydrazone

FCS Foetal calf serum

FDC Follicular dendritic cells

FITC Fluorescein isothiocyanate

FLT3 Fms-like tyrosine kinase 3

FSC Forward scatter

G6PD Glucose-6-phosphate dehydrogenase

GAPDH glyceraldehyde 3-phosphate dehydrogenase

gDNA Genomic DNA

GFP Green fluorescent protein

GLS Glutaminase

GLS2 Glutaminase 2

GLUD1 Glutamate dehydrogenase 1

GLUD2 Glutamate dehydrogenase 2

GLUT1 Glucose transporter 1

Gy Gray

HDMPR High dose methylprednisolone

HIF1A Hypoxia inducible factor 1 alpha

HIF-1α Hypoxia inducible factor 1 alpha

HK1 Hexokinase 1

HK2 Hexokinase 2

HRP Horse radish peroxidase

HSC Haemopoietic stem cell

IFC Integrated fluidic circuit

Ig Immunoglobulin

IgM Immunoglobulin M

IgVH Immunoglobulin heavy chain variable region

IL-4 Interleukin 4

IL-7R Interleukin 7 receptor

INSIG2 Insulin induced gene 2

IPO8 Importin 8

J Joining

kDa Kilodaltons

L Litre

LDHA Lactate dehydrogenase A

LDT Lymphocyte doubling time

LMPP Lymphoid multipotent progenitor

mA Milliamps

M-CLL Mutated chronic lymphocytic leukaemia

MCS Multiple cloning site

MCT Monocarboxylate transporter

MCT1 Monocarboxylate transporter 1

MCT4 Monocarboxylate transporter 4

ME1 Malic enzyme 1

ME2 Malic enzyme 2

ME3 Malic enzyme 3

mg Milligrams (10^{-3} grams)

MGB Minor groove binder

miR microRNA

mL Millilitre (10^{-3} litre)

mM Millimolar (10^{-3} molar)

M-MLV RTase Moloney murine leukemia virus reverse transcriptase

MPP Multipotent progenitor

mpH Milli-power of hydrogen

NaCl Sodium chloride

NAD Nicotinamide adenine dinucleotide

NDUFB2 NADH dehydrogenase (ubiquinone) 1 beta subcomplex subunit 2

NDUFB5 NADH dehydrogenase (ubiquinone) 1 beta subcomplex subunit 5

NDUFB9 NADH dehydrogenase (ubiquinone) 1 beta subcomplex subunit 9

NHL Non-Hodgkin's lymphoma

nm Nanometer (10^{-9} meter)

OCR Oxygen consumption rate

PAPRG Proliferation activator receptor gamma

Par Parental fibroblasts

PBS Phosphate buffered saline

PDK1 Pyruvate dehydrogenase lipoamide kinase isozyme 1

PDK4 Pyruvate dehydrogenase lipoamide kinase isozyme 4

PDP1 Pyruvate dehydrogenase phosphatase catalytic subunit 1

PE Phycoerythrin

PFH Paraformaldehyde

PFKB1 6-phosphofructo-2-kinase/fructose-2,6 biphosphatase 1

PFKB2 6-phosphofructo-2-kinase/fructose-2,6 biphosphatase 2

PFKB3 6-phosphofructo-2-kinase/fructose-2,6 biphosphatase 3

PFKB4 6-phosphofructo-2-kinase/fructose-2,6 biphosphatase 4

PHA Phytohaemagglutinin

PHGDH Phosphoglycerate dehydrogenase

PI Propidium iodide

pMoles Picomole (10^{-9} moles)

poly-HEMA poly(2-hydroxyethyl methacrylate)

PPARA Peroxisome proliferator-activated receptor alpha

PPARG Peroxisome proliferator-activated receptor gamma

PPIA Protein phosphatase 1 A

PSAT1 Phosphoserine aminotransferase 1

QC Quality control

qRT-PCR Quantitative real time polymerase chain reaction

RAG Recombination activating gene

RBC Red blood cell

RCF Relative centrifugal force

RNA Ribonucleic acid

RNase Ribonuclease

ROX 6-Carboxyl-X-Rhodamine

RPM Revolutions per minute

RPMI Roswell park memorial institute media

sCD40L Soluble CD40L

SDS Sodium dodecyl sulphate

SDS-PAGE Sodium dodecyl sulphate-polyacrylamide gel electrophoresis

SEM Standard error of the mean

SFM Serum free media

SHM Somatic hypermutation

sIgm Surface immunoglobulin

siRNA Small interfering RNA

SNARE Soluble NSF attachment protein receptor

SOC Super optimal broth with catabolite repression

SOD1 Superoxide dismutase 1

SOD2 Superoxide dismutase 2

SREBF1 Sterol regulatory element-binding transcription factor 1

SREBF2 Sterol regulatory element-binding transcription factor 2

SSC Side scatter

TBS-T Tris-buffered saline-tween 20

TCA cycle Tricarboxylic acid cycle

Tdt Terminal deoxynucleotidyl transferase

TE Tris-EDTA

TEMED N,N,N',N'-tetramethyl-ethane-1,2-diamine

TGN Trans-golgi network

TKTL-11 Transketolase

TMD Transmembrane domain

TRFC Transferrin receptor

UM-CLL Unmutated chronic lymphocytic leukaemia

UT Untreated

V Variable

VEGF Vascular endothelial growth factor

VEGFA Vascular endothelial growth factor A

WBC White blood cell

ZAP-70 Zeta chain associated protein kinase 70

VII. PUBLICATIONS

Clapham CE, Pettitt AR, and Slupsky JR. 2014. Targeting cell metabolism in chronic lymphocytic leukaemia (CLL); a viable therapeutic approach? *Journal of Hematology and Oncology Research*, 1, 1-17.

1 CHAPTER 1: GENERAL INTRODUCTION

1.1 OVERVIEW

The subject of this thesis is whether therapeutic targeting of cell metabolism through the inhibition of monocarboxylate transport is a viable strategy for the treatment of chronic lymphocytic leukaemia (CLL). Disruption of metabolic processes in other cancer types has been shown to have synergy with conventional therapies, reducing the development of drug resistance and the process of relapse. Specifically, monocarboxylate transporter (MCT) -1 and -4 are of interest due to their function in preventing intracellular accumulation of lactic acid. Inhibition of these transporters has been shown to induce cell death in cancerous and non-cancerous cells (Murray et al., 2005, Halestrap and Wilson, 2012). Investigation into therapeutic targeting of metabolic processes within CLL cells has not received extensive scientific attention, possibly because expansion of the malignant clone in this disease was attributed to failed apoptosis as opposed to deregulated proliferation. The aim of this thesis is to examine MCT-1 and -4 as therapeutic targets in the treatment of CLL. Thus, the first chapter provides an introduction and justification of this aim. Chapter 2 examines the expression characteristics of MCT -1 and -4 as well as a chaperone required for cell surface expression, CD147. Chapter 3 builds upon this work by investigating the influence of microenvironment, specifically CD40 ligation, on MCT -1 and -4 expression. Chapter 3 also examines the effect of CD40 ligation on the expression of genes associated with metabolism and on metabolic flux in CLL cells. Finally, chapter 4 assesses the sensitivity of CLL cell lines to the MCT1 inhibitor, AZD3965 and explores compensatory mechanisms by disrupting MCT4 function to determine whether combined inhibition of both MCT -1 and -4 is a potential therapeutic approach for this disease.

1.2 B CELL LYMPHOCYTES

1.2.1 Haematopoiesis and lymphoid cell fate

Chronic lymphocytic leukaemia is a malignancy of B cell origin (Caporaso et al., 2007). B cells are produced during haematopoiesis, a process whereby haemopoietic stem cells (HSC) undergo a series of cell fate decisions to differentiate into cellular blood components such as red blood cells (RBC), white blood cells (WBC) and platelets. HSC's follow one of two paths of differentiation becoming either myeloid or lymphoid progenitor cells, a decision that is influenced by growth factors, cytokines, interleukins, transcription factors and the surrounding microenvironment (He et al., 2013).

B cells are produced during lymphopoiesis which occurs in the primary lymphoid tissues; the foetal liver and the bone marrow (LeBien and Tedder, 2008, Zhang et al., 2013). The HSC's progress through numerous developmental steps mediated by transcription factors such as Ikaros, fms-like tyrosine kinase 3 (FLT3), PU.1, interleukin 7 receptor (IL-7R), E2A, EBF1, Pax5, recombination activating gene (RAG) and terminal deoxynucleotidyl transferase (Tdt) (Ye and Graf, 2007, Melchers, 2005, Clark et al., 2014) (Figure 1.1). The expression of these factors drives the cells to become; multipotent progenitor (MPP) cells, followed by lymphoid multipotent progenitor (LMPP) cells and then common lymphoid progenitor (CLP) cells. The formation of pro-B cells is observed when expression of the gene coding for the B cell receptor (BCR) is induced, and differentiation to pre-B and immature B cells happens when intact BCR is produced and expressed on the cell surface allowing the B cell to respond to antigenic challenge (Figure 1.1 (A)) (Cambier et al., 2007, Nutt and Kee, 2007).

Generation of the BCR from immunoglobulin (Ig) light and heavy chains during the pro-B cell and pre-B cell stages is when the cell becomes committed to becoming a B cell. Heavy and light chain polypeptides collectively form the immunoglobulin molecule. Both heavy and light chain polypeptides contribute to the antigen binding sites and allow recognition of antigen by the BCR (Pleyer et al., 2009). To increase the range of antigens to which the individual can respond, diversity is created from the recombination of the variable (V), diversity (D) and joining (J) regions in the heavy

chain at the pro-B cell stage. At the pre-B cell stage a selection step occurs where the immature or pre-BCR is engaged. This is followed by recombination of the V and J regions of the light chain which undergoes a second selection step to avoid the production of self-reactive clones (Perez-Vera et al., 2011). If the BCR receptor does not pass this tolerance check either the BCR Ig chains undergo receptor editing to generate a new BCR, the cell undergoes apoptosis, or the cell enters the periphery and is induced into a failsafe anergic state where it is unresponsive to stimuli (Cambier et al., 2007).

Following this the immature B cell progresses becoming a transitional B cell and exits the marrow, entering the peripheral circulation and secondary tissues such as the spleen and lymph nodes (Zenz et al., 2010) (Figure 1.1 (B)). Here the cells begin to express surface markers such as CD23 and they continue to develop either becoming follicular B cells or marginal-zone B cells (Cambier et al., 2007). Upon antigenic engagement in order to generate the specific antibody needed against the antigen a process called somatic hypermutation (SHM) occurs which induces mutations within the Ig variable region in order to produce a B cell with a high affinity for the antigen, a process termed affinity maturation. B cells which are autoreactive or have a low affinity are removed following interaction with T helper cells and follicular dendritic cells (FDCs). The approved B cell then transverses the germinal center migrating into the light zone where the cell proliferates and matures into plasma cells and memory B cells (Figure 1.1 (B)) (Perez-Vera et al., 2011).

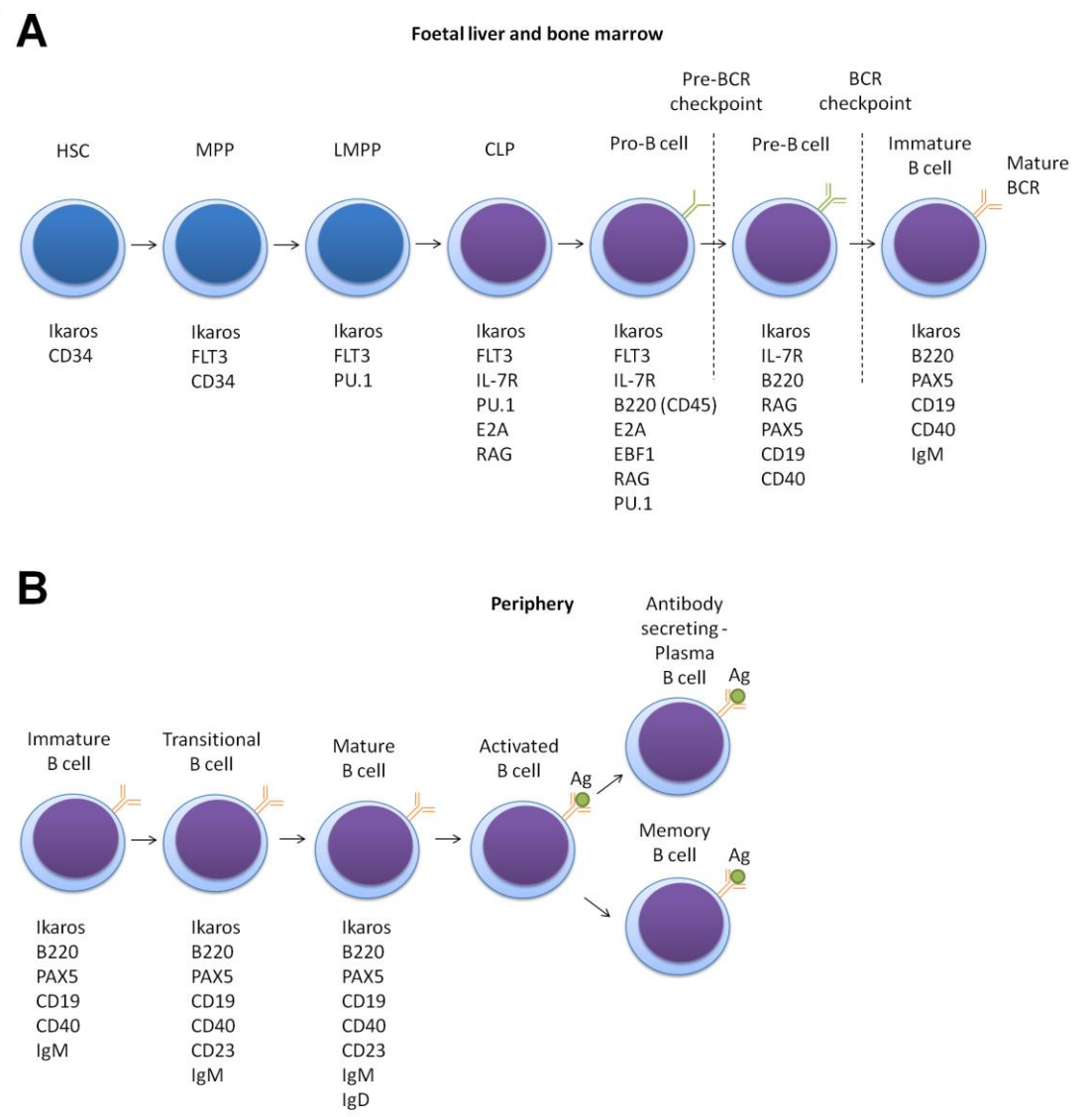

Figure 1.1: Normal B cell development. (A) Haemopoietic stem cells (HSC's) progress through developmental steps mediated by transcription factors such as Ikaros, fms-like tyrosine kinase 3 (FLT3), PU.1, interleukin 7 receptor (IL-7R), E2A, EBF1, Pax5, recombination activating gene (RAG) and terminal deoxynucleotidyl transferase (Tdt) to become immature B cells which express a mature BCR (Ye and Graf, 2007, Melchers, 2005, Clark et al., 2014). **(B)** In the periphery these cells encounter antigen in the secondary tissues (Zenz et al., 2010) and undergo somatic hypermutation (SHM) to generate a B cell specific to a particular epitope. The cell then transverses the germinal center and begins to proliferate and matures into plasma cells and memory B cells. Image adapted from Cambier et al. (2007), Nutt and Kee (2007), Nagasawa (2006).

1.2.2 CLL cell development

CLL is a B cell malignancy which has been shown to arise from a population of mature cells (Klein et al., 2001) which have aberrant expression of CD5 (Seifert et al., 2012). However, the stage in B cell development from which CLL arises has yet to be shown. Comparison of two major subtypes of CLL indicate that CLL cells may derive from two cell types (Ferrarini, 2009). These subtypes are patients with mutated IgVH genes (M-CLL) and patients with unmutated IgVH (UM-CLL) genes which code for the BCR and are respectively associated with stable and progressive disease (Dighiero and Hamblin, 2008). Studies show both clones to be antigen experienced with a BCR gene repertoire differing from that of naïve B cells, and this suggests that CLL clones are selected prior to oncogenic transformation (Messmer et al., 2004). This notion is important because it indicates that CLL may arise from a single stimulus. Moreover, that a distinct selection of genes are used to produce a "stereotyped BCR" in UM-CLL suggests that cells are repeatedly stimulated with a single antigen or are less selective being poly-reactive to multiple antigens including self-antigens (Rego et al., 2012, Ferrarini, 2009).

The degree of SHM in CLL cells is a feature which differs between M-CLL cells and UM-CLL cells and supports the notion that CLL has multiple cells of origin because M-CLL cells undergo SHM in the GC while UM-CLL cells have yet to reach the GC. However, gene expression analyses of the two subtypes has revealed similarities which coupled with the fact both subtypes resemble antigen experienced memory B cells suggests a single cell may be the site of CLL ontogeny (Damle et al., 2002, Chiorazzi and Ferrarini, 2011). At present there are two main hypotheses which describe CLL cells to originate from a single cell type. The first is that CLL cells are derived from human B1 cells. Evidence for this hypothesis comes from murine studies (Dorshkind and Montecino-Rodriguez, 2007) and is supported by studies in human B1 cells showing presence of CD5 and Zeta-chain-associated protein kinase (ZAP-70) as well as the expression of various markers (CD20+/CD27+/CD43+/CD70-) to be the same on both cell types (Griffin et al., 2011). Moreover, the restricted BCR gene repertoire used by CLL cells is also indicative of B1 cell origin.

The second hypothesis is that CLL cells originate from marginal zone B cells which are located in the spleen (Chiorazzi and Ferrarini, 2011). Support for this notion is provided by a study showing that the functional and expression characteristics between CLL cells and marginal zone B cells is similar (Griffin et al., 2011). Further evidence is provided by studies which show that marginal zone B cells and CLL cells respond similarly to antigen engagement (Dono et al., 1996a, Dono et al., 1996b), and that CLL cells and MZ cells express the BCR using a similar range of IgVH genes (Rossi and Gaidano, 2010). Malignant transformation in CLL is thought to be driven, therefore, by chronic activation of MZ cells through constitutive engagement with self- or non-self-antigens (Caligaris-Cappio, 2009). Finally, SHM does not occur in human B1 cells (Griffin et al., 2011), whereas the same can occur within MZ cells (Rossi and Gaidano, 2010).

Despite these studies investigating the origin of CLL cells the source of this disease is still under debate. Understanding the ontogeny of CLL cells is of value because it allows a deepened understanding of the pathology of this disease, particularly as it relates to outcomes as will be discussed below.

1.3 CHRONIC LYMPHOCYTIC LEUKAEMIA (CLL)

1.3.1 Epidemiology

Chronic lymphocytic leukaemia (CLL) is the most common form of leukaemia in the Western world, and accounts for 25% of blood cancer diagnoses with approximately 2,800 people each year being diagnosed in the UK alone (Cancer research UK, 2010). Affecting primarily older adults, the median age at diagnosis is 72 years. CLL is rare in younger people, with only 20-30% of cases arising in patients less than 55 years of age (Howlader et al., 2012, Hayden et al., 2009). Males are at greater risk of CLL than females with the incidence rate being almost double. This disease is also more common in the Caucasian population as opposed to other ethnicities (Landgren et al., 2007, Oscier et al., 2012), and has been shown to have a familial link as relatives of CLL patients have a predisposition to other lymphoid malignancies (Goldin and Caporaso, 2007, Crowther-Swanepoel and Houlston, 2009).

1.3.2 Aetiology

Although the cause of CLL has not been fully elucidated migrant studies have highlighted how genetic rather than environmental factors play a crucial role in the aetiology of CLL. These studies have shown that migrant populations maintain the CLL rate of their native country (Caporaso et al., 2007, Linet et al., 2007). As previously discussed, this is supported by familial studies where it is shown that first degree relatives of CLL patients are seven times more likely to develop the disease (Sherborne and Houlston, 2010, Linet et al., 2007) as well as studies that refute the involvement of environmental factors (Caporaso et al., 2007).

1.3.3 Clinical overview

1.3.3.1 Clinical features

Enhanced proliferation and cell survival combine to create a characteristic lymphocytosis of CLL cells with CD5, CD20 and CD23 positivity in the peripheral blood, lymphoid tissues and bone marrow (Moran et al., 2002, Goldin and Caporaso, 2007). The accumulation of B cells is gradual which is reflected by chronic nature of this disease as symptoms develop slowly. Because of this approximately 70-80% of cases are diagnosed following routine blood testing, and 25% of these patients may be asymptomatic (Oscier et al., 2012). Symptoms of CLL include; frequent infections, lethargy, bone pain, abdominal pain, splenomegaly, hepatomegaly, feeling unwell, lymphadenopathy, bruising, bleeding i.e. epistaxis, weight loss, dyspnoea, anaemia, headaches, fever, and night sweats (Oscier et al., 2012).

1.3.3.2 Diagnosis

The symptoms listed above are considered alongside tests for the diagnosis of this disease. In patients with CLL, lymphocytosis is a characteristic finding in the full blood count (FBC) usually exceeding 5×10^9/L. Such a finding prompts examination of blood film morphology (Oscier et al., 2012) where lymphocytosis and smear cells are characteristic features (Bennett et al., 1989, Nowakowski et al., 2007). Following blood film examination, immunophenotyping is used to identify CLL cells based upon the expression of characteristic markers such as surface membrane immunoglobulin (smIg), CD5, CD23, FMC7, CD22 or CD79b and a scoring system is used to distinguish CLL from other B cell malignancies (Moreau et al., 1997).

Additional investigations to aid diagnosis and monitor disease progression also include; lymph node biopsy, bone marrow biopsy, cytogenetics, chest x-ray and CT (Oscier et al., 2012).

1.3.3.3 Staging and prognostic factors

Clinical staging of CLL is based upon the Rai (Rai et al., 1975) and Binet (Binet et al., 1981) systems which take into consideration clinical factors such as the degree of; lymphocytosis, lymphoid tissue involvement, bone marrow suppression and hepatosplenomegaly. These staging systems are important because of the heterogenous nature of this disease, and, as such, are used to guide treatment. However, limitations with both of these systems has led to the identification of a multitude of prognostic factors at the molecular level which are able to distinguish indolent from progressive disease more confidently and enable a more personalised approach to treatment (Dighiero and Hamblin, 2008). For instance, ZAP-70, CD38, serum β2-microglobulin, thymidine kinase, CD23 and IgVH mutational status have all been shown to be valuable tools for predicting prognosis (Defoiche et al., 2008, Damle et al., 1999, Gonzalez et al., 2011, Crespo et al., 2003). Other factors such as *TP53* status can affect the type of therapy a patient may receive. For instance, with agents such as fludarabine the killing effect is dependent on p53 function, and therefore would not be an appropriate treatment regime if p53 function was disrupted due to mutation or deletion (Dohner et al., 1995, Pettitt et al., 1999).

However, despite the information these molecular factors provide about disease prognosis and the pathology of CLL, their ability to reliably predict disease progression on a patient by patient basis is limited. Prior to the commencement of therapy a "wait and watch" strategy is used which uses the rate of lymphocyte doubling, or the lymphocyte doubling time (LDT), over a 6 month period to assess when to start treatment (Molica and Alberti, 1987, Montserrat et al., 1986). For instance, if the LDT is less than 6 months this suggests there is an increased likelihood of disease progression due to the increasing tumour burden. In addition, if a patient begins to experience symptoms or complications therapy is also started as this is also an indicator that the lymphocyte count is increasing (Oscier et al., 2004).

1.3.3.4 Treatment

As previously described, treatment may not be commenced straight away for patients who present with CLL which is non-aggressive and is administered based on clinical stage, age, and fitness (Oscier et al., 2012). To date CLL remains incurable and treatment strategies are focused upon managing this disease by decreasing tumour burden through the destruction of CLL cells via chemotherapy and biological therapy, as well as managing complications such as anaemia, autoimmunity, immunosuppression and infection (Morrison, 2010, Oscier et al., 2012).

The first line treatment for CLL is chemotherapy where fludarabine is the basis for the majority of treatment plans (Oscier et al., 2012). However, as previously discussed, fludarabine induces cell death by inhibiting DNA synthesis in a p53 dependent manner, and this can give rise to refractory disease in patients with either p53 mutation/deletion (Dohner et al., 1995, Pettitt et al., 1999). To curb the development of drug resistance and limit non-specific toxicity, fludarabine-combined chemotherapy is used (Hallek and Eichhorst, 2004). For instance, fludarabine is given alongside; cyclophosphamide (FC), cyclophosphamide and rituximab (FCR), cyclophosphamide and mitoxantrone (FCM), and cyclophosphamide, mitoxantrone and rituximab (FCMR) (Oscier et al., 2012, O'Brien et al., 2001, Hillmen, 2004).

While combination of fludarabine with cyclophosphamide is the foundation for the majority of regimes, new alkylating agents have entered the clinic in place of cyclophosphamide and another drug, chlorambucil, and are used for combination therapy where treatment with FC based options are no longer appropriate (Oscier et al., 2012). For instance, bendamustine (B), may be used with fludarabine as it is well tolerated by patients (El-Mabhouh et al., 2014, Woods et al., 2012). This compound is also used in parallel with rituximab (BR) (Oscier et al., 2012, Zaja et al., 2013), a monoclonal antibody that is B cell-specific and targets CD20 to induce cell death via antibody-dependent cell-mediated-cytotoxicity (ADCC) (Alduaij and Illidge, 2011). This biological therapy may also be used in combination with fludarabine and cyclophosphamide, [FR and (C+R respectively)] (Oscier et al., 2012). Other monoclonal antibodies such as alemtuzumab have even greater specificity for B cells

because it binds to CD52, a marker of B cell maturity (Tembhare et al., 2013). This antibody is used in combination with fludarabine (FA) as well as cyclophosphamide, fludarabine, and rituximab (CFAR) (Oscier et al., 2012). These monoclonal antibodies may also be used alongside glucocorticoids such as dexamethasone and high dose methylprednisolone (HDMPR) (Smolej et al., 2012).

Steroids such as these are commonly used following relapse as second line treatments because they are associated with side effects. CHOP, cyclophosphamide, doxorubicin, vincristine and prednisolone is a common second line combination therapy that is also used for the treatment of non-Hodgkin's lymphoma (Hamblin, 2001). If this round of second line treatment is ineffective, a stem cell transplant may be performed. However, this approach is only suitable for younger, fit patients and is uncommon (Oscier et al., 2012).

New agents for the treatment of this disease are being developed to therapeutically target factors contributing to CLL pathogenesis. For instance, compounds such as lenalidomide disrupt the interaction between CLL cells and the tumour microenvironment (Chen, 2013), while Bruton's tyrosine kinase (Btk) inhibitors such as ibrutinib are directed against BCR signaling (Hendriks et al., 2014).

1.3.3.5 Pathogenesis

The treatment options described above focus on inducing cell death, however, anti-proliferative agents are also likely to have value because of the role of proliferation in CLL pathogenesis (Messmer et al., 2005). In the past the characteristic accumulation of lymphocytes seen in this disease was attributed to enhanced cell survival (Brody et al., 1969). This was because early studies showed CLL cells to be arrested in G_0 of the cell cycle (Dameshek, 1967, Brody et al., 1969), and that these cells over express the anti-apoptotic proteins, Mcl-1 and Bcl-2 as well as under express pro-apoptotic Bax (Gottardi et al., 1995, Zenz et al., 2010, Pepper et al., 1997, Kitada et al., 1998). However, this paradigm was challenged when CLL cells were demonstrated to have a significant level of proliferative activity in a study by Messmer et al. (2005) whereby

deuterium was used to label the DNA of newly-formed CLL cells. Further studies using deuterium labelling of CLL cells showed that the level of cell division was reduced in comparison to normal B cells (Defoiche et al., 2008, van Gent et al., 2008), but that deuterium labeled CLL cells remained in circulation for longer than their healthy counterparts, suggesting that they have a prolonged survival. Collectively, these studies showed that the characteristic lymphocytosis seen in this disease arises due to both cell division and enhanced cell survival.

Proliferation of CLL cells is localised to proliferation centers in the haemic tissues such as the lymph node (Ramsay and Rodriguez-Justo, 2013). Interaction within the microenvironment is important in the pathogenesis of this disease because it is here that CLL cells come into contact with supportive cells such as helper T cells, nurse like cells, follicular dendritic cells (FDC) and stroma cells which provide survival and proliferative stimuli (Pleyer et al., 2009). For instance, stimulation of CLL cells by helper T cells expressing CD40 ligand (CD40L) has been shown to induce proliferation (Patten et al., 2008, Pascutti et al., 2013). However, despite controversy surrounding the role of T cells within the proliferation center the presence of CD40L has been shown to be localised in the germinal center following treatment with anti-CD40L (Han et al., 1995). Soluble factors such as IL-21 and IL-4 are also secreted by T cells to further stimulate cell division of CLL cells (Ahearne et al., 2013). In addition to this, stimulation of CLL cells via CD40-CD40L interaction contributes to disease pathogenesis by providing anti-apoptotic signals. For instance, CD40 ligation has been shown to induce the expression of Bcl-xl and Mcl-1 as well as reducing Bcl-2 levels having the effect of promoting cell survival (Willimott et al., 2007). Moreover, stimulation via CD40L can mediate resistance to purine analogues such as fludarabine (Citores et al., 2010).

B cell activation via B cell receptor (BCR) signaling is another contributor to CLL pathogenesis, and factors affecting disease prognosis such as IgVH mutational status are involved in BCR signaling as well as ZAP-70 and CD38 (Burger and Chiorazzi, 2013).

1.4 THE IMPORTANCE OF CELL METABOLISM IN CLL

As discussed above, proliferation is important to the pathogenesis of CLL. This, combined with the fact that cell division is an energetically demanding process (Garedew et al., 2012), makes it reasonable to assume that cell metabolism may also be important by proxy. A hallmark of malignancy is that cancer cells rapidly consume glucose and switch to a glycolytic phenotype even in the presence of ample oxygen, a phenomenon known as the Warburg effect (Warburg et al., 1924). However, this effect has also been seen in non-cancerous cells such as lymphocytes which use this mechanism to provide quick energy to support rapid proliferation as part of the immune response (Dang, 2012). In order to assess whether CLL cells experience the Warburg effect first it is important to understand the metabolic characteristics of their healthy counterpart, normal B cells.

1.4.1 Normal B cell metabolism

Normal B cells have been shown to change their preferred means of energy generation in response to antigenic engagement (Garcia-Manteiga et al., 2011). For instance, in naïve and memory B cells, which are generally inactive, oxidative phosphorylation is the primary means of cell metabolism (Chacko, 2013). However, once the cell is activated it undergoes differentiation and develops into a plasma cell, inducing aerobic glycolysis as well as promoting glutaminolysis to support antibody secretion (Kominsky et al., 2010). Metabolic flux analyses using mouse B cells show that BCR crosslinking (BCR-XL) increases both the acidity of the extracellular environment indicative of enhanced glycolytic activity, and the degree of oxygen consumed required for oxidative phosphorylation (Capasso et al., 2010). Studies by Doughty et al. (2006), and Fu et al. (2004) provide evidence that the main substrate metabolised by these cells is glucose, as activating stimuli such as BCR-XL and phytohaemagglutinin (PHA) induce the expression of glucose transporters such as GLUT1 to facilitate glucose uptake.

Taken together, these studies provide a basis with which to model the metabolism of CLL cells in order to assess whether the Warburg effect is a feature of CLL.

1.4.2 CLL cell metabolism

The studies in normal B cells suggest that the Warburg effect may be also a feature of malignant transformation in CLL because of the 'Warburg like' glycolytic phenotype that is adopted by lymphocytes during cell division (Dang, 2012). Although glycolysis is less efficient than oxidative phosphorylation, there are numerous benefits associated with a glycolytic phenotype for malignant cells. For example, glycolysis promotes cell migration (Gallagher et al., 2007, Cheung and Vousden, 2010, Su et al., 2009), aids nutrient uptake, promotes cell survival and protects from oxidative stress (Vander Heiden et al., 2009, Bensaad and Vousden, 2007, Cheung and Vousden, 2010, Sloan and Ayer, 2010).

However, studies examining the metabolic characteristics of CLL cells indicate that rapid consumption of glucose does not occur in these cells. In contrast to what is seen in other malignancies, CLL cells have been shown to have a lower glucose requirement when compared to normal B cells (Brody et al., 1969, Warburg et al., 1924). This is supported by studies using fluorodeoxyglucose positron emission tomography (FDG-PET), a technique which exploits rapid glucose uptake. The use of FDG-PET is not sensitive enough to estimate disease progression in CLL because glucose consumption is at a low level (Karam et al., 2006). These studies contradict the Warburg paradigm, but do not take into consideration the likely low energy requirements of circulating CLL cells which are arrested in G_0 of the cell cycle.

Recent work has begun to clarify the metabolic requirements of CLL cells. Jitschin et al. (2014) have shown that the level of oxidative phosphorylation is increased in CLL cells compared to normal B cells, an observation that is in keeping with studies from this department where CLL cells were shown to have considerable levels of oxidative stress (Moran et al., 2002). In the absence of increased glucose uptake, CLL cells may metabolise other substrates in order to support survival and proliferation. For instance,

glutamine, glycogen (Mitus et al., 1958, Jones et al., 1962), or fatty acids as recently described by Spaner et al. (2013) could all act as energy reservoirs. Glutaminolysis has been shown to be augmented in cervical cancer as opposed to glycolysis (Reitzer et al., 1979, Vousden and Ryan, 2009), whereas enhanced oxidative phosphorylation is a feature of breast cancer (Jose et al., 2011, Bonuccelli et al., 2010a), similar to what is reported by Jitschin et al. (2014) in the context of CLL. Thus, although CLL cells do not appear to exhibit archetypal characteristics of the Warburg effect, these cells do show signs of metabolic derangement.

Evidence that the metabolism of CLL cells is altered is provided by MacIntyre et al. (2010) in a study whereby serum levels of metabolites are measured and compared in M-CLL cells and UM-CLL cells. This shows lactate, fumarate and uridine levels to be increased in patients with UM-CLL suggesting changes in the pathobiology of these cells may alter cell metabolism. However, because this study examined serum samples this may reflect the metabolic activity of not only circulating cells but proliferating cells in the secondary tissues also. This would fit in with the switching between metabolic pathways seen in normal B cells following B cell activation (Garcia-Manteiga et al., 2011, MacIntyre et al., 2010) and account for the differences in serum metabolites between M-CLL and UM-CLL cells because UM-CLL cells are chronically stimulated via the BCR (Chiorazzi and Ferrarini, 2003, Krysov et al., 2010).

The differences between these two prognostic groups suggest that metabolic reprogramming, a known feature of the Warburg effect is occurring in these cells. Studies by Rodriguez et al. (2013) and Tili et al. (2012) support this notion as mutation of sucrose isomaltase (Rodriguez et al., 2013) and reduced *miR-125b* (Tili et al., 2012) have both been demonstrated to cause increased expression of genes specific to glucose metabolism. Furthermore, the study by Tili et al. (2012) correlated *miR-125b* expression, and consequently increased glucose metabolism, with poor prognosis.

Taken together these reports indicate that although CLL cells have not been shown to have enhanced glycolysis or rapid glucose consumption typical of the Warburg effect the aspects of their metabolism differs from normal B cells. CLL cells likely use

oxidative phosphorylation when located in the circulation and switch to a more glycolytic phenotype during cell division, akin to normal B cells. However, increased levels of oxidative phosphorylation in the absence of increased glucose uptake suggest that these cells may utilise alternative substrates. Moreover, metabolic reprogramming is a feature in CLL.

1.5 THERAPEUTIC TARGETING OF CELL METABOLISM IN CLL

Although CLL cells have not been shown to promote glycolysis over oxidative phosphorylation, the importance of glycolysis to the pathophysiology of this disease can be demonstrated by inhibiting this process. For example, inhibition of hexokinase, a key glycolytic enzyme, using lonidamine results in decreased cell viability *in vitro* as well as reducing lymphocyte count, lymphadenopathy and splenomegaly when it is used *in vivo* (Tura et al., 1984). Furthermore, inhibition of the glycolytic pathway using 2-deoxyglucose (2DG) has also been shown to cause a reduction in cell viability as well as attenuating ATP production (Tidmarsh et al., 2004). Clearly inhibition of glycolysis has an effect in these cells. Therapeutic targeting of cell metabolism is an approach that has had a degree of success for the treatment of some cancers (Zhao et al., 2013b). One strategy has been to target lactate transport out of the cell because a consequence of enhanced glycolytic activity is the accumulation of lactic acid, a toxic bi-product (Polanski et al., 2014). The export of lactate has been shown to be mediated by the monocarboxylate transporter (MCT) -1 and -4, inhibition of which has been shown to cease proliferation and induce cell death (Halestrap and Wilson, 2012).

1.5.1 Monocarboxylate transporters (MCTs)

MCTs are a family of membrane transport proteins of which 14 members have been identified thus far (Halestrap and Price, 1999, Halestrap and Meredith, 2004). The protein consists of 12 highly conserved transmembrane domains (TMDs) which have the N and C termini situated in the cytoplasm (Figure 1.2) (Visser et al., 2007).

Sequence variations between isoforms can be observed in the C terminus and a large intracellular loop located between TMDs 6 and 7 which are thought to be involved in regulation and confer substrate specificity (Halestrap and Price, 1999, Morris and Felmlee, 2008). This is demonstrated in studies by Halestrap and Price (1999) and Rahman et al. (1999) where substitution of Phe^{360} to Cys in the TMD 10 in Chinese-hamster MCT1 reduced the affinity of MCT1 for lactate and pyruvate, and substitution of Asp^{302} to Glu in the TMD 8 in rat MCT1 eliminated lactate transport. The N terminus is thought to be involved in maintenance, plasma membrane insertion and energy coupling, i.e. binding of a proton (Halestrap and Price, 1999).

MCT's have been shown to transport a wide range of substrates such as monocarboxylates; lactate, pyruvate, butylate; oxo-acids, and ketone bodies (Halestrap and Price, 1999, Morris and Felmlee, 2008). Of the 14 identified MCT's, only MCT's 1-4 have been found to be proton-linked co-transporting a single proton in association with the substrate across the plasma membrane (Morris and Felmlee, 2008, Halestrap and Meredith, 2004).

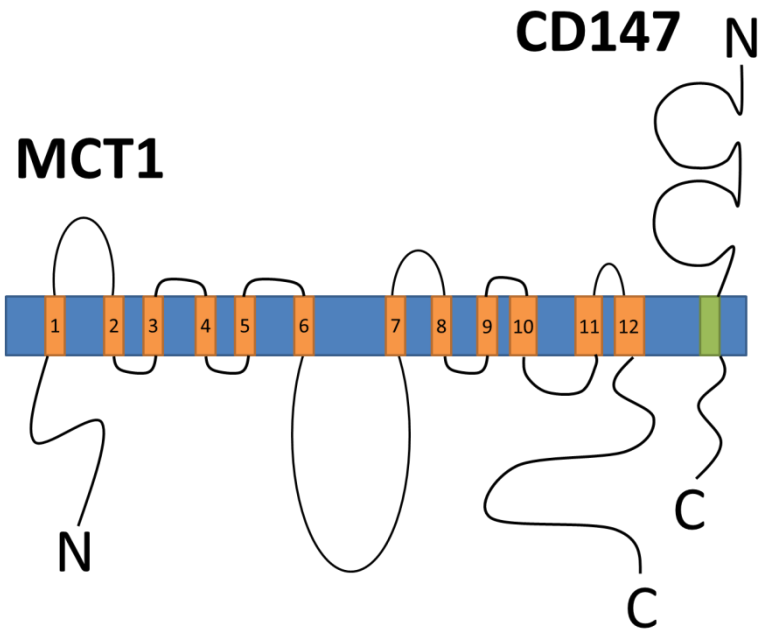

Figure 1.2: Structure of MCT1 and CD147. MCT1; the diagram illustrates 12 TMD's, a large intracellular loop between TMD 6 and TMD 7, the N terminus and C termini both located in the cytoplasm. CD147; the diagram shows two extracellular Ig-like domains, a highly conserved a single transmembrane domain with and a short C terminus situated in the cytosol the latter two are thought to be responsible for association with MCT's. Image adapted from Halestrap and Meredith (2004).

1.5.1.1 Monocarboxylate transporter 1 (MCT1)

MCT1 (SLC16A1, human gene locus 1p13.2) is 40-50kDa protein which has ubiquitous tissue expression (Halestrap and Meredith, 2004). A proton-dependent co-transporter/exchanger it is situated in the apical and basolateral membranes when active (Morris and Felmlee, 2008). Substrates transported by MCT1 include; short chain un-branched aliphatic monocarboxylates i.e. propionate and acetate, in addition to other monocarboxylates such as pyruvate, acetoacetate, lactate, α-ketoisovalerate, α-oxoisohexanoate, α-oxoisovalerate, XP13512 and butyrate (Morris and Felmlee, 2008, Halestrap and Meredith, 2004).

MCT1 also has the ability to function as a monocarboxylate exchanger transporting substrates such as lactate out of the cell while bringing in substrates such as pyruvate for use in the Tricarboxylic acid cycle (Halestrap and Meredith, 2004). Transportation may be bi-directional, however MCT1 has been shown to be mainly used for substrate uptake (Morris and Felmlee, 2008).

1.5.1.2 Monocarboxylate transporter 4 (MCT4)

MCT4 (SLC16A3, human gene locus 17q25.3) is a 54kDa protein expressed mainly in cells which have a high level of glycolytic activity (Halestrap and Meredith, 2004). For example WBCs, tumors, astrocytes, chondrocytes, the brain, kidneys, retinal pigment epithelium (RPE), placenta, heart, lungs and small intestine, all express MCT4 (Halestrap and Meredith, 2004, Morris and Felmlee, 2008). It is located in the basolateral membrane when active, similarly to MCT1, and is also a proton linked co-transporter transporting substrates such as; lactate, pyruvate, acetoacetate, α-ketobutyrate, α-ketoisocaproate, α-ketoisovalerate, and D-β-hydroxybutyrate (Morris and Felmlee, 2008).

1.5.1.3 Monocarboxylate transporter (MCT) 2 and 3

MCT2 (SLC16A7, human gene locus 12q14.1) and MCT3 (SLC16A8, human gene locus 22q13.1) similarly to MCT -1 and -4, are proton linked co-transporters and are expressed on the basolateral membrane (Morris and Felmlee, 2008). Unlike MCT1 which has ubiquitous expression, expression of MCT -2 and -3 is restricted akin to MCT4 . MCT2 expression has been demonstrated in the testis, liver, kidney, skeletal muscle, heart, brain, spleen, and pancreas (Halestrap and Meredith, 2004). MCT3 expression has been shown to be more restricted arising in the Retinal pigment epithelium (RPE), choroids plexus, aorta, placenta, and kidney (Halestrap and Meredith, 2004). Surface expression of these proteins is dependent on the presence of an accessory protein. MCT -1, -3, and -4 share the same protein, CD147 which is discussed in the next section. For the surface expression of MCT2 gp70 (EMBIGIN) is required (Halestrap and Price, 1999, Morris and Felmlee, 2008). The focus of this study is the inhibition of lactate transport mediated by MCTs. MCT2 transports pyruvate, lactate and ketone bodies while MCT3 transports lactate (Halestrap and Meredith, 2004). For the purposes of this study MCT3 was not considered because of its restricted expression however, MCT2 has been shown to be present in normal B cells by Merezhinskaya et al. (2004). The inhibitors in development by AstraZeneca are targeted against MCT1 and 4. AZD3965 directed against MCT1 is known to inhibit MCT2 also. For this reason MCT2 was not investigated in this study.

1.5.1.3.1 CD147

For the surface expression of both MCT -1 and -4 a chaperone protein, CD147, is required (Halestrap and Meredith, 2004, Gallagher et al., 2007). A extracellular matrix metalloproteinase, CD147 has a single highly conserved transmembrane domain (Figure 1.2) with two extracellular Ig-like domains in addition to a short C terminal situated in the cytosol (Halestrap and Meredith, 2004, Kirk et al., 2000). CD147 is highly conserved and widely expressed with increased quantities being noted in RPE, tumors, activated T cells, and on the neonatal blood-brain barrier (Su et al., 2009, Kirk et al., 2000). The vital role of CD147 for the expression of MCT -1 and -4 is demonstrated by Kirk et al. (2000) and Gallagher et al. (2007) whereby silencing of CD147 in breast

cancer resulted in degradation of MCT4 while sole transfection of MCT -1 or -4 into mammalian cell lines resulted in low levels of surface expression in comparison to co-transfection of MCT -1 or -4 with CD147.

The process of MCT -1 or -4 surface expression is described in a general model by Mellman and Nelson (2008) and begins in the endoplasmic reticulum (ER). Here the core-glycosylated form of CD147 (30kDa) is synthesized and accumulated alongside MCT -1 and -4 before forming a complex with either MCT -1 or -4 which triggers a conformation change in CD147 producing the fully-glycosylated form. Dimerization then occurs with a second complex and the MCT-CD147 heterodimer is deposited into a vesicle mediated by coatomer protein complex-II (COPII). This vesicle is then transported to the golgi complex by soluble NSF attachment protein receptor (SNARE) and vesicle tethering mechanisms where coatamer protein complex-I (COPI) mediates translocation of the heterodimer to the trans-golgi network (TGN). From the TGN the heterodimer is transported to the plasma membrane via the cytoskeleton using similar mechanisms modulated by SNARE and vesicle tethering (Mellman and Nelson, 2008).

1.5.1.4 Regulation of MCT -1 and -4

Surface expression of MCT -1 and -4 has been shown to be differentially regulated. Factors such as CD147, substrate concentration, pH, hormones, hypoxia, and transcription factors such as MYC have been shown to mediate the expression of MCT -1 and -4 (Halestrap and Meredith, 2004). However, while some factors such as AMPK, testosterone, chronic stimulation/exercise and CD147 have been shown to upregulate expression for both these transporters other factors have been shown to have differing effects specific for each isoform. For instance, MCT1 message is known to increase in response to increased lactate and butyrate concentrations (Halestrap and Price, 1999, Hashimoto et al., 2007, Kennedy and Dewhirst, 2010a) and is specific to MCT1 having no effect on MCT4 expression. Other factors such as weight loss, obesity and hypoxia have opposing effects on MCT -1 and -4 expression. For example, weight loss and hypoxia downregulate MCT1 while obesity promotes MCT1 expression, with the reverse being true for MCT4 (Kennedy and Dewhirst, 2010a, Ullah et al., 2006,

Gallagher et al., 2007). In addition to transcriptional regulation differences between message and protein studies examining the expression of MCT-1 and -4 indicate that these transporters are regulated by post-transcriptional and post-translational mechanisms also (Halestrap and Wilson, 2012).

1.6 AIMS AND HYPOTHESIS

1.6.1 Aims

In order to establish whether monocarboxylate transporter (MCT) -1 and -4 are possible therapeutic targets in CLL the first aim of this investigation was to characterise MCT-1 and -4 expression in these cells. The presence of the chaperone protein CD147, required for the function of these proteins, was measured using flow cytometry. Localisation of MCT1 was performed using immunocytochemistry and confocal microscopy. Protein and message levels for both transporters was examined using Western blotting and qRT-PCR in CLL cells as well as normal B cells in addition to two CLL cell lines; MEC-1 and HG3 cells.

The second aim of the study was to assess the expression of these transporters following CD40 ligation to examine the influence of microenvironmental stimuli. Moreover, to provide further insight into CLL cell metabolism and identify novel targets a Fluidigm Biomark™ chip was used to assess the expression of genes associated with cell metabolism such as glycolysis while real time measurements were obtained using the SeahorseXF24 metabolic flux analyser.

The third aim of the study was to evaluate whether MCT -1 and -4 are potential therapeutic targets, using the MCT1 inhibitor AZD3965 and siRNA specific for MCT4. The sensitivity of the CLL cell lines, MEC-1 and HG3 to the compound was assessed by staining for cell death using 3,3'-dihexyloxacarbocyanine iodide ($DiOC_6$) and propidium iodide (PI). In addition cell viability was measured using Alamar blue®. To assess

whether the compound inhibited proton mediated transport by MCT1 extracellular acidification rate (ECAR) was measured in real time using the SeahorseXF24.

1.6.2 Hypotheses

1) MCT -1 and -4 are expressed by CLL cells [H_1].

MCT -1 and -4 are not expressed by CLL cells [H_0].

2) The need for monocarboxylate transport is increased when CLL cells are induced to proliferate [H_1].

The need for monocarboxylate transport is unaffected when CLL cells are induced to proliferate [H_0].

3) CLL cells are sensitive to MCT -1 and/or -4 inhibition resulting in cell death [H_1].

CLL cells are resistant to MCT -1 and/or -4 inhibition [H_0].

2 CHAPTER 2: CHARACTERISATION OF MCT -1 AND -4 EXPRESSION IN CLL CELLS

2.1 INTRODUCTION

2.1.1 MCT -1 and -4 expression in cancer cells

As previously discussed, one consequence of enhanced glycolysis is the accumulation of lactic acid in the cytoplasm. In order for a high level of glycolytic activity to be maintained MCT -1 and -4 fulfill a crucial role mediating lactate transport out of the cell. This is particularly important for the Warburg effect, as in various cancers the expression of both these transporters, along with the accessory protein CD147, is increased in order to cope with the increased demand for lactate export (Pinheiro et al., 2012, Halestrap and Wilson, 2012). Expression of MCT-1 and -4 has also been correlated with poor prognosis in multiple types of cancer such as breast (Pinheiro et al., 2010), gastric (Torres de Oliveira et al., 2012, Pinheiro et al., 2009), prostate (Pertega-Gomes et al., 2011), and bone (Zhao et al., 2014). In relation to B cell malignancies, CD147 expression has been associated with prognosis in acute lymphocytic leukaemia (ALL) as well as non-Hodgkin's lymphoma (NHL). This illustrates further the importance of these proteins in cancer biology and haemato-oncology (de Vries et al., 2010).

However, whilst these transporters have been investigated in the context of solid tumors, few studies have examined haematological malignancies such as CLL (Hartmann et al., 2012).

2.1.2 MCT -1 and -4 expression in B cells

The aim of this chapter is to examine the expression of both MCT -1 and -4 in primary CLL cells and normal B cells. Few studies have assessed the expression profile of MCTs in normal B cells. The very first study of MCT expression on haemic cells

reported that MCT4 was present on white blood cells (WBCs) without differentiating between subtypes (Halestrap and Price, 1999). Later, a specific investigation of lymphocytes by Merezhinskaya et al. (2004) showed expression of MCT -1, -2 and -4 although this study did not distinguish between B and T cells. The expression of these transporters is not surprising considering that normal lymphocytes are known to adopt a Warburg-like phenotype following activation. This switch to a glycolytic phenotype supports the rapid cell division required to mount an efficient immune response (Garcia-Manteiga et al., 2011). In this chapter the expression of these transporters and the ancillary protein CD147 was investigated using flow cytometry, immunocytochemistry, Western blot analysis and qRT-PCR to determine their expression on CLL cells.

2.2 MATERIALS AND METHODS

2.2.1 Recovery of cryopreserved samples

2.2.1.1 Primary chronic lymphocytic leukaemia (CLL) cells

CLL cells were acquired from CLL patients following informed consent and the approval of the Liverpool Research Ethics Committee. Peripheral blood was obtained via venepuncture and protected from coagulation with the addition of heparin. WBCs were isolated by slowly layering the blood sample on to Lymphoprep™ (Axis-Shield, Stockport, UK) solution in a 2:1 ratio followed by centrifuged for 30 minutes at 800 rcf. The isolated mononuclear cells were then washed using Roswell Park Memorial Institute (RPMI) media (Biosera, Uckfield, UK) and resuspended in RPMI supplemented with 10% heat inactivated foetal calf serum (FCS) (Sigma, Gillingham, UK). To heat inactivate the FCS, a bottle was thawed at room temperature or at 4°C, and then heated at 58.8°C for 1 hour in a water bath. In preparation for cryopreservation, cooled RPMI media containing 10% FCS and 20% dimethyl sulfoxide (DMSO) (Sigma, Gillingham, UK) was added drop wise until a final concentration of 10% DMSO was attained. 1mL aliquots of this cell suspension were then frozen at -80°C prior to storage at -150°C within the University of Liverpool Leukaemia Biobank.

Cryopreserved CLL cells were recovered on ice by drop wise addition of RPMI media modified with 100 units/mL penicillin-streptomycin (Invitrogen, Paisley, UK), 2mM L-glutamine (Invitrogen, Paisley, UK), and 0.5% filtered bovine serum albumin (BSA) (Sigma, Gillingham, UK). Once a final volume of 10mL was achieved, samples were centrifuged (500 rcf, 5 minutes, 4°C) and washed in modified media to remove DMSO which is toxic at room temperature. Only cells which had a minimum viability of 70% were used.

2.2.1.2 Normal B cells

Normal B cells were analysed fresh from whole blood (flow cytometry only) from healthy consenting volunteers or isolated from buffy coats purchased from the National Health Service Blood and Transplant (NHSBT, Speke, UK). Mononuclear cells were separated from buffy coat samples using density-gradient centrifugation as detailed in section 2.2.1.1 except the buffy coat samples were diluted 1:4 with RPMI media prior to layering on to the Lymphoprep™. These samples were then stored at -150ºC.

2.2.1.3 Suspension cell lines

Raji (Burkitt's lymphoma cell line) and MEC-1 (CLL cell line) cells were purchased from the Leibniz Institute DSMZ-German Collection of Microorganisms and Cell Cultures (Braunschweig, Germany). MDA-MB-231 (breast cancer cell line) cells were kindly donated by Dr Guozheng Wang and Dr Helen Kalirai (University of Liverpool).

Raji, MDA-MB-231, and MEC-1 cells were recovered at 37°C in a water bath for 5 minutes prior to the addition of 10mL of RPMI media or for the MEC-1 cells, Dulbecco's Modified Eagle's Medium (DMEM) (Sigma, Gillingham, UK), modified with 100 units/mL penicillin-streptomycin, 2mM L-glutamine, 10% heat inactivated FCS.

2.2.2 Cell viability

Assessment of cell viability was done using Trypan blue exclusion. Viable cells remain colourless because cell membranes remain intact and exclude the dye. Non-viable cells absorb Trypan blue because the membrane is compromised thereby making them appear blue under microscopic examination (Altman et al., 1993). 0.1% Trypan blue (Sigma, Gillingham, UK) was added to the cell suspension at an appropriate dilution. Live cell count, dead cell count, cell viability and live cell concentration were determined using the Cellometer™ AutoT4 cell counter (Peqlab Ltd, Sarisbury Green, UK). The Cellometer™ AutoT4 cell counter was focused according to the manufacturer's instructions to avoid falsely low or falsely high counts.

2.2.3 B cell purification

Mononuclear separation of peripheral blood was undertaken using Lymphoprep™ as described in 2.2.1.1. B lymphocytes were isolated using negative selection using the MACS B cell purification Kit II (Miltenyi Biotec, Bisley, UK) as per the manufacturer's instructions. The cell suspension was incubated with biotin conjugated antibodies specific for non-B cells (anti-CD2, anti-CD14, anti-CD16, anti-CD36, anti-CD43, and anti-glycophorin A) followed by incubation with microbeads coated with anti-biotin (IgG1). The cell suspension was then passed through a MACS column where the microbeads become immobilised due to the presence of a magnetic field and trap non-B cells, while B cells are eluted. The quality of the purified specimen was assessed using flow cytometry for CD19-PE. Autofluoresence and non-specific binding were accounted for using conjugated isotype specific control; IgG1,y1-PE (BD Biosciences, Oxford, UK). The BD FACS Calibur™ (FACS Calibur, BD Biosciences, Oxford, UK) was calibrated using BD CaliBRITE™ beads (BD Biosciences, Oxford, UK) to compensate for spectral overlap (BD CellQuestPro User guide, 2002).

2.2.4 B-CLL cell purification

The malignant B cells from CLL patients were purified by negative selection using a cell purification kit designed for this purpose [MACS B Cell isolation kit (B-CLL) (Miltenyi Biotec, Bisley, UK)] following the manufacturer's guidelines. The same quality assurance measures were taken as described in section 2.2.3.

2.2.5 Antibodies

Rabbit polyclonal anti-MCT1 (AZ5565) (AstraZeneca, Manchester, UK), rabbit polyclonal anti-MCT4 (AZ5570) (AstraZeneca, Manchester, UK); rabbit polyclonal anti-MCT1 (ab85021) (Abcam, Cambridge, UK), rabbit polyclonal anti-MCT4 (ab74109) (Abcam, Cambridge, UK); isoform specific rabbit polyclonal anti-MCT1, isoform specific rabbit polyclonal anti-MCT4 kindly provided by Dr Nancy Philp

(Thomas Jefferson University, PA, USA); mouse monoclonal anti-MCT1 (H-1) (sc-365501) (Insight Biotechnology, Wembley, UK), mouse monoclonal anti-MCT4 (sc-376101) (Insight Biotechnology, Wembley, UK), rabbit polyclonal anti-MCT4 (HS-90) (sc-50329) (Insight Biotechnology, Wembley, UK).

2.2.6 Flow cytometry for the detection of CD147

CLL cells and normal B cells from buffy coats that had been recovered from -150ºC storage were centrifuged and resuspended in modified ice cold phosphate buffered saline (PBS) (Fisher Bioreagents®, Fischer Scientific, Leicestershire, UK) pH 7.2 containing 1% BSA and 0.1% sodium azide (Sigma, Gillingham, UK) to a concentration of 5 x 10^6 cells/mL. Following manufacturer's guidelines, fluorophore-conjugated antibodies were added to a 96 well U bottomed plate along with 100µL of cell suspension. For the purposes of this study anti-CD5-R-PE (IgG1) (ab27372; Abcam, Cambridge, UK) (578nm), anti-CD20-APC (IgG1) (340908; BD Biosciences, Oxford, UK) (660nm), anti-CD23-PerCP-Cy™5.5 (IgG1,k) (561166; BD Biosciences, Oxford, UK) (695nm) were used to identify the presence of CLL cells (CD5+/CD20+/CD23+) and normal B cells (CD5-/CD20+/CD23+). Anti-CD147-FITC (IgG1) (ab69771; Abcam, Cambridge, UK) (520nm), was then used to examine CD147 expression specifically on these cells.

Following addition of antibody the cell suspension was incubated in the dark 30 minutes on ice. 100µL of modified PBS was then added and the plate was centrifuged at 500 rcf for 3 minutes at 4°C. The supernatant was then removed, and the cell pellet was resuspended in 100µL of modified PBS and 400µL of sheath fluid ready for analysis.

To account for autofluoresence and non-specific binding conjugated isotype specific controls were used; IgG1,y1-FITC (345815; BD Biosciences, Oxford, UK), IgG1-R-PE (345816; BD Biosciences, Oxford, UK), IgG1-APC (554681; BD Biosciences, Oxford, UK), and IgG1,k-PerCp™-Cy5.5 (552834; BD Biosciences, Oxford, UK). The analyser was calibrated as detailed in 2.2.3.

For the analysis of normal B cells from fresh whole blood specimens samples were treated with red cell lysis buffer [150mM NH_4Cl (Sigma, Gillingham, UK), 10mM $NaHCO_3$ (Sigma, Gillingham, UK), 1mM $EDTANa_2$ (Sigma, Gillingham, UK), in 1L sterile ddH_2O (Fresenius Kabi sterile water, Runcorn, UK)]. This was followed by a washing step and resuspension of the remaining cells in 200µL of sterile PBS. Staining of the cells followed the procedure outlined above.

2.2.7 Immunocytochemistry

2.2.7.1 Alkaline phosphatase (APAAP) staining

Cytospin slides were prepared using a Cytospin 2 (Shandon, Block Scientific Inc, NY, USA) to which 100µL of a 5 x 10^6/mL cell suspension was added. The slide was subsequently fixed in acetone (Fischer Scientific, Leicestershire, UK) for 3 minutes, air dried, and blocked using 10% BSA and stored at -20ºC for future use. The slides were then thawed for 30 minutes and incubated with anti-MCT1 (1:100) or normal rabbit IgG control (1:100) (Insight Biotechnology, Wembley, UK). For the Raji cell positive control a dilution of 1:200 was used. After a 1 hour incubation period slides were washed with PBS and treated with biotinylated anti-rabbit IgG (H+L) (Vector Laboratories Inc, Peterborough, UK) for 1 hour. Slides were then washed and incubated with extravidin® alkaline phosphatase (Sigma, Gillingham, UK) for 30 minutes. Next slides were washed in PBS and incubated with 0.45µm filtered VECTOR® Blue Alkaline Phosphatase Substrate Kit III (SK-5300) (Vector Laboratories Inc, Peterborough, UK), washed, and counterstained with haematoxylin (Sigma, Gillingham, UK). Finally slides were rinsed in tap water and cover slipped. Images were taken using a Nikon DMX2100 Digital camera.

2.2.7.2 Confocal microscopy

Recovered CLL cells were resuspended at 1 x 10^7 cells/mL in PBS. 500µL aliquots were fixed with the addition of an equal volume of 4% paraformaldehyde (PFH) (Sigma,

Gillingham, UK) for a 10 minute period and then washed by centrifugation at 1600 rpm for 3 minutes. Cells were then permeablised using 0.2% Triton-X-100 (Sigma, Gillingham, UK) for 5 minutes and washed. Prior to staining, cells were blocked by treatment with a blocking solution (0.1% gelatin (Sigma, Gillingham, UK), 0.5% BSA, 0.1% sodium azide) for 30 minutes. Cells were then incubated at 1:20 with anti-MCT1 (H-1) (mouse) (sc-365501), or purified mouse monoclonal IgG1 isotype control (1:100) (R&D systems, Abingdon, UK) for 1 hour at followed by incubation with anti-mouse AlexaFluor®555 (1:100) (Invitrogen, Paisley, UK) for 1 hour and centrifuged at 1600 rpm for 3 minutes. Cells were subsequently resuspended in PBS and added to poly-L-lysine (Sigma, Gillingham, UK) coated microscopy slides and air dried. Slides were then mounted and cover slipped ready for examination.

2.2.8 Western blot analysis for MCT -1 and -4

2.2.8.1 Lysate preparation

Samples were centrifuged at 500 rcf for 5 minutes at 4°C and resuspended in 1mL of modified media. Next the samples were transferred to pre chilled 1.5mL eppendorfs and centrifuged at 500 rcf for 5 minutes at 4°C prior to washing using PBS to remove excess albumin. The samples were then lysed using 200µL of clear SDS-PAGE lysis buffer (buffer recipes in appendix) per 1 x 10^7 cells. To release cellular fragments and shear DNA, specimens were sonicated for 5-10 seconds using a Sonics Vibracell™ Ultrasonic processor. Samples were then heated in a heat block at 100°C for 5 minutes as a denaturation step. Finally, the samples were centrifuged at 14,000 rpm for 10 minutes, and then transferred to a fresh eppendorf and stored at -20°C.

2.2.8.2 Protein determination

0, 0.125, 0.25, 0.5, 1.0 and 2.0mg/mL BSA protein standards were produced using clear SDS–PAGE sample buffer. These standards were loaded into a 96 well flat bottomed plate alongside appropriate dilutions of each sample. Protein determination was

performed using a DC Protein assay kit (Bio-Rad-Laboratories Ltd, Hemel Hempstead, UK) as per the manufacturer's instructions, and read at 630nm using the MQX200 µQuant plate reader (BioTek®, Potton, UK). Clear SDS–PAGE sample buffer was used as a blank reference.

2.2.8.3 Gel preparation

10-12% acrylamide resolving gels were used in this study. Gels were cast using the following protocol; 6.45mL ddH_2O, 4.25mL 4x Protogel® Resolving buffer (Geneflow Ltd, Lichfield, UK), 6.3mL Protogel® Acrylamide Ultra Pure (Geneflow Ltd, Lichfield, UK), 50µL ammonium per sulphate (APS) (Sigma, Gillingham, UK), and 15µL N,N,N',N'-tetramethyl-ethane-1,2-diamine (TEMED) (Sigma, Gillingham, UK). 5% acrylamide stacking gels were cast using this protocol; 4.36mL ddH_2O, 1.9mL Protogel® Stacking buffer (Geneflow Ltd, Lichfield, UK), 1.24mL Protogel® Acrylamide Ultra Pure, 50µL APS and 15µL TEMED.

The gel apparatus used was the Bio-Rad mini-Protean system, using 1.5mm thick gels with a calculated volume of 7.5mL for the resolving gel and 2.5mL for the stacking gel.

2.2.8.4 Sodium dodecyl sulphate-polyacrylamide gel electrophoresis (SDS-PAGE)

To separate proteins SDS-PAGE gel electrophoresis was used. 10µg (15µL) of protein was loaded into designated wells. A molecular weight marker (Precision Plus Protein™ Kaleidoscope™ Standards, Bio-Rad-Laboratories Ltd, Hemel Hempstead, UK) was used (10µL) as a set of standards to identify protein size. This was diluted to 15µl with 5µL 1x Sample buffer. 1x Sample buffer was also used to adjust the final volume of positive control lysates (5µg in 7.5µL) to 15µL. Once all gel lanes had been filled, the gel tank was filled with 1x SDS-PAGE running buffer and run at 30mA/gel for approximately 60 minutes.

Electrophoretic transfer of gel-separated proteins was performed using a Bio-Rad mini-Transblot apparatus. Gels were washed in Transfer buffer (Geneflow Ltd, Lichfield,

UK) prior to assembly of the transfer sandwich. Millipore™ Immoblion® Transfer membranes (Millipore, Watford, UK) (9cm x 6cm) were prepared by first wetting with methanol for 30 seconds (Fischer Scientific, Leicestershire, UK) and then placing them into Transfer buffer. The transfer sandwich was assembled in the following order: a bottom sponge soaked in Transfer buffer was overlayed with Whatman paper (10cm x 8cm) (Fischer Scientific, Leicestershire, UK). This was followed by the gel and then the transfer membrane. The sandwich was completed with another layer of Whatman paper and an upper sponge. This sandwich was then put into the transfer tank along with an ice block and filled with Transfer buffer, noting the direction of transfer towards the transfer membrane. The transfer tank was then run for 1 hour at 400mA constant current.

2.2.8.5 Western blotting

In order to prevent non-specific binding of probe antibodies the membranes were incubated in a blocking buffer for 30-60 minutes. Probing membranes with primary antibodies was performed using antibody dilutions of either 1:1000 or 1:2000. Probe solutions were made up using 5mL of blocking buffer plus antibody to make up the appropriate dilution. The membranes were then incubated overnight at 4ºC with constant shaking. Membranes were then washed with TBS-T (2x30 seconds, 2x5 minutes and 1x15 minutes washes) and then incubated with either HRP conjugated anti-rabbit or anti-mouse IgG secondary antibodies (1:5000) for 1 hour at room temperature. This was followed by another washing step with TBS-T.

2.2.8.6 Detection

For detection either Amersham ECL prime or Lumigen™ Advanced ECL detection reagents (GE Healthcare, Belfast, UK) were used according to the manufacturer's instructions. A Fujifilm Intelligent dark box (Fujifilm, Bedford, UK) and Fujifilm LAS-100 Camera (Fujifilm, Bedford, UK) were used to measure chemiluminescence.

2.2.8.7 Densitometry

Densitometry analysis of gel images was performed using Aida image analyzer software (Version 3.52) (Raytest Gmbh, Straubenhardt, Germany). All protein amounts are reported relative to the expression of β-actin detected using mouse monoclonal anti-β-actin (clone AC-74) (Sigma, Gillingham, UK).

2.2.9 Polymerase chain reaction (PCR)

2.2.9.1 RNA extraction

Purified samples (>71% CD19+) were centrifuged at 500 rcf for 5 minutes at 4°C and resuspended to 5 x 10^6 cells/mL in media. Samples were then transferred in 1mL aliquots to pre-chilled 1.5mL eppendorf tubes, and then centrifuged at 500 rcf for 5 minutes at 4°C, washed in PBS, and re-centrifuged for a further 5 minutes. Pellets were stored at -80°C prior to use.

RNA extraction was performed using a QIAshredder™ (Qiagen, Manchester, UK) and a RNeasy® minikit (Qiagen, Manchester, UK) as per the manufacturer's instructions in a Fisherbrand UV4PCR hood. Quantification of extracted RNA was performed using a NanoDrop 2000c spectrophotometer (Thermo scientific, Leicester, UK). Only samples with a 260:280 ratio of <2 were used.

2.2.9.2 cDNA synthesis

Diluted RNA (0.08µg/µL, 12.5µL volume) was reverse transcribed using 1µL of oligo $(dT)_{15}$ primer (Eurofins MWG Operon, Ebersberg, Germany) and a RT master mix consisting of: 4µL 5x RT Buffer (Promega, Southampton, UK), 1µL 10mM dNTP's (Promega, Southampton, UK), 0.5µL RNasin plus (Promega, Southampton, UK), and 1µL M-MLV RTase, (Promega, Southampton, UK). Final volume was 20µL, and reaction tubes were centrifuged at 11,000 rcf for 30 seconds. Samples were then incubated for 1 hour at 37°C and then heated at 65°C for 10 minutes.

2.2.9.3 Quantitative real-time PCR (qRT-PCR)

Diluted cDNA (1:4) was added to each designated well in an Mx3000P® 96 well plate (Agilent technologies, Wokingham, UK) running each sample in triplicate. The master mix (MCT1, MCT4 or β-actin) was produced using TaqMan® gene expression master mix (Applied Biosystems, Life technologies, Paisely, UK) and the corresponding primers and probe: MCT1; TaqMan® gene expression assay Hs00161826_m1* (Applied Biosystems, Life technologies, Paisely, UK), MCT4; TaqMan® gene expression assay Hs00358829_m1 (Applied Biosystems, Life technologies, Paisely, UK), human ACTB (β actin) endogenous control (FAM / MGB Probe, Non-Primer Limited) (Applied Biosystems, Life technologies, Paisely, UK). The master mix was then added to the plate as per the manufacturer's instructions. Once loading was completed the plate was sealed using Mx3000P® optical strip caps (Agilent technologies, Wokingham, UK) and centrifuged for 1 minute at 500 rcf. The PCR reaction was then run using a Stratagene Mx3005P QPCR system (Agilent technologies, Wokingham, UK). The following cycling variables were used as suggested by TaqMan®; 50°C, 2 minutes, 95°C, 10 minutes, 95°C 15 seconds, 60°C, 1 minute, for 40 cycles.

2.2.10 Quality assurance

For the detection of CD147 using flow cytometry a Raji cell line was used as a positive control because these cells have been previously reported to express CD147 (Vangeepuram et al., 1997, Lambert et al., 2002).

For immunocytochemistry, confocal microscopy, Western blot analysis and qRT-PCR either a MEC-1 cell line or a Raji cell line was used as positive control for MCT1 as they have both been shown to express this transporter (Lin et al., 1998b).

For the Western blot analysis and qRT-PCR a MDA-MB-231 cell line was used as a positive control for MCT4 as expression of MCT4 was confirmed by Gallagher et al.

(2007). As a negative control a Raji cell line was used as MCT4 has been reported to absent in these cells (Lin et al., 1998b).

2.2.11 Statistical analysis

Statistical analyses were performed using Graphpad Prism (Version 6.01, Graphpad Software Inc., CA, USA). The statistical tests used are identified when and where they are used within the results section of this chapter. A P value of $P \leq 0.05$ was considered to be statistically significant.

2.3 RESULTS

2.3.1 Assessment of CD147 expression in CLL and normal B cells using flow cytometry

As previously described CD147 is a chaperone protein required for the surface expression of MCT -1 and -4, and is specific for these members of the MCT family (Halestrap and Meredith, 2004, Gallagher et al., 2007, Morris and Felmlee, 2008). Commercially available antibodies targeting MCT -1 and -4 are directed against cytoplasmic C-terminal epitopes of their respective proteins, and make surface expression analysis difficult. Therefore, CD147 can be used as surrogate marker of surface expressed MCT -1 and -4, and this was assessed on CLL and normal B cells using flow cytometry.

B cells from 20 CLL patients and 14 normal controls (consisting of fresh samples from 10 healthy volunteers and 4 cryopreserved samples prepared from buffy coats) were analysed for CD147. The antibody used is specific for CD147 because it targets the N terminus of a fully glycosylated form of the protein that is only expressed on the cell surface (Gallagher et al., 2007). A four colour profile consisting of CD5, CD20 and CD23 was used to identify CLL (CD5+/CD20+/CD23+) and normal B cells (CD5-/CD20+/CD23+). Multi-colour flow cytometry was used at this point, and the optimal combination of fluorophores was determined using the BD Fluorescence Spectrum Viewer (Figure 2.1). Figure 2.2 shows the gating strategy used to identify CLL and normal B cells using CD5 and CD20. Further characterisation of these cells was achieved using CD23 (Oscier et al., 2012). To test the validity of this analytical strategy Raji cells were used as a positive control (Figure 2.3) (Lambert et al., 2002, Vangeepuram et al., 1997). Thus, analysis of CD147 expression on CLL and normal B cells showed the presence of this protein on the cell surface of both cell types (Figure 2.4), and comparison of expression levels demonstrate that CD147 levels are significantly higher on normal B than on CLL cells (** $P = 0.0014$, Mann Whitney U test).

To account for any effect of cryopreservation on CD147 expression comparisons were made between fresh and cryopreserved normal B cells, and CLL cells and cryopreserved normal B cells (Figure 2.5). This figure demonstrates no difference between CD147 expression on fresh versus cryopreserved normal B cells ($P = 0.7333$, Mann Whitney U test). Comparison of CD147 expression between CLL and cryopreserved normal B cells shows that the observations made in Figure 2.4 are preserved and B cells express significantly more CD147 than do CLL cells (*** $P = 0.0006$).

Taken together, these data confirm surface expression of CD147 on CLL and normal B cells, with expression being higher on the latter cell type. This indicates that MCT1 and/or MCT4 are likely to be expressed on these cells, and that one or the other transporter may be higher on normal B cells in comparison to CLL cells.

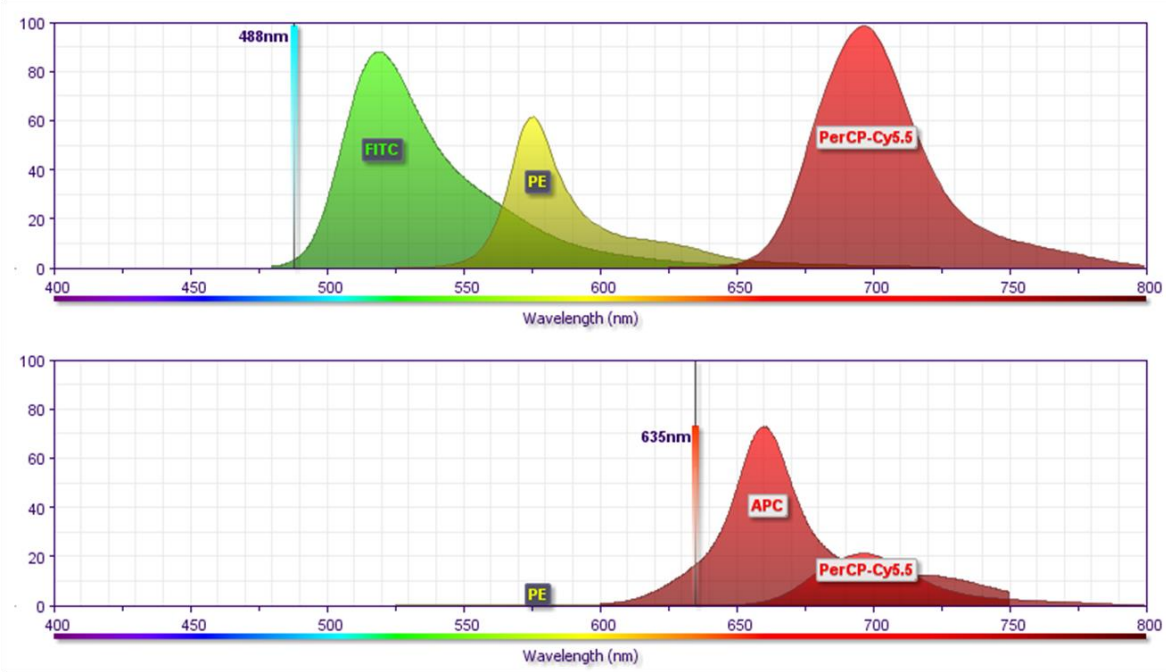

Figure 2.1: Emission spectra of the fluorophores used for multi-colour colour flow cytometry. The top histogram shows how the emission spectra for FITC, PE and PerCP-Cy5.5 overlap when excited with a 488nm laser. The bottom histogram shows the emission spectra for APC and PerCP-Cy5.5 overlap when excited with a 635nm laser. These spectra were used to design the best possible antibody profile for the detection of CD147 on CLL and normal B cells namely; anti-CD5-R-PE, anti-CD20-APC, anti-CD23-PerCP-Cy™5.5 and anti-CD147-FITC.

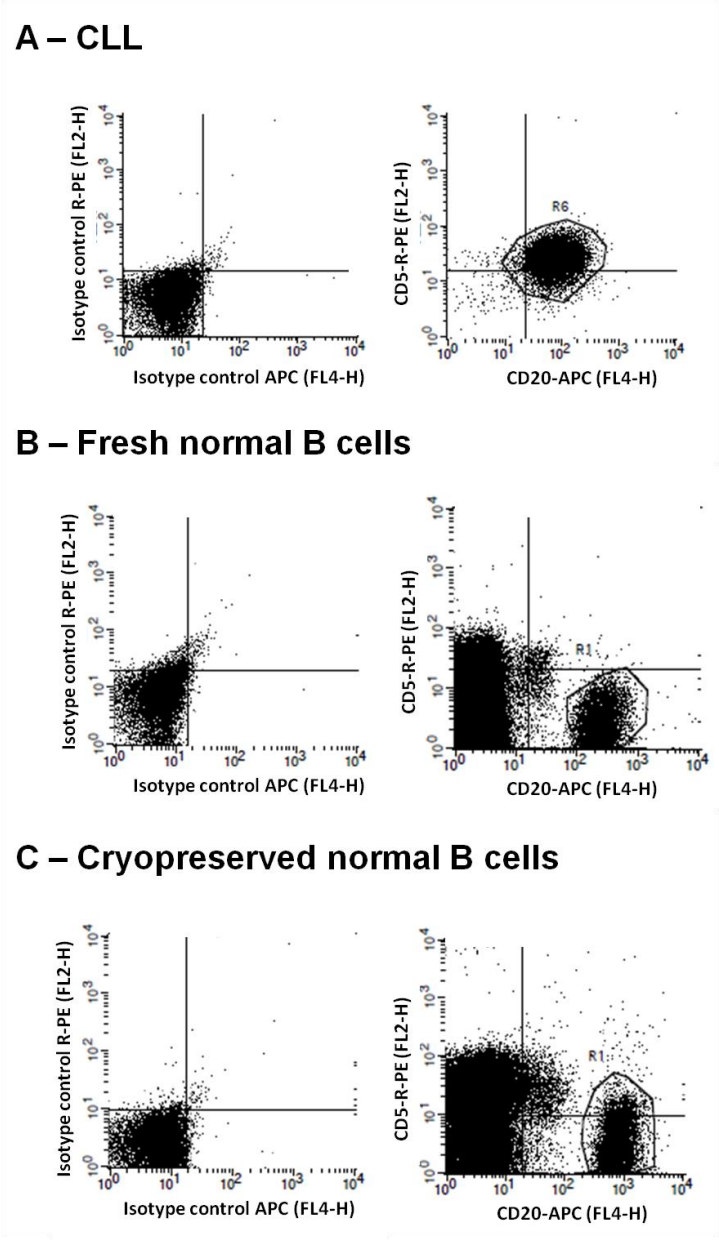

Figure 2.2: Identification of CLL cells and normal B cells using flow cytometry. **(A)** CLL cells were identified based on CD5-PE and CD20-APC positivity. **(B)** Fresh normal B cells (CD5- and CD20+). **(C)** Cryopreserved normal B cells from a buffy coat sample (CD5- and CD20+). The left plot demonstrates the isotype controls for PE and APC while the right plot shows gated cells.

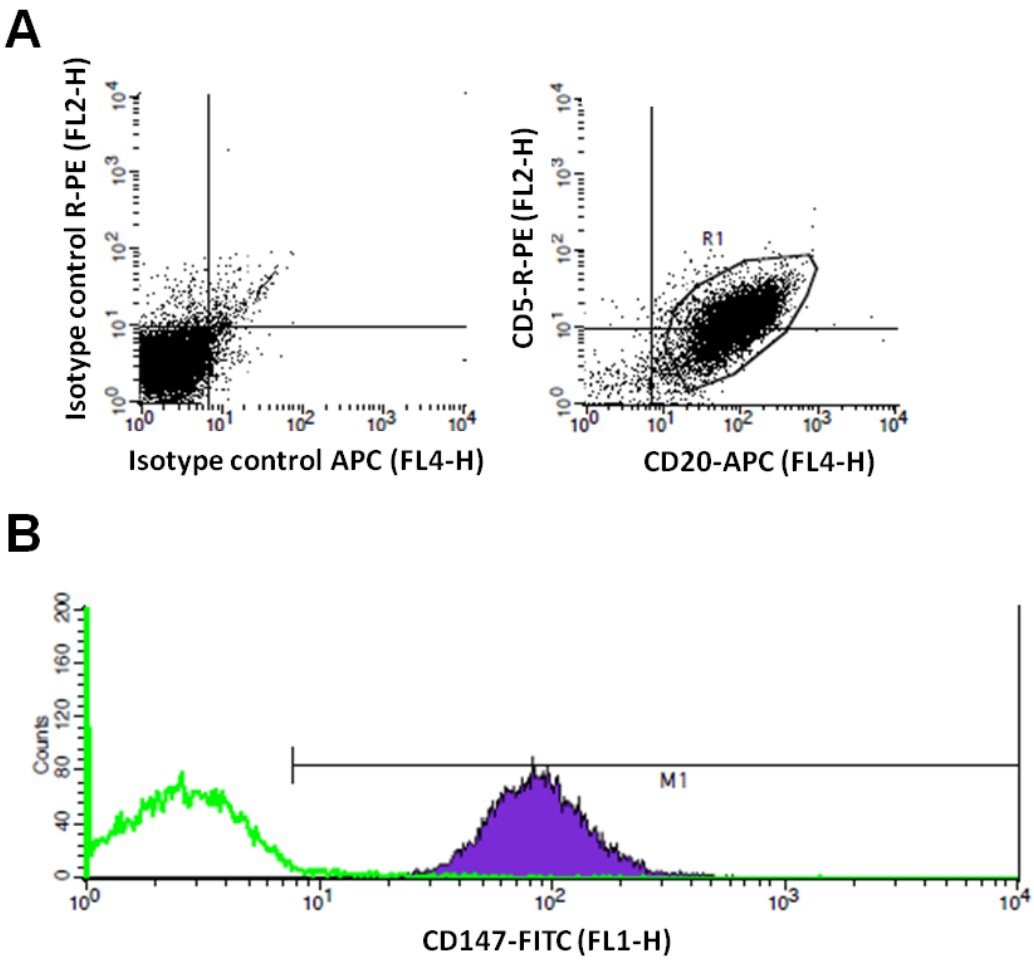

Figure 2.3: Raji cell line positive control for CD147. (A) Raji cells were identified based on CD5 and CD20 positivity. The left plot demonstrates the isotype controls for PE and APC while the right plot shows gated cells. **(B)** Histogram showing Raji cells to express CD147. The green line shows non-specific fluorescence measured using the isotype control FITC (FL1-H) while the section highlighted purple shows the fluorescence associated with the expression of CD147 (CD147-FITC (FL1-H)).

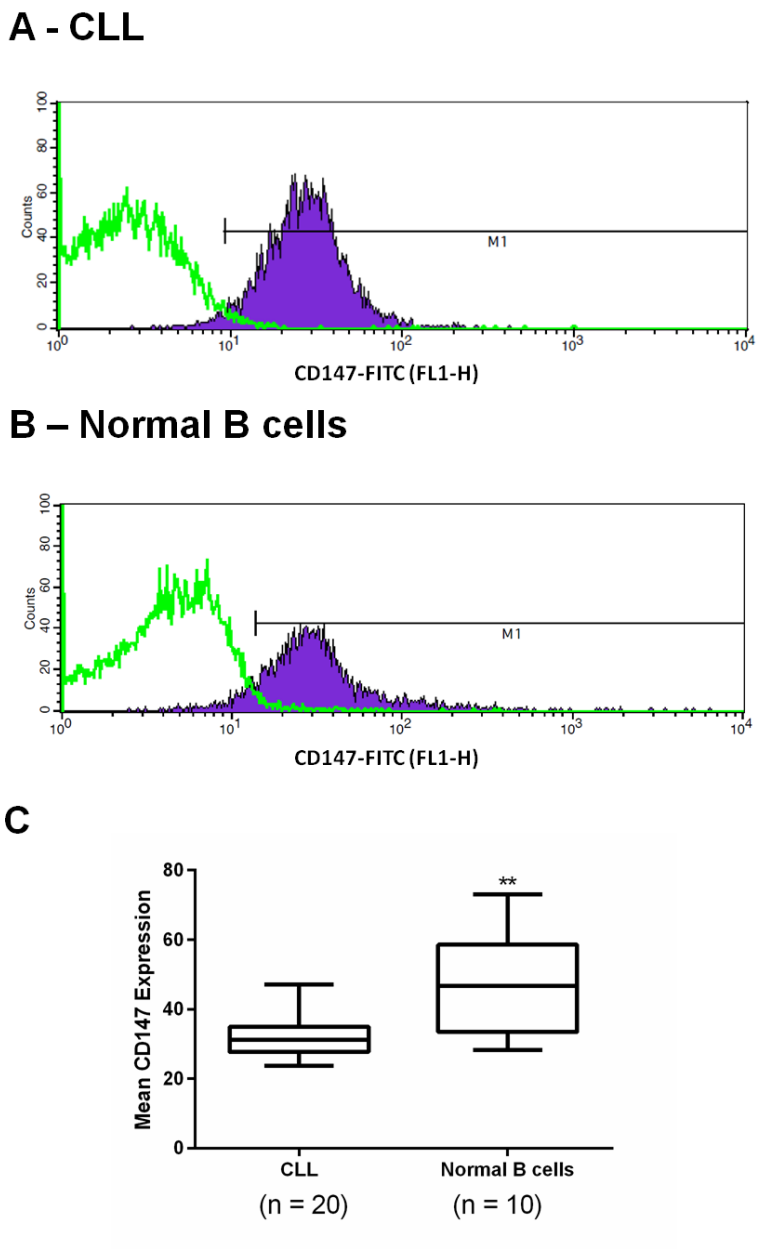

Figure 2.4: CD147 expression in CLL and normal B cells. **A)** 20 CLL samples were analysed for surface expression of CD147 using flow cytometry. CLL cells were gated as CD5+, CD20+, and CD23+. **(B)** Fresh normal B cells from 10 whole blood samples from healthy volunteers were analysed for CD147. Normal B cells were gated as CD5-, CD20+ and CD23+. For both **(A)** and **(B)** the green line shows non-specific fluorescence (isotype control FITC (FL1-H)) while the purple section shows the fluorescence associated with the expression of CD147 (CD147-FITC (FL1-H)). M1

indicates cells expressing CD147. **(C)** Box and whisker plot comparing mean CD147 expression in 20 CLL patients and 10 healthy volunteers. A Mann Whitney U test revealed that there to be greater CD147 expression in fresh normal B cells in comparison to CLL cells (** $P = 0.0014$).

A

Case no.	Mean CD147 Expression (G1)
1M	50.45
2M	72.22
3F	33.84
4F	28.30
5F	53.99
6F	72.99
7F	50.20
8M	41.99
9M	32.20
10M	43.32

B

Case no.	Mean CD147 Expression (G1)
2370	49.52
2371	48.25
3272	65.90
3273	44.15

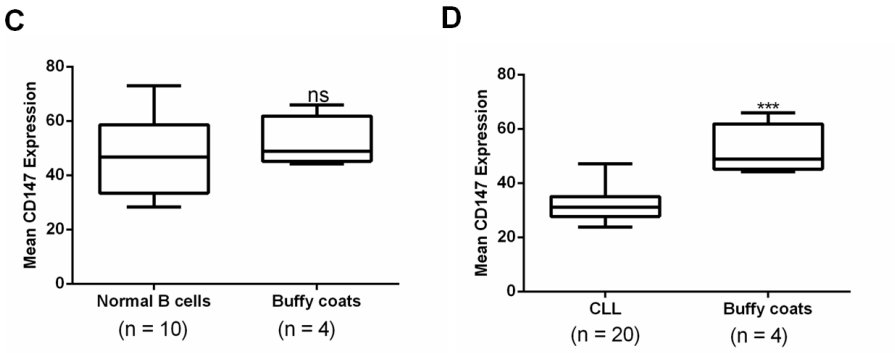

Figure 2.5: The effect of cryopreservation on CD147 expression in normal B cells. **(A)** Mean CD147 expression in fresh normal B cells from the whole blood of 10 healthy volunteers. **(B)** Mean CD147 expression in cryopreserved normal B cells from 4 buffy coats. **(C)** Box and whisker plot comparing mean CD147 expression in 10 fresh normal B cell samples and 4 cryopreserved normal B cell samples. A Mann Whitney U test revealed that was no significant difference between normal B cells and buffy coat samples ($P = 0.7333$). **(D)** Box and whisker plot comparing CD147 expression on B cells from 20 CLL patients and 4 healthy control subjects (cryopreserved buffy coat samples). A Mann Whitney U test revealed that there is a significant difference between CD147 expression in CLL cells in comparison to cryopreserved normal B cells (*** $P = 0.0006$).

2.3.2 Alkaline phosphatase (APAAP) staining for MCT -1 and -4 in CLL cells

To examine expression and verify the localisation of MCT -1 and -4 on CLL cells alkaline phosphatase staining (APAAP) was used. The results of this staining are shown in Figures 2.6 and 2.7. Figure 2.6 shows MCT1 expression in cells from 2 CLL patients as well as Raji cells used as a positive control. The antibody used was a rabbit polyclonal anti-MCT1 (Ab85021) from Abcam against a cytoplasmic epitope of the protein. In this figure specific staining appears concentrated within the cytoplasm of cells however it was difficult to distinguish between cytoplasmic and membrane localisation. Because Raji cells express MCT1 is high amounts, a more dilute solution (1:200) of the antibody was prepared from the 1:100 dilution used for the CLL cells. Nevertheless, these results show that MCT-1 is expressed on CLL and Raji cells.

The result generated using the Ab85021 antibody was then validated using a second rabbit polyclonal anti-MCT1 (AZ5565) developed in-house by AstraZeneca (Manchester, UK). Again, cells from 2 CLL patients and Raji cell line were examined, and similar to the images in Figure 2.6, the use of AZ5565 showed cytoplasmic staining in both cell types (Figure 2.7).

Validation of MCT4 expression in CLL cells was not possible because none of the antibodies available could be successfully used for this technique, particularly with respect to the positive control, MDA-MB-231 cells (data not shown) (Gallagher et al., 2007).

Moreover, further use of APAAP staining for the detection and quantification of MCT1 expression was considered unsatisfactory. Attempts were made to optimise the staining technique, but reproducibility remained a problem particularly with respect to intensity of staining. Thus, although similar results were generated using two different antibodies, lending confidence to the notion that MCT1 is expressed by CLL cells, comparison between cells from different CLL patients and/or with normal B cells would be unreliable.

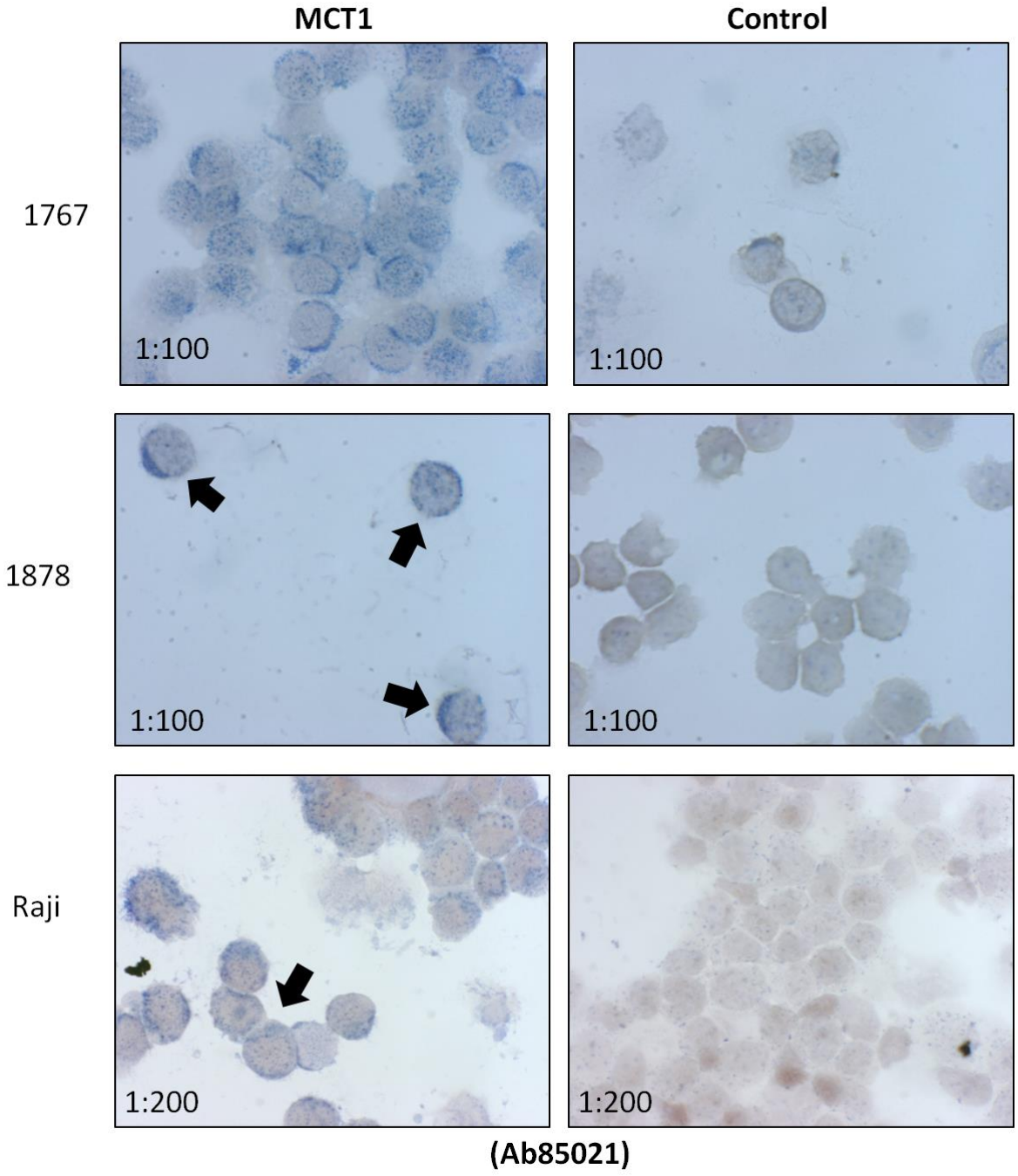

Figure 2.6: APAAP staining for MCT1 expression and localisation in CLL cells. MCT1 expression and distribution in 2 cases of CLL and Raji cell positive control treated with a 1:100 and 1:200 dilution of rabbit polyclonal anti-MCT1 (Ab85021) (Abcam, Cambridge, UK) respectively. Normal rabbit IgG was used as a negative control (1:100). Blue staining indicates the expression of MCT1.

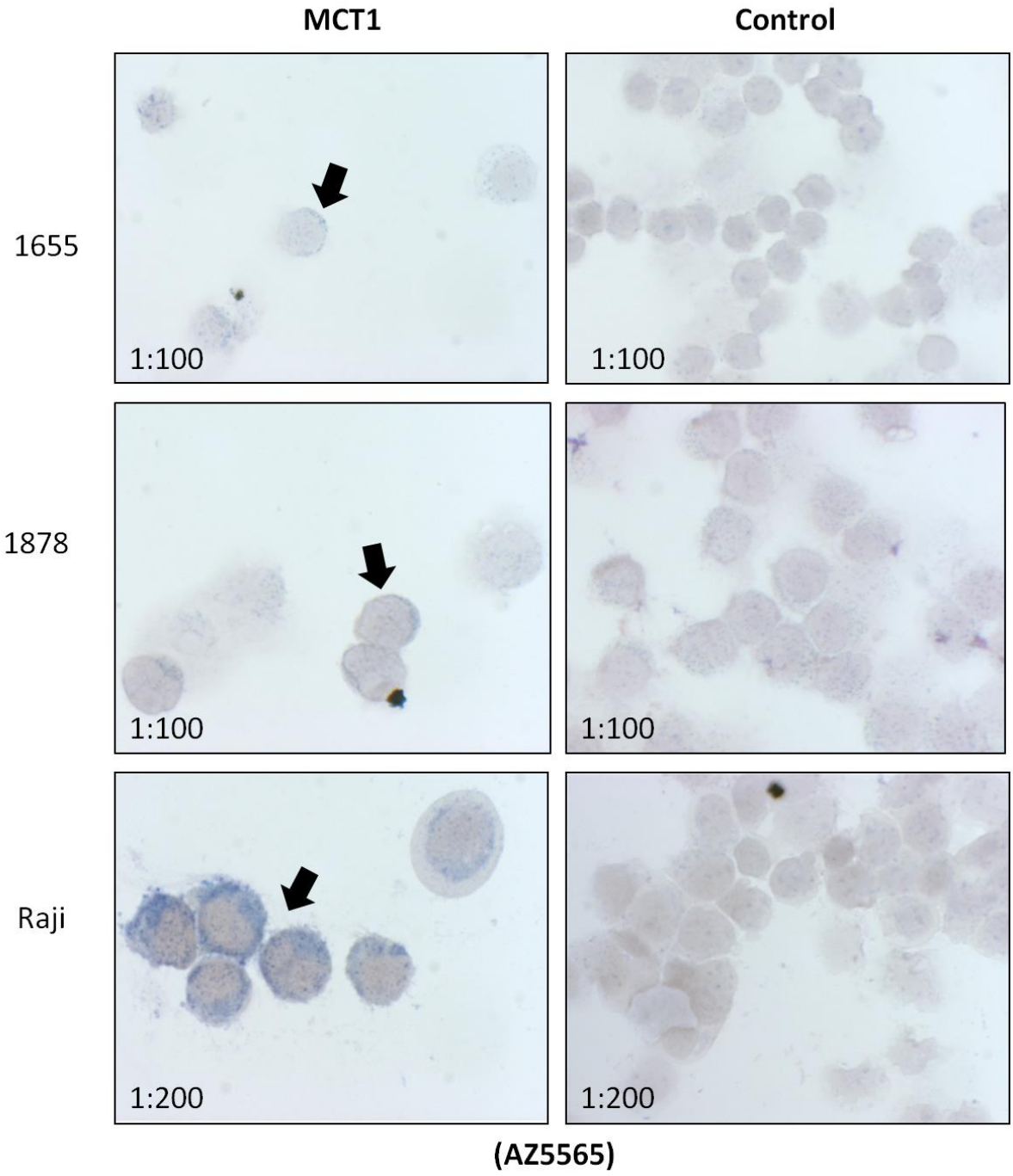

Figure 2.7: APAAP staining for MCT1 expression and localisation in CLL cells. MCT1 expression and distribution in 2 cases of CLL and Raji cell positive control treated with a 1:100 and 1:200 dilution of rabbit polyclonal anti-MCT1 (AZ5565) (AstraZeneca, Manchester, UK) respectively. Normal rabbit IgG was used as a negative control (1:100). Blue staining indicates the expression of MCT1.

2.3.3 Confocal microscopy for MCT -1 and -4 localisation in CLL cells

An attempt was made to assess immunocytochemical detection of MCT1 expression on CLL cells using confocal microscopy as a means of reducing the effects of preparation that is incumbent with the APAAP technique. The results of this analysis are shown in Figure 2.8, where analysis of MCT1 expression in cells from 3 CLL patients is presented. Here cells were stained with a mouse monoclonal anti-MCT1 antibody (sc-365501) from Insight Biotechnology. Staining with this antibody appeared restricted to a ring that likely corresponds to the cell cytoplasm, confirming the results generated with the polyclonal anti-MCT1 antibodies (Figures 2.6 and 2.7). However, this technique was not pursued owing to technical problems concerning reliability.

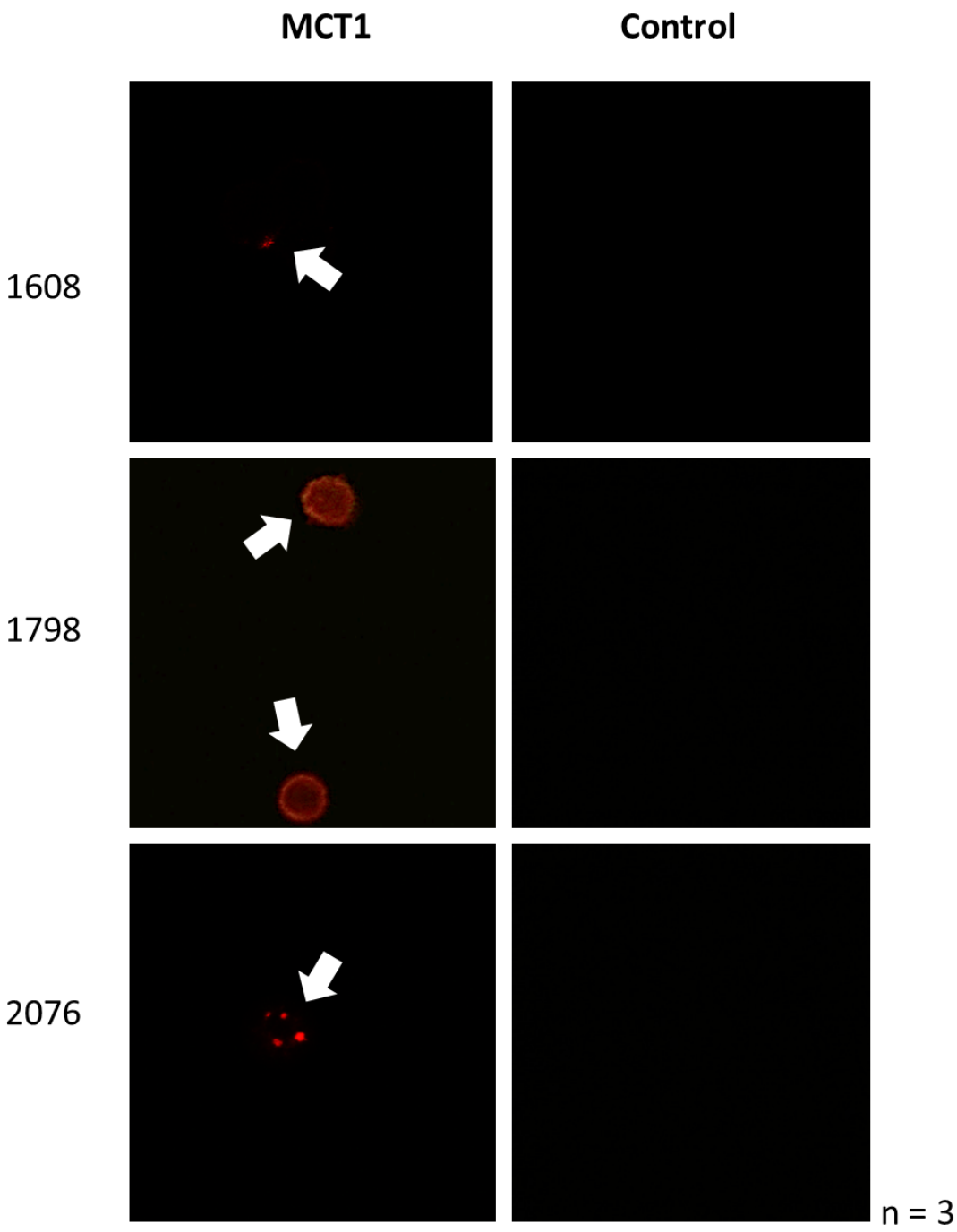

Figure 2.8: Confocal microscopy for MCT1 expression and localisation in CLL cells. CLL cells from 3 different patients were stained with mouse monoclonal anti-MCT1 (sc-365501) or with normal mouse IgG control. CLL cell purity for the cases used was 88.75% (1608), 99.21% (1798) and 89.23% (2076). Specific fluorescence associated with sc-365501 staining was determined by setting threshold fluorescence to the maximum associated with the non-specific control.

2.3.4 Western blot analysis for MCT -1 and -4 in CLL and normal B cells

Immunocytochemistry indicated expression of MCT1 on CLL cells. However, owing to problems with reliability these techniques were unsuitable for quantitative analysis. Therefore, for further exploration of MCT -1 and -4 protein levels in CLL cells Western blot analysis was used.

Figure 2.9 confirms MCT1 expression in Raji cells, which were used as a positive control for the immunocytochemistry. In these experiments MCT1 was detected in whole cell lysates as a single 48kDa band using the antibody AZ5565 and the rabbit polyclonal anti-MCT1 provided by Dr Philp. The mouse monoclonal anti-MCT1 antibody (sc-365501) used for the immunocytochemistry was not used in this section as this work was performed prior to the confocal analysis. Figure 2.9 also shows MCT1 expression in MEC-1 cells, a CLL cell line. As with the Raji cells, MCT1 was identified as a 48kDa band, a band that was identified by three antibodies developed against MCT1 (Ab85021, AZ5565, and anti-MCT1 provided by Dr Philp). Moreover, it was noted that MEC-1 cells seemed to express less MCT1 than did Raji cells despite equal protein loading. Taken together, these data suggest that Western blotting can be used to quantitatively assess MCT1 expression in CLL cells.

Antibody performance was further assessed using whole cell lysates prepared from the malignant cells from 19 CLL cases. This experiment compared the performance of each antibody; Ab85021, AZ5565, and anti-MCT1 (provided by Dr Philp). Figure 2.10 shows that all of the antibodies can be used to detect MCT1 expression in CLL cells. The results obtained using AZ5565 and the anti-MCT1 provided by Dr. Philp were consistent with each other. However, the results generated with Ab85021 antibody seemed unreliable owing to the presence of additional bands, particularly in the region where MCT1 was present. Because of the availability and apparent reliability of the AZ5565 antibody, it was chosen for further quantitative studies.

A comparison of MCT1 expression in CLL and normal B cells was then carried out. Cell lysates were prepared using purified normal B cells (>76% purity), and equal amounts of protein were analysed for the presence of MCT1. Figure 2.11 shows the

results of this comparison with MCT1 levels being significantly raised in purified normal B cells compared to CLL cells (** $P = 0.0081$, Mann Whitney U test). This is in keeping with the CD147 analysis (Figure 2.4). Thus, taken together, these data show that MCT1 is under expressed on CLL cells.

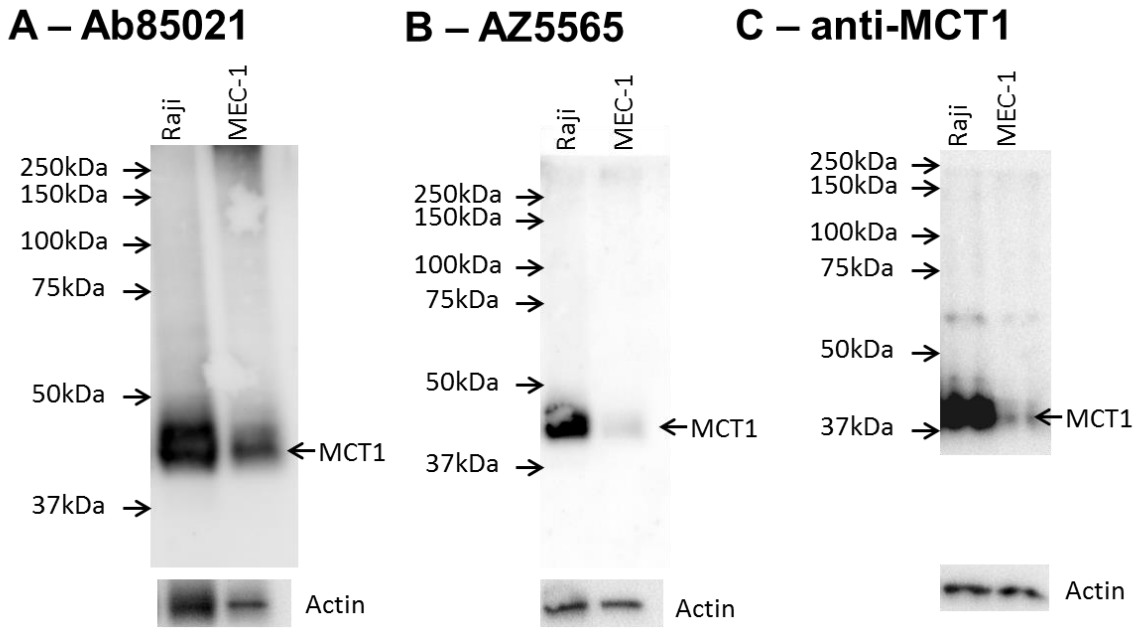

Figure 2.9: MCT1 protein expression in Raji and MEC-1 cell lines. 3 immunoblots showing MCT1 expression in Raji and MEC-1 cells when treated with either **(A)** rabbit polyclonal anti-MCT1 (Ab85021) (1:2000) (Abcam, Cambridge, UK), or **(B)** rabbit polyclonal anti-MCT1 (AZ5565) (1:1000) (AstraZeneca, Manchester, UK), or **(C)** rabbit polyclonal anti-MCT1 (1:2000) provided by Dr Philp (Thomas Jefferson University, PA, USA). MCT1 is visible at a molecular weight of 48kDa. Blots were probed with mouse monoclonal anti-β-actin (clone AC-74) as a control to ensure equal protein loading.

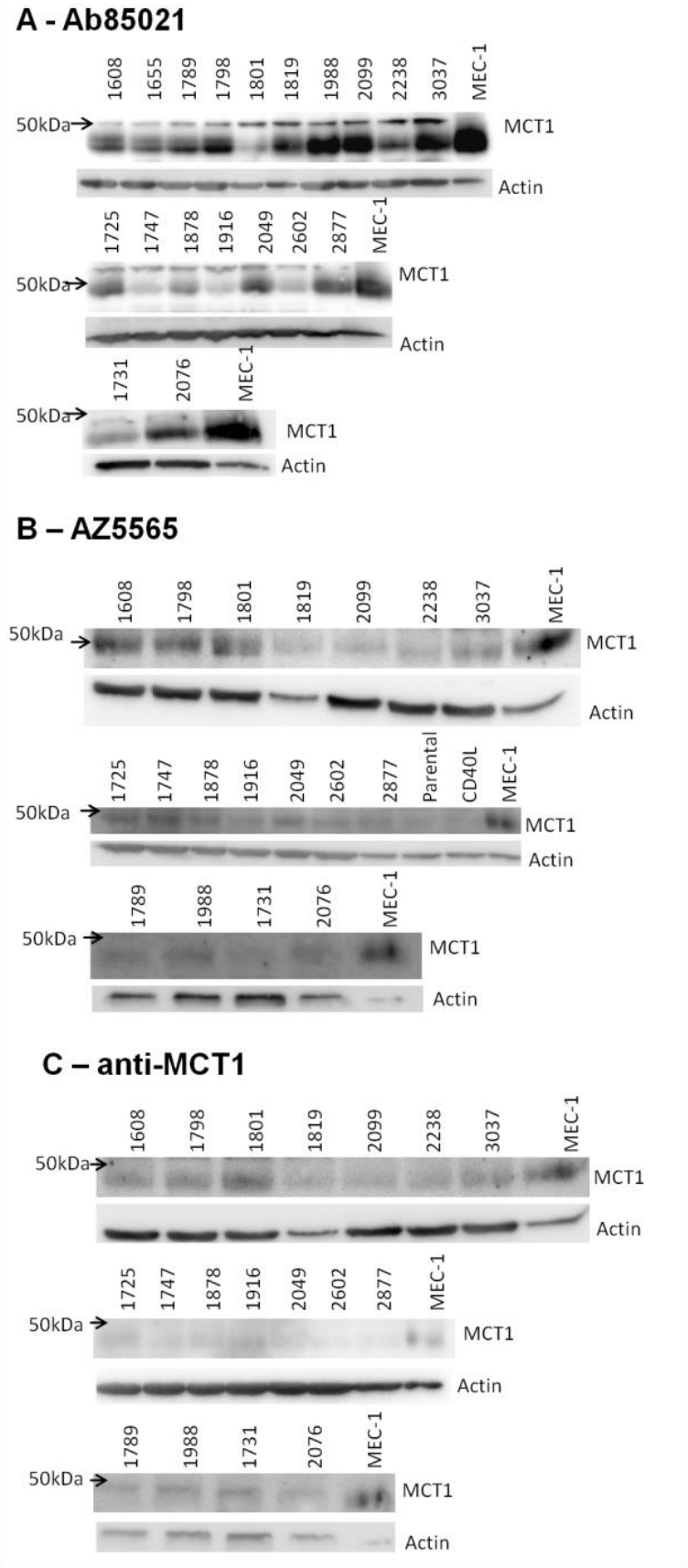
A - Ab85021
1608
1655
1789
1798
1801
1819
1988
2099
2238
3037
MEC-1
50kDa
MCT1
Actin
1725
1747
1878
1916
2049
2602
2877
MEC-1
50kDa
MCT1
Actin
1731
2076
MEC-1
50kDa
MCT1
Actin
B – AZ5565
1608
1798
1801
1819
2099
2238
3037
MEC-1
50kDa
MCT1
Actin
1725
1747
1878
1916
2049
2602
2877
Parental
CD40L
MEC-1
50kDa
MCT1
Actin
1789
1988
1731
2076
MEC-1
50kDa
MCT1
Actin
C – anti-MCT1
1608
1798
1801
1819
2099
2238
3037
MEC-1
50kDa
MCT1
Actin
1725
1747
1878
1916
2049
2602
2877
MEC-1
50kDa
MCT1
Actin
1789
1988
1731
2076
MEC-1
50kDa
MCT1
Actin

Figure 2.10: MCT1 protein expression in CLL cells – assessing antibody specificity and validation of controls. 9 immunoblots showing a total of19 CLL cases which heterogeneously express MCT1 when treated with either **(A)** a 1:1000 or a 1:2000 dilution of rabbit polyclonal anti-MCT1 (Ab85021) (Abcam, Cambridge, UK), or **(B)** rabbit polyclonal anti-MCT1 (AZ5565) (1:1000) (AstraZeneca, Manchester, UK), or **(C)** rabbit polyclonal anti-MCT1 (1:2000) provided by Dr Philp (Thomas Jefferson University, PA, USA). MCT1 is visible at a molecular weight of 48kDa. Blots were probed with mouse monoclonal anti-β-actin (clone AC-74) as a control to ensure equal protein loading. A MEC-1 cell line was used as a positive control for MCT1 (AstraZeneca, Manchester, UK).

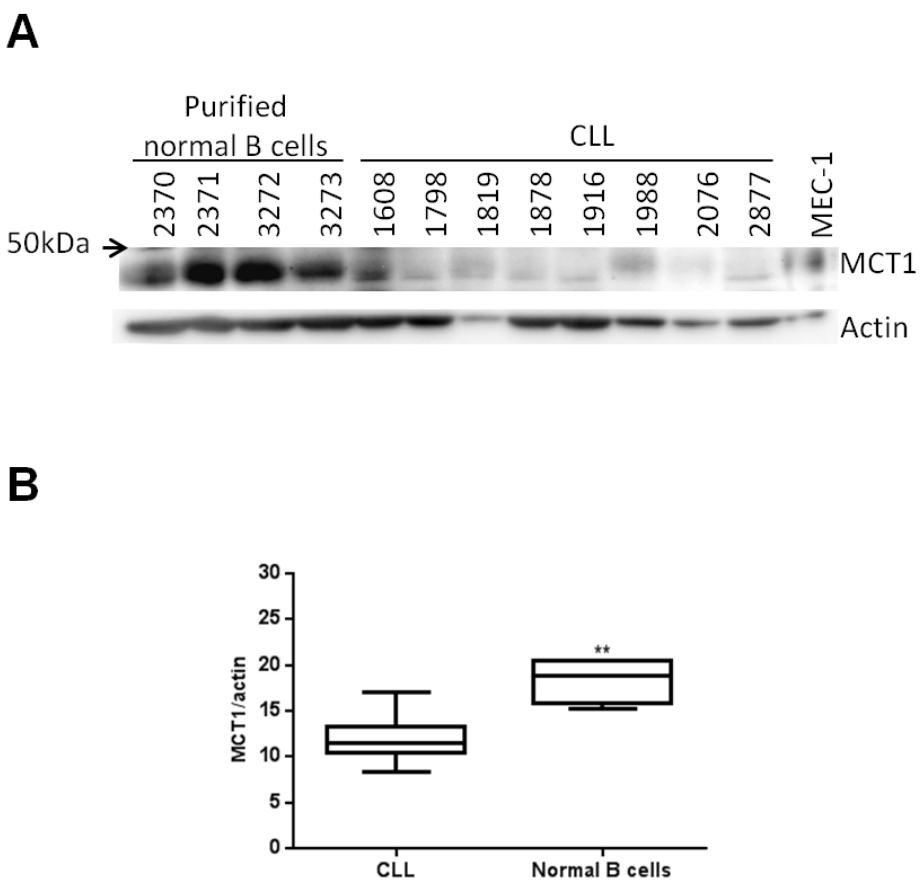

Figure 2.11: MCT1 protein expression in purified normal B cells versus CLL cells. **(A)** Immunoblot showing 4 purified normal B cells (>76% purity) and 8 CLL cells expressing MCT1 when treated with rabbit polyclonal anti-MCT1 (AZ5565) (1:1000) (AstraZeneca, Manchester, UK). MCT1 is visible at a molecular weight of 48kDa. Blots were probed with mouse monoclonal anti-β-actin (clone AC-74) as a control to ensure equal protein loading. A MEC-1 cell line was used as a positive control for MCT1 (AstraZeneca, Manchester, UK). **(B)** Quantitative comparison of MCT1 expression, calculated as a ratio of MCT1/actin expression, in CLL and normal B cell lysates using the data presented in part **(A)**. Statistical significance was determined using a Mann Whitney U test (** $P = 0.0081$).

MCT4 expression in CLL cells was next assessed. MDA-MB-231 cells were used as a positive control (Gallagher et al., 2007). Raji cells were used as a negative control because they are reported to lack MCT4 (Lin et al., 1998b). Three antibodies targeting MCT4 expression were assessed in protein lysates prepared from MDA-MB-231, MEC-1, and Raji cells; Ab74109, AZ5570, the rabbit polyclonal anti-MCT4 antibody provided by Dr Philp. Figure 2.12 shows the results of this assessment. MCT4 has a predicted molecular weight of 54kDa, but is reported to migrate with a lower molecular weight on SDS-PAGE gels (Halestrap and Wilson, 2012, Merezhinskaya et al., 2004). Thus, MCT4 appears as a single migrating band with an apparent molecular weight that is slightly below the 50kDa marker. This band was strongly present in the control lane, and weakly observed in the lanes corresponding to MEC-1 cells using the AZ5570 antibody, the anti-MCT4 antibody provided by Dr Philp. Raji cell lysates showed absence of this band using these antibodies, confirming that MCT4 expression is absent from these cells. With respect to the Ab74109 antibody, a band was visible, but was equally present in both the positive (MDA-MB-231 cells) and negative (Raji cells) control lysates, indicating that this antibody was unsuitable.

Figure 2.13 shows that MCT4 protein levels are variable between patient samples. Largely similar results were obtained using the AZ5570 and the anti-MCT4 provided by Dr Philp. Ideally, either of these antibodies could have been used for further analysis. However, neither were available in sufficient quantity. Thus, additional antibodies targeted against MCT4 were purchased and validated based on the molecular weight at which a band was visible and the behavior with the positive and negative controls, the MDA-MB-231 and the Raji cell lines respectively. Issues with availability meant that the antibodies sc-376101 and sc-50329 were used in subsequent experiments to detect MCT4.

A comparison of MCT4 expression in CLL and normal B cells was then carried out. (Figure 2.14). Here the mouse monoclonal antibody sc-376101 was used to detect MCT4. The figure shows MCT4 levels in normal B cells are observed at significantly higher levels than in CLL cells (** $P = 0.0040$, Mann Whitney U test). This result is in concordance with the findings relating to MCT1 and CD147 (Figures 2.11 and 2.4).

Taken together, the results from this section indicate that CLL cells express both MCT -1 and -4, but at significantly lower levels than are observed on normal B cells.

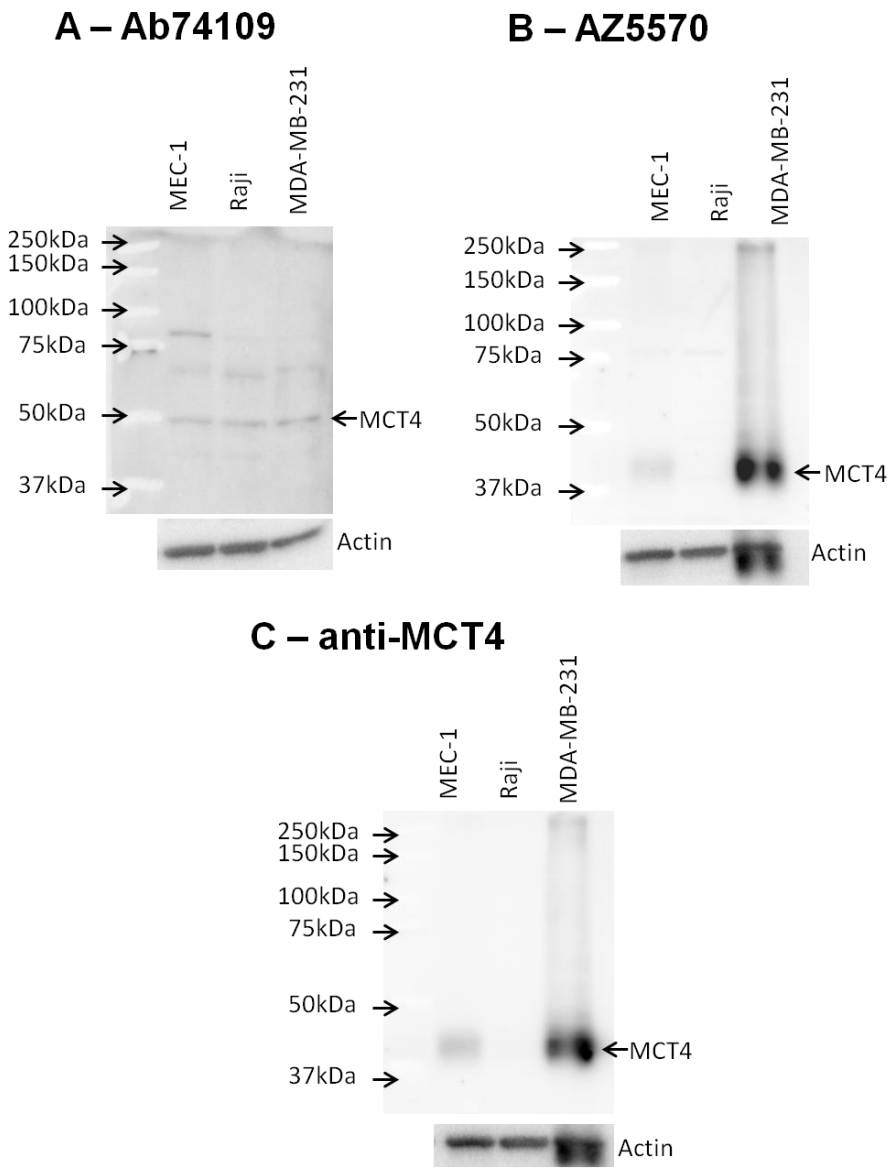

Figure 2.12: MCT4 protein expression in MEC-1 and Raji cell lines. 3 immunoblots showing MCT4 expression in MEC-1 and Raji cells when treated with **(A)** rabbit polyclonal anti-MCT4 (Ab74109) (1:2000) (Abcam, Cambridge, UK), **(B)** rabbit polyclonal anti-MCT4 (AZ5570) (1:1000) (AstraZeneca, Manchester, UK), or **(C)** isoform specific rabbit polyclonal anti-MCT4 (1:2000) kindly provided by Dr Philp (Thomas Jefferson University, PA, USA). MCT4 is visible just below 50kDa. Blots were probed with mouse monoclonal anti-β-actin (clone AC-74) as a control to ensure equal protein loading. A MDA-MB-231cell line was used as a positive control (Gallagher et al., 2007). A Raji cell line was used as a negative control (Lin et al., 1998b).

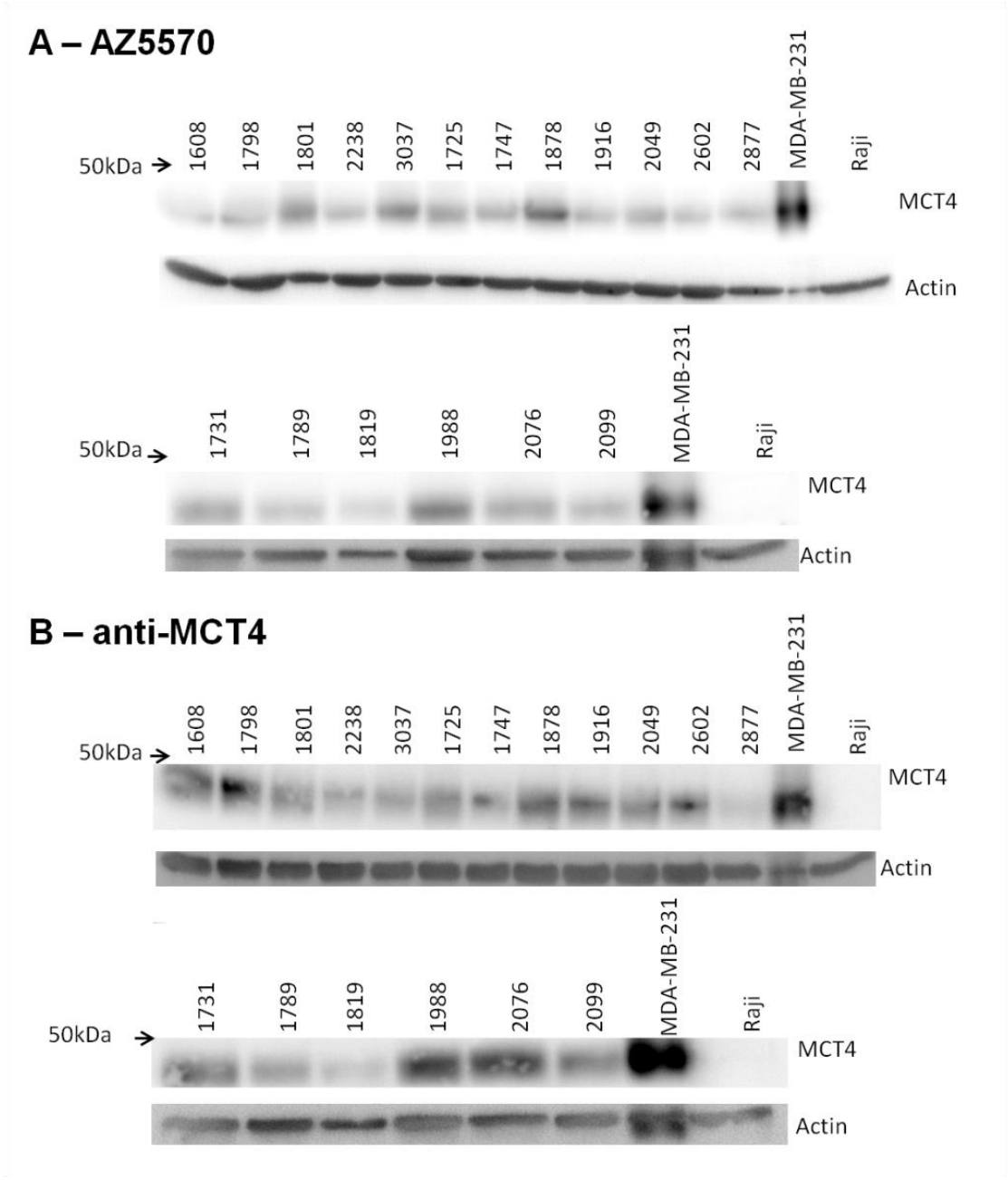

Figure 2.13: MCT4 protein expression in CLL cells – assessing antibody specificity and validation of controls. 4 immunoblots showing a total of 18 CLL cases which heterogeneously express MCT4 when treated with either **(A)** rabbit polyclonal anti-MCT4 (AZ5570) (1:1000) (AstraZeneca, Manchester, UK), or **(B)** isoform specific rabbit polyclonal anti-MCT4 (1:2000) kindly provided by Dr Philp (Thomas Jefferson University, PA, USA). MCT4 is visible just below 50kDa. Blots were probed with

mouse monoclonal anti-β-actin (clone AC-74) as a control to ensure equal protein loading. A MDA-MB-231cell line was used as a positive control (Gallagher et al., 2007). A Raji cell line was used as a negative control (Lin et al., 1998b).

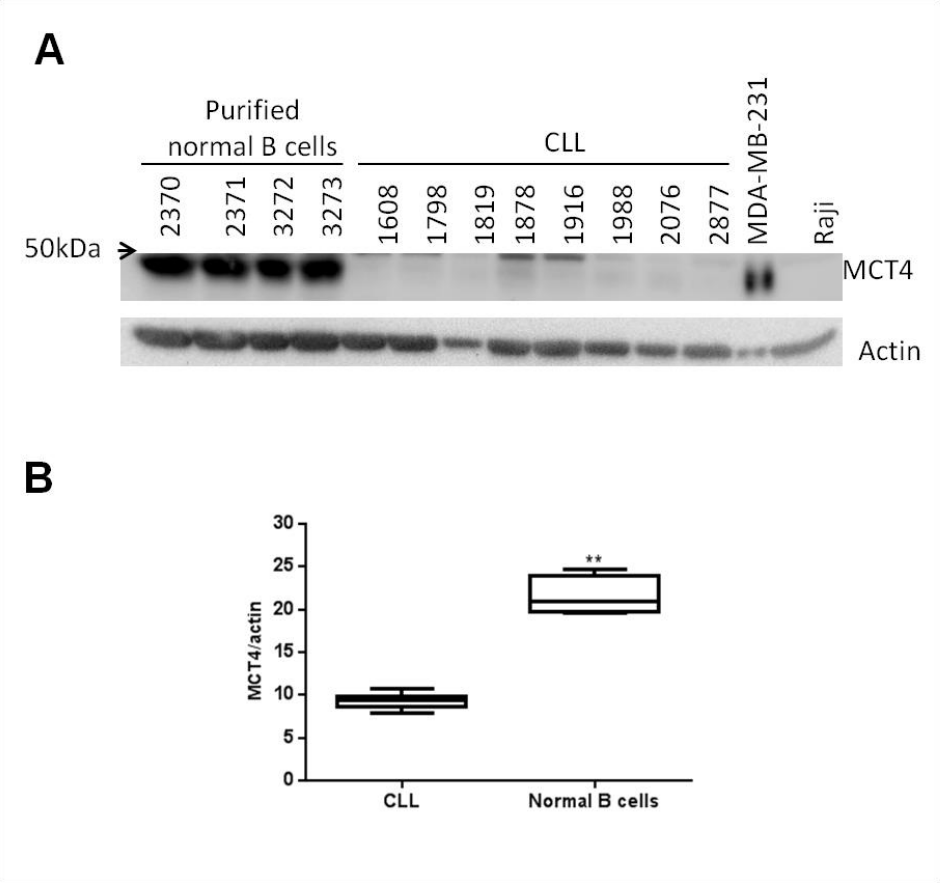

Figure 2.14: MCT4 protein expression in purified normal B cells versus CLL cells. **(A)** Immunoblot showing 4 purified normal B cells (>76% purity) and 8 CLL cells expressing MCT4 when treated with mouse monoclonal anti-MCT4 (sc-376101) (1:1000) (Insight Biotechnology, Wembley, UK). MCT4 is visible just below 50kDa. Blots were probed with mouse monoclonal anti-β-actin (clone AC-74) as a control to ensure equal protein loading. A MDA-MB-231 cell line was used as a positive control for MCT4 (Gallagher et al., 2007). A Raji cell line was used as a negative control for MCT4 (Lin et al., 1998b). **(B)** Quantitative comparison of MCT4 expression, calculated as a ratio of MCT4/actin expression, in CLL and normal B cell lysates using the data presented in part **(A)**. A Mann Whitney U test revealed a significant difference in MCT4 levels between CLL cells and purified normal B cells (** $P = 0.0040$).

2.3.5 Quantitative real-time PCR (qRT-PCR) analysis for MCT -1 and -4 in CLL and normal B cells

To examine the mRNA expression profiles of MCT -1 and -4 in CLL and normal B cells quantitative real-time PCR (qRT-PCR) was used.

Figure 2.15 (A) shows the mean MCT1 mRNA levels in MEC-1 and Raji cell lines. As expected, both cell lines expressed MCT1 message in agreement with the Western blot data (Figure 2.9) and Raji cells seemed to express more MCT1 than did MEC-1 cells. With respect to MCT4, MDA-MB-231 cells were used as a positive control and Raji cells were used as a negative control in agreement with the data shown in Figure 2.12 (Figure 2.15 (B)). MEC-1 cells expressed detectable levels of MCT4 mRNA. Taken together, these data confirm Western blot data using these cell lines, and show that MCT-1 and -4 expression can be assessed by qRT-PCR.

MCT-1 and -4 expression were next measured in CLL cells. Figures 2.16 (A) and (B) show qRT-PCR data for mean MCT1 and mean MCT4 expression in purified CLL cells from 16 patient samples. The quality of the CLL cell purification was assessed using flow cytometry for CD19, and all cases had >71% purity. MCT -1 and -4 mRNA levels are seen to vary between patient samples, reminiscent of the heterogeneity seen upon examination of MCT -1 and -4 proteins by Western blot (Figures 2.10 and 2.13). Figures 2.16 (C) and (D) show mRNA expression levels for MCT -1 and -4 in purified B cells (>91% purity) isolated from 3 buffy coat samples. A comparison of MCT1 expression between CLL and normal B cells showed significantly higher levels of this mRNA species in normal B cells (*** $P = 0.0002$) (Figure 2.16 (E)), and is consistent with Western data comparing MCT1 protein in these cell types. However, MCT4 mRNA expression showed no significant difference between CLL and normal B cells (Figure 2.16 (F)) ($P = 0.7053$), suggesting that the lower levels of MCT4 protein in CLL cells is not due to down regulation of gene expression.

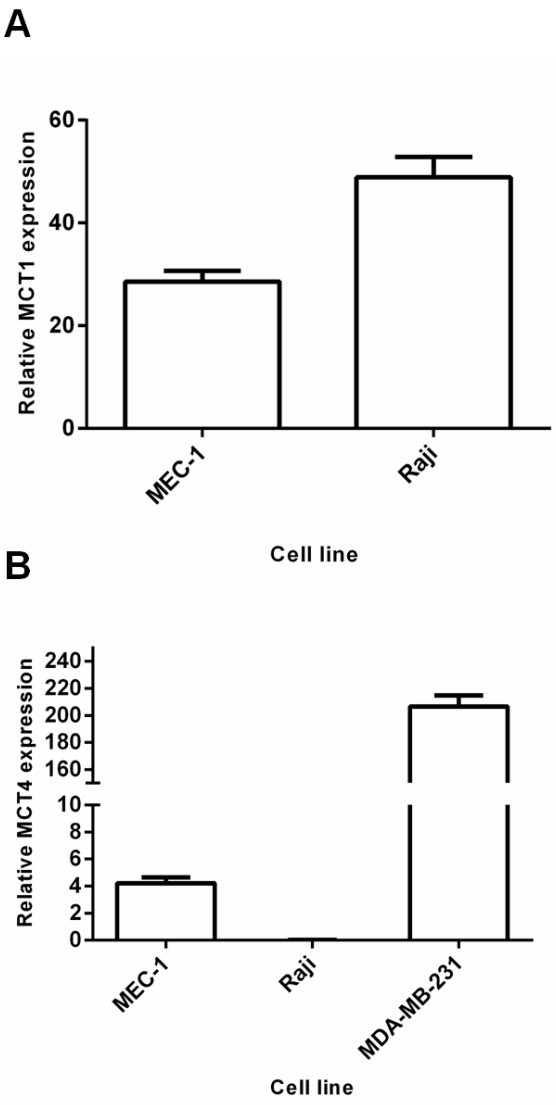

Figure 2.15: qRT-PCR analysis of MCT -1 and -4 mRNA levels in MEC-1, Raji and MDA-MB-231 cell lines. qRT-PCR analysis of MCT -1 and -4 mRNA was carried out according to the method described in section 2.2.9, and quantitation was determined relative to expression of actin. **(A)** Mean MCT1 expression in MEC-1 and Raji cell lines. Data was derived from 3 technical replicates, **(B)** Mean MCT4 expression in MEC-1, Raji and MDA-MB-231 cell lines. Data were derived from 3 technical replicates. Error bars represent the SEM.

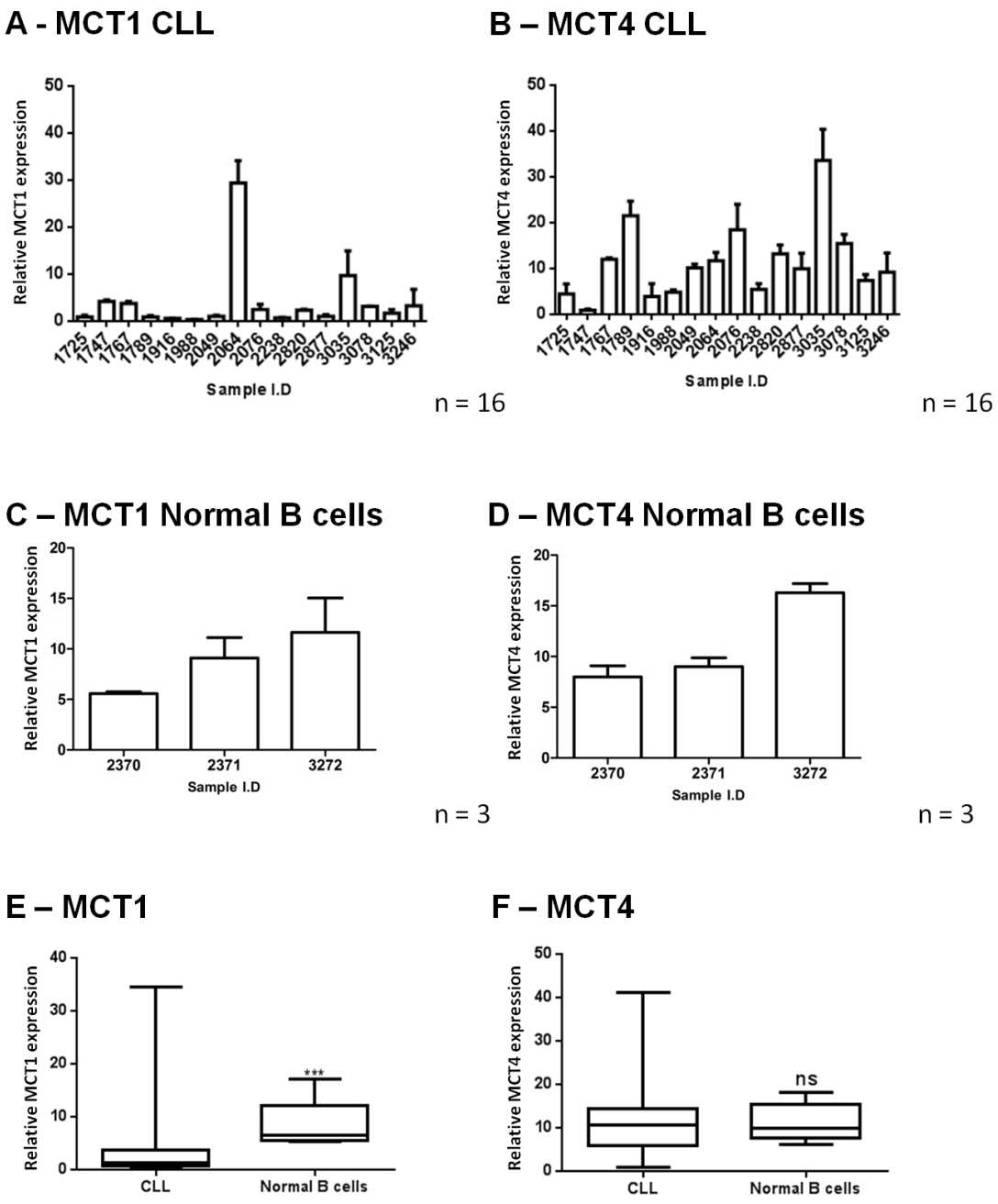

Figure 2.16: Comparison of MCT -1 and -4 mRNA levels in CLL and normal B cells. For all sections MCT-1 and -4 mRNA levels are determined relative to actin mRNA levels in the same cell. qRT-PCR data for; **(A)** mean MCT1 expression and, **(B)** mean MCT4 expression in purified CLL cases from 16 patients (>71% purity) derived from 3 technical replicates. **(C)** mean MCT1 expression and, **(D)** mean MCT4 expression, in purified B cells prepared from 3 buffy coat samples (> 91% purity)

derived from 3 technical replicates. **(E)** A Mann Whitney U test revealed MCT1 expression to be significantly higher (*** $P = 0.0002$) in normal B cells (n = 3). **(F)** There was no significant difference in MCT4 expression ($P = 0.7053$). Error bars represent the SEM.

2.3.6 Comparison of MCT -1, -4 and CD147 expression in IgVH mutated and IgVH unmutated CLL

The observation that MCT -1, -4 and CD147 expression on CLL cells was variable between patient samples loans itself to the heterogeneous nature of this disease. A characteristic marker of this heterogeneity in CLL is IgVH mutation status, whereby disease in UM-CLL cases is generally progressive and in M-CLL cases it is not (Oscier et al., 2012). Moreover, IgVH mutational status was chosen for this comparison because it has been reported to be associated with increased proliferation and replicative capacity (Vilpo et al., 2005, Rampazzo et al., 2012). This implies that in UM cases the rate of CLL proliferation may be higher and that this may be accompanied by increased glycolytic activity and dependency on lactate export out of the cell. Therefore, a comparison of MCT -1, -4 and CD147 expression on CLL cells from M and UM-CLL cases was made.

Figure 2.17 compares CD147 expression on the malignant cells from 10 M-CLL and10 UM-CLL cases, as assessed by flow cytometry. No difference was observed with respect to expression of this antigen between these cohorts of patient samples (P = 0.2475, Mann Whitney U test). A comparison of MCT -1 and -4 protein expression showed that MCT1 expression is significantly lower on M-CLL compared to UM-CLL cells (* P = 0.0317), whereas MCT4 expression was similar (P = 0.2222) (Figure 2.18). For these experiments a mouse monoclonal (sc-365501) antibody was used to detect MCT1 and a rabbit polyclonal (HS-90) (sc-50329) antibody was purchased and used to detect MCT4. These antibodies were validated by comparing the molecular weight at which bands became visible to the antibodies previously used as well as their behavior with positive and negative controls for both MCT -1 and -4. This was necessary due to the lack of availability of AZD3965, AZ5570 and the anti-MCT4 provided by Dr Philp. At the gene expression level both MCT -1 and -4 mRNA levels were found to be decreased in the malignant cells from M-CLL cases than in those from UM-CLL cases (respectively ****P = <0.0001 and * P = 0.0342, Mann Whitney U test) (Figure 2.19). Taken together, these data show that patients with M-CLL are likely to have lower levels of MCT1 expression in comparison to patients with UM-CLL. Whether this is

related to disease progression, as is reported for the malignant cells of other cancers (Pinheiro et al., 2010, Torres de Oliveira et al., 2012, Pinheiro et al., 2009, Pertega-Gomes et al., 2011, Zhao et al., 2014), remains to be determined.

Case no.	V gene usage (%)	IGVH Mutational status (< 2% = unmutated)	Mean CD147 Expression (G1)
1608	21.13	Mutated	30.97
1655	6.10	Mutated	28.83
1789	2.48	Mutated	34.35
1886	6.60	Mutated	33.84
1916	2.67	Mutated	23.76
2049	2.41	Mutated	33.28
2238	5.21	Mutated	29.43
2602	2.80	Mutated	23.82
2686	10.64	Mutated	27.28
3037	2.43	Mutated	31.34
1767	0.37	Unmutated	35.68
1878	0.00	Unmutated	46.11
2064	0.33	Unmutated	35.91
2389	1.75	Unmutated	26.69
2673	0.34	Unmutated	28.14
2715	0.03	Unmutated	26.03
3035	0.69	Unmutated	28.17
3078	0.00	Unmutated	31.17
3125	0.00	Unmutated	38.39
3246	0.69	Unmutated	47.08

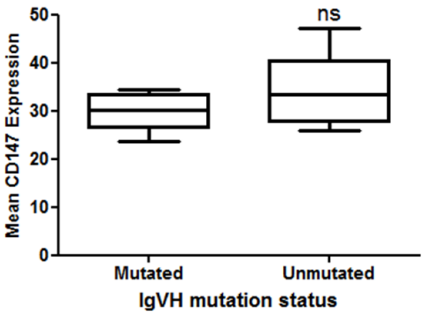

Figure 2.17: Comparison of CD147 expression on CLL cells from IgVH mutated versus IgVH unmutated cases. CD147 expression in 10 M-CLL and10 UM-CLL cases was determined by flow cytometry (inset table), and then compared graphically. A Mann Whitney U test revealed no significant difference in expression (P = 0.2475).

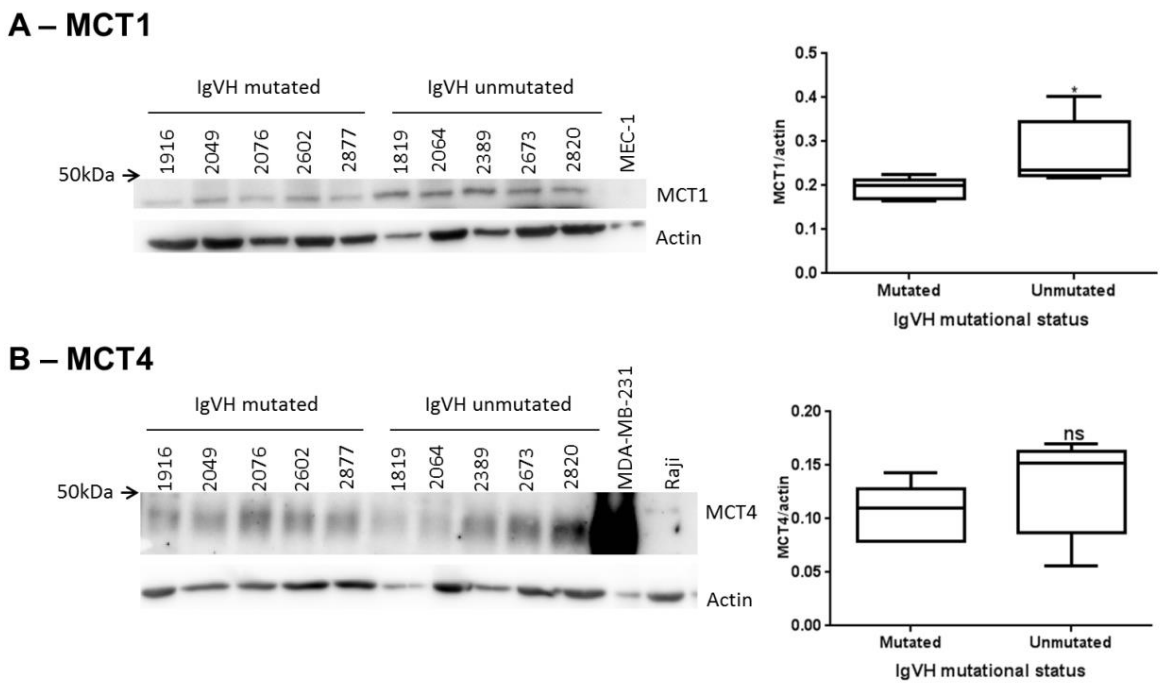

C

Case no.	V gene usage (%)	IgVH Mutational status (< 2% = unmutated)
1916	2.67	Mutated
2049	2.41	Mutated
2076	2.64	Mutated
2602	2.8	Mutated
2877	8.5	Mutated
1819	1.74	Unmutated
2064	0.33	Unmutated
2389	1.75	Unmutated
2673	0.34	Unmutated
2820	1.74	Unmutated

Figure 2.18: Comparison of MCT -1 and -4 protein expression in CLL cells from IgVH mutated versus IgVH unmutated cases. Protein lysates made from CLL cells from 5 M-CLL versus 5 UM-CLL cases. **(A)** Western blot analysis of MCT1 expression (left panel). Blots were treated with a 1:1000 dilution of mouse monoclonal anti-MCT1 (sc-365501.) Graphical comparison of the MCT1/actin ratio derived by

densitometry of the bands (right panel). **(B)** Western blot analysis of MCT4 expression (left panel). Blots were treated with a 1:1000 dilution of rabbit polyclonal anti-MCT4 (HS-90) (sc-50329). Graphical comparison of the MCT4/actin ratio derived by densitometry of the bands (right panel). For **(A)** and **(B)** a MEC-1 cell line was used as a positive control (AstraZeneca, Manchester, UK) and MDA-MB-231 and Raji cell lines were used as positive and negative controls respectively (Gallagher et al., 2007., Lin et al., 1998b). Blots were probed with mouse monoclonal anti-β-actin (clone AC-74) as a control to ensure equal protein loading. **(C)** Table listing IgVH mutational status for the CLL cases used.

A

Case no.	V gene usage (%)	IgVH Mutational status (< 2% = unmutated)
1789	2.48	Mutated
1916	2.67	Mutated
1988	6.83	Mutated
2049	2.41	Mutated
2076	2.64	Mutated
2238	5.21	Mutated
2877	8.50	Mutated
1767	0.37	Unmutated
2064	0.33	Unmutated
2820	1.74	Unmutated
3035	0.69	Unmutated
3078	0.00	Unmutated
3125	0.00	Unmutated
3246	0.69	Unmutated

B – MCT1

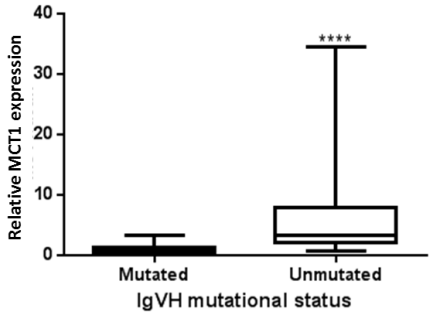

C – MCT4

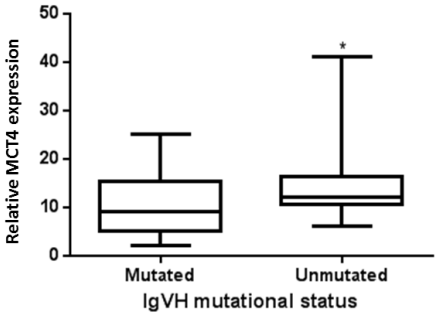

Figure 2.19: Comparison of MCT -1 and -4 mRNA levels in CLL cells from IgVH mutated versus IgVH unmutated cases. qRT-PCR was used to analyse MCT -1 and -4 expression relative to actin. **(A)** Table listing the IgVH mutational status for the 14 cases of CLL used in this part of the study. **(B)** Graphical comparison of MCT1 mRNA levels in CLL cells from M and UM-CLL cases (****P = <0.0001). **(C)** Graphical comparison of MCT4 mRNA levels in CLL cells from M and UM-CLL cases (* P = 0.0342). Statistical significance was determined using a Mann Whitney U test.

2.4 DISCUSSION

The expression of the monocarboxylate transporters, MCT -1 and -4, and the accessory protein CD147 have not been previously investigated in CLL. The present study is the first to examine the expression profile of these proteins in this disease, as well as confirm their expression in normal B cells (Merezhinskaya et al., 2004, Deeg et al., 2001, Koch et al., 1999, Kasinrerk et al., 2006).

As previously discussed, CD147 can be considered a surrogate marker of MCT -1 and -4 expression because of the chaperone function of this protein in bringing these transporters to the cell membrane (Gallagher et al., 2007). Although other transport proteins are chaperoned by CD147 (Zhu et al., 2013) the results of the present study show concordance between CD147 and MCT1/4 expression on CLL and normal B cells. That is, CLL cells express lower levels of CD147, MCT -1 and -4 than do normal B cells.

The expression of MCT1 on CLL cells was demonstrated by immunocytochemistry, and detected using antibodies raised against different epitopes. The same antibodies detected a band of expected molecular weight in Western blot analysis of whole cell lysates, indicating with confidence that CLL and normal B cells express this protein. Further to this, qRT-PCR showed that expression of the gene could be seen at the message level. Similarly, the detection of MCT4 on CLL and normal B cells was carried out using different antibodies to probe for this protein by Western blotting of whole cell lysates, and by using qRT-PCR to assess mRNA levels.

The expression of MCT -1 and -4 in CLL and normal B cells is not unexpected because a previous study has shown the presence of these transporters in normal lymphocytes, although this study did not distinguish between B and T cells (Merezhinskaya et al., 2004). In addition to this, MCT1 seems to be ubiquitously expressed by all cells (Halestrap and Price, 1999, Halestrap and Wilson, 2012). However, the expression of MCT4 is more restricted and is seen mainly in cells which are glycolytically active, including WBCs (Halestrap and Price, 1999, Halestrap and Wilson, 2012). Although the expression of these transporters has been in examined in other types of cancer

(Pinheiro et al., 2010, Torres de Oliveira et al., 2012, Pinheiro et al., 2009, Pertega-Gomes et al., 2011, Zhao et al., 2014), in lymphoid malignancy expression of MCT -1 and -4 has not been widely studied. As previously discussed, the expression of MCT1 has been shown in Raji cells, a cell line derived from Burkitt's lymphoma as well as in a MOLT-4 cell line, which is derived from acute ALL (Lin et al., 1998b). These findings were verified by other studies showing that MCT1 expression is raised across a panel of B cell malignancies compared to their normal counterparts (Arendt et al., 2012, de Vries et al., 2010, Liu et al., 2009, Thorns et al., 2002, Nabeshima et al., 2004, Shi et al., 2003). More recently, a study by Doherty et al. (2013) showed that MCT1 correlated with MYC expression in numerous types of cancer cell lines including Raji cells. The implication of this finding is that the higher proliferative activity associated with high MYC expression necessitates greater need of lactate import/export by MCT1. This is important because MYC has been shown to be important to CLL pathobiology (Refaeli et al., 2008, Put et al., 2012, Halina et al., 2010).

The results of this chapter show that the expression of MCT -1 and -4 in CLL cells is less than that in normal B cells. This finding contrasts with those of others studying other lymphoid malignancies (Arendt et al., 2012, de Vries et al., 2010, Liu et al., 2009, Thorns et al., 2002, Nabeshima et al., 2004, Shi et al., 2003), but is likely related to the pathophysiology of CLL cells. Although CLL has been shown to have a significant proliferative component (Messmer et al., 2005) the rate of CLL cell proliferation is lower than that of normal B cells (Defoiche et al., 2008). Furthermore, expansion of the malignant clone in CLL is localised to proliferation centres in the secondary haemic tissues where these cells encounter mitogenic stimuli (van Gent et al., 2008). The experiments presented in this chapter use CLL cells from circulation, and these are known to be arrested in G_0 of the cell cycle but are functionally incompetent and have impaired metabolism in comparison to normal B cells (Dasanu, 2008, Brody et al., 1969, Dameshek, 1967). That the levels of MCT -1 and -4 as well as CD147 on CLL cells are down regulated is in keeping by studies which show the activity of glycolytic enzymes such as aldolase and glucose-6-phosphate isomerase to be lower in these cells compared to normal B cells (Vives Corrons et al., 1989, Ho et al., 1982, Musolino et al., 1992). Moreover, these findings are also in agreement with more recent work showing

increased oxidative phosphorylation in CLL cells but not increased aerobic glycolysis (Jitschin et al., 2014). Normal B cells are also arrested in G_0 and have been shown to rely on oxidative phosphorylation for energy homeostasis (Garcia-Manteiga et al., 2011), but the need of these cells to respond to antigenic challenge with induction of glycolysis (Garcia-Manteiga et al., 2011) may require the presence of higher baseline expression levels of MCT1 and MCT4.

Like normal B cells, CLL cells are also capable of becoming activated, particularly those which bear the UM-CLL genotype. In this respect, similarly to the comparison between normal B cells and CLL cells, MCT1 expression was observed higher on CLL cells from UM-CLL cases in comparison to M-CLL cases. As MCT1 is known to function both as an importer or exporter of substrates the increased expression of MCT1 on UM-CLL cells may be a reflection of the higher metabolic needs of these cells over M-CLL cells.

In conclusion, the data presented in this chapter shows for the first time the expression of MCT -1 and -4 as well as their obligate chaperone CD147 on circulating CLL cells. In comparison to normal B cells, the expression of these proteins is low suggesting different metabolic requirement of these two cell types. This chapter did not address the expression of these proteins on CLL cells within areas where microenvironmental influences can affect their survival and proliferation. This is the subject of the next chapter where the influence of CD40 ligation is investigated.

3 CHAPTER 3: INVESTIGATING THE INFLUENCE OF THE MICROENVIRONMENT ON THE METABOLISM OF CLL CELLS

3.1 INTRODUCTION

The data in chapter 2 show that the expression of MCT -1 and -4 is decreased in circulating CLL cells in comparison to normal B cells. However, the levels of these transporters may change when the cells enter secondary tissues where they encounter microenvironmental stimuli that induce their activation and proliferation. Studies by Garcia-Manteiga et al. (2011) show that normal B cells switch to a glycolytic phenotype in order to sustain proliferation when they come into contact with antigenic stimuli. A primary mediator of B cell proliferation in germinal centers is CD40 engagement and IL-4 provided by cognate helper T cells (Patten et al., 2008). CD40 engagement and IL-4 also promote CLL cell proliferation (Hamilton et al., 2012), and, similar to normal B cells, such engagement on CLL cells may promote a metabolic switch to glycolysis that then requires increased expression of MCT -1 and/or -4.

The aim of this chapter is to investigate the effect of microenvironmental stimuli on the expression profile of MCT -1 and -4 in CLL cells. This chapter focuses on the effects of CD40 ligation and does not consider the additional effects of IL-4 or other cytokines. It was found that CD40 engagement on CLL cells resulted in specific upregulation of MCT4 protein expression. The metabolic processes requiring such regulation of MCT4, such as glycolysis, were investigated using a Fluidigm Biomark™ qRT-PCR chip array to examine gene expression and the SeahorseXF24 extracellular flux analyser to assess changes in metabolic flux.

3.2 MATERIALS AND METHODS

3.2.1 Culture of adherent cell lines

Mouse parental and CD40L (human) expressing mouse fibroblasts were provided by Professor Gerry Cohen (MRC Toxicology, University of Leicester, UK). Cells were recovered from -150°C storage at 37°C in a water bath for 5 minutes prior to the addition of 10mL of DMEM supplemented with 100 units/mL penicillin-streptomycin, 2mM L-glutamine and 10% heat inactivated FCS. Samples were subsequently centrifuged (250 rcf, 5 minutes, 4°C) and washed in modified media to remove DMSO cryopreservative before being seeded at a density of 3×10^5 cells/mL. Cells were cultured at 37°C under an atmosphere containing 5% CO_2, and passaged every 2-3 days whereby the cells were washed in PBS and trypsinised [Trypsin-EDTA (0.05%) (Invitrogen, Paisley, UK)] for approximately 3 minutes at 37ºC. Loosened cells were washed in modified DMEM media and made ready for re-seeding.

3.2.2 Poly-HEMA-coating of culture surfaces

Culture of CLL cells took place in tissue culture plates coated with poly(2-hydroxyethyl methacrylate) (poly-HEMA) (Sigma, Gillingham, UK) which were prepared by incubating a volume (dependent on the size of the tissue culture plate) of 1.2mg/mL of poly-HEMA dissolved in 95% ethanol at 37°C for a minimum of 48 hours.

3.2.3 Activation of CLL cells using soluble CD40 ligand (sCD40L)

Soluble CD40 ligand (sCD40L) for stimulation of CLL cells was prepared from a kit (Enzo Life Sciences, Exeter, UK) according to the manufacturer's instructions. The concentrations used in this study were 100, 200 and 400ng/mL of sCD40L. Following addition of the prepared sCD40L solution, CLL cells were incubated at 37°C and 5% CO_2 for either 24 or 48 hours in poly-HEMA plates. Generally 4×10^6 CLL cells were stimulated per condition.

3.2.4 Activation of CLL cells by co-culture with CD40 ligand (CD40L) expressing fibroblasts

Irradiated CD40L and parental fibroblasts which had a minimum viability of 70% were used for these experiments. Trypsinised cells (6 x 10^5 cells/mL) were suspended in modified DMEM and irradiated using the GAMMACELL® 3000 (Best Theratronics, Slough, UK). The dosage of gamma radiation delivered was 75Gy, and following irradiation the cells were plated at 1.8 x 10^6 cells/well and incubated overnight at 37°C and 5% CO_2 to adhere. Prior to co-culture experiments the monolayer washed using PBS.

CLL cells were recovered from storage at -150ºC as described in 2.2.1.1 and resuspended to 1 x 10^7 cells/mL in media. 3 x 10^7 CLL cells/well were then added to fibroblasts, and then the co-culture was allowed to incubate at 37°C and 5% CO_2 for 48 hours. In some cases, untreated control (UT) CLL cells were prepared by culturing 3 x 10^7 cells/well in a 6 well plate pre-treated poly-HEMA.

3.2.4.1 Confirmation of CD40 ligand (CD40L) expression

Prior to commencement of these experiments, the fibroblasts were checked for CD40L expression. This was done by preparing a suspension of the fibroblasts and then staining with either Mouse anti-CD40L-FITC (IgG1k) (555699, BD Biosciences, Oxford, UK) or IgG1,y1-FITC Isotype control (345815, BD Biosciences, Oxford, UK) and analysing CD40L expression by flow cytometry.

3.2.5 Antibodies

As detailed in section 2.2.5. Additional antibodies used included; goat anti-human IgM (2020-01) (Southern Biotech, Cambridge, UK), donkey anti-goat IgG-HRP (Insight Biotechnology, Wembley, UK).

3.2.6 Western blot analysis

A similar procedure was used and is detailed in section 2.2.8.

3.2.7 Flow cytometry for the detection of CD147

As detailed in section 2.2.6.

3.2.8 Polymerase chain reaction (PCR)

RNA extraction, cDNA synthesis and qRT-PCR analysis were performed as described previously in section 2.2.9, however glyceraldehyde 3-phosphate dehydrogenase (GAPDH) was used as the reference gene to obtain relative quantitation (FAM/ MGB Probe, Non-Primer Limited) (Applied Biosystems, Life technologies, Paisely, UK).

3.2.9 Fluidigm Biomark™ array

3.2.9.1 Sample preparation

Samples were prepared from CLL cells co-cultured with parental and CD40L fibroblasts as detailed in section 3.2.4.

3.2.9.2 RNA extraction

RNA extraction was performed using QIAshredder™ and RNeasy® minikits as per the manufacturer's instructions and using a QIAcube (Qiagen, Manchester, UK). Quantification of extracted RNA was performed using a NanoDrop 2000c spectrophotometer. Only samples with a 260:280 ratio of <2 were used.

3.2.9.3 cDNA synthesis

A high capacity cDNA reverse transcription kit (Applied Biosystems, Life technologies, Paisely, UK) was used to synthesise cDNA from RNA (50ng/20µL) as per the manufacturer's guidelines. The following cycling variables were used for the thermal cycler; 25°C 10 minutes, 37°C 120 minutes, 85°C 5 seconds.

3.2.9.4 cDNA pre-amplification and preparation of the sample plate

A panel reflecting genes involved in cellular metabolism was selected and is listed for human genes in Table 3.1 and mouse genes in Table 3.2. The analysis is based on a TaqMan® gene expression assay, and all genes analysed were done using kits purchased from Applied Biosystems. For the human analysis (CLL cells) a panel of housekeeping genes including; actin, IPO8, and PPIA were additionally used. For the mouse analysis (fibroblasts) a panel of housekeeping genes including; 18S and IPO8 were additionally used.

To create a pre-amplification (PreAmp) pool for the genes of interest 1µL of each gene expression assay (these are the PCR primers) was added to a single RNase free eppendorf tube. To this PreAmp pool, Tris-EDTA (TE) buffer (pH 8.0) (Ambion, CA, USA) was added to produce a final volume of 100µL, and this was subsequently mixed and spun in a microcentrifuge. Next, 200µL of TaqMan® PreAmp mastermix (Applied Biosystems, Life technologies, Paisely, UK) was added as a final step to create the PreAmp pool.

The sample plate was prepared by placing 3.75µL of the PreAmp pool into each well of a 96 well plate. 1.25µL of cDNA prepared in section 3.2.9.3 was placed into pre-designated wells, corresponding to the samples used, and then mixed using a multi-channel pipette and finally centrifuged briefly to collect fluid in the bottom of each well. The plate was then sealed using optical adhesive cover (Applied Biosystems, Life technologies, Paisely, UK) and Microseal A film (Bio-Rad-Laboratories Ltd, Hemel

Hempstead, UK) and run on a thermal cycler. The following cycling variables were used 95°C 10 minutes, 95°C 15 seconds, 60°C, 4 minutes, for 14 cycles.

Following this thermal cycling step, 20µL of TE buffer (Ambion, Life technologies, Paisely, UK) was added to each well of the plate using a multi-channel pipette to obtain a 1:5 dilution of amplified cDNA. The plate was again sealed with an optical adhesive cover, mixed, and spun. 4.5µL of this final amplified cDNA solution was then added to a fresh 96 well plate into pre-designated wells. This plate, termed the "sample plate" was then sealed, centrifuged and stored at -20ºC if not used immediately.

3.2.9.5 Fluidigm Biomark™ qRT-PCR

3.2.9.5.1 Preparation of the assay plate containing the primer-probe sets (assay plate)

Preparation of the assay plate was performed by placing 7.5µL of each primer-probe sets (FAM MGB) for the genes of interest into designated wells of a 96 well plate. These plates were stored at 4ºC until used.

3.2.9.5.2 Priming of the 48 x 48 Fluidigm Biomark™ chip

To prepare the 48 x 48 Fluidigm Biomark™ chip (Fluidigm, CA, USA) control line fluid was added into the accumulator valves (Figure 3.1) whilst holding the plate at a 45º angle. Next the plate was loaded into an IFC (integrated fluidic circuit) MX-48 machine (Fluidigm, CA, USA) and primed. This ensures that the interface valves are closed to prevent premature mixing of the samples and assays.

3.2.9.5.3 Preparation of the assay and sample plates prior to loading of the Fluidigm Biomark™ chip

To the assay plate prepared in section 3.2.9.5.1, 7.5µL/well of 2x DA assay loading reagent (Fluidigm, CA, USA) was added to each of the wells. The assay plate was then sealed with an optical adhesive cover and kept at 4ºC in the dark until assay loading of the Fluidigm Biomark™ chip (Fluidigm, CA, USA).

The sample plate was prepared for loading in the following manner. 30µL of 20x DA sample loading reagent was added to 300µL of gene expression mastermix and mixed in a 1.5mL eppendorf tube. 5.5µL of this solution was added to each well of the sample plate prepared in section 3.2.9.4. This sample plate is now ready for loading into the Fluidigm Biomark™ chip and was kept at 4ºC in dark, sealed with an optical adhesive cover.

3.2.9.5.4 Loading of the Fluidigm Biomark™ chip

5µL from each well of the assay plate was transferred to their designated assay inlets on the Fluidigm Biomark™ chip (Figure 3.1). Following this 5µL from each well of the sample plate was transferred to their designated sample inlets on the Fluidigm Biomark™ chip (Figure 3.1). The Fluidigm Biomark™ chip was subsequently loaded on to the IFC MX-48 machine which loads the chip.

3.2.9.5.5 Analysis of the Fluidigm Biomark™ chip

Following the loading step the chip was transferred to the Biomark™ machine and run using the following protocol; 50°C 2 minutes, 95°C 10 minutes, 95°C 15 seconds, 60°C, 1 minute, for 40 cycles. ROX™ was used as a passive reference to normalise well to well differences (Appendix 6.4).

3.2.9.5.6 Data analysis of the Fluidigm Biomark™ chip

A revised panel of genes was produced by evaluating the amplification efficiency for each gene using a sample of reference RNA as a positive control. Genes which had a Ct value of <24 were included in further analysis. The panel of genes was further refined by assessing the specificity of the primers for cDNA and by including a sample of gDNA as a negative control. Genes which were amplified (Ct <24) were excluded from further analysis. Following this inter-individual variation across the samples was assessed using either a Kruskal-Wallis test or ANOVA. This was to ensure that the samples were of similar quality and that the genes have performed reliably and with similar efficiencies to provide confidence that any variation observed in future comparative analyses is not due to experimental variation. Post hoc tests were performed where variation was significant. Following this a comparative analysis was done. Here, linear fold change in gene expression was used to guide subsequent statistical analysis comparing gene expression between conditions and cell types. A minimum threshold of ≥ 1.5 fold change was used as an indicator of upregulation, while a threshold of ≤ 0.5 was used as an indicator of downregulation. Finally analysis of global changes in metabolic pathways was assessed by grouping genes into metabolic pathways.

	Gene	Metabolic pathway		Gene	Metabolic pathway
1	SLCA19	Amino acid transport	24	Glutamate dehydrogenase 1 (GLUD1)	Glutamine metabolism
2	SLC1A4	Amino acid transport	25	Glutamate dehydrogenase 1 (GLUD2)	Glutamine metabolism
3	SLC1A5	Amino acid transport	26	Glutaminase (GLS)	Glutamine metabolism
4	SLC6A14	Amino acid transport	27	Glutaminase (GLS2)	Glutamine metabolism
5	SLC7A5	Amino acid transport	28	Hexokinase 1 (HK1)	Glycolysis
6	SLC7A10	Amino acid transport	29	Hexokinase 2 (HK2)	Glycolysis
7	SLC7A11	Amino acid transport	30	Lactate dehydrogenase A (LDHA)	Glycolysis
8	SLC22A6	Amino acid transport	31	6-phosphofructo-2-kinase/fructose-2,6-biphosphatase 1 (PFKFB1)	Glycolysis
9	SLC22A8	Amino acid transport	32	6-phosphofructo-2-kinase/fructose-2,6-biphosphatase 3 (PFKFB3)	Glycolysis
10	SLC25A10	Amino acid transport	33	Hypoxia inducible factor 1 alpha (HIF1A)	Hypoxia
11	SLC25A11	Amino acid transport	34	Vascular endothelial growth factor A (VEGFA)	Hypoxia
12	SLC38A1	Amino acid transport	35	SLC16A1	Monocarboxylate transporter 1
13	SLC38A2	Amino acid transport	36	SLC16A3	Monocarboxylate transporter 4
14	SLC38A7	Amino acid transport	37	Pyruvate dehydrogenase lipoamide kinase isozyme 1 (PDK1)	Pyruvate metabolism
15	Acetyl-CoA carboxylase alpha (ACACA)	Fatty acid metabolism	38	Pyruvate dehydrogenase lipoamide kinase isozyme 4 (PDK4)	Pyruvate metabolism
16	Acetyl-CoA carboxylase beta (ACACB)	Fatty acid metabolism	39	Phosphoglycerate dehydrogenase (PHGDH)	Serine metabolism
17	Acyl-CoA synthetase short-chain family member 2 (ACSS2)	Fatty acid metabolism	40	Phosphoserine aminotransferase 1 (PSAT1)	Serine metabolism
18	ATP citrate lyase (ACLY)	Fatty acid metabolism	41	Activating transcription factor 4 (ATF4)	Stress
19	Carnitine palmitoyltransferase I A (CPT1A)	Fatty acid metabolism	42	Superoxide dismutase 1 (SOD1)	Stress
20	Diacylglycerol acyltransferase-1 (DGAT1)	Fatty acid metabolism	43	Malic enzyme 1 (ME1)	Tricarboxylic acid (TCA) cycle
21	Elongation of long-chain fatty acids family member 5 (ELOVL5)	Fatty acid metabolism	44	Malic enzyme 2 (ME2)	Tricarboxylic acid (TCA) cycle
22	Elongation of long-chain fatty acids family member 6 (ELOVL6)	Fatty acid metabolism	45	Malic enzyme 3 (ME3)	Tricarboxylic acid (TCA) cycle
23	Fatty acid synthase (FASN)	Fatty acid metabolism			

Table 3.1: Genes of interest for the human Fluidigm Biomark™ array.

	Gene	Metabolic pathway		Gene	Metabolic pathway
1	SLC1A5	Amino acid transport	24	Hexokinase 2 (HK2)	Glycolysis
2	SLC7A5	Amino acid transport	25	Lactate dehydrogenase A (LDHA)	Glycolysis
3	SLC25A1	Amino acid transport	26	6-phosphofructo-2-kinase/fructose-2,6-biphosphatase 1 (PFKFB1)	Glycolysis
4	SLC25A11	Amino acid transport	27	6-phosphofructo-2-kinase/fructose-2,6-biphosphatase 2 (PFKFB2)	Glycolysis
5	Acetyl-CoA carboxylase alpha (ACACA)	Fatty acid metabolism	28	6-phosphofructo-2-kinase/fructose-2,6-biphosphatase 3 (PFKFB3)	Glycolysis
6	Acetyl-CoA carboxylase beta (ACACB)	Fatty acid metabolism	29	6-phosphofructo-2-kinase/fructose-2,6-biphosphatase 4 (PFKFB4)	Glycolysis
7	ATP citrate lyase (ACLY)	Fatty acid metabolism	30	Hypoxia inducible factor 1 alpha (HIF1A)	Hypoxia
8	Carnitine palmitoyltransferase I A (CPT1A)	Fatty acid metabolism	31	SLC16A1	Monocarboxylate transporter 1
9	Carnitine palmitoyltransferase I A (CPT1B)	Fatty acid metabolism	32	SLC16A3	Monocarboxylate transporter 4
10	Diacylglycerol acyltransferase-1 (DGAT1)	Fatty acid metabolism	33	Glucose-6-phosphate dehydrogenase (G6PD)	Pentose phosphate pathway
11	Elongation of long-chain fatty acids family member 5 (ELOVL5)	Fatty acid metabolism	34	Transketolase (TKTL-11)	Pentose phosphate pathway
12	Elongation of long-chain fatty acids family member 6 (ELOVL6)	Fatty acid metabolism	35	Pyruvate dehydrogenase lipoamide kinase isozyme 1 (PDK1)	Pyruvate metabolism
13	Fatty acid synthase (FASN)	Fatty acid metabolism	36	Pyruvate dehydrogenase lipoamide kinase isozyme 4 (PDK4)	Pyruvate metabolism
14	Insulin induced gene 2 (INSIG2)	Fatty acid metabolism	37	Pyruvate dehydrogenase phosphatase catalytic subunit 1 (PDP1)	Pyruvate metabolism
15	Peroxisome proliferator-activated receptor alphas (PPARA)	Fatty acid metabolism	38	Phosphoglycerate dehydrogenase (PHGDH)	Serine metabolism
16	Peroxisome proliferator-activated receptor gamma (PPARG)	Fatty acid metabolism	39	Calcium/calmodulin-dependent protein kinase kinase 2 (CAMKK2)	Stress
17	Proliferation activation receptor gamma (PAPRG)	Fatty acid metabolism	40	Superoxide dismutase 1 (SOD1)	Stress
18	Sterol regulatory element-binding transcription factor 1 (SREBF1)	Fatty acid metabolism	41	Superoxide dismutase 2 (SOD2)	Stress
19	Sterol regulatory element-binding transcription factor 2 (SREBF2)	Fatty acid metabolism	42	Malic enzyme 1 (ME1)	Tricarboxylic acid (TCA) cycle
20	Transferrin receptor (TRFC)	Fatty acid metabolism	43	Malic enzyme 2 (ME2)	Tricarboxylic acid (TCA) cycle
21	Glutamate dehydrogenase 1 (GLUD1)	Glutamine metabolism	44	NADH dehydrogenase [ubiquinone] 1 beta subcomplex subunit 2 (NDUFB2)	Tricarboxylic acid (TCA) cycle
22	Glutaminase (GLS)	Glutamine metabolism	45	NADH dehydrogenase [ubiquinone] 1 beta subcomplex subunit 5(NDUFB5)	Tricarboxylic acid (TCA) cycle
23	Hexokinase 1 (HK1)	Glycolysis	46	NADH dehydrogenase [ubiquinone] 1 beta subcomplex subunit 9 (NDUFB9)	Tricarboxylic acid (TCA) cycle

Table 3.2: Genes of interest for the mouse Fluidigm Biomark™ array.

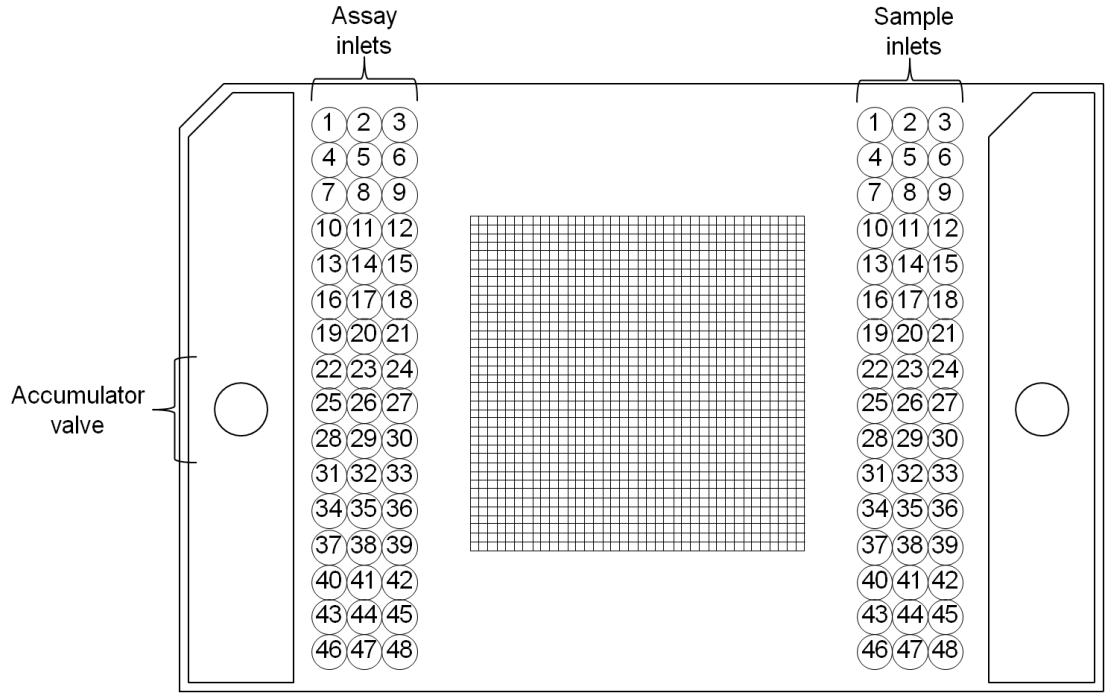

Figure 3.1: Assay and sample layout for the 48x48 Fluidigm Biomark™ chip.

3.2.10 Metabolic flux analysis using the SeahorseXF24 metabolic flux analyser

3.2.10.1 Media preparation

Unbuffered RPMI media (10x) stock (Sigma, Gillingham, UK) diluted with dH_2O to produce 1x RPMI media was supplemented with 2mM L-glutamine, 2.5μM folic acid (Sigma, Gillingham, UK), and 2mM of sodium pyruvate (Sigma, Gillingham, UK). This was then adjusted to pH 7.4 and sterile filtered. This media will be herein referred to as "Seahorse media."

3.2.10.2 Immobilisation of non-adherent cells with Matrigel™

To immobilise suspension cells to the XF24 cell culture microplate (Seahorse Bioscience, Saint Marcell, France) the cells were seeded on to a surface treated with the cellular adhesive Matrigel™ (BD Biosciences, Oxford, UK). To prepare the Matrigel™ a frozen aliquot was thawed on ice and kept at 4ºC to prevent it from polymerising. This was diluted with Seahorse media in a 1:4 dilution and 38μL was added to each well using pre-chilled pipette tips. The plate was subsequently left for 1 hour at room temperature after which excess Matrigel™ was removed and 100μL of Seahorse media was added to each well. The plate was then stored at 4ºC overnight and used within 24 hours.

3.2.10.3 Calibration of the SeahorseXF24 metabolic flux analyser

To calibrate the analyser 1mL of SeahorseXF calibrant solution (Seahorse Bioscience, Saint Marcell, France) was added per well to the XF24 calibration microplate and incubated overnight in the SeahorseXF24 Prep station (Seahorse Bioscience, Saint Marcell, France) at 37ºC under ambient atmospheric conditions and used within 24 hours.

3.2.10.4 Sample preparation

Cryopreserved CLL cells were recovered as detailed in section 2.2.1.1. Fresh CLL cells were either resuspended to a concentration of 2 x 10^7 cells/mL and left to acclimatise in the incubator at 37ºC and 5% CO_2 overnight or the cells were added to a fibroblast monolayer as detailed in section 3.2.4 and co-cultured for a 48 hour period. CLL cells were then removed from the fibroblast monolayer and prepared as described in the next section (3.2.10.5).

3.2.10.5 Preparation of the XF24 cell culture microplate

Cells were used at a density of 2 x 10^7 cells/mL. For the adhesion of cells on to the pre-prepared Matrigel™ treated microplate, cells were first resuspended in media and supplemented with 2mM L-glutamine and 2mM sodium pyruvate, but without added FCS or BSA. 100µL of this suspension was added per well except for the blanks; A1, B4, C3 and D6. This was then incubated in the SeahorseXF Prep station at 37ºC under ambient atmospheric conditions for 1 hour. Following this adhesion step the plate was examined under a microscope to assess the monolayer, and then the overlying media was removed. Next 450µL of pre-warmed Seahorse media was slowly added per well without disrupting the monolayer. The integrity of the monolayer was then re-checked and the plate was left to equilibrate for 20 minutes in the SeahorseXF Prep station prior to analysis. The plate was loaded following the calibration of the instrument using the XF24 calibration plate prepared previously.

3.2.10.6 Mitochondrial stress test

10x stock concentrations of each of the following compounds were prepared in Seahorse media so that upon injection a final concentration of 1.26µM oligomycin (Sigma, Gillingham, UK), 1.5µM trifluoromethoxy carbonyl cyanide phenylhydrazone (FCCP) (Sigma, Gillingham, UK) and 1µM each of antimycin-A (Sigma, Gillingham, UK) and rotenone (Sigma, Gillingham, UK) was added.

To start the assay a baseline was established. This was done my taking a measurement, then mixing the plate for 2 min, allowing a delay of 2 minutes and then taking a measurement (mix 2 min, wait 2 min, measure 2 min). This cycle was repeated five times to establish a robust baseline OCR (pMoles/min). Following this the oligomycin was injected using port A. Oligomycin inhibits ATP synthase and causes a drop in OCR which reflects the amount of oxygen consumed to produce ATP (Figure 3.2) (Chacko, 2013). The addition of this compound also causes a change in ECAR in response to the inhibition of ATP synthase, a component required for oxidative phosphorylation, and this change in ECAR reflects glycolytic capacity. Three measurement cycles were then taken (mix 2 min, wait 2 min, measure 2 min) prior to the injection of port B (FCCP) after which three more readings of measurement cycles were obtained. The addition of FCCP uncouples the mitochondria from the electron transport chain and maximises respiration (Figure 3.2) (Chacko, 2013). Finally, antimycin-A and rotenone were added through port C. These compounds inhibit complex I and II on mitochondria to cease respiration completely, after which two measurement cycles were taken (mix 2 min, wait 2 min, measure 2 min) (Figure 3.2) (Chacko, 2013). From this data parameters such as baseline respiration, ATP production, maximal respiration, proton leak, spare capacity and glycolytic capacity can be calculated from the change in OCR and ECAR (Figure 3.2).

3.2.10.7 Normalisation to total cellular DNA

In order to compare metabolic measurements between cell samples, normalisation of the OCR and ECAR data was necessary. Thus, after completion of the metabolic analyses on the SeahorseXF24 the media was removed from each of the wells and the plate was stored at -80ºC.

The measurements obtained from the SeahorseXF24 were normalised to DNA content using a CyQUANT® cell proliferation assay kit (Invitrogen, Paisley, UK) as per the manufacturer's instructions. Lysis buffer was prepared using 19mL of solution containing 180mM NaCl in 1mM of EDTA and 1mL of CyQUANT® cell lysis buffer.

5mL of this lysis buffer was taken and 100µL of RNase A (Qiagen, Manchester, UK) was added. 100µL of this final solution was added per well of the plate and left on the orbital shaker for 1 hour at room temperature to extract DNA. After this lysis step, the lysed cells were transferred to pre-designated wells of a blacked out 96 well plate and diluted 1:10 with lysis buffer without RNase A. DNA concentration in the cell lysis samples was determined using a standard curve for DNA content (0, 10, 50, 100, 200, 400, 800, 1000 ng/mL), also made up with lysis buffer without RNase A. Following this, dye solution was added to each well in a 1:1 dilution and this was left for 2 minutes prior to measurement on the POLARstar Omega plate reader (BMG LABTECH, Germany). Fluorescence measurements were taken where an excitation wavelength of 508nm and emission wavelength at 520nm was used.

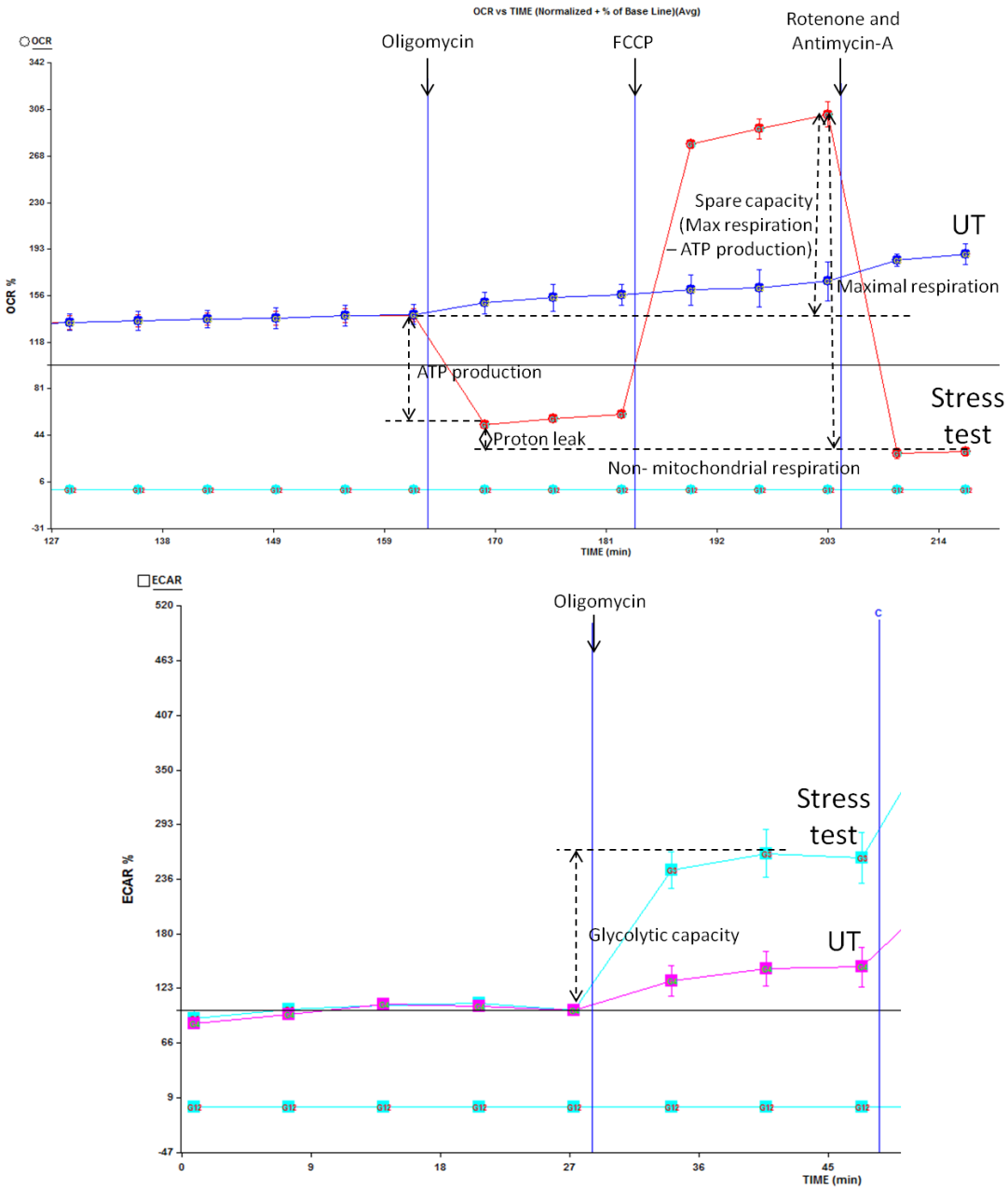

Figure 3.2: Parameters calculated in response to mitochondrial stressors. The sequential addition of oligomycin, FCCP and rotenone and antimycin-A causes characteristic changes in % oxygen consumption rate (OCR) (pMoles/min). Using these measurements parameters such as baseline respiration, ATP production, maximal respiration, proton leak and spare capacity can be determined. Change in % extracellular acidification rate (ECAR) (mpH/min) enables the calculation of glycolytic capacity.

3.2.11 Quality assurance

To ensure confidence in Western blot analysis of fibroblasts during co-culture, a quality assurance system was developed to detect contamination of CLL cells within fibroblast cell preparations. This was done by assessing the presence of IgM. CLL cell lysate was used as a positive control.

For the Fluidigm Biomark™ array a sample of reference RNA was used as a positive control to test the efficiency of the assay. This was denoted as HqPCR and MqPCR. As a negative control genomic DNA was used (HgDNA and MgDNA).

In addition to this the quality assurance steps taken in section 2.2.10 were also taken.

3.2.12 Statistical analysis

Statistical analyses were performed using GraphPad Prism (Version 6.01, GraphPad Software Inc., CA, USA). The statistical tests used are identified when and where they are used within the results section of this chapter. A *P* value of $P = <0.05$ was considered to be statistically significant.

3.3 RESULTS

3.3.1 MCT -1 and -4 expression in CLL cells following co-culture with CD40 ligand (CD40L) expressing fibroblasts

Various *in vitro* models have been developed to mirror the interactions which occur *in vivo* between CLL cells and the microenvironment (Hamilton et al., 2012). As such, CLL cells can be maintained in co-culture with cell lines such as parental fibroblasts as well as fibroblasts which express CD40L to simulate the role of T helper cells (Patten et al., 2008). This system was chosen to investigate the effects of such interaction on expression MCT -1 and -4 in CLL cells.

CD40L and parental fibroblasts were regularly assessed to insure cell line integrity. Figure 3.3 shows how flow cytometry was used to confirm the presence or absence of CD40L on the CD40L fibroblasts and the parental fibroblasts respectively. Use of these fibroblast lines was done in lots. Fibroblasts from a frozen aliquot were grown to confluence in several T75 tissue culture flasks, the cells would be removed and irradiated and frozen down again for subsequent use in co-culture experiments. This approach kept the passage number of the fibroblast lines low, and, in this way, experimental consistency could be maintained.

For co-culture experiments CLL cells were incubated with irradiated CD40L or parental fibroblasts, and, following co-culture for 48 hours, the CLL cells were harvested and MCT -1 and -4 expression was assessed using Western blot analysis. Figure 3.4 shows that co-culture of CLL cells with either CD40L or parental fibroblasts induces increased expression of MCT1 compared to non-co-cultured CLL cells (n = 3). However, CD40 ligation did not seem to induce further expression of MCT1 on the CLL cells (Figure 3.5). There was variability between samples, but overall there was no significant change as assessed by a Wilcoxon matched-pairs signed rank test ($P = 0.0938$) (n = 6).

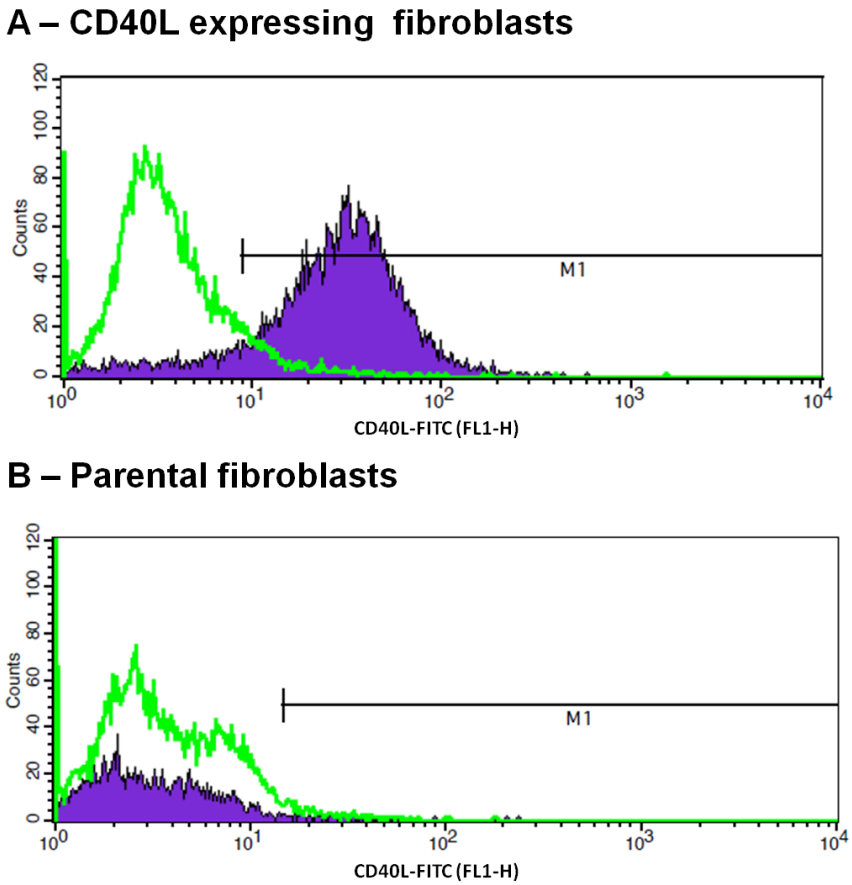

Figure 3.3: Confirmation of CD40L expression in fibroblasts using flow cytometry. **(A)** CD40L fibroblasts are shown to express CD40L. **(B)** Parental fibroblasts are shown to be negative for CD40L. The green histogram is associated with isotype control antibodies, whereas the purple histogram is associated with CD40L antibodies. M1 shows cells selected as being positive for CD40L expression.

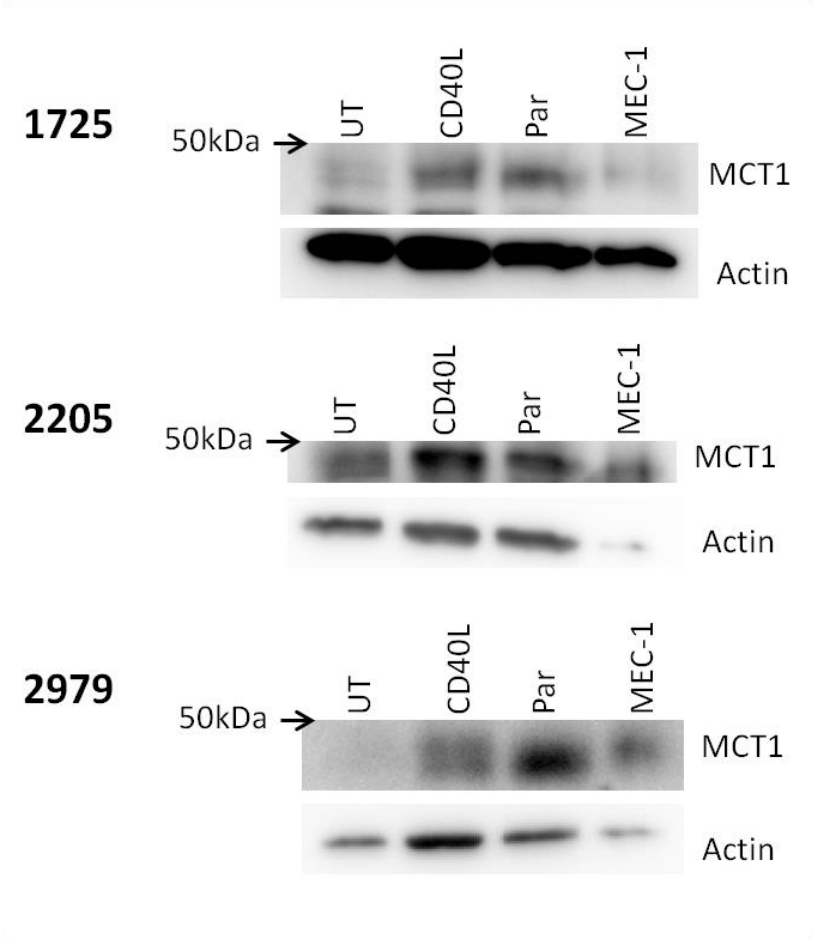

Figure 3.4: MCT1 expression in CLL cells co-cultured with CD40L and parental fibroblasts. Western blot analysis of MCT1 and actin expression in whole cell lysates prepared from CLL cells co-cultured with CD40L and parental (Par) fibroblasts, or cultured in their absence (UT). As a positive control, whole cell lysates of MEC-1 cells was included. The MCT1 antibody used for these blots is AZ5565 (1:1000). Blots were probed with mouse monoclonal anti-β-actin (clone AC-74) as a control to ensure equal protein loading.

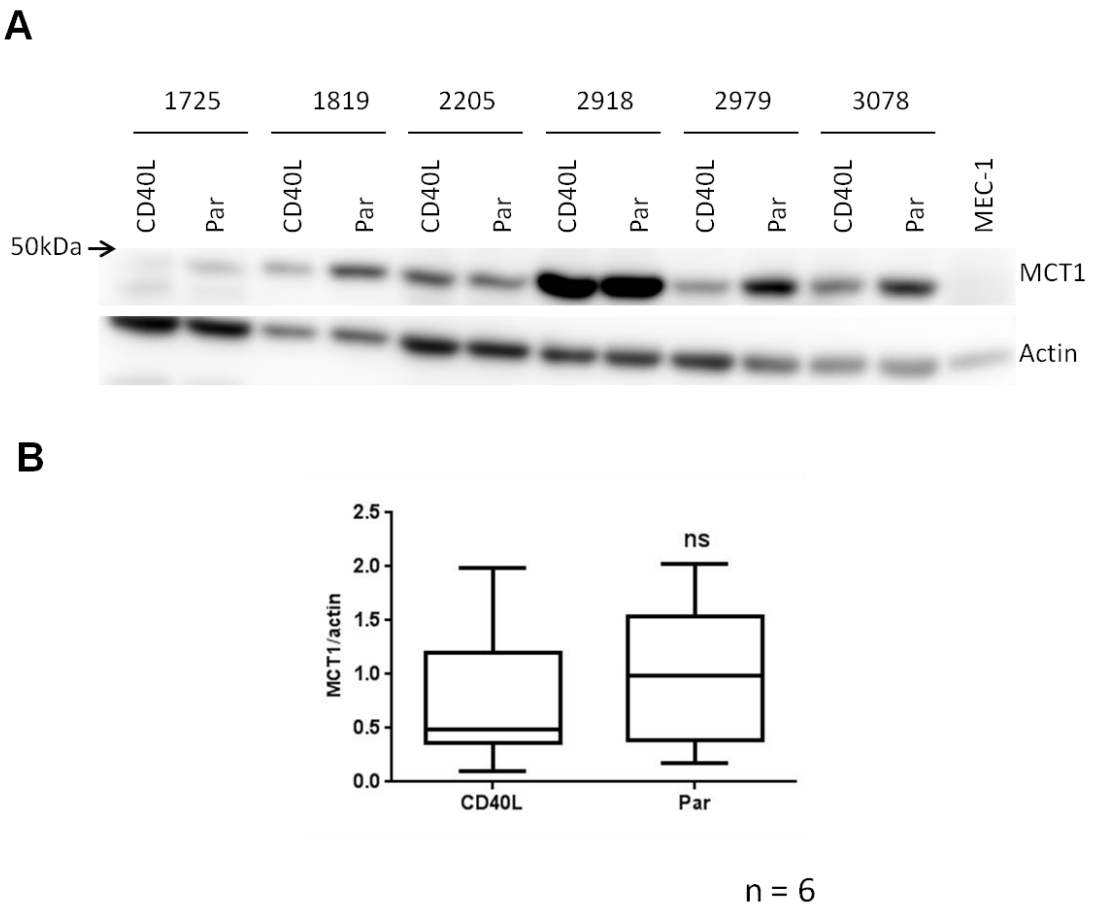

Figure 3.5: MCT1 expression is not induced in CLL cells following CD40L stimulation. The malignant cells from 6 cases of CLL were co-cultured with CD40L and parental (Par) fibroblasts for 48 hours. **(A)** Western blot analysis of whole CLL cell lysates for the indicated proteins. MCT1 expression was detected using mouse monoclonal anti-MCT1 (H-1) (sc-365501) (1:1000) (Insight Biotechnology, Wembley, UK). A MEC-1 cell lysate was used as a positive control for MCT1. Blots were probed with mouse monoclonal anti-β-actin (clone AC-74) as a control to ensure equal protein loading. **(B)** Graphical representation of the data shown in part **(A)**. MCT1 expression was determined as a densitometric ratio of MCT1:actin. A Wilcoxon matched-pairs signed rank test revealed there to be no significant difference in MCT1 expression between the groups ($P = 0.0938$).

With respect to MCT4 expression, there seemed to be no difference between control CLL cells and CLL cells co-cultured with parental fibroblasts (Figure 3.6). However, CLL cells co-cultured with CD40L fibroblasts show a distinct upregulation of MCT4 (Figure 3.6), a finding that is verified in Figure 3.7 which shows there is significant change in MCT4 expression on CLL cells co-cultured on CD40L fibroblasts compared to those cultured on parental fibroblasts (* $P = 0.0313$, n = 6, Wilcoxon matched-pairs signed rank test).

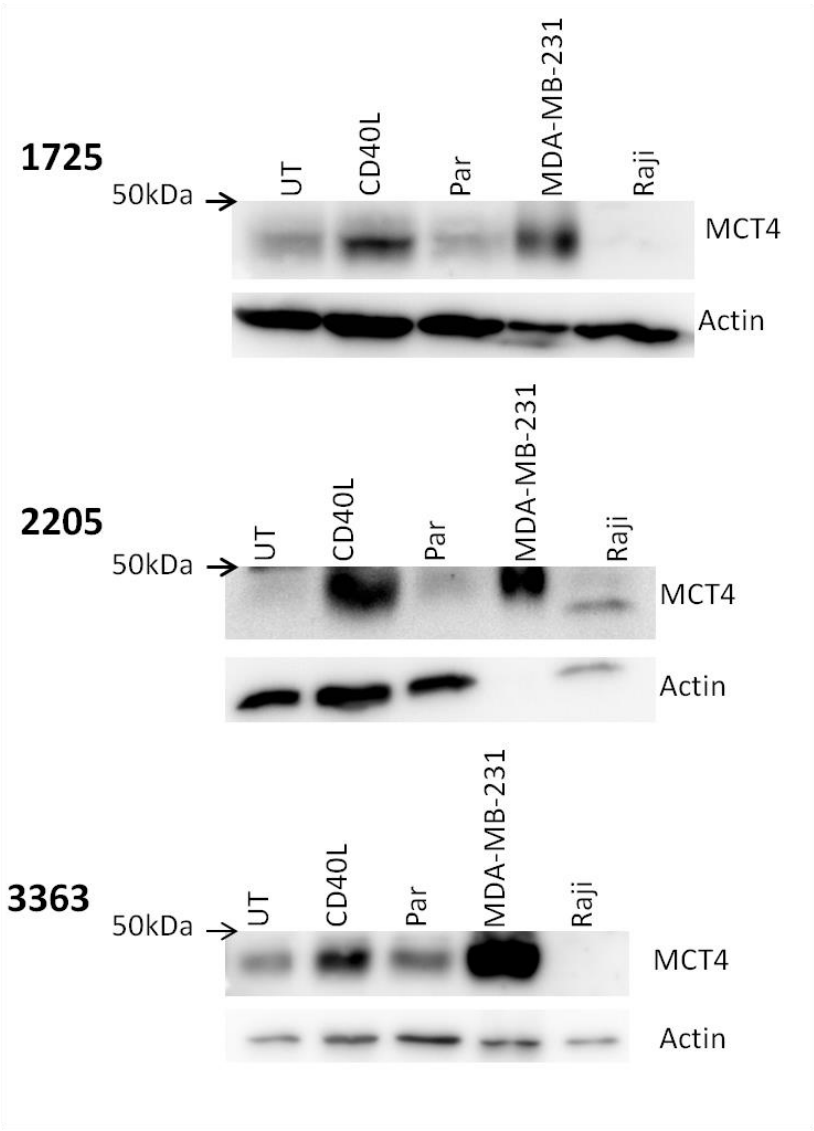

Figure 3.6: MCT4 expression in CLL cells following co-cultured with CD40L and parental fibroblasts. Western blot analysis of MCT4 and actin expression in whole cell lysates prepared from CLL cells co-cultured with CD40L and parental (Par) fibroblasts, or cultured in their absence (UT). As a positive control, whole cell lysates of MDA-MB-231 cells was included. As a negative control, whole cell lysates of Raji cells was included. The MCT4 antibody used for these blots is a rabbit polyclonal anti-MCT4 (HS-90) (sc-50329) (1:1000) (Insight Biotechnology, Wembley, UK). Blots were probed with mouse monoclonal anti-β-actin (clone AC-74) as a control to ensure equal protein loading.

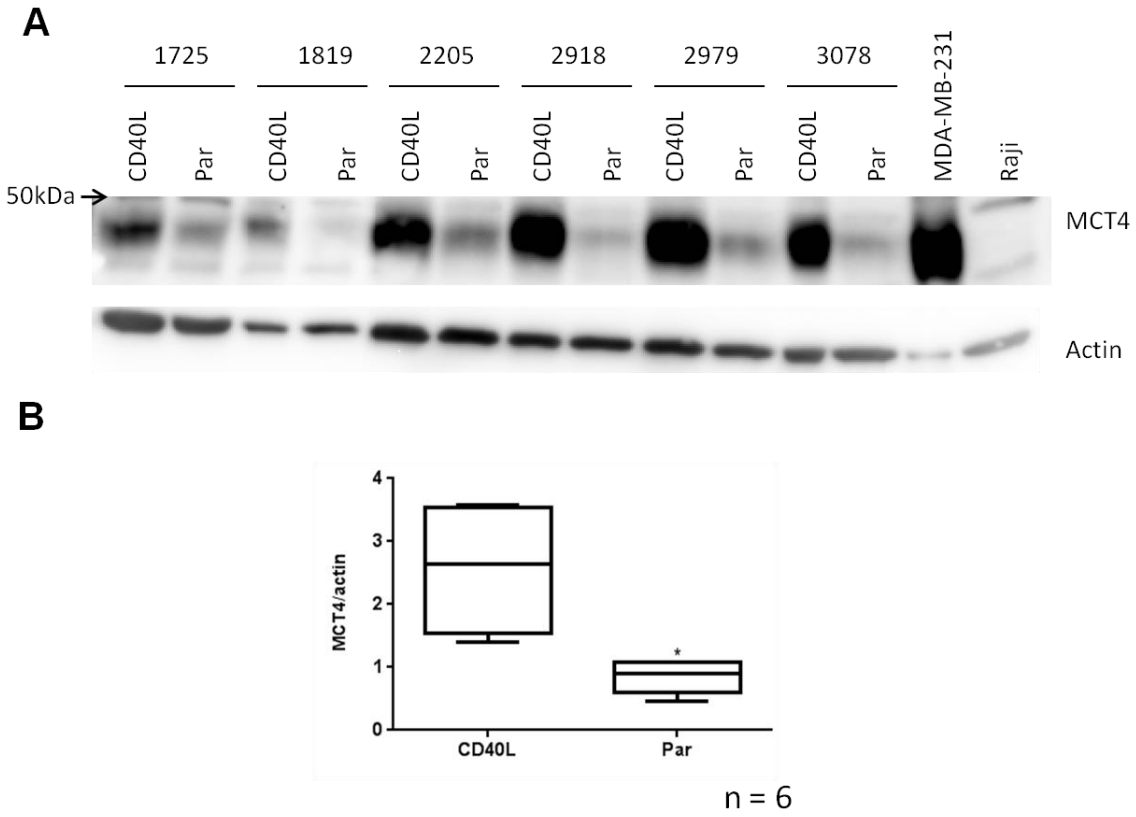

Figure 3.7: MCT4 expression in CLL cells following CD40L stimulation. The malignant cells from 6 cases of CLL were co-cultured with CD40L and parental (Par) fibroblasts for 48 hours. **(A)** Western blot analysis of whole CLL cell lysates for the indicated proteins. MCT4 expression was detected using sc-50329. A MDA-MB-231 cell lysate was used as a positive control for MCT4. Blots were probed with mouse monoclonal anti-β-actin (clone AC-74) as a control to ensure equal protein loading. **(B)** Graphical representation of the data shown in part **(A)**. MCT4 expression was determined as a densitometric ratio of MCT4:actin. A Wilcoxon matched-pairs signed rank test revealed there to be a significant difference in MCT4 expression between the groups (* $P = 0.0313$).

3.3.2 MCT -1 and -4 expression in CLL cells following incubation with soluble CD40 ligand (sCD40L)

Hypoxia has been shown to regulate MCT -1 and -4 expression on cells, causing MCT1 levels to decrease and MCT4 expression to increase (Kennedy and Dewhirst, 2010b, Gallagher et al., 2007). To determine that the effects on MCT-1 and -4 observed on CLL cells exposed to CD40L fibroblasts was not an artefact of hypoxia, soluble CD40L (sCD40L) was used.

CLL cells were incubated with increasing concentrations (100, 200, and 400ng/mL) of sCD40L plus enhancer for a 24 hour period. This concentration range and incubation time were selected based on previous work in this laboratory examining the effect of sCD40L stimulation on vascular endothelial growth factor (VEGF) expression (Farahani et al., 2005). Figure 3.8 shows that there is no difference in MCT1 expression on untreated or sCD40L-stimulated CLL cells. With respect to MCT4, there appeared to be an increase in expression of this protein using the highest concentration of sCD40L (Figure 3.9 (A)). Repeat experiments using different CLL cases showed a similar effect, (Figure 3.9 (B)), but quantitation failed to show significant change (Figure 3.9 (C), P = 0.2500 Wilcoxon matched–pairs signed ranks test).

3.3.3 CD147 expression following stimulation with CD40 ligand (CD40L)

CD147 is a chaperone of MCT-1 and -4 membrane expression (Kirk et al., 2000). Considering that incubation of CLL cells with CD40 expressing fibroblasts upregulates only MCT4, it seemed logical to assume that any increase in MCT4 expression would be accompanied by concomitant increase in CD147. This notion was investigated by flow cytometry. Figure 3.10 shows that there was no change in CD147 expression between untreated CLL cells and CLL cells cultured on parental fibroblasts. However, culture of CLL cells on CD40L fibroblasts resulted in a significant increase in CD147 expression compared to either untreated CLL cells (*** P = 0.0005) or CLL cells cultured on parental fibroblasts (**** P = <0.0001). These data indicate that CD147 expression on CLL cells can be used as a surrogate marker of MCT4 upregulation in subsequent experiments analysing gene expression.

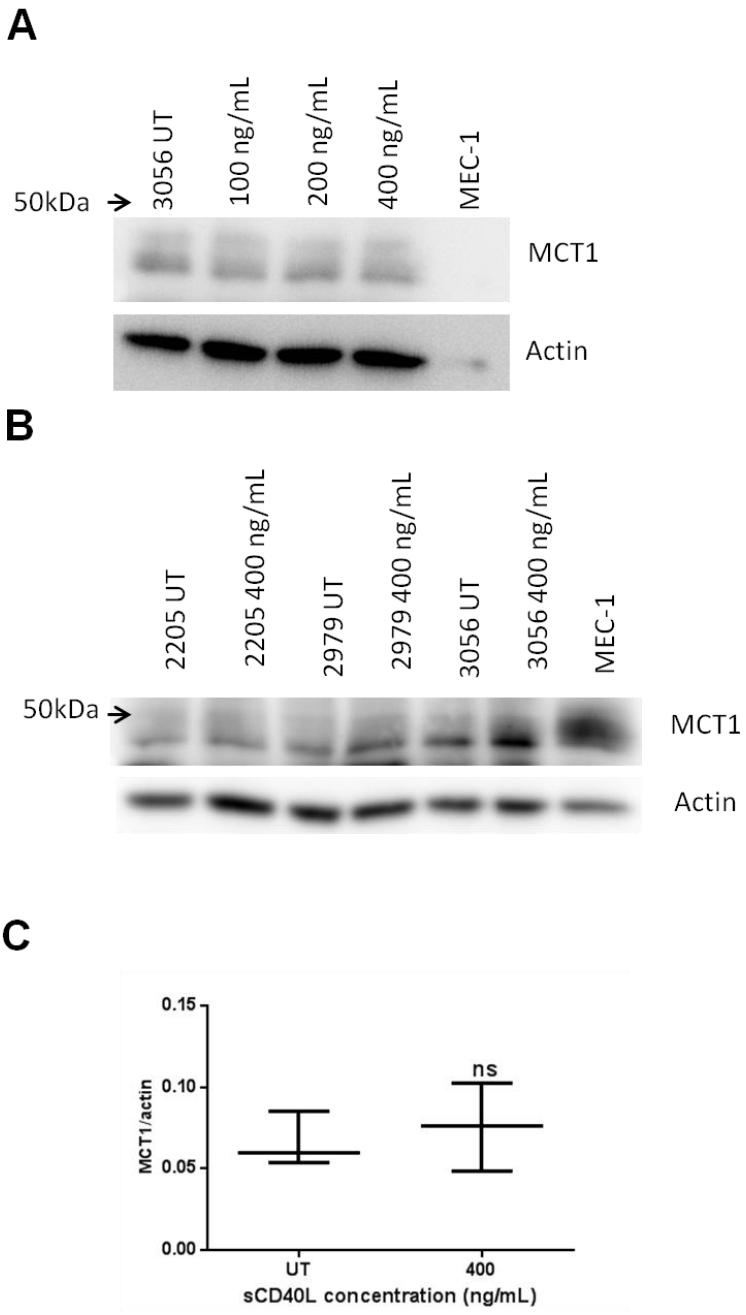

Figure 3.8: MCT1 expression following treatment with sCD40L (24hrs). A) CLL cells were treated with increasing concentrations of sCD40L (100, 200 and 400ng/mL) for 24 hours. **(B)** Malignant cells from 3 cases of CLL treated with 400ng/mL of sCD40L. For **(A)** and **(B)** MCT1 was detected using mouse monoclonal anti-MCT1 (sc-365501) (1:1000) (Insight Biotechnology, Wembley, UK) in whole cell lysates using Western blotting. A MEC-1 cell lysate was used as a positive control. Blots were

probed with mouse monoclonal anti-β-actin (clone AC-74) as a control to ensure equal protein loading. **(C)** Graphical representation of the data shown in part **(B)**. MCT1 expression was determined as a densitometric ratio of MCT1:actin. A Wilcoxon matched–pairs signed ranks test showed no significant difference in MCT1 expression in UT versus CLL cells treated with 400ng/mL sCD40L ($P = 0.5000$).

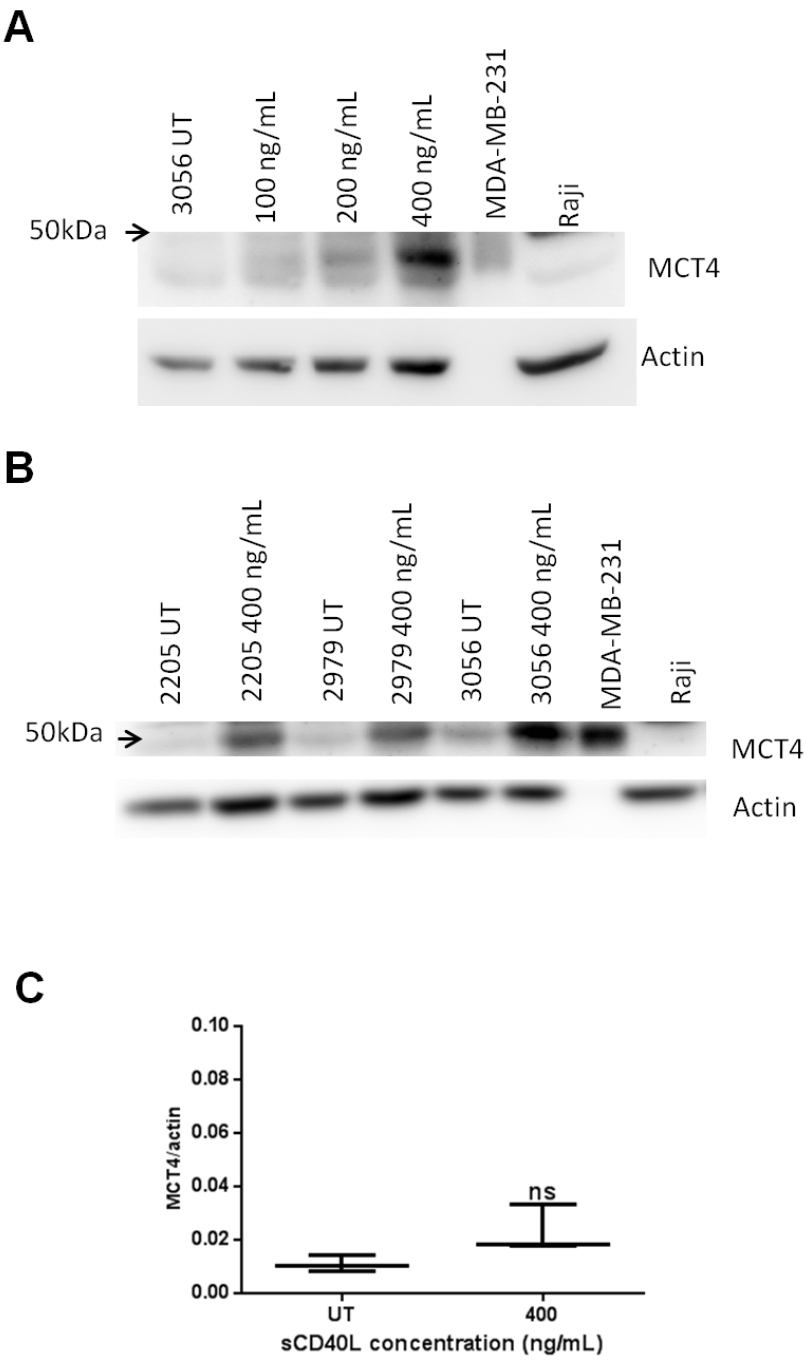

Figure 3.9: MCT4 expression following treatment with sCD40L (24hrs). (A) CLL cells were treated with increasing concentrations of sCD40L (100, 200 and 400ng/mL) for 24 hours. **(B)** Malignant cells from 3 cases of CLL treated with 400ng/mL of sCD40L. MCT4 was detected using rabbit polyclonal anti-MCT4 (sc-376101) (1:1000) (Insight Biotechnology, Wembley, UK) in whole cell lysates using Western blotting.

MDA-MB-231 and Raji cell lysates were used as positive and negative controls respectively. Blots were probed with mouse monoclonal anti-β-actin (clone AC-74) as a control to ensure equal protein loading. **(C)** Graphical representation of the data shown in part **(B)**. MCT4 expression was determined as a densitometric ratio of MCT4:actin. A Wilcoxon matched–pairs signed ranks test showed no significant difference in MCT4 expression in UT versus CLL cells treated with 400ng/mL sCD40L ($P = 0.2500$).

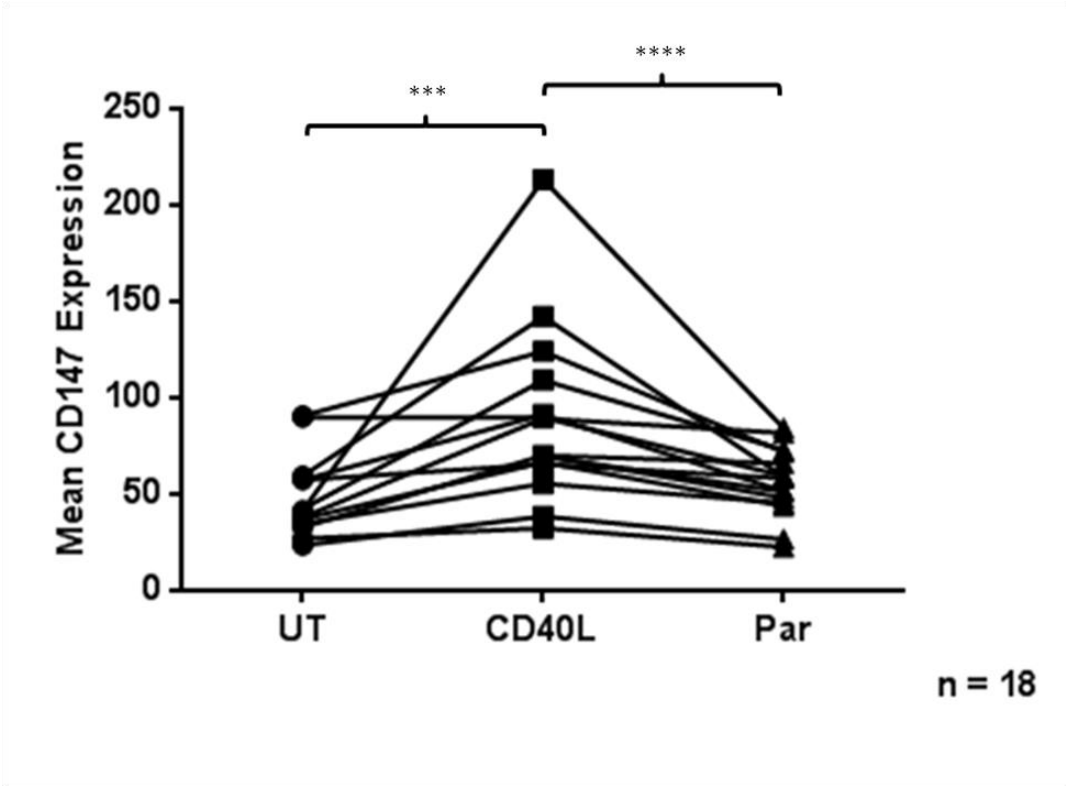

Figure 3.10: CD147 levels following co-culture of CLL cells on CD40L and parental fibroblasts. CD147 levels were measured on 18 cases of CLL following co-culture using flow cytometry. CLL cells were gated as CD5+, CD20+, and CD23+. Statistical analyses revealed there to be a significant increase in the mean CD147 expression following the incubation of CLL cells with CD40L fibroblasts in comparison to untreated cells (*** $P = 0.0005$). The same was true when comparing cells co-cultured with parental fibroblasts versus co-culture with CD40L fibroblasts (**** $P = < 0.0001$). Untreated CLL cells compared to CLL cells co-cultured on the parental (Par) fibroblasts showed no significant difference in mean CD147 expression ($P = 0.2163$).

3.3.4 MCT -1 and -4 mRNA levels following stimulation with CD40L

Following the assessment of protein levels for both MCT-1 and -4, qRT-PCR was used to evaluate whether any change observed was also seen at the mRNA level. GAPDH expression was chosen as a reference gene in preference to actin because expression of the latter gene appeared to vary less between CLL cells cultured on parental fibroblasts and CLL cells cultured on CD40L fibroblasts (Figure 3.11). However, both housekeeping genes appeared to have increased Ct values in untreated CLL cells compared to fibroblast co-cultured CLL cells. As such, only co-cultured CLL cells were considered for future experiments.

qRT-PCR analysis of MCT-1 and -4 mRNA levels show that co-culture of CLL cells with CD40L fibroblasts does not stimulate gene expression of these proteins (Figure 3.12). In fact, mRNA levels of both MCT-1 and -4 were reduced by co-culture of CLL cells with CD40L fibroblasts. CD147 expression was used as a marker to insure activation of the CD40L-stimulated cells (data not shown). This suggests that upregulation of MCT4 protein in CLL cells co-cultured with CD40L fibroblasts is likely to result from post-translational regulation rather than transcriptional regulation of gene expression. However, because there is slight variation in the level of GAPDH for both the CLL cells co-cultured with the CD40L and parental fibroblasts this could have meant changes present in the samples were not observed.

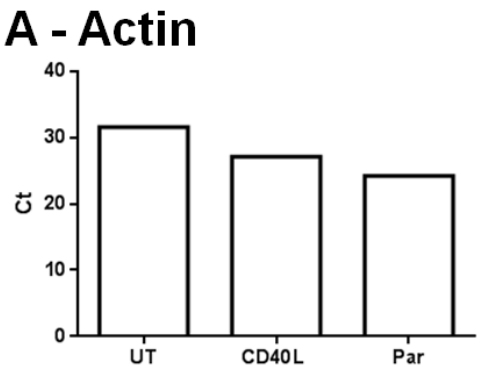

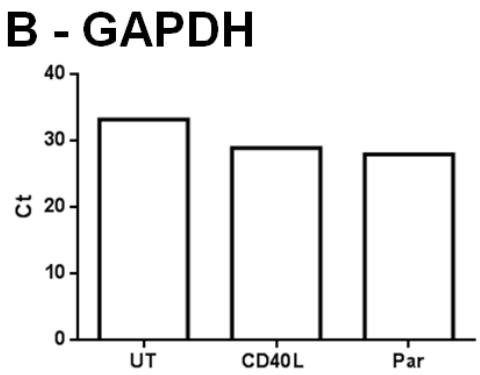

C

	UT (Ct)	CD40L (Ct)	Par (Ct)
Actin	31.54	27.08	24.23
GAPDH	33.23	28.96	27.98

Figure 3.11: Assessing appropriate reference genes for PCR following immobilised CD40L stimulation. CLL cells co-cultured on CD40L fibroblasts (CD40L) and parental (Par) fibroblasts and cultured in the absence of fibroblasts (UT); **(A)** relative to actin, and **(B)** relative to GAPDH. **(C)** Data table showing the Ct values for each candidate control. GAPDH appears to be the most reliable endogenous control with respect to comparing between CLL cells co-cultured on CD40L fibroblasts and those cultured on parental fibroblasts. Comparison with the UT control is not appropriate here due to the large difference in Ct values.

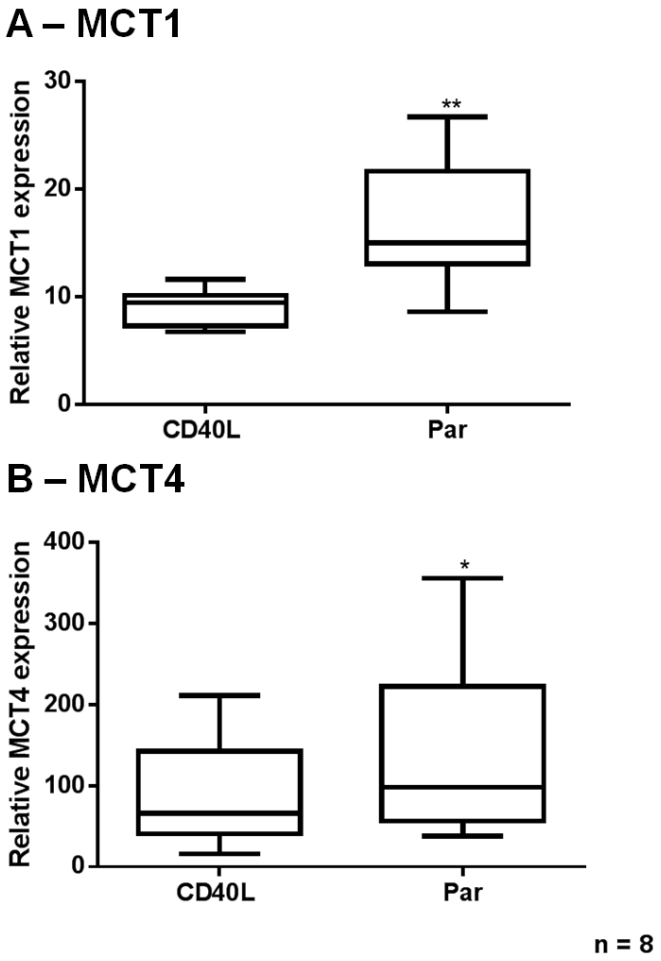

Figure 3.12: MCT -1 and -4 mRNA levels in CLL cells following CD40L stimulation. qRT-PCR analysis of MCT1 **(A)** and MCT4 **(B)** mRNA expression relative to GAPDH in CLL cells following co-culture with CD40L and parental (Par) fibroblasts. The comparison is derived from three technical replicates of n = 8 CLL cases, and is shown as the mean±SEM. A Wilcoxon matched-pairs signed rank test revealed there was a significant change in both MCT 1 (** $P = 0.0078$) and MCT4 mRNA (* $P = 0.0391$).

3.3.5 MCT4 expression in fibroblast cell lines following co-culture with CLL cells

The experiments thus far have examined the influence of fibroblasts on the expression of MCT -1 and -4 in CLL cells. In this section, the effect of CLL cells on MCT -1 and -4 in fibroblasts is assessed.

Figure 3.13 shows that MCT-1 and -4 expression in CD40L and parental fibroblasts is low compared to control cells (MEC-1 and MDA-MB-231 cell lysates). Co-culture of the parental fibroblasts with CLL cells did not affect this low level of expression of either MCT-1 or -4 (Figure 3.14). However, co-culture of CD40L fibroblasts with CLL cells resulted in an increase in MCT4 expression by the fibroblasts (Figure 3.14 (A)). To insure that the induced increase in MCT4 expression was not an artefact of CLL cell contamination, IgM expression in the fibroblast cell lysates was assessed (Figure 3.14 (B)). IgM in CD40L fibroblasts co-cultured with CLL cells was very low in comparison to IgM in CLL cell lysates, suggesting little, if any, gross contamination of the fibroblast lysates with CLL cells. This suggests that metabolic changes may occur in the CD40L fibroblasts in response to co-culture which require enhanced monocarboxylate transport mediated by MCT4.

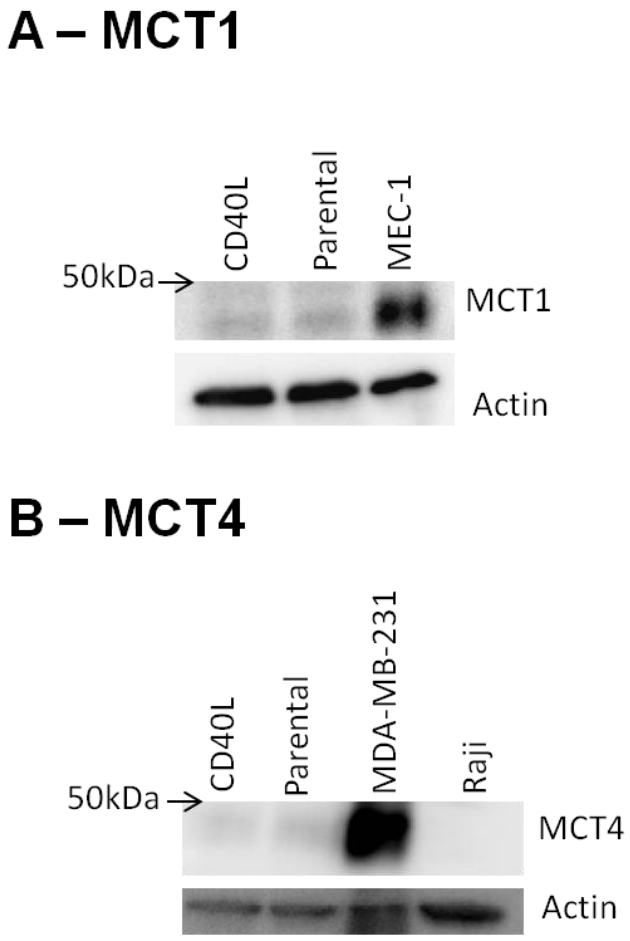

Figure 3.13: MCT -1 and -4 expression in CD40L and parental fibroblasts. Western blot analysis of MCT1 **(A)** and MCT4 **(B)** in cell lysates prepared from CD40L and parental (Par) fibroblast cell lines. MCT1 was detected using AZ5565 while MCT4 was detected using AZ5570. As a positive control for MCT1 expression, whole cell lysates of MEC-1 cells were used in part **(A)**. Whole cell lysates of MDA-MB-231 and Raji cells were used as positive and negative controls for MCT4 expression. Blots were probed with mouse monoclonal anti-β-actin (clone AC-74) as a control to ensure equal protein loading.

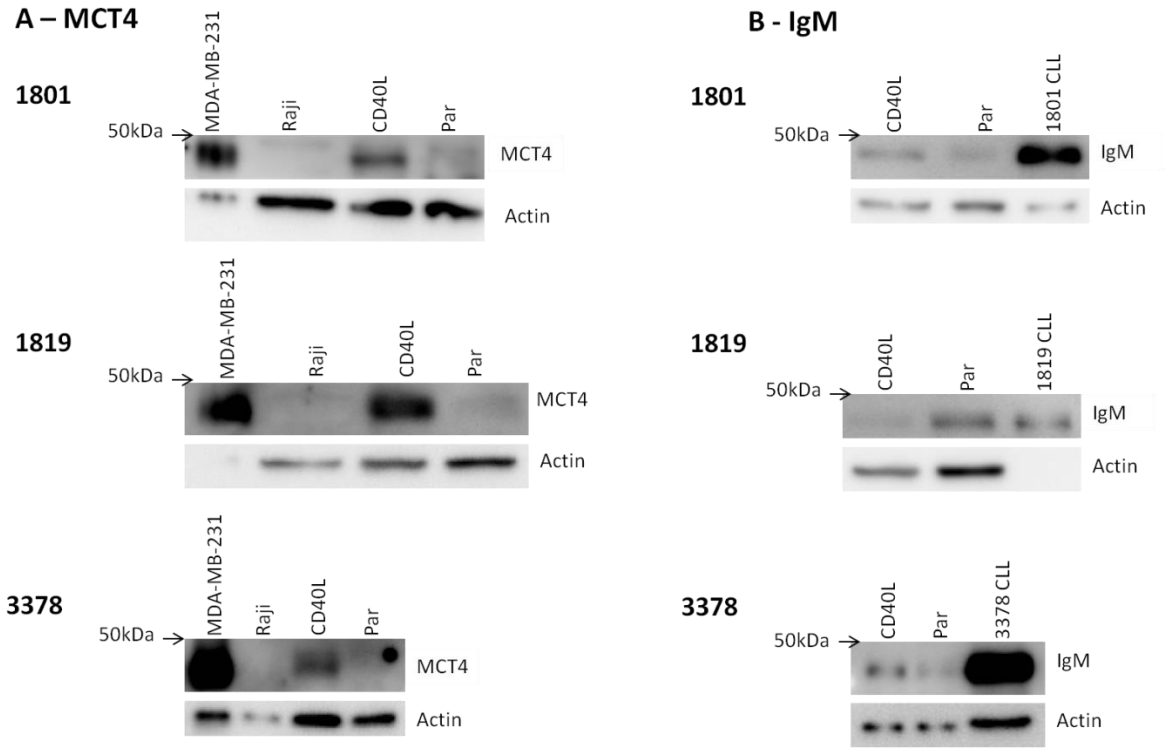

Figure 3.14: MCT4 and IgM expression in fibroblast cell lines following co-culture with CLL cells. Western blot analysis of MCT4 **(A)** and IgM **(B)** in cell lysates prepared from CD40L and parental (Par) fibroblast cell lines which had been in co-culture with CLL cells for 48 hours (as indicated by case adjacent CLL case number). MCT4 was detected using sc-376101 while IgM was detected using goat anti-human IgM (2020-01) (Southern Biotech, Cambridge, UK). Whole cell lysates of MDA-MB-231 and Raji cells were used as positive and negative controls for MCT4 expression in part **(A)**. As a positive control for IgM a UT CLL cell lysate was used. Blots were probed with mouse monoclonal anti-β-actin (clone AC-74) as a control to ensure equal protein loading.

3.3.6 Fluidigm Biomark™ gene array analysis of metabolic gene expression in CLL cells co-cultured with CD40L fibroblasts

Upregulation of MCT4 in CLL cells co-cultured with CD40L fibroblasts implies that there are metabolic changes within CLL cells that require the increased expression of MCT4. To understand this change, gene expression analysis was performed using a Fluidigm Biomark™ chip. The 45 genes profiled in the array are detailed in Table 3.1.

Figure 3.15 shows a heat map of the Ct values for each gene across individual samples i.e. CLL cells co-cultured with CD40L and parental fibroblasts. Amplification data which was not classified as linear was automatically excluded by the Fluidigm Biomark™ Real Time PCR Analysis Software (Version 3.1.3) (indicated by an 'X' on Figure 3.15). Verification that the cDNA synthesis and pre-amplification steps used during sample preparation were successful was performed using human reference RNA (HqPCR, row 1 of array data). This showed that 43 of 45 genes were amplified (Ct <24); the genes which were not, ACACB, and GLUD2 were excluded from further analysis. Human genomic DNA (HgDNA, row 7 of the array data) was used as a negative control for the PCR reaction. Here, 3 genes were amplified (Ct <24), LDHA, ATF4, and PPIA. Whereas LDHA and ATF4 were excluded from further analysis, PPIA was not because the amplification curve for this gene was poor for the HgDNA sample. Moreover, the Ct value (Ct = 19) for PPIA amplified from HgDNA was outside the range obtained for the analysed samples (Ct 10-18) using cDNA, indicating that more PPIA was present in the samples than in the genomic control.

In order to select the most suitable gene for sample normalisation, the expression of 3 housekeeping genes; actin, IPO8 and PPIA was investigated. Figure 3.16 shows the Ct values for these housekeeping genes (n = 14). PPIA was selected as the most appropriate housekeeping gene because the Ct values demonstrated the least variability between CD40L and parental fibroblast co-cultured CLL cells (P = 0.0781, Wilcoxon test). One case of CLL, 2565, failed on the chip (Ct >999) and was excluded from further analysis.

Specificity of the primers used for the Fluidigm chip for human cDNA over mouse cDNA was verified by the inclusion of mouse-only control samples. Here, irradiated CD40L and parental fibroblasts that had not come into contact with CLL cells were used. Two of three preparations of these cells (rows 28 and 29 for CD40L fibroblasts and rows 34 and 35 for parental fibroblasts) showed no or very little amplification, indicating that the primers used are specific for human genes. However, one preparation (row 30 for CD40L fibroblasts and row 36 for parental fibroblasts) showed amplification of the genes used for the chip. One possible explanation is that this preparation was made separately from the other two, and could reflect inadvertent contamination. Nevertheless, it was assumed that the array was specific for human genes based on the results obtained with the first two preparations.

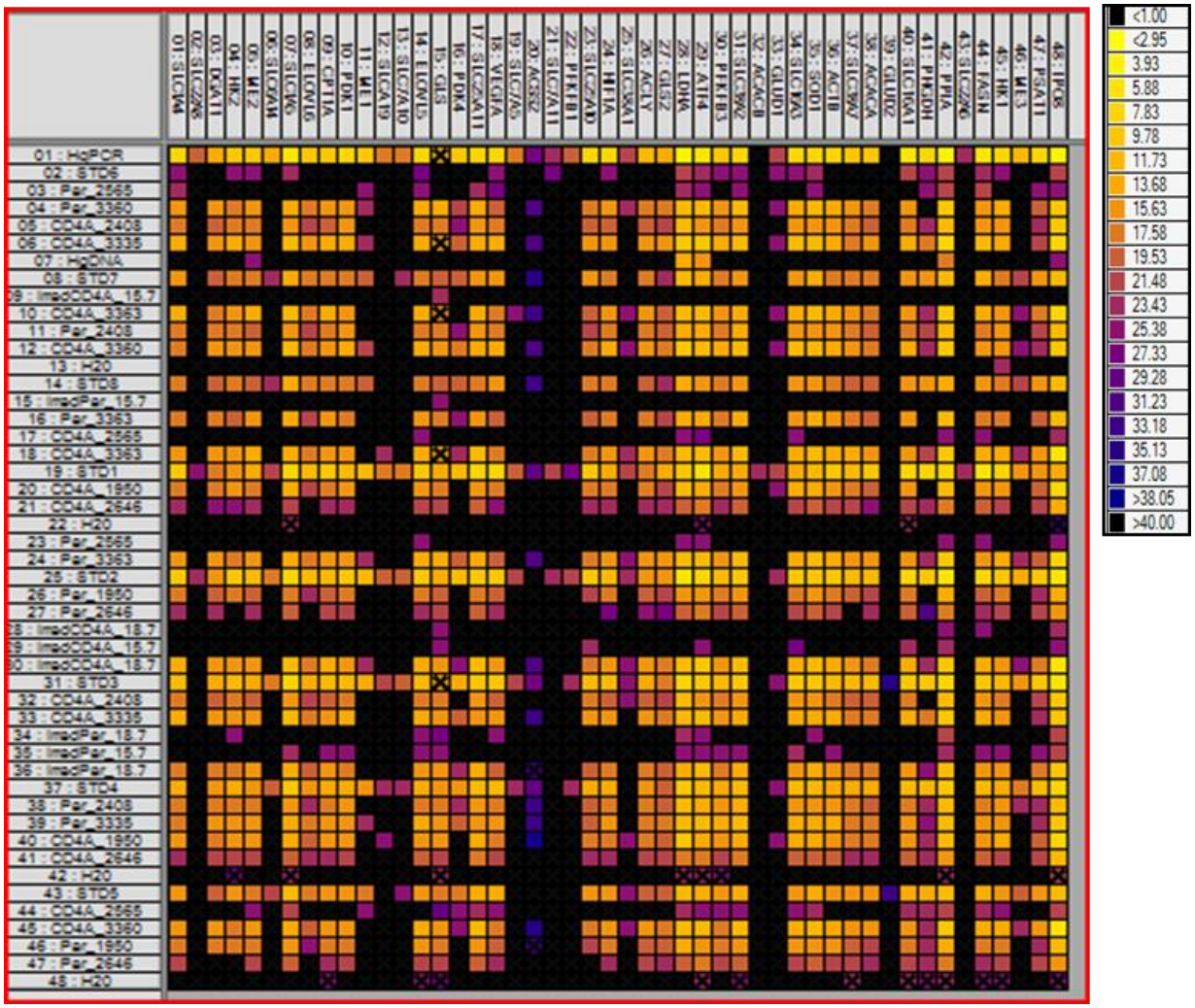

Figure 3.15: Fluidigm Biomark™ chip array for metabolic genes in CLL cells co-cultured with CD40L and parental fibroblasts. Heat map of the Ct values obtained for each gene across individual samples. Amplification data which was not classified as linear was automatically excluded by the Fluidigm Biomark™ Real Time PCR Analysis Software (Version 3.1.3) (indicated by an 'X').

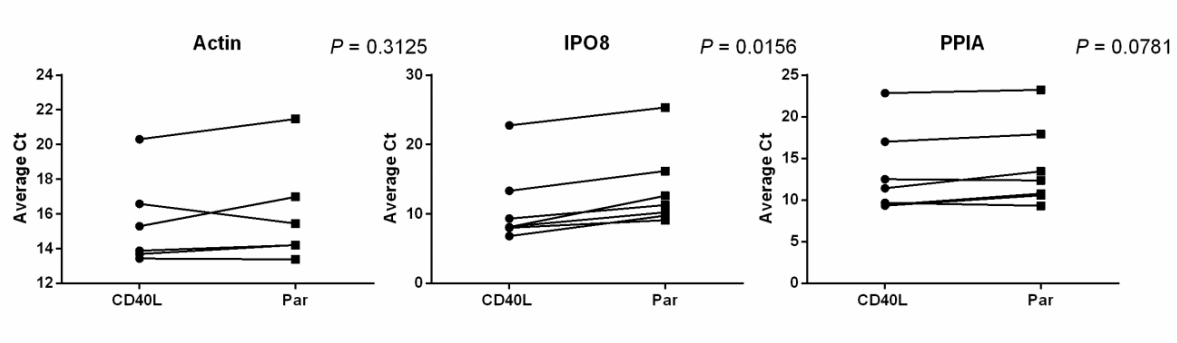

Figure 3.16: Selection of housekeeping genes for Fluidigm Biomark™ chip array in CLL cells co-cultured with CD40L and parental fibroblasts. PPIA was selected as most appropriate housekeeping gene for normalisation of gene expression because it showed the least variability across the samples (P = 0.0781, Wilcoxon test) (n = 14).

After establishing the most appropriate housekeeping gene, relative expression of the genes of interest on the chip relative to PPIA were then calculated and plotted as heat map (Figure 3.17). At this point in the analysis, 11 genes (SLCA19, SLC6A14, SLC7A5, SLC7A10, SLC7A11, SLC22A6, SLC22A8, ACSS2, PFKFB1, ME1 and ME3) out of the original 45 were excluded because they failed to amplify (Ct >999). A further 4 genes (SLC38A1, GLUD1, PDK4 and PHGDH) were also excluded from further analysis because there was less than n = 3 measurements for these genes, making them unsuitable for statistical analyses.

The next step was to assess inter-individual variation between the cases used, and variability under each condition. Figures 3.18 and 3.19 show relative gene expression in CLL cells co-cultured, respectively, with CD40L and parental fibroblasts. Here, dCt is used as a measure of expression (gene of interest relative to housekeeping gene), and low dCt values correspond to higher gene expression. A Kruskal-Wallis test was used to assess the inter-individual variation between cases. In CLL cells co-cultured with CD40L fibroblasts there was no significant inter-individual variation in gene expression except for ATF4 (* $P = 0.0271$), SLC1A4 (* $P = 0.0178$) and SLC25A10 (* $P = 0.0362$). Further post hoc analyses using a Dunn's test for multiple comparisons revealed that this apparent inter-individual variation was not significant ($P = >0.05$). In CLL cells co-cultured with parental fibroblasts there was no significant inter-individual variation in gene expression except for PSAT1 (** $P = 0.0095$) and SLC1A5 (* $P = 0.0381$). Again, post hoc analyses using a Dunn's test for multiple comparisons revealed that this apparent inter-individual variation was not significant ($P = >0.05$).

Taken together, these data suggest that the RNA extraction method yields samples of comparable quality and provides reassurance that the genes have performed reliably and with similar efficiencies. Furthermore, these findings provide confidence that any variation observed in future comparative analyses between CLL cells co-cultured with CD40L fibroblasts versus CLL cells co-cultured with parental fibroblasts will likely be due to differential gene modulation and not experimental variation. Thus, the analysis can now move to comparative study.

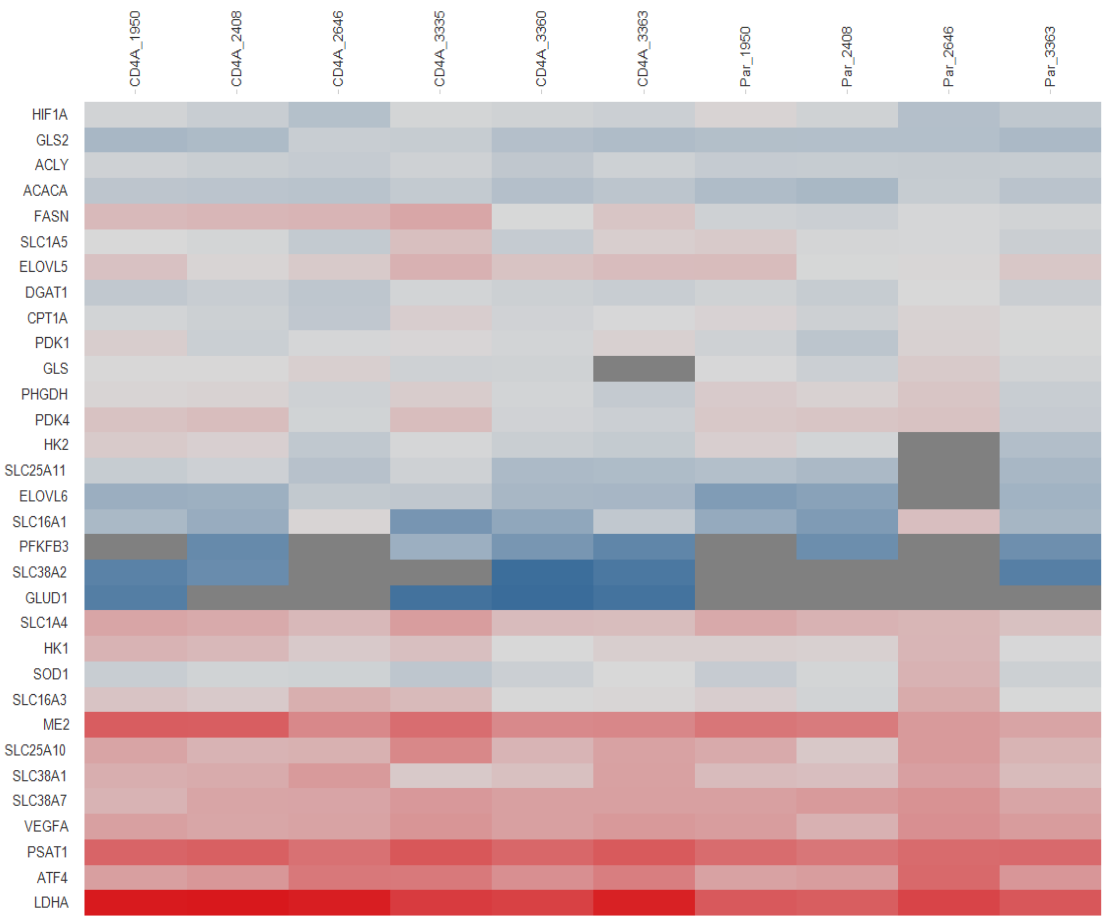

Figure 3.17: Heat map showing gene expression in CLL cells co-cultured with CD40L and parental fibroblasts. Hierarchical clustering of gene expression was performed based upon negative dCt values. Genes with higher levels of expression are coloured red and clustered towards the bottom of the heat map while genes with lower levels of gene expression are coloured blue and clustered towards the top of the heat map.

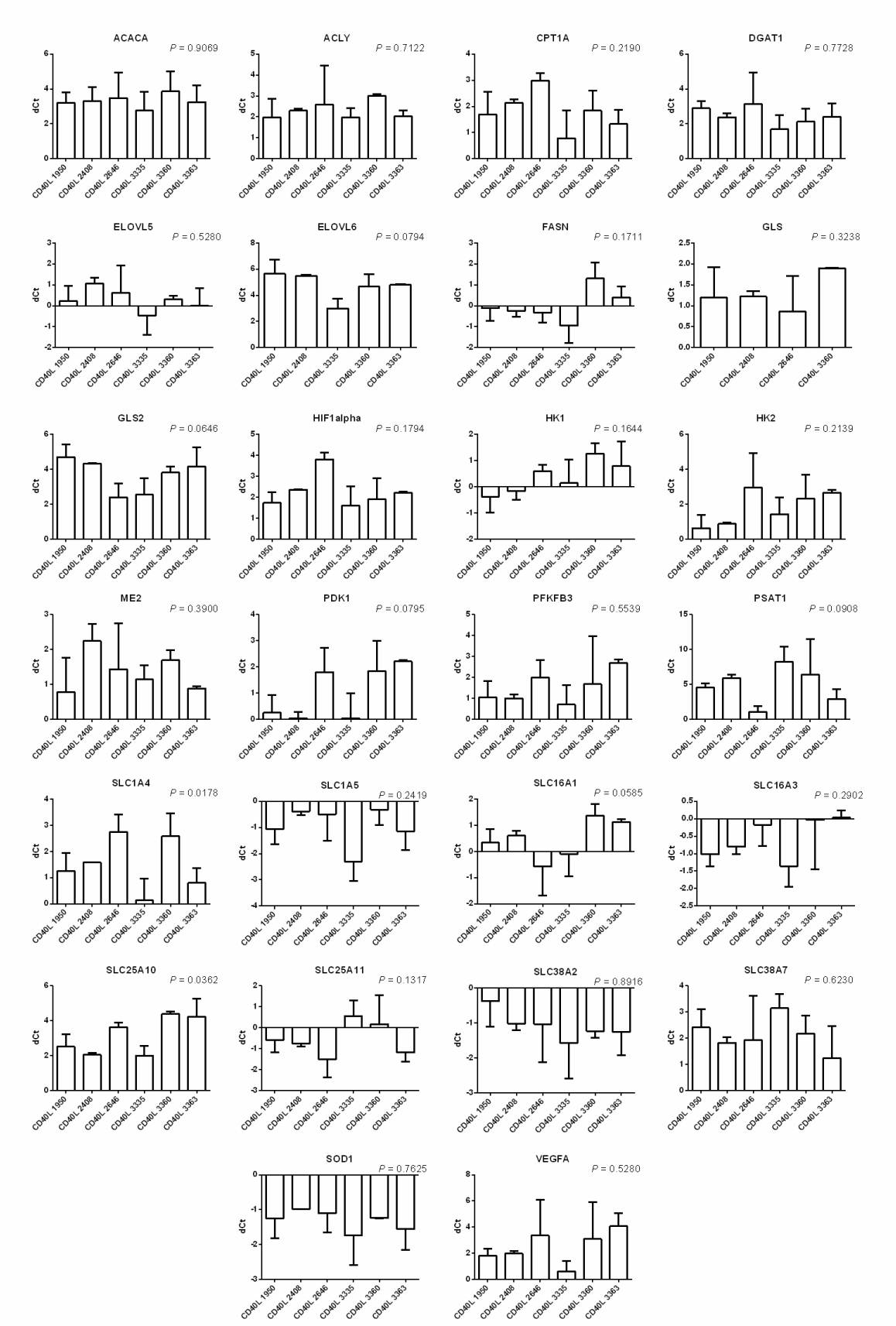
ACACA
P = 0.9069
ACLY
P = 0.7122
CPT1A
P = 0.2190
DGAT1
P = 0.7728
ELOVL5
P = 0.5280
ELOVL6
P = 0.0794
FASN
P = 0.1711
GLS
P = 0.3238
GLS2
P = 0.0646
HIF1alpha
P = 0.1794
HK1
P = 0.1644
HK2
P = 0.2139
ME2
P = 0.3900
PDK1
P = 0.0795
PFKFB3
P = 0.5539
PSAT1
P = 0.0908
SLC1A4
P = 0.0178
SLC1A5
P = 0.2419
SLC16A1
P = 0.0585
SLC16A3
P = 0.2902
SLC25A10
P = 0.0362
SLC25A11
P = 0.1317
SLC38A2
P = 0.8916
SLC38A7
P = 0.6230
SOD1
P = 0.7625
VEGFA
P = 0.5280
dCt
CD40L 1950
CD40L 2408
CD40L 2646
CD40L 3335
CD40L 3360
CD40L 3363

Figure 3.18: Assessing inter-individual variation between CLLs co-cultured with CD40L fibroblasts. Inter-individual variation in genes associated with cell metabolism. Values are relative to PPIA. A Kruskal-Wallis test was used to assess the inter-individual variation between cases. In CLL cells co-cultured with CD40L fibroblasts there was no significant inter-individual variation in gene expression except for ATF4 (* $P = 0.0271$), SLC1A4 (* $P = 0.0178$) and SLC25A10 (* $P = 0.0362$). Further post hoc analyses using a Dunn's test for multiple comparisons revealed that this apparent inter-individual variation was not significant ($P = >0.05$). Error bars are the SEM derived from 3 technical replicates.

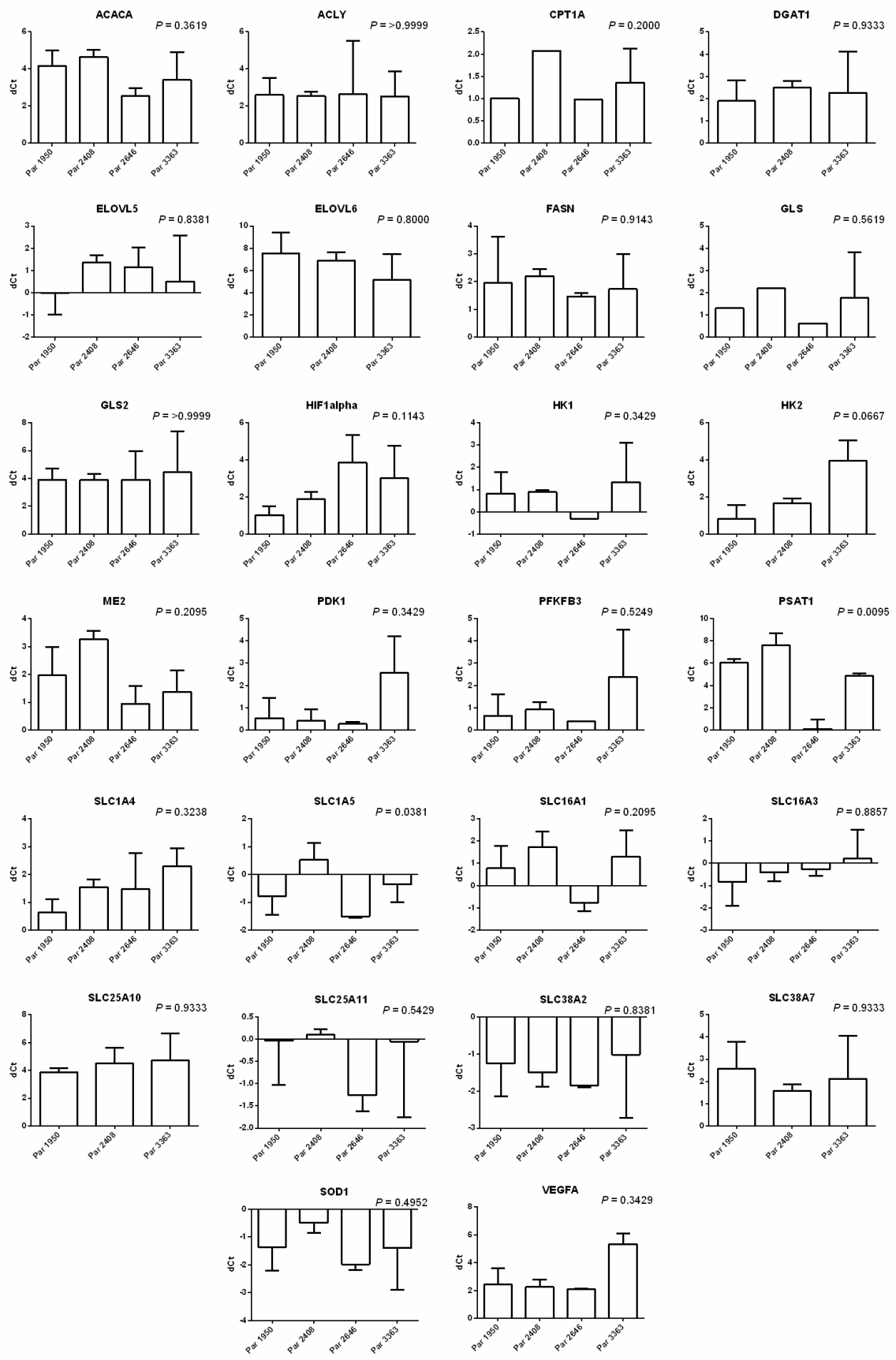
ACACA
P = 0.3619
ACLY
P = >0.9999
CPT1A
P = 0.2000
DGAT1
P = 0.9333
ELOVL5
P = 0.8381
ELOVL6
P = 0.8000
FASN
P = 0.9143
GLS
P = 0.5619
GLS2
P = >0.9999
HIF1alpha
P = 0.1143
HK1
P = 0.3429
HK2
P = 0.0667
ME2
P = 0.2095
PDK1
P = 0.3429
PFKFB3
P = 0.5249
PSAT1
P = 0.0095
SLC1A4
P = 0.3238
SLC1A5
P = 0.0381
SLC16A1
P = 0.2095
SLC16A3
P = 0.8857
SLC25A10
P = 0.9333
SLC25A11
P = 0.5429
SLC38A2
P = 0.8381
SLC38A7
P = 0.9333
SOD1
P = 0.4952
VEGFA
P = 0.3429
dCt
Par 1950
Par 2408
Par 2646
Par 3363

Figure 3.19: Assessing inter-individual variation between CLL co-cultured with parental fibroblasts. Inter-individual variation in genes associated with cell metabolism. Values are relative to PPIA. A Kruskal-Wallis test was used to assess the inter-individual variation between cases. In CLL cells co-cultured with parental fibroblasts there was no significant inter-individual variation in gene expression except for PSAT1 (** $P = 0.0095$) and SLC1A5 (* $P = 0.0381$). Again, post hoc analyses using a Dunn's test for multiple comparisons revealed that this apparent inter-individual variation was not significant ($P = >0.05$). Error bars are the SEM derived from 3 technical replicates.

Figure 3.20 (A) shows a heat map illustrating changes in gene expression in CLL cells co-cultured with CD40L fibroblasts normalised to gene expression in CLL cells co-cultured with parental fibroblasts (parental control) (n = 4). From this figure it was immediately obvious that CLL case 2646 did not behave in the same way as the three other CLL cases. Moreover, the Ct associated with PPIA was higher than the other cases, suggesting insufficient starting material for the assay. Thus, the values associated with this case were excluded from further study.

The values associated with the three remaining CLL cases were then averaged, to produce average linear fold changes [shown in Figure 3.20 (B)]. None of the genes within this panel showed downregulation below a 0.5 fold threshold. Increase in expression was observed for ELOVL6 (* $P = 0.0257$) and FASN (* $P = 0.0385$), these were the only genes where the P value was ≤ 0.05 (Figure 3.21). However, if the P value is raised to ≤ 0.1 it is possible to include ACACA ($P = 0.1$), HK1 ($P = 0.09$), HK2 ($P = 0.1$), ME2 ($P = 0.09$), SLC1A5 ($P = 0.06$), SLC25A11, ($P = 0.06$), and VEGFA, ($P = 0.1$) (Figure 3.21). In keeping with the hierarchical cluster analysis shown in Figure 3.20, all of these genes showed a minimum 1.5 fold increase in expression. Three additional genes, GLS, PSAT1, SLC1A4, SLC16A1 and SLC25A10, were upregulated past this 1.5 fold threshold. For GLS there were only two measurements, and with PSAT1, SLC1A4, SLC16A1 and SLC25A10 the P value associated with the observed increase was greater than 0.1. Although the increased expression observed in these 12 latter genes could not termed significant based on 95% confidence ($P \leq 0.05$) (Figure 3.21), they were still used in pathway analysis to provide insight into global changes in metabolism (Figure 3.22).

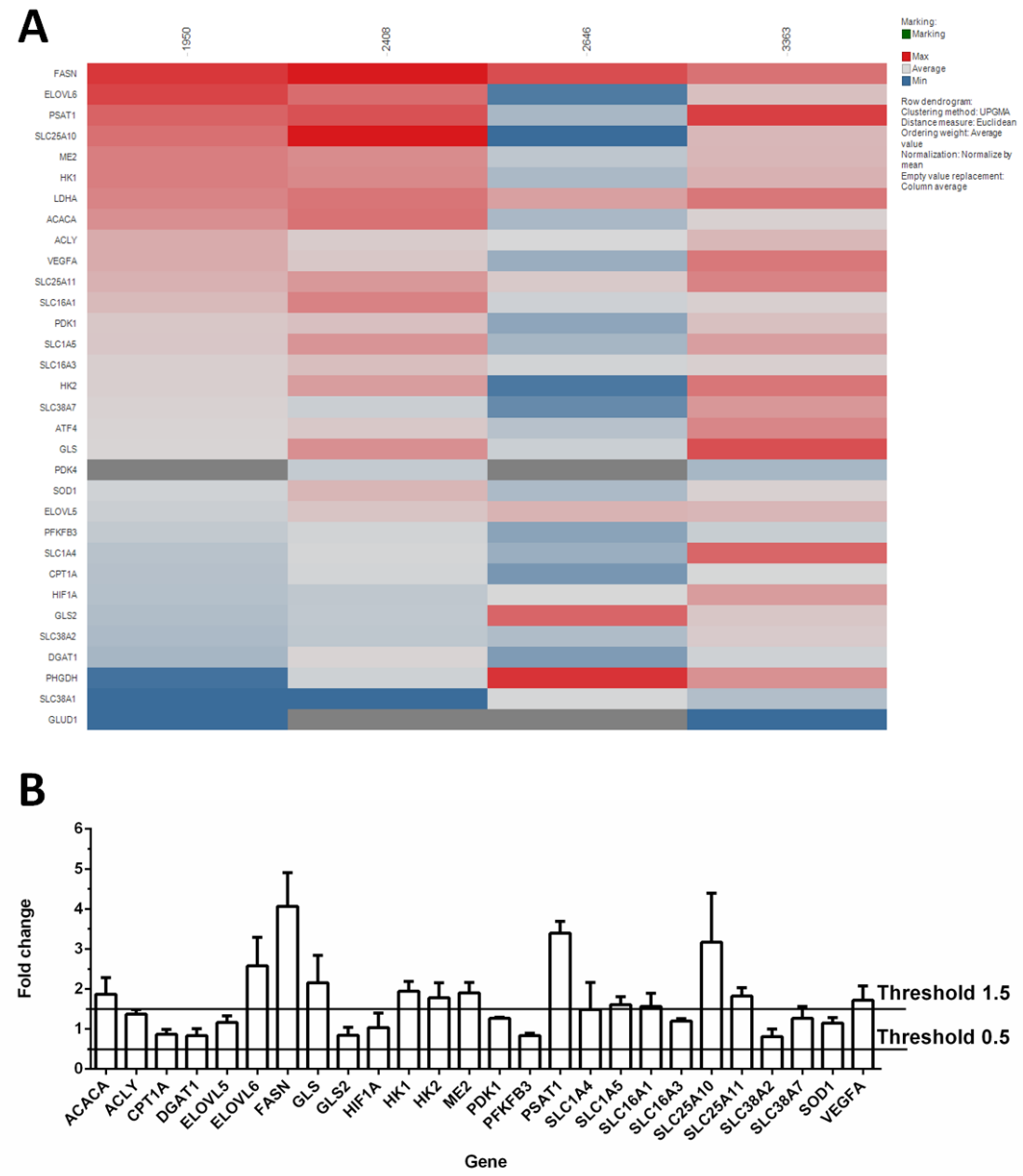

Figure 3.20: Fold change in gene expression in CLL cells in response to CD40L stimulation (n = 4). (A) Hierarchical clustering of gene expression based upon a log 2 fold change. Values were made relative to PPIA and normalised to the parental control. Genes with higher levels of expression are coloured red and clustered towards the top while genes with lower levels of expression are coloured blue and clustered towards the bottom of the heat map. **(B)** Linear fold changes for each case of CLL (n = 3). A fold change of >1.5 indicates increased gene expression. A fold change of <0.5 indicates decreased gene expression. Error bars are the SEM.

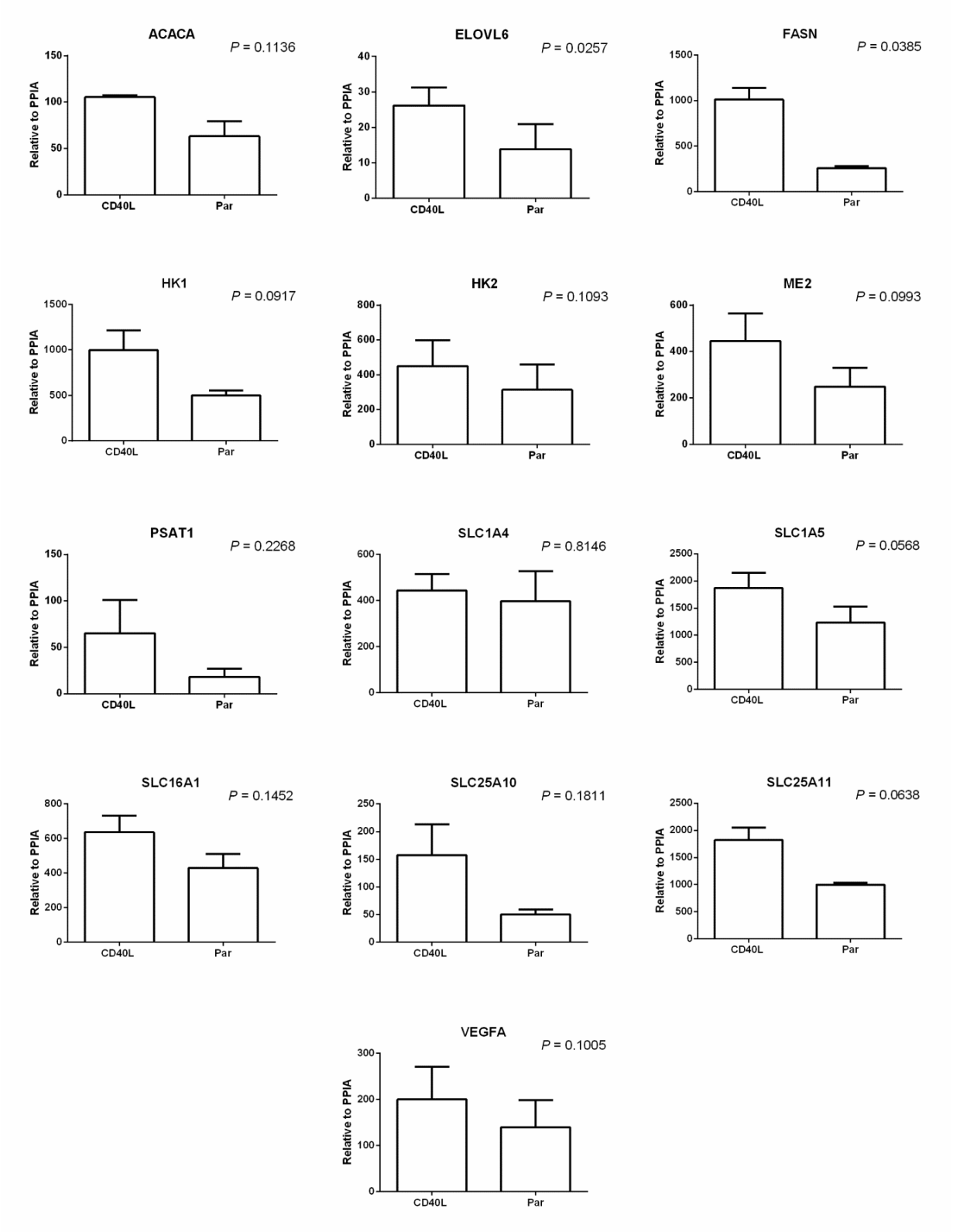

Figure 3.21: Increased gene expression in CLL cells following co-culture with CD40L fibroblasts. Values were made relative to PPIA. A paired t test shows a

significant increase in expression was for ELOVL6 (* $P = 0.0257$) and FASN (* $P = 0.0385$). Error bars are the SEM.

Metabolic pathway analyses are illustrated in Figure 3.23. Co-culture of CLL cells on CD40L fibroblasts appeared to stimulate fatty acid metabolism as indicated by the upregulation of ELOVL6 and FASN, and, to a lesser extent ACACA. Pathways of energy production were also affected because HK1 and HK2, within the glycolysis pathway, and GLS and ME2, within the TCA pathway, were upregulated. Levels of genes involved in amino acid transport (SLC1A4, SLC1A5, SLC25A10, and SLC25A11) and serine metabolism (PSAT1) also increased. Finally, in keeping with a previous observation from this department (Farahani et al., 2005), VEGFA expression was also upregulated by CD40 ligation on CLL cells.

Taken together, these data suggest that there is a global upregulation of metabolic activity in CLL cells exposed to CD40 stimulation. In particular, the upregulation of genes involved in glycolysis support a hypothesis that this pathway is activated in CD40-stimulated CLL cells requiring upregulation of MCT4 protein to mediate lactate transport and prevent cytosolic acidification. However, correction has not been made for the use of multiple statistical testing and validation of this data is required.

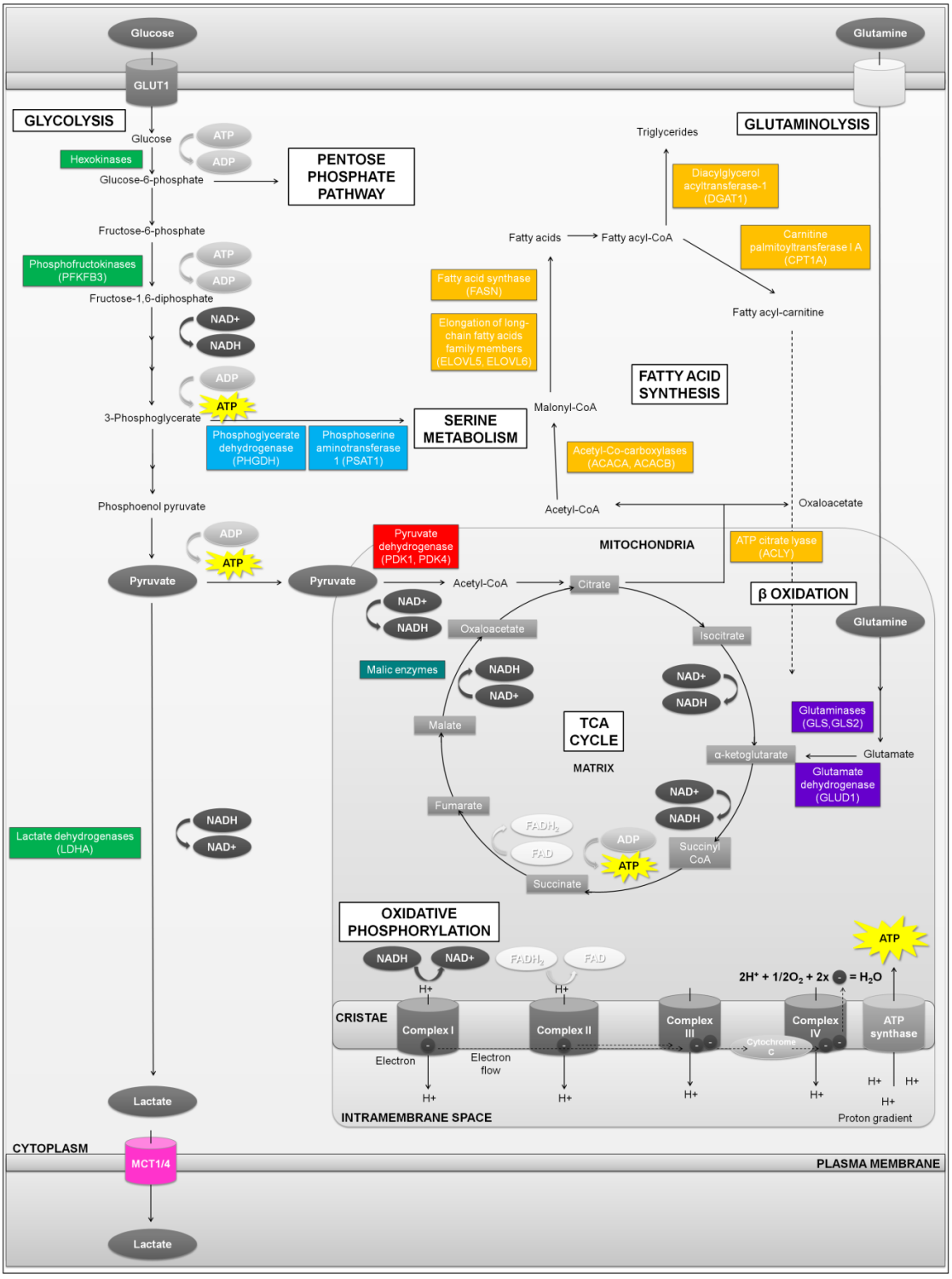

Figure 3.22: Diagrammatic representation of the metabolic pathways investigated using the Fluidigm Biomark™ array. Fatty acid metabolism (orange), glutamine metabolism (purple), glycolysis (green), monocarboxylate transporters (pink), pyruvate metabolism (red), serine metabolism (blue), TCA cycle (teal).

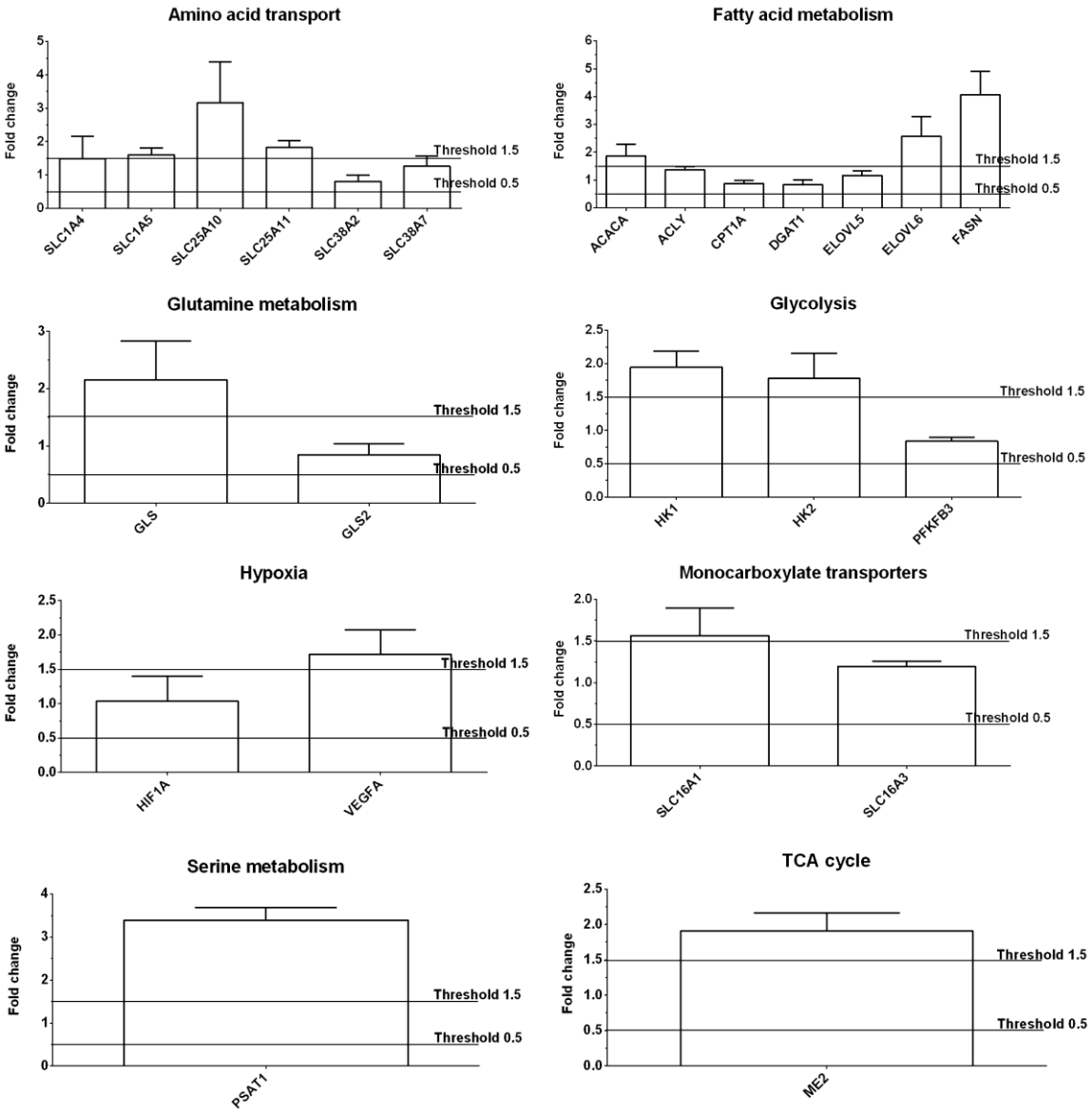

Figure 3.23: Examining the changes in metabolic processes in CLL cells following co-culture with CD40L fibroblasts. Linear fold changes relative to CLL cells co-cultured with parental fibroblasts with a threshold of plus 1.5 and 0.5 to highlight the greatest increases and decreases in mRNA expression (n = 3). Error bars are the SEM.

3.3.7 Fluidigm Biomark™ gene array analysis of metabolic gene expression in CD40L and parental fibroblasts following co-culture with CLL cells

Co-culture of CLL cells with CD40L fibroblasts clearly has an effect on CLL cells. However, what is not clear is whether CLL cells have an effect on their stromal support, in this case CD40L and parental fibroblasts. Evidence shown in Figure 3.14 (A) suggests that such co-culture induces MCT4 expression in CD40L fibroblasts, indicating the possibility of changes in metabolism. This notion is not unfounded as a symbiotic relationship between cancer cells and the tumour microenvironment has been described in the literature (Bonuccelli et al., 2010b, Feron, 2009). To investigate whether co-culture with CLL cells induces change in the expression of genes associated with cell metabolism in supporting fibroblast cells a mouse Fluidigm Biomark™ chip was used. The 46 genes used in this analysis are detailed in Table 3.2.

Figure 3.24 shows a heat map of the Ct values for each gene across CD40L and parental fibroblasts co-cultured with CLL cells. Amplification data which was not classified as linear was automatically excluded by the Fluidigm Biomark™ Real Time PCR Analysis Software (Version 3.1.3) (indicated by an 'X' on Figure 3.24). As with the human array a mouse reference RNA (MqPCR, row 1 of array data) sample was used as a positive control to verify that the cDNA synthesis and pre-amplification steps of the protocol were successful. This data showed that all of the 46 genes within the array were amplified (Ct <24) except for TKTL-11 which was subsequently excluded from further analysis. Once again, a genomic DNA sample was used as a negative control for the PCR reaction (MgDNA, row 7 of array data). One gene was amplified, 18S, however the Ct value was >Ct 24 and this was deemed acceptable considering that the Ct value within the fibroblast samples was approximately 10. Thus, 18S was included in the analyses.

A housekeeping gene was selected from a panel of two genes; 18S and IPO8. Figure 3.25 shows the average Ct values for these genes (n = 12). 18S was selected as the most appropriate housekeeping gene because the Ct values associated with this gene when amplified from CD40L and parental fibroblasts were similar. The same could not be

said of IPO8 where the Ct value associated with this gene amplified from parental fibroblasts looked to be lower than that from CD40L fibroblasts. Moreover, the Ct value of IPO8 was much higher than that of 18S. One experiment, enumerated 2565, highlighted a problem where the Ct value of 18S was high. Further examination of the genes of interest showed this sample had failed on the chip, and this was also evident from the analysis of the CLL cells associated with this experiment. Case 2565 was therefore excluded from further analysis.

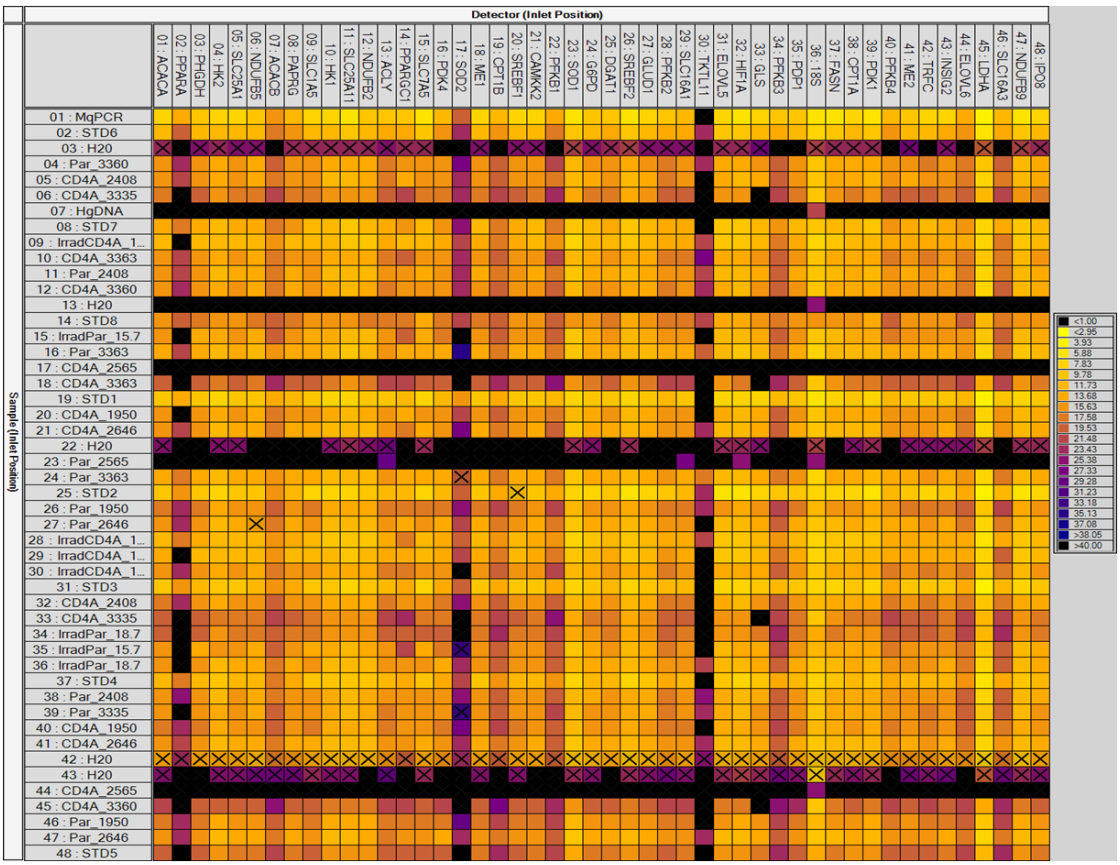

Figure 3.24: Fluidigm Biomark™ chip array for metabolic genes in CD40L and parental fibroblasts co-cultured with CLL cells. Heat map of the Ct values obtained for each gene across individual samples. Amplification data which was not classified as linear was automatically excluded by the Fluidigm Biomark™ Real Time PCR Analysis Software (Version 3.1.3) (indicated by an 'X').

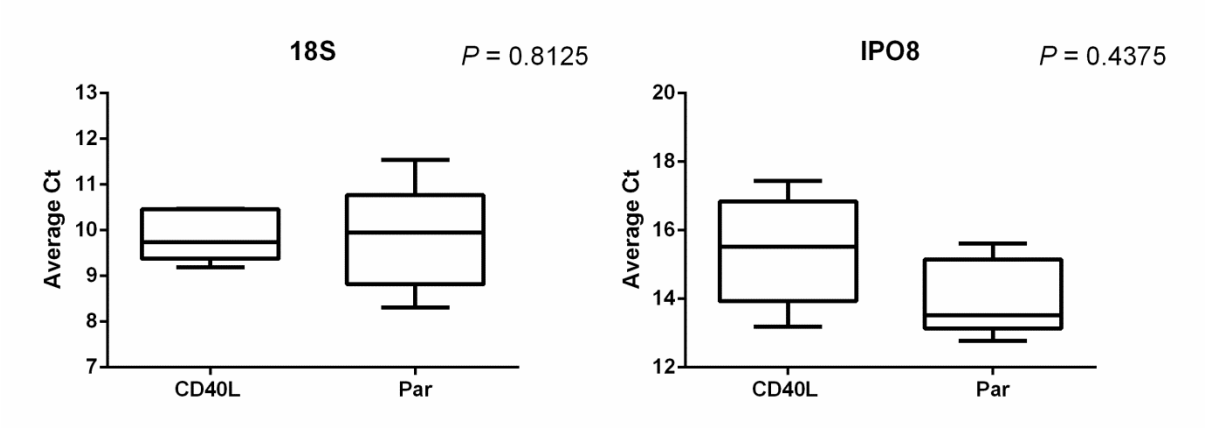

Figure 3.25: Selection of housekeeping genes for Fluidigm Biomark™ chip array in CD40L and parental fibroblasts co-cultured with CLL cells. 18S was selected as the best housekeeping gene to which the genes of interest were normalised because it showed the least variability (P = 0.8125, unpaired t test) (n = 12).

The heat map shown in Figure 3.26 illustrates expression of the genes of interest relative to expression of 18S. From this figure it is obvious that the sample designated CD40L 3335 did not behave in the same way as did the three other CD40L cases and was excluded from further study.

As done previously for the human array, an ANOVA was used to assess the inter-individual variation between preparations of CD40L fibroblasts which had been co-cultured with CLL cells (Figure 3.27 and 3.28). At this point in the analysis PPARG was excluded from further analyses due to undetectable levels of expression (Ct >999), and PPARα was excluded because there were less than n = 3 measurements for this gene. For each of the remaining genes of interest there was no significant inter-individual variation (P = >0.05).

Examination of the parental fibroblast preparations is shown in Figure 3.29 and 3.30. Once again PPARG was excluded from the analysis due to undetectable levels of expression (Ct >999). For each of the genes there was no significant inter-individual variation except for ACACA (* P = 0.0250), ME2 (* P = 0.0483), PDK4 (** P = 0.0040), PHGDH (* P = 0.0400), SLC16A1 (* P = 0.0225) and SREBF2 (* P = 0.0263). Post hoc analyses using a Tukey's multiple comparison test revealed that there was no significant variation in ME2 (P = >0.05). However, significant variation was seen for the other genes listed above highlighting Par 2646 to be the source of the variation. As such this sample was excluded from further analyses.

Taken together, these data suggest that the extraction method yields samples of comparable quality and provides reassurance that the genes have performed reliably and with similar efficiencies. Thus, the analysis can now move to comparative study.

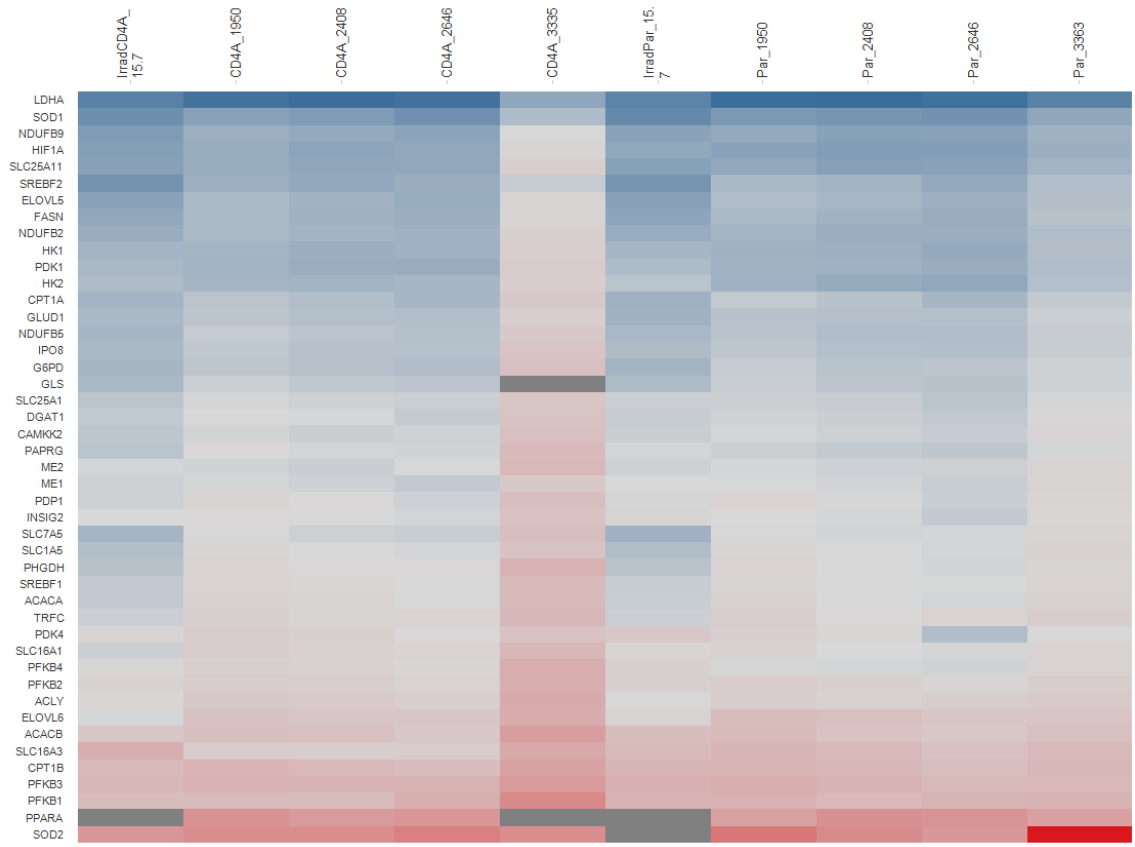

Figure 3.26: Heat map showing changes in gene expression for genes in CD40L and parental fibroblasts co-cultured with CLL cells. Hierarchical clustering of gene expression was performed based upon negative dCt values. Genes with higher levels of expression are coloured red and clustered towards the bottom of the heat map while genes with lower levels of gene expression are coloured blue and clustered towards the top of the heat map. Grey is used to depict the absence of gene expression data.

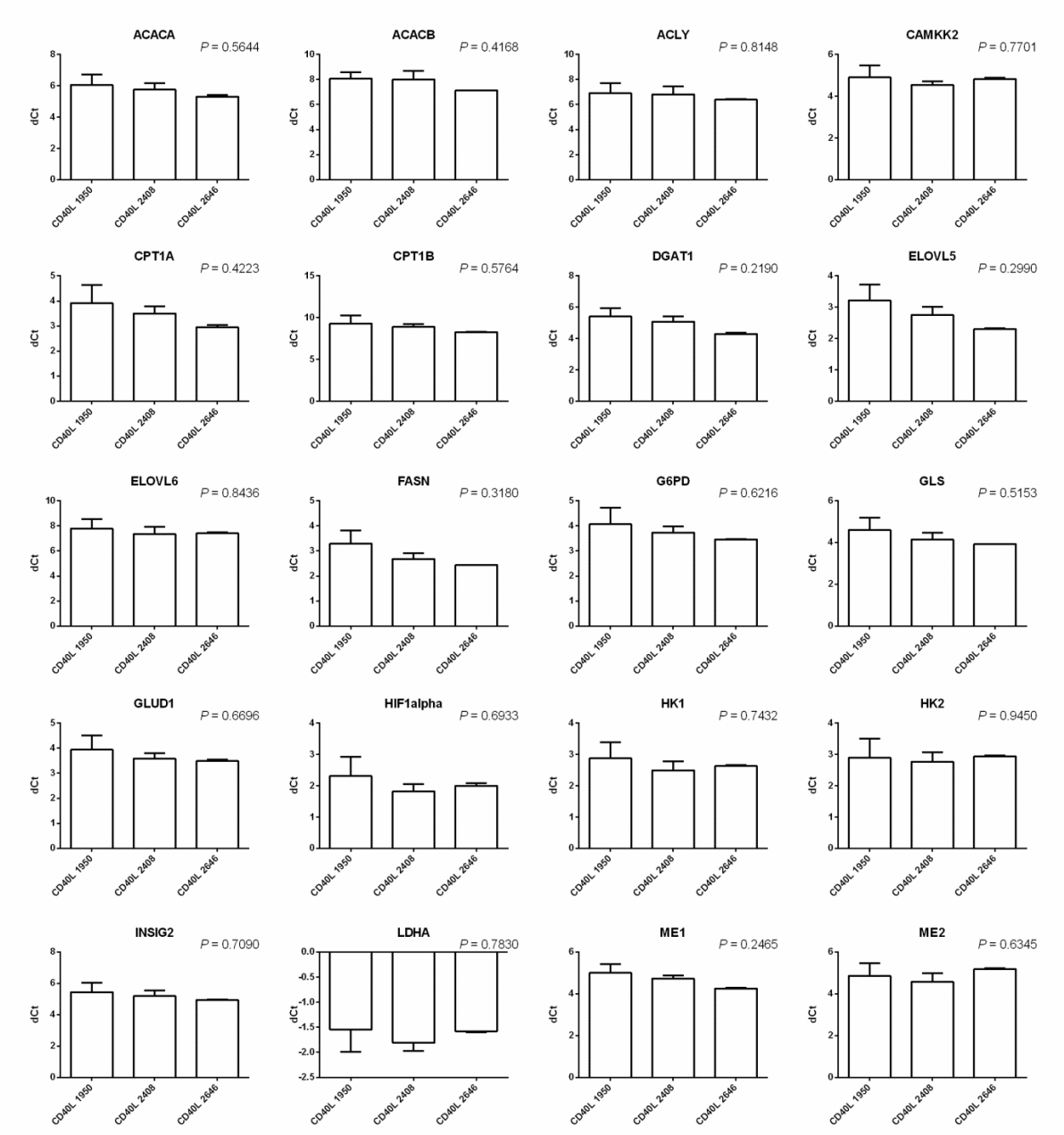

Figure 3.27: Assessing variation in metabolic gene expression in CD40L fibroblasts co-cultured with CLL cells. An ANOVA was used to assess the inter-individual variation between preparations of CD40L fibroblasts which had been co-cultured with CLL cells. Values were normalised to 18S. There was no significant inter-individual variation (P = >0.05). Error bars are the SEM derived from 3 technical replicates.

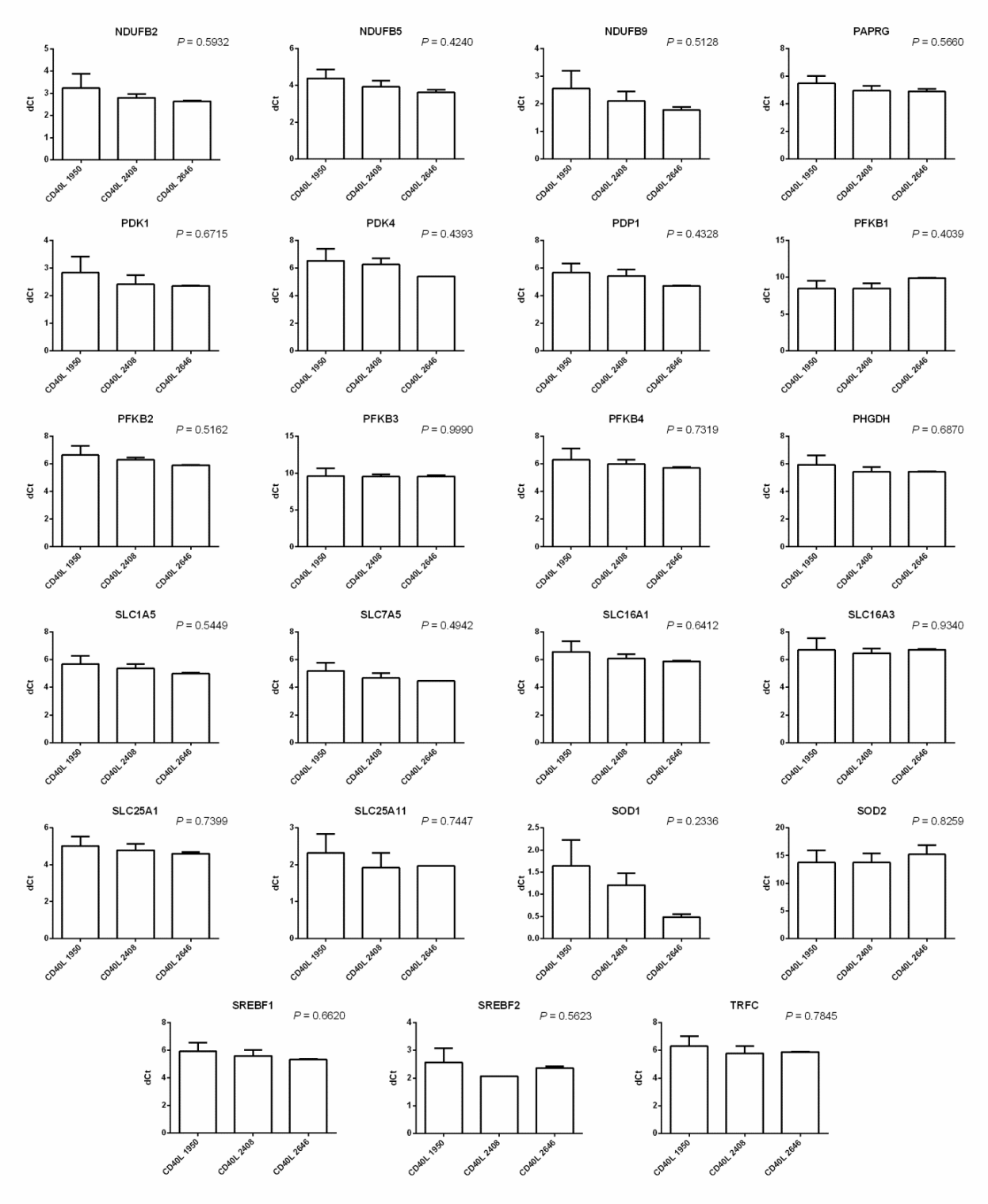

Figure 3.28: Assessing variation in metabolic gene expression in CD40L fibroblasts co-cultured with CLL cells. An ANOVA was used to assess the inter-individual variation between preparations of CD40L fibroblasts which had been co-

cultured with CLL cells. Values were normalised to 18S. PPARG was excluded due to undetectable levels of expression (Ct >999), and PPARα was excluded as there were less than n = 3. For the remaining genes of interest there was no significant inter-individual variation (P = >0.05). Error bars are the SEM derived from 3 technical replicates.

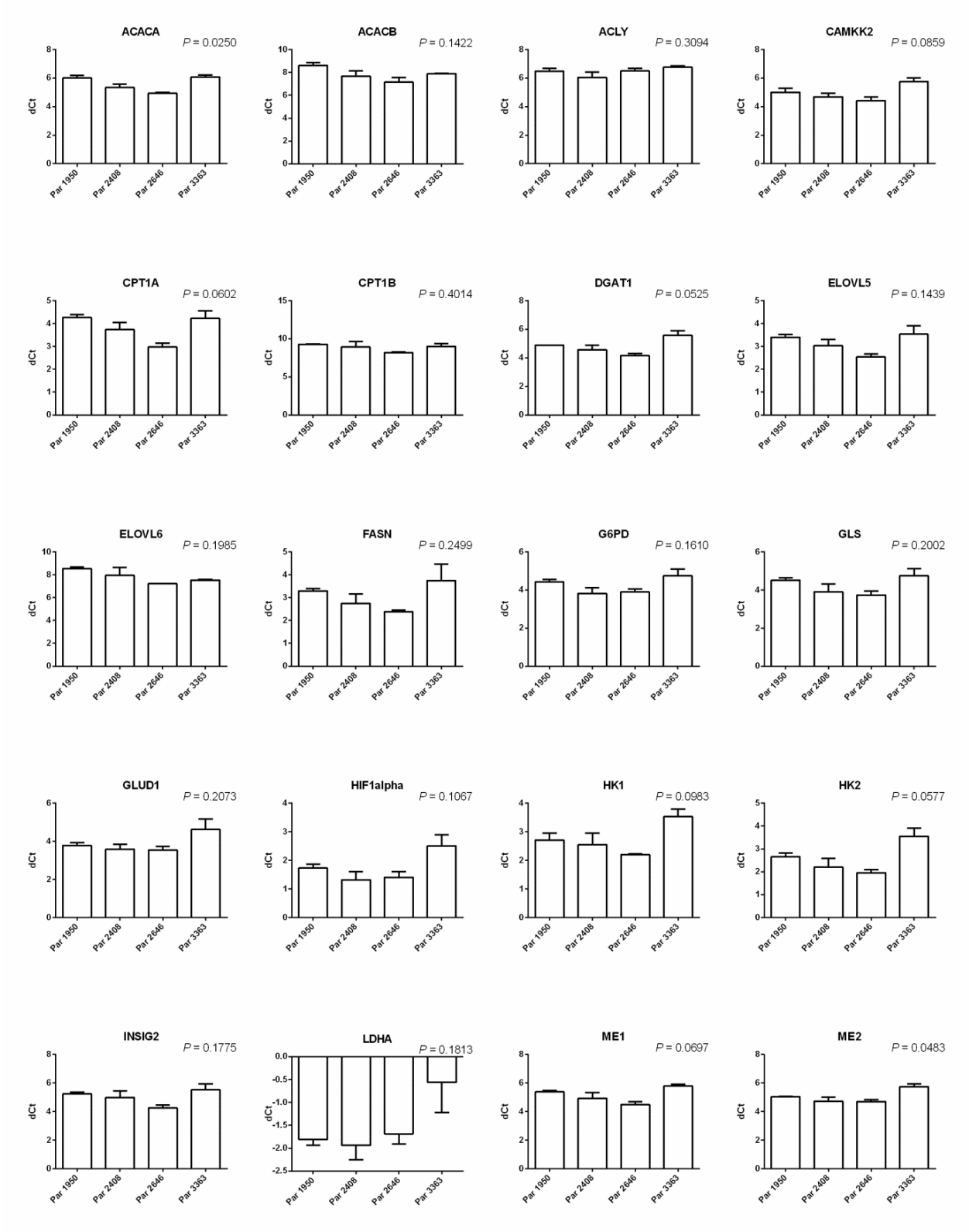

Figure 3.29: Assessing variation in metabolic gene expression in parental fibroblasts co-cultured with CLL cells. An ANOVA was used to assess the inter-

individual variation between preparations of parental fibroblasts which had been co-cultured with CLL cells. Values were normalised to 18S. There was no significant inter-individual variation except for ACACA (* $P = 0.0250$) and ME2 (* $P = 0.0483$). Post hoc analyses using a Tukey's multiple comparison test revealed that there was no significant variation in ME2 ($P = >0.05$). However, significant variation was seen for the other genes highlighting Par 2646 to be the source of the variation. As such this sample was excluded from further analyses. Error bars are the SEM derived from 3 technical replicates.

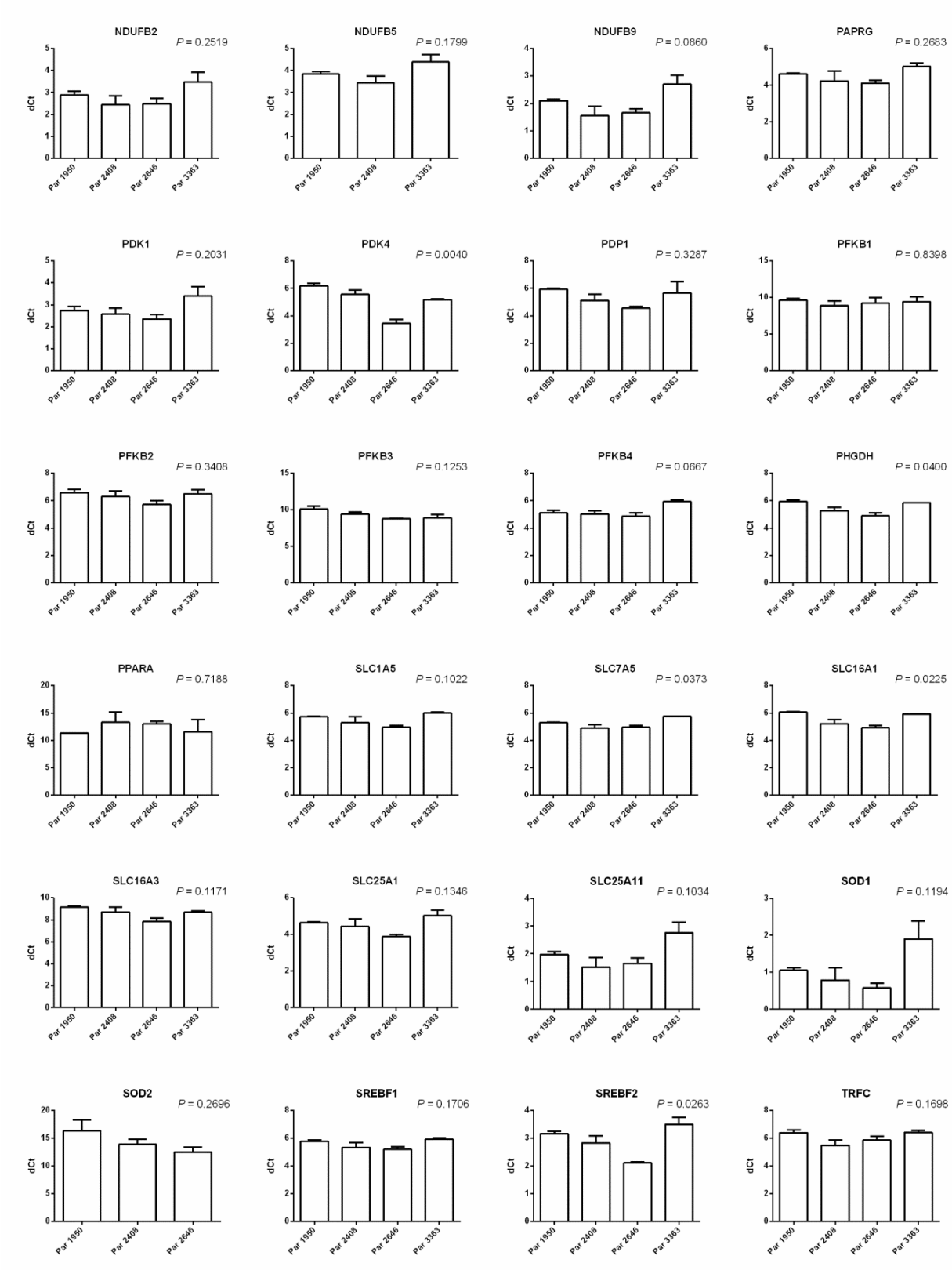
NDUFB2
P = 0.2519
NDUFB5
P = 0.1799
NDUFB9
P = 0.0860
PAPRG
P = 0.2683
PDK1
P = 0.2031
PDK4
P = 0.0040
PDP1
P = 0.3287
PFKB1
P = 0.8398
PFKB2
P = 0.3408
PFKB3
P = 0.1253
PFKB4
P = 0.0667
PHGDH
P = 0.0400
PPARA
P = 0.7188
SLC1A5
P = 0.1022
SLC7A5
P = 0.0373
SLC16A1
P = 0.0225
SLC16A3
P = 0.1171
SLC25A1
P = 0.1346
SLC25A11
P = 0.1034
SOD1
P = 0.1194
SOD2
P = 0.2696
SREBF1
P = 0.1706
SREBF2
P = 0.0263
TRFC
P = 0.1698
dCt
Par 1950
Par 2408
Par 2646
Par 3363

Figure 3.30: Assessing variation in metabolic gene expression in parental fibroblasts co-cultured with CLL cells. An ANOVA was used to assess the inter-individual variation between preparations of parental fibroblasts which had been co-cultured with CLL cells. Values were normalised to 18S. PPARG was excluded from the analysis due to undetectable levels of expression (Ct >999). For each of the genes there was no significant inter-individual variation except for PDK4 (** $P = 0.0040$), PHGDH (* $P = 0.0400$), SLC16A1 (* $P = 0.0225$) and SREBF2 (* $P = 0.0263$). Post hoc analyses using a Tukey's multiple comparison test revealed that there was significant variation highlighting Par 2646 to be the source of the variation. As such this sample was excluded from further analyses. Error bars are the SEM derived from 3 technical replicates.

The influence of CLL cells on supportive fibroblasts was assessed by comparing gene expression in CD40L and parental fibroblasts co-cultured with CLL cells relative to those which were not. The CD40L and parental fibroblast control samples (those cultured in the absence of CLL cells) were prepared at a different time to the co-cultured samples; however, the conditions of this preparation were the same. Inter-variation between preparations of the control fibroblast (CD40L and parental) samples was assessed (Table 3.3), and at this point SOD2 was excluded from the analysis for both CD40L and parental fibroblasts because there were less than 3 measurements. No significant variation was seen between the different preparations except for PPARGC1 in the CD40L fibroblast samples (* $P = 0.0351$, unpaired t test). Because of this variance, this gene was excluded from further analysis. Taken together, these data provide confidence that any variation seen in future comparative analyses between fibroblast cells co-cultured with CLL cells versus those cultured in the absence of CLL cells will likely be due to CLL cell-induced changes in gene expression and not experimental variation. Therefore, the study can progress to make comparisons between these culture conditions.

Figure 3.31 shows a heat map illustrating changes in gene expression in CD40L and parental fibroblasts that have been co-cultured with CLL cells and normalised to control fibroblast preparations (n = 3). The effect of CLL cell co-culture on CD40L fibroblasts was assessed first. The average fold change in gene expression in co-cultured CD40L fibroblasts is illustrated in Figures 3.32 and 3.33; 4 genes (HK2, LDHA, PDK1 and SLC16A3) showed significant upregulation above a 1.16 fold threshold, and 18 genes showed significant downregulation below a 0.61 fold threshold (ACACA, ACLY, ELOVL5, ELOVL6, FASN, G6PD, GLS, NDUFB5, NDUFB9, PAPRG, PHGDH, SLC1A5, SLC7A5, SLC16A1, SLC25A1, SREBF1, SREBF2 and TRFC).

A – CD40L

Gene	*P* value	Gene	*P* value	
ACACA	0.5172	NDUFB9	0.5452	
ACACB	0.7547	PAPRG	0.3126	
ACLY	0.7744	PDK1	0.9802	
CAMKK2	0.3773	PDK4	0.6612	
CPT1A	0.7698	PDP1	0.9475	
CPT1B	0.9068	PFKB1	0.5884	
DGAT1	0.6645	PFKB2	0.7375	
ELOVL5	0.5397	PFKB3	0.7437	
ELOVL6	0.5299	PFKB4	0.5973	
FASN	0.6502	PHGDH	0.3539	
G6PD	0.7840	PPARGC1	0.0351	*
GLS	0.5382	SLC1A5	0.4501	
GLUD1	0.6476	SLC7A5	0.3576	
HIF1A	0.4463	SLC16A1	0.4720	
HK1	0.6982	SLC16A3	0.2983	
HK2	0.6549	SLC25A1	0.6031	
INSIG2	0.8102	SLC25A11	0.6008	
LDHA	0.8826	SOD1	0.5790	
ME1	0.7594	SREBF1	0.5471	
ME2	0.6043	SREBF2	0.4657	
NDUFB2	0.5266	TRFC	0.4001	
NDUFB5	0.4952			

B - Par

Gene	*P* value	Gene	*P* value
ACACA	0.6391	NDUFB9	0.8530
ACACB	0.5417	PAPRG	0.7995
ACLY	0.6898	PDK1	0.3917
CAMKK2	0.8339	PDK4	0.4508
CPT1A	0.7683	PDP1	0.8961
CPT1B	0.8350	PFKB1	0.9290
DGAT1	0.9367	PFKB2	0.8915
ELOVL5	0.5948	PFKB3	0.9716
ELOVL6	0.4859	PFKB4	0.7577
FASN	0.6212	PHGDH	0.4357
G6PD	0.6282	PPARGC1	0.1771
GLS	0.7979	SLC1A5	0.3692
GLUD1	0.6622	SLC7A5	0.2352
HIF1A	0.7993	SLC16A1	0.5978
HK1	0.7741	SLC16A3	0.7084
HK2	0.4935	SLC25A1	0.8365
INSIG2	0.5071	SLC25A11	0.8677
LDHA	0.4627	SOD1	0.6535
ME1	0.8921	SREBF1	0.6431
ME2	0.8121	SREBF2	0.3164
NDUFB2	0.8121	TRFC	0.5845
NDUFB5	0.7734		

Table 3.3: Comparing inter-individual variation between untreated irradiated fibroblast (CD40L and parental) controls. Variation between irradiated control samples cultured in the absence of CLL cells (untreated, UT). **(A)** Comparison of UT irradiated control preparations of CD40L fibroblasts showed significant variation with one gene, PPARGC1, using an unpaired t test. **(B)** Comparison of UT irradiated control preparations of parental (Par) fibroblasts showed no significant variation. $P \leq 0.05$.

Figure 3.31: Change in gene expression in CD40L fibroblasts and parental fibroblasts following co-culture with CLL cells. Linear fold changes were calculated by normalisation of CD40L and parental fibroblasts co-cultured with CLL cells to irradiated CD40L and parental fibroblasts which had not been in contact with CLL cells respectively. Upregulation of gene expression is coloured red and downregulation in blue.

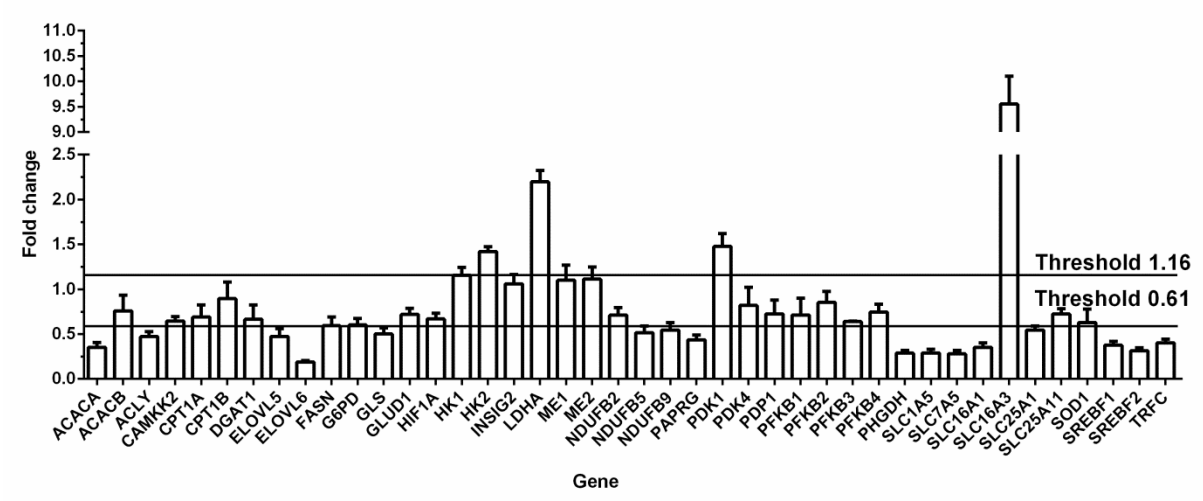

Figure 3.32: Fold change in gene expression in CD40L fibroblasts following co-culture with CLL cells (n = 3). Linear fold increases for CD40L fibroblasts co-cultured with CLL cells made relative to an irradiated CD40L fibroblast control. A minimum threshold fold change of ≥1.16 indicates there are 5 genes which are upregulated; HK1, HK2, LDHA, PDK1 and SLC16A3 (n = 3) while a minimum threshold of ≤ 0.61 suggests there are 19 genes which are downregulated; ACACA, ACLY, ELOVL5, ELOVL6, FASN, G6PD, GLS, NDUFB5, NDUFB9, PAPRG, PHGDH, SLC1A5, SLC7A5, SLC16A1, SLC25A1, SOD1, SREBF1, SREBF2 and TRFC.

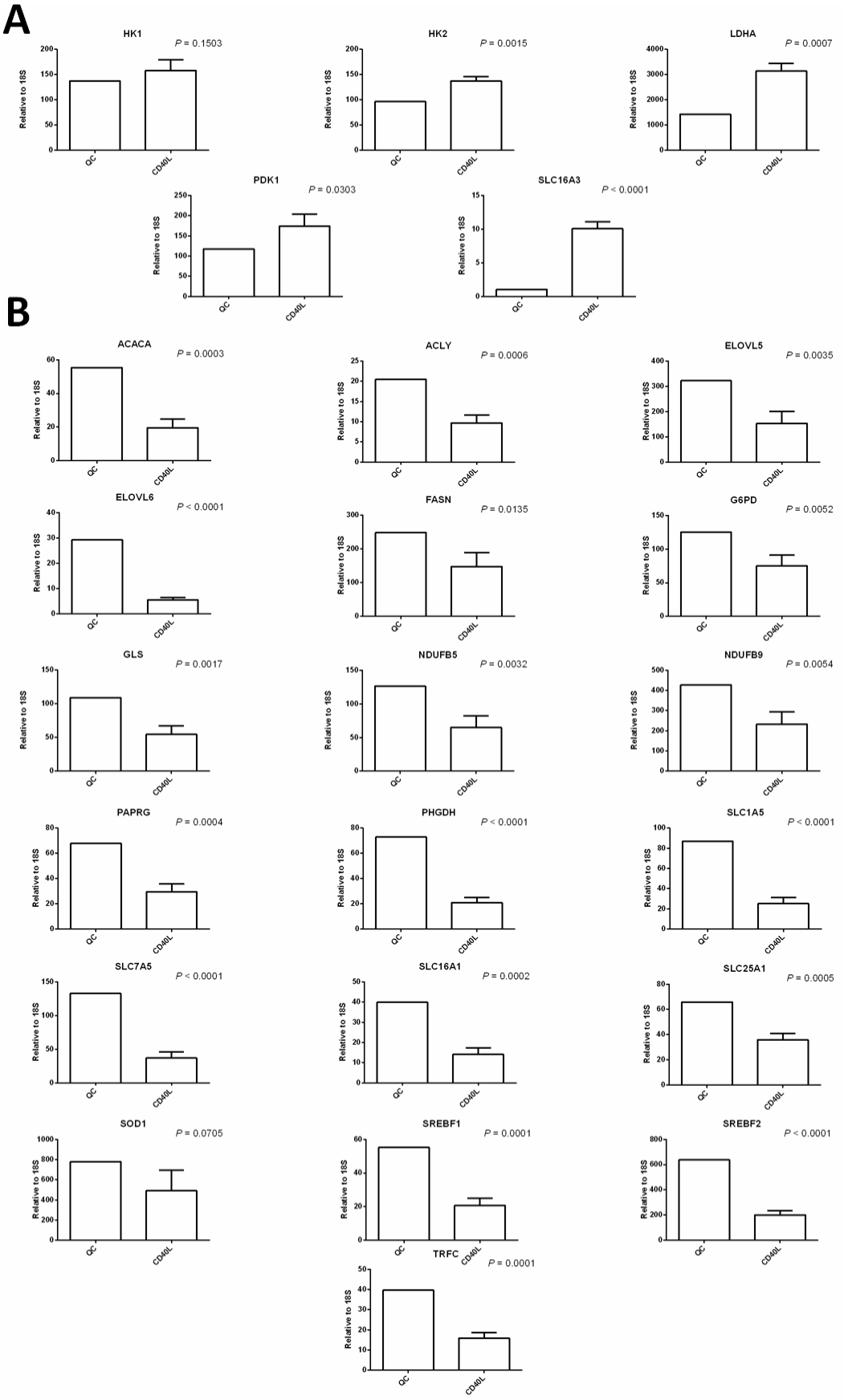
A
HK1
P = 0.1503
HK2
P = 0.0015
LDHA
P = 0.0007
PDK1
P = 0.0303
SLC16A3
P < 0.0001
B
ACACA
P = 0.0003
ACLY
P = 0.0006
ELOVL5
P = 0.0035
ELOVL6
P < 0.0001
FASN
P = 0.0135
G6PD
P = 0.0052
GLS
P = 0.0017
NDUFB5
P = 0.0032
NDUFB9
P = 0.0054
PAPRG
P = 0.0004
PHGDH
P < 0.0001
SLC1A5
P < 0.0001
SLC7A5
P < 0.0001
SLC16A1
P = 0.0002
SLC25A1
P = 0.0005
SOD1
P = 0.0705
SREBF1
P = 0.0001
SREBF2
P < 0.0001
TRFC
P = 0.0001
Relative to 18S
QC
CD40L

Figure 3.33: Increased and decreased gene expression in CD40L fibroblasts following co-culture with CLL cells. (A) An unpaired t test showed significant upregulation of HK2, LDHA, PDK1 and SLC16A3 (n = 3). **(B)** An unpaired t test showed significant downregulation of ACACA, ACLY, ELOVL5, ELOVL6, FASN, G6PD, GLS, NDUFB5, NDUFB9, PAPRG, PHGDH, SLC1A5, SLC7A5, SLC16A1, SLC25A1, SREBF1, SREBF2 and TRFC.

The effect of CLL cell co-culture on parental fibroblasts was next assessed. Figures 3.34 and 3.35 show the data for the comparative analysis between parental fibroblasts co-cultured with CLL cells and control parental fibroblasts. Thresholds for gene upregulation and downregulation were set at 1.5 and 0.66 fold, respectively. In terms of upregulated genes, only two (INSIG2 and PDK4) of the 9 potentially upregulated genes showed significance ($P < 0.05$). 16 genes (ACACA, CPT1A, ELOVL5, ELOVL6, FASN, GLS, G6PD, GLUD1, NDUFB5, PHGDH, SLC1A5, SLC7A5, SOD1, SREBF1, SREBF2 and TRFC) showed significant downregulation in parental fibroblasts co-cultured with CLL cells compared to control. Taken together with the data generated using CD40L fibroblasts, these data show that co-culture with CLL cells affects gene expression in fibroblasts. However, correction has not been made for the use of multiple statistical testing and validation of this data is required.

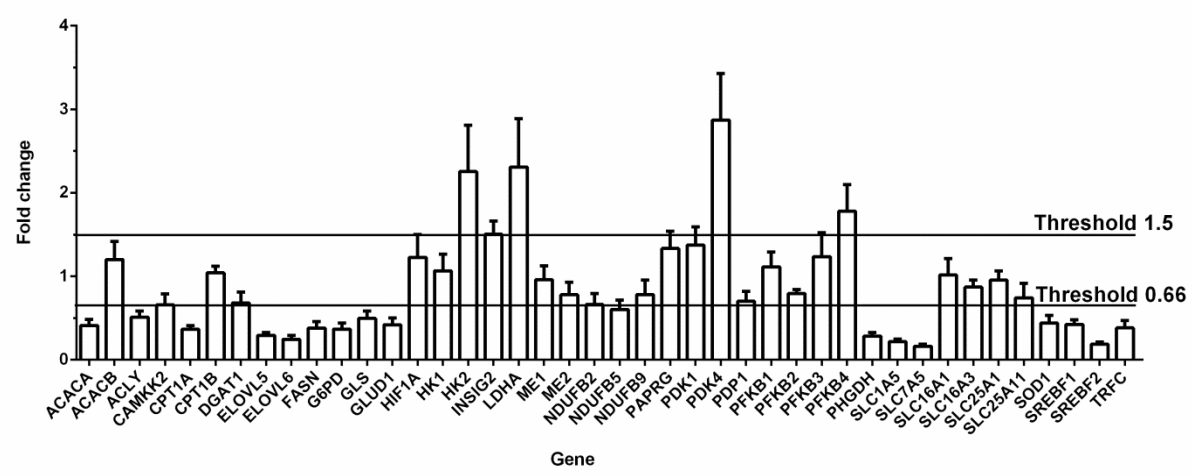

Figure 3.34: Fold change in gene expression in parental fibroblasts following co-culture with CLL cells (n = 3). Linear fold change increases for parental fibroblasts co-cultured with CLL cells made relative to an irradiated parental fibroblast control. A minimum threshold fold change of ≥1.5 indicates there are 9 genes which are upregulated, HIF1A, HK2, INSIG2, LDHA, PAPRG, PDK1, PDK4, PFKB3, PFKB4, while a minimum threshold of ≤ 0.66 suggests there are 17 genes which are downregulated; ACACA, CAMKK2, CPT1A, ELOVL5, ELOVL6, FASN, GLS, G6PD, GLUD1, NDUFB5, PHGDH, SLC1A5, SLC7A5, SOD1, SREBF1, SREBF2 and TRFC.

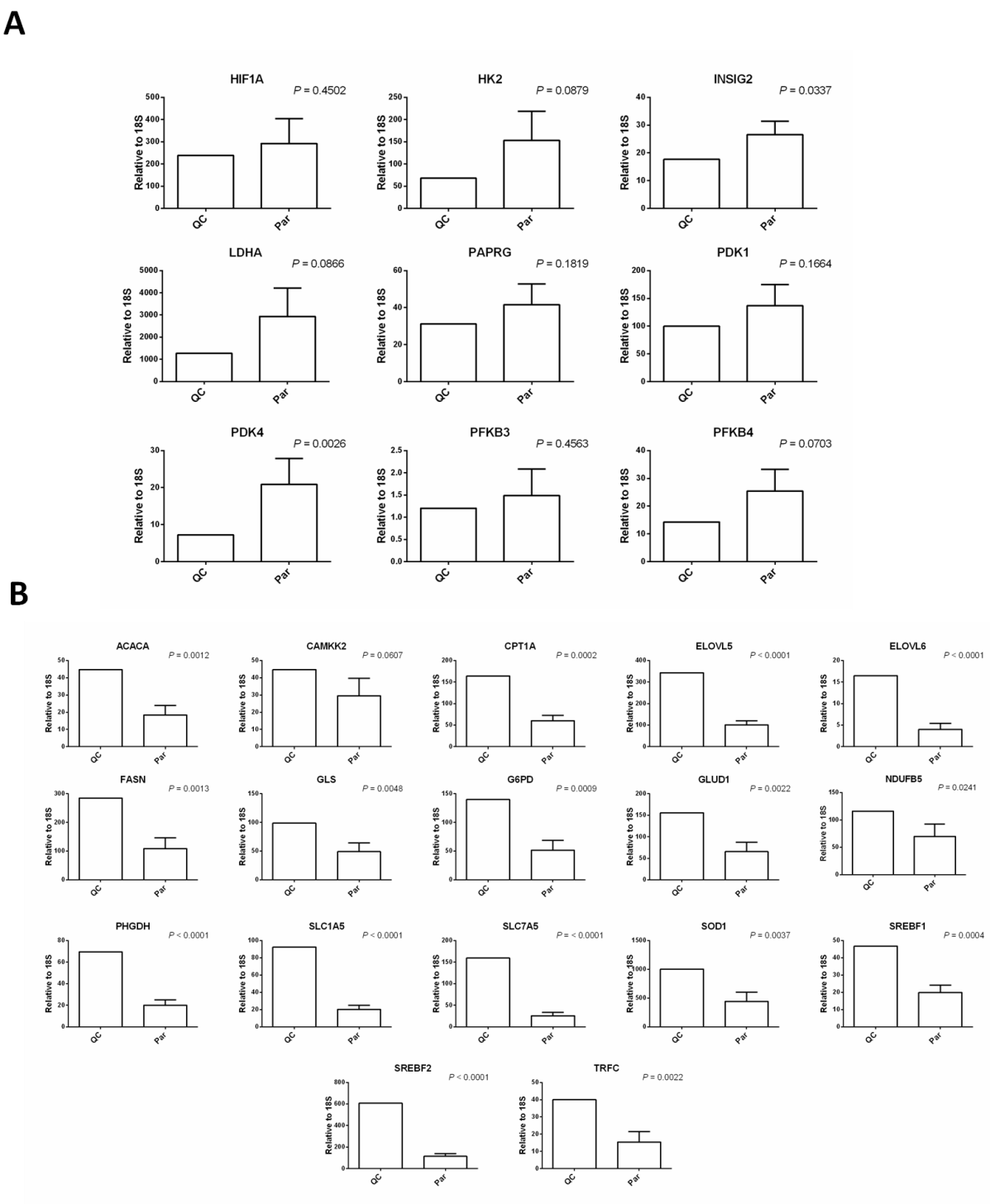

Figure 3.35: Changes in gene expression in parental fibroblasts following co-culture with CLL cells. (A) An unpaired t test revealed 2 genes to be significantly upregulated, INSIG2 and PDK4 (n = 3). **(B)** 16 genes were shown to be significantly down regulated using an unpaired t test (n = 3).

Following on from the comparative analyses, changes in gene expression were examined in relation to metabolic pathways as was done when CLL cells were analysed (Figure 3.36). Incubation of CD40L fibroblasts with CLL cells seemed to promote energy generating processes such as glycolysis (HK1, HK2, LDHA) as well as pyruvate metabolism (PDK1). SLC16A3 (the gene which codes for MCT4) is upregulated, likely as a consequence of enhanced glycolytic activity, and is in agreement with protein data (Figure 3.14). Incubation of CD40L fibroblasts with CLL cells also seemed to suppress amino acid transport (SLC1A5, SLC7A5, SLC25A1), fatty acid metabolism (ACACA, ACLY, ELOVL5, ELOVL6, PAPRG, SREBF1, SREBF2 and TRFC), glutamine metabolism (GLS), and serine metabolism (PHGDH). Interestingly, a similar gene profile was suppressed in parental fibroblasts co-cultured with CLL cells. Thus, genes involved in amino acid transport (SLC1A5, SLC7A5), fatty acid metabolism (ACACA, ACLY, CPT1A, ELOVL5, ELOVL6, FASN, SREBF1, SREBF2 and TRFC), glutamine metabolism (GLS, GLUD1) the pentose phosphate pathway (G6PD), serine metabolism (PHGDH) and were all downregulated. This suggests that there are common effects of CLL cells on their stromal support. However, the strong upregulation of SLC16A3 in the CD40L fibroblasts indicates a specific effect of engaged CD40L, caused either within the CD40L fibroblast itself (a signalling effect) or by the increased metabolic requirements of CD40-stimulated CLL cells.

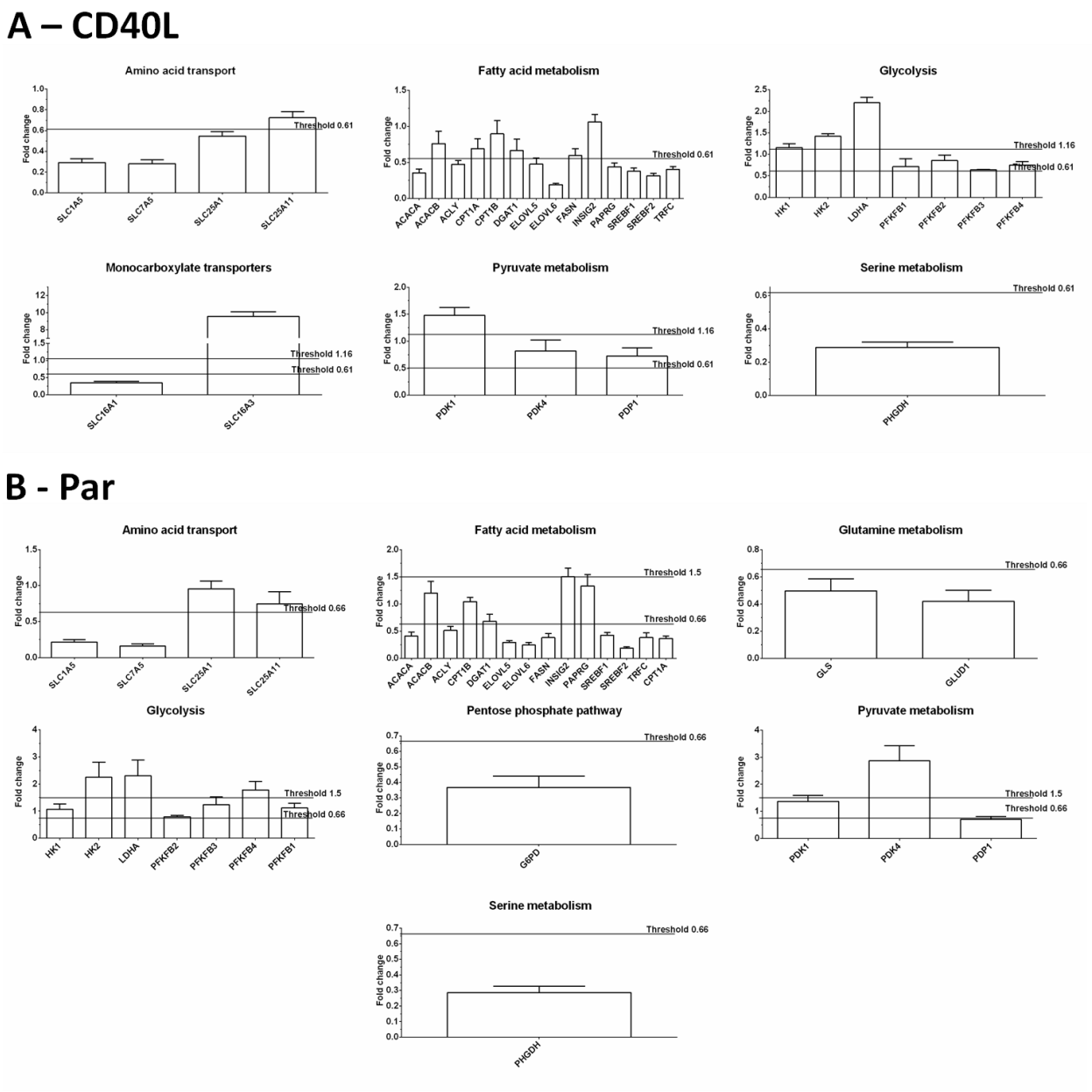

Figure 3.36: Examining the changes in metabolic processes in CD40L and parental fibroblasts following co-culture with CLL cells. Linear fold changes relative to irradiated controls with a threshold of plus 1.5 and 0.5 to highlight the greatest increases and decreases in mRNA expression (n = 3). Error bars are the SEM.

3.3.8 Assessing mitochondrial function in CLL cells using the SeahorseXF24 metabolic flux analyser

Co-culture of CLL cells with CD40L fibroblasts results in upregulation of MCT4 protein and is accompanied by a switch in gene expression favouring fatty acid metabolism and glycolysis. This switch in energy metabolism was next analysed using the SeahorseXF24 metabolic flux analyser. This method was chosen to compliment the Fluidigm array data and provide real time information about the metabolic phenotype of these cells. To assess oxidative phosphorylation OCR (**o**xygen **c**onsumption **r**ate) was measured while ECAR (**e**xtra**c**ellular **a**cidification **r**ate) was used as an indicator of glycolytic activity. By examining changes in both OCR and ECAR it is possible to assess metabolic competency through the addition of agents such as; oligomycin, FCCP, rotenone and antimycin-A to produce parameters such as; basal respiration, ATP turnover, proton leak, maximal respiration, spare respiratory capacity and glycolytic capacity.

First of all it was necessary to optimise this measuring technique for the analysis of CLL cells. Attempts were made to use cryopreserved CLL cells, however, addition of oligomycin, FCCP, rotenone and antimycin-A produced little change in the measurements despite using different cell numbers [Figure 3.37 (A)]. Addition of pyruvate to the analysis media, as is suggested by a paper by Chacko (2013) using primary B cells, showed that CLL cells became responsive to mitochondrial stressors [Figure 3.37 (B)]. However, in this case repeat experiments using the same case did not generate reproducible results. Finally, fresh CLL cells were used, and these showed good responses to mitochondrial stressors in comparison to cryopreserved CLL cells [Figure 3.37 (C)]. This is supported in the literature where it is described how cryopreservation may irreparably damage mitochondria (Trusal et al., 1984, Larsen et al., 2012, Tsutsaeva and Gordienko, 1982). Moreover, in lymphocytes specifically, cryopreservation has been demonstrated to alter the phenotype of cells as well as change the expression of adhesion molecules which may also have a role in regulating metabolic function (Faint et al., 2011, Costantini et al., 2003, Deneys et al., 1999).

Thus, CLL cell responsiveness to the mitochondrial stressors was always robust when fresh cells were used.

The next step in measuring metabolic flux in CLL cells involved further optimisation titrating the concentration of FCCP. This is because the effects of this compound can vary between different cell types, and because too much or too little can affect final measurement. Figure 3.38 shows OCR data following the addition of FCCP at 0.5, 0.75, 1.0, 1.5 and 3µM concentrations. 1.5µM FCCP was selected because this concentration was consistent with data generated using cell lines that is presented later in this thesis, and because maximal mitochondrial uncoupling was induced.

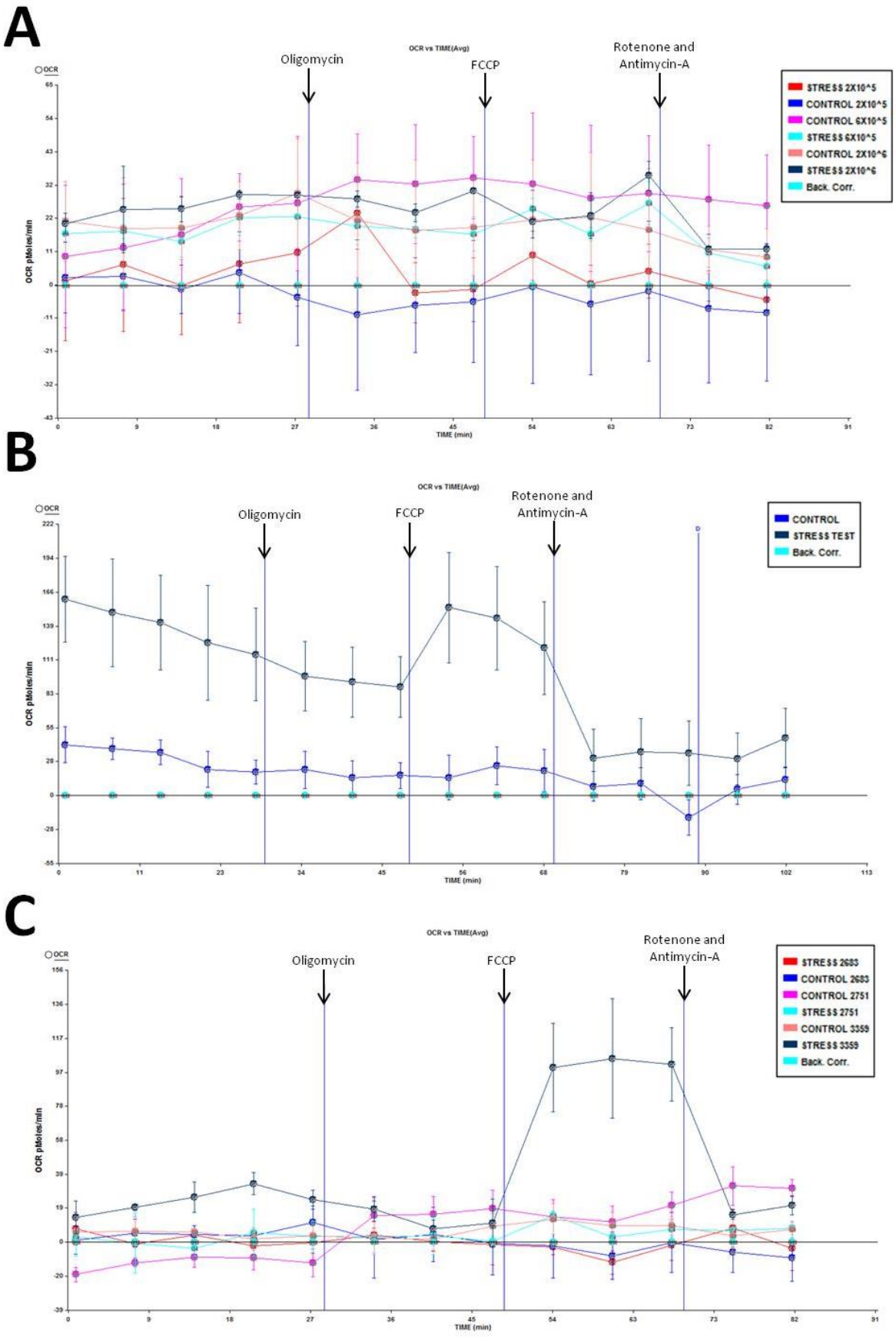
A
OCR vs TIME(Avg)
Oligomycin
FCCP
Rotenone and Antimycin-A
OCR
OCR pMoles/min
TIME (min)
STRESS 2X10^5
CONTROL 2X10^5
CONTROL 6X10^5
STRESS 6X10^5
CONTROL 2X10^6
STRESS 2X10^6
Back. Corr.
B
OCR vs TIME(Avg)
Oligomycin
FCCP
Rotenone and Antimycin-A
OCR
OCR pMoles/min
TIME (min)
CONTROL
STRESS TEST
Back. Corr.
C
OCR vs TIME(Avg)
Oligomycin
FCCP
Rotenone and Antimycin-A
OCR
OCR pMoles/min
TIME (min)
STRESS 2683
CONTROL 2683
CONTROL 2751
STRESS 2751
CONTROL 3359
STRESS 3359
Back. Corr.

Figure 3.37: Optimisation of the SeahorseXF24 analysis technique. (A) To assess seeding density CLL cells were plated out at 2 x 10^5 cells/well, 6 x 10^5 cells/well, and 2 x 10^6 cells/well and subjected to a mitochondrial stress test (oligomycin 1.26μM, FCCP 1.5μM and rotenone and antimycin-A 1μM). **(B)** CLL cells (2 x 10^6 cells/well) were shown to be responsive to mitochondrial stressors following the addition of 2mM sodium pyruvate to analysis media. **(C)** Fresh CLL cells (case 3359) and thawed CLL cells (cases 2683 and 2751) (2 x 10^6 cells/well) were subjected to a mitochondrial stress test. Fresh cells were seen to respond to stressors while the thawed cells were unresponsive.

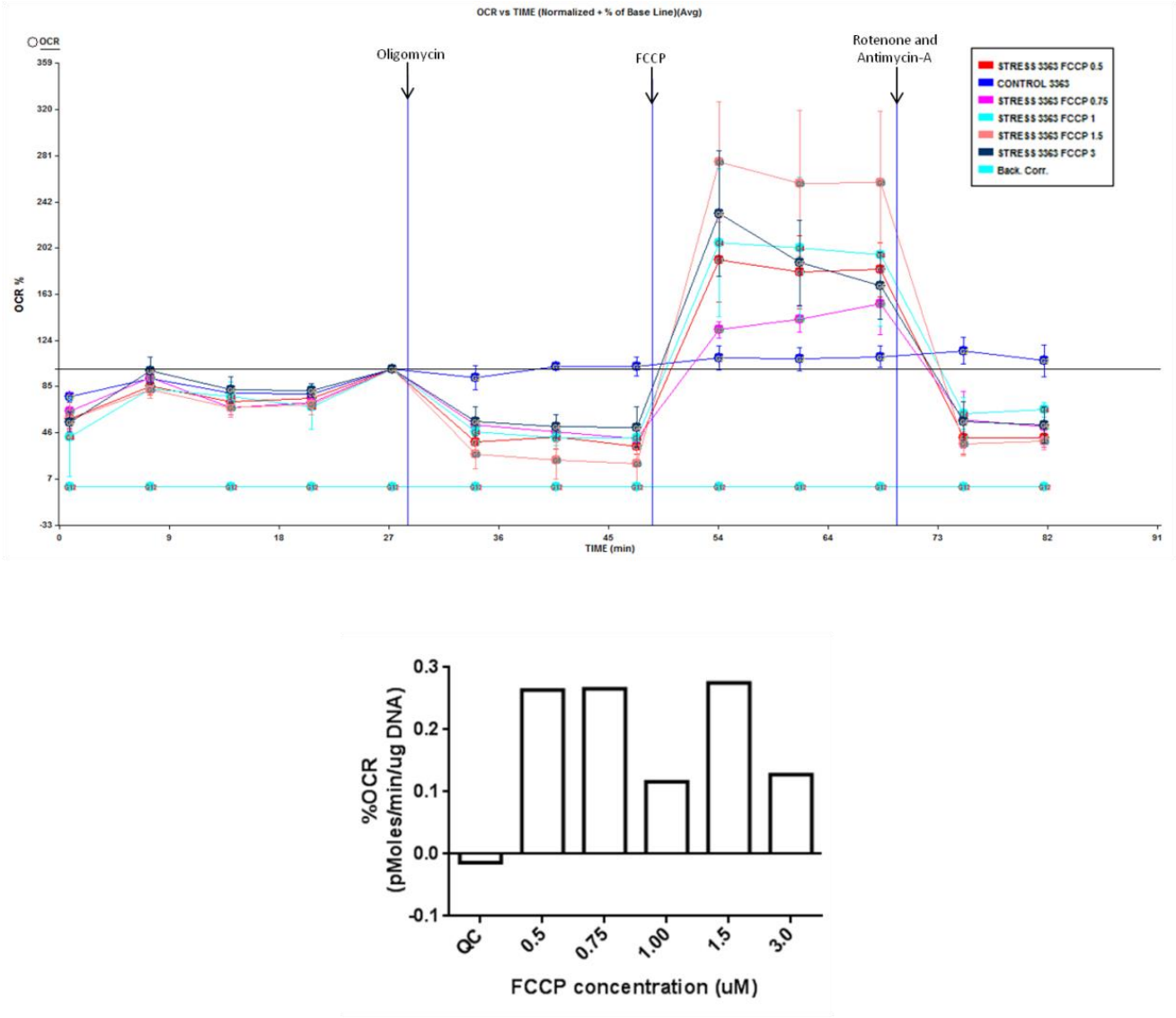

Figure 3.38: FCCP titration. Fresh CLL cells (2 x 10^6 cells/well) were subjected to a mitochondrial stress test (oligomycin 1.26µM, FCCP 0.5, 0.75, 1.0, 1.5 and 3µM and rotenone and antimycin-A 1µM). OCR (pMoles/min) was measured. Data was made relative to the baseline (%) and normalised to DNA content (µgDNA). 1.5µM was chosen for use in future experiments.

Mitochondrial respiration of cultured (untreated) and co-cultured CLL cells (with CD40L and parental fibroblasts) were next examined to determine whether CD40 ligation induces changes in metabolic flux. This was done by removing the CLL cells from the fibroblast monolayer and plating them out to create a monolayer from which OCR (pMoles/min/μgDNA) could be measured in response to mitochondrial stressors (oligomycin 1.26μM, FCCP 1.5μM, and rotenone and antimycin-A 1μM).

This experiment was performed using freshly isolated CLL cells from 5 patients. In all cases co-culture of the CLL cells with CD40L fibroblasts induced MCT4 expression (Figure 3.39). This shows that the CLL cells from the cases used responded as expected. Figure 3.40 shows the recorded OCR traces of variously cultured CLL cells as they respond to the different mitochondrial stressors. Figure 3.41 captures this data as baseline respiration, ATP production, maximal respiration, proton leak, and spare capacity. Culture of CLL cells on fibroblasts, either CD40L or parental, seems to support CLL cell metabolism because baseline respiration, ATP production, maximal respiration and spare capacity all increased in the co-cultured CLL cells. Variability was observed on a case to case basis and tests for statistical significance proved inconclusive. However, this variability seemed confined to the untreated and parental fibroblast co-cultured CLL cells [respectively the red and dark blue traces in Figures 3.40(A-E)]. Where consistency was observed is in the CD40L fibroblast co-cultured CLL cells [light blue trace in Figures 3.40(A-E)]. Here, addition of oligomycin lowered OCR consistent with inhibition of ATP synthase in all cases tested. Addition of FCCP to induce maximal respiration raised OCR in all cases tested. Taken together, these data imply that co-culture of CLL cells with CD40L fibroblasts induces intracellular conditions consistent with fully functional mitochondria.

The glycolytic capacity of CLL cells under these culture conditions was next assessed. This was done by measuring changes in ECAR (mpH/min/μgDNA) in response to oligomycin (1.26μM). Figure 3.42 shows the response of each case individually. ECAR was largely unaffected by the addition of oligomycin in untreated CLL cells consistent with the low level of oxygen-dedicated ATP production measured in Figure 3.41 (B). In CLL cells cultured on parental fibroblasts, ECAR was also unaffected by

oligomycin addition in 3 of the 5 cases tested (Figure 3.42). However, addition of oligomycin to CLL cells co-cultured on CD40L fibroblasts consistently increased glycolytic capacity in these cells, and this is in line with the consistent ability of oligomycin to decrease oxygen consumption in these cells (Figure 3.40). Taken together, these data suggest that CD40 ligation on CLL cells induces increased glycolysis, providing support for the data generated by the Fluidigm™ chip.

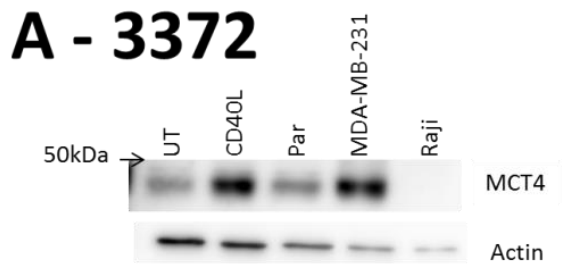
A - 3372
50kDa
UT
CD40L
Par
MDA-MB-231
Raji
MCT4
Actin

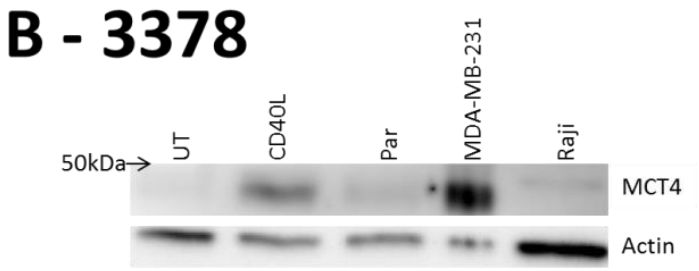
B - 3378
50kDa
UT
CD40L
Par
MDA-MB-231
Raji
MCT4
Actin

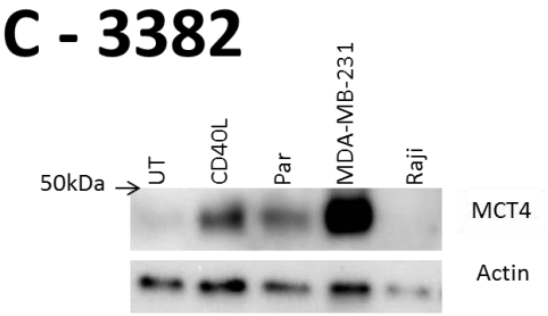
C - 3382
50kDa
UT
CD40L
Par
MDA-MB-231
Raji
MCT4
Actin

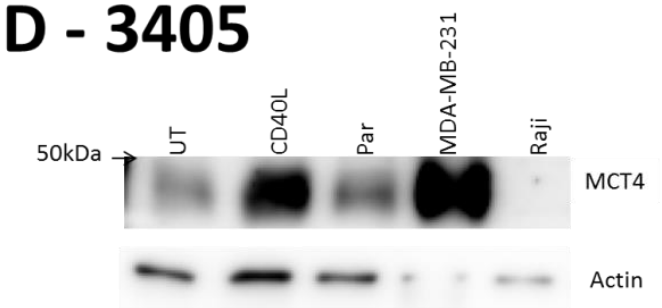
D - 3405
50kDa
UT
CD40L
Par
MDA-MB-231
Raji
MCT4
Actin

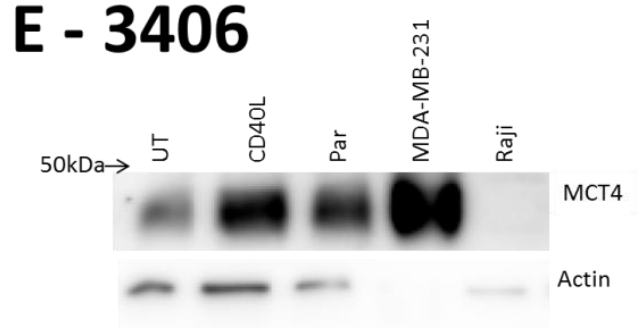
E - 3406
50kDa
UT
CD40L
Par
MDA-MB-231
Raji
MCT4
Actin

Figure 3.39: Western blot analysis to check for MCT4 upregulation following CD40 ligation in samples used for metabolic flux analyses. As a positive control for CD40L stimulation MCT4 expression was assessed using Western blotting for each of the cases used analysed using the SeahorseXF24 **(A-E)**. Blots were treated with rabbit polyclonal anti-MCT4 (sc-376101) (1:1000) (Santa Cruz Biotechnology, CA, USA). Blots were probed with mouse monoclonal anti-β-actin (clone AC-74) as a control to ensure equal protein loading. A MDA-MB-231cell line and a Raji cell line were used as positive and negative controls for expression (Gallagher et al., 2007, Lin et al., 1998a).

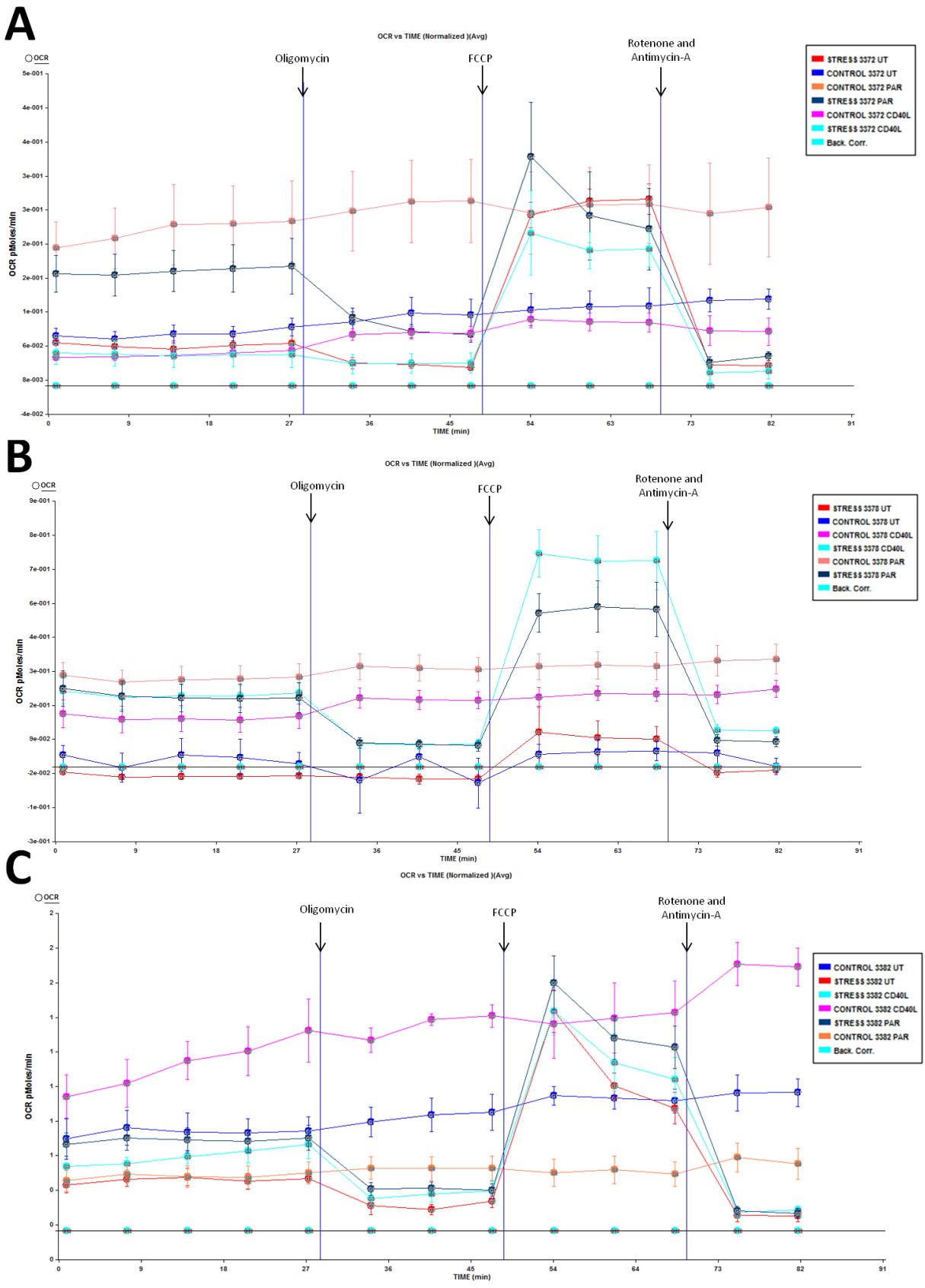
A
OCR vs TIME (Normalized)(Avg)
OCR
Oligomycin
FCCP
Rotenone and
Antimycin-A
STRESS 3372 UT
CONTROL 3372 UT
CONTROL 3372 PAR
STRESS 3372 PAR
CONTROL 3372 CD40L
STRESS 3372 CD40L
Back. Corr.
OCR pMoles/min
TIME (min)
B
OCR vs TIME (Normalized)(Avg)
OCR
Oligomycin
FCCP
Rotenone and
Antimycin-A
STRESS 3378 UT
CONTROL 3378 UT
CONTROL 3378 CD40L
STRESS 3378 CD40L
CONTROL 3378 PAR
STRESS 3378 PAR
Back. Corr.
OCR pMoles/min
TIME (min)
C
OCR vs TIME (Normalized)(Avg)
OCR
Oligomycin
FCCP
Rotenone and
Antimycin-A
CONTROL 3382 UT
STRESS 3382 UT
STRESS 3382 CD40L
CONTROL 3382 CD40L
STRESS 3382 PAR
CONTROL 3382 PAR
Back. Corr.
OCR pMoles/min
TIME (min)

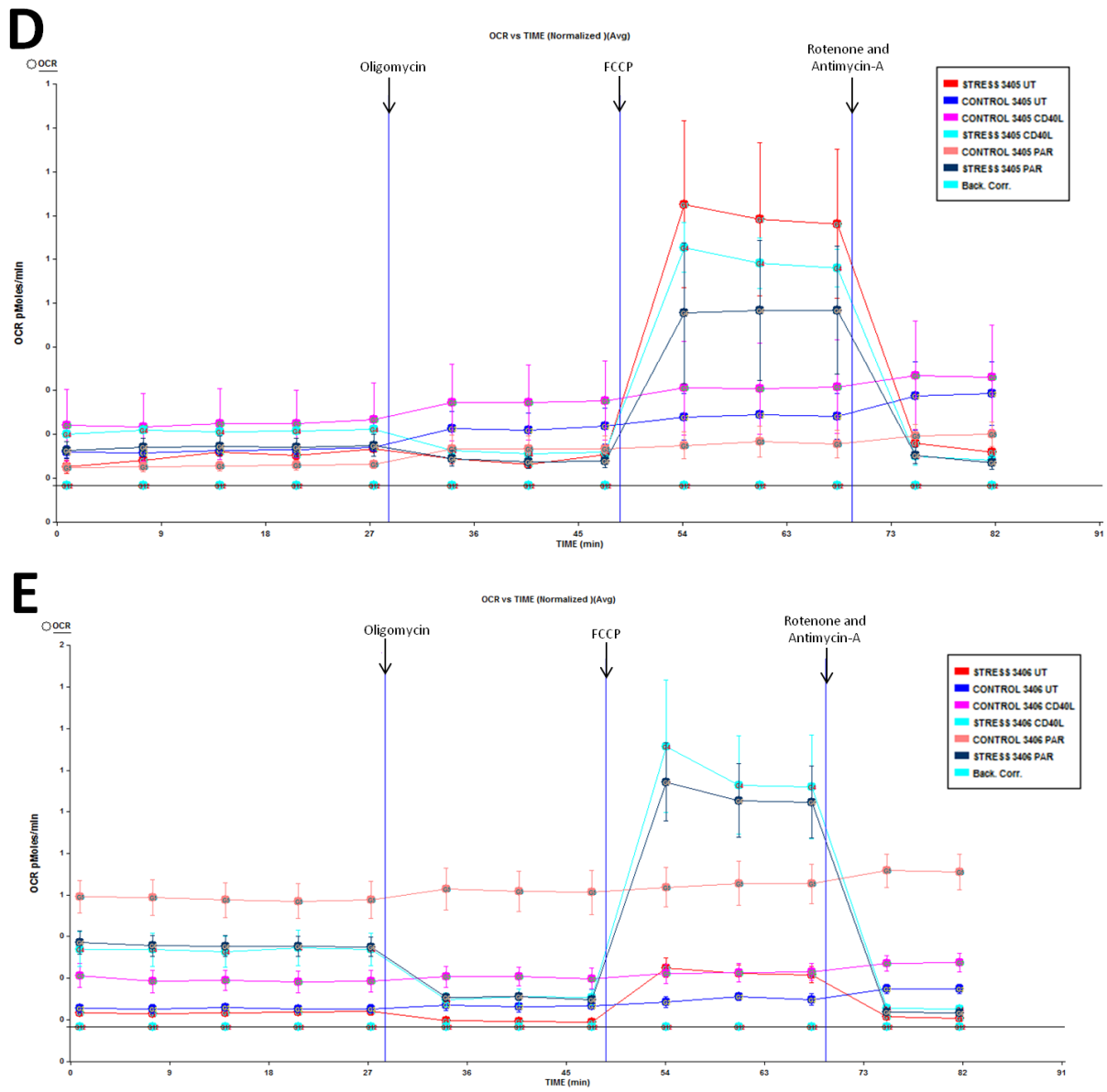

Figure 3.40: Change in OCR in response to mitochondrial stressors. Fresh CLL cells (2 x 10^6 cells/well) were co-cultured with CD40L or parental fibroblasts or cultured alone (UT) for 48 hours. Cells were subjected to a mitochondrial stress test (oligomycin 1.26µM, FCCP 1.5µM, and rotenone and antimycin-A 1µM). OCR (pMoles/min/µgDNA) was measured.

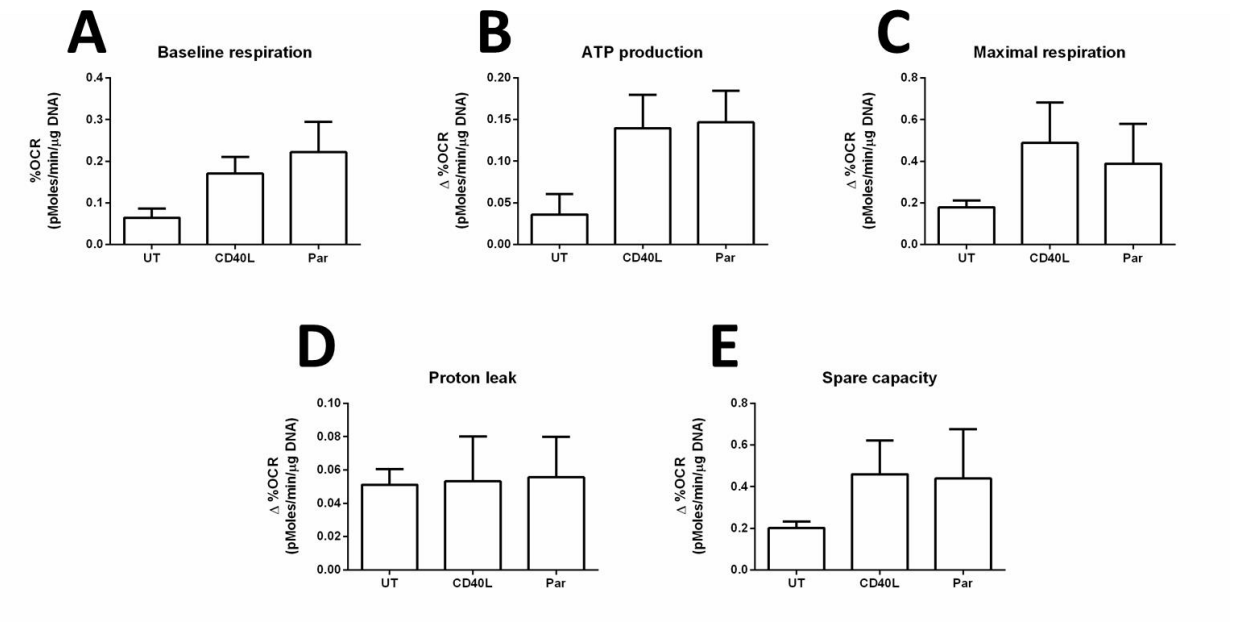

Figure 3.41: Examining the effect of CD40L stimulation on oxidative phosphorylation. Graphical presentation of data shown in Figure 3.40. Changes in OCR (pMoles/min/µgDNA) were measured in response to the mitochondrial stressors to calculate; basal respiration, ATP production, proton leak, maximal respiration, and spare respiratory capacity (n = 5). A Wilcoxon test revealed there to be no significant change in any of these parameters in CLL cells following co-culture with CD40L and parental fibroblasts (P = > 0.05).

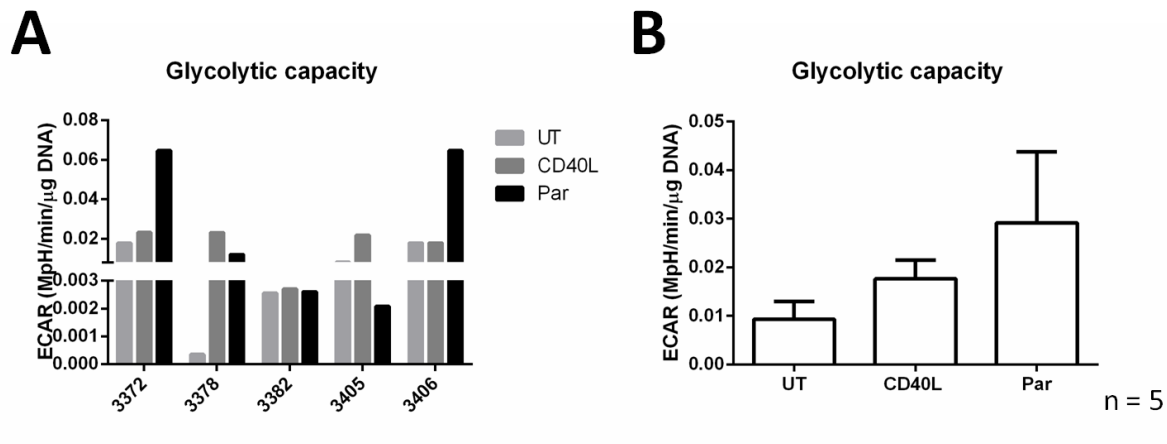

Figure 3.42: Examining the effect of CD40L stimulation on glycolysis. Fresh CLL cells (2 x 10^6 cells/well) were co-cultured with either; no supportive cells (UT), CD40L fibroblasts or parental fibroblasts for 48 hours. To assess glycolytic capacity oligomycin 1.26µM was added and ECAR (mpH/min/µgDNA) was measured (n = 5). **(A)** Shows the glycolytic capacity for each case under each culture condition. **(B)** Comparison of all of the cases tested showed there to be no significant change in the glycolytic capacity of CLL cells following co-culture with CD40L and parental fibroblasts (P = > 0.05, Wilcoxon test).

3.4 DISCUSSION

This chapter further examines MCT -1 and -4 expression on CLL cells by assessing the expression of these transporters in response to microenvironmental stimuli, specifically CD40 ligation. Chapter 2 showed that MCT -1 and -4 expression is reduced in non-dividing CLL cells located in the circulation in comparison to their healthy counterparts. As previously discussed, proliferation of CLL cells is localised in the secondary tissues (van Gent et al., 2008) and stimulation of CLL cells using CD40L has been shown to induce cell division (Pascutti et al., 2013, Scielzo et al., 2011). This process is likely associated with an increase in metabolic activity because entry of normal B cells into S phase has been shown to prompt a metabolic switch to glycolysis (Garcia-Manteiga et al., 2011) thus it is likely that CLL cell contact with CD40L causes proliferation associated metabolic changes and may have increased reliance on monocarboxylate transport. The aim of this chapter was to examine the effect of CD40-CD40L engagement on expression of MCT -1 and -4, and whether this is associated with enhanced metabolic activity.

The principle finding of this chapter is that ligation of CD40 on primary CLL cells upregulates MCT4 expression. This upregulation is best observed when CLL cells are co-cultured with CD40L fibroblasts. However, co-culture of CLL cells with fibroblasts, either CD40L or parental, induces expression of MCT1. This suggests that the microenvironment affects CLL cells such that they require increased monocarboxylate transport. This effect seems to work reciprocally, especially under the condition where CLL cells are co-cultured with CD40L fibroblasts. Here, MCT4 expression is stimulated in the host fibroblasts.

To investigate why MCT4 expression increases in CD40-stimulated CLL cells an analysis of metabolic gene expression was carried out using a Fluidigm Biomark™ array. For this experiment only cells more than 70% viability were used to ensure that fibroblasts with the maximum potential for stimulating CLL cells and CLL cells with the maximum potential for being stimulated were used. Here is was found that in response to CD40L there is an upregulation in expression of genes involved in glycolysis and fatty acid metabolism. This is in keeping with a study by Gricks et al.

(2004) whereby gene expression was assessed in normal B cells and CLL following CD40 activation. In this study it was reported that such stimulation results in increased metabolic gene expression. Changes in metabolic gene expression in CLL cells responding to CD40 engagement are also reported by Willimott and Wagner (2012) and Jiang et al. (2012) where the expression of microRNA's (miR's) was examined. Here, miR's, such as *miR-155*, are increased in CLL cells in response to CD40 ligation, and the effect of these miR's is to influence the expression of genes involved in glucose metabolism such as HK2 (Jiang et al., 2012). The results of the current study show increase in expression of HK1 and HK2.

To further study glucose metabolism in CD40-stimulated CLL cells direct analysis of cell metabolism was performed by metabolic flux analysis. Thus, CLL cells co-cultured with CD40L fibroblasts consistently increase glycolytic capacity in agreement with the data generated by the gene array. This finding is in keeping with what is observed in normal B cells which have been stimulated to proliferate (Garcia-Manteiga et al., 2011). However, CD40 ligation on CLL cells does not induce proliferation, a second stimulus, either IL-4 or IL-21, is required (Pascutti et al., 2013, Ghia et al., 2005). CD40 stimulation alone may therefore prepare CLL cells metabolically for entry into S phase of the cell cycle. Variability in the extent of glycolytic capacity induction between patient samples limits the strength of this interpretation; further replicates are required to provide verification.

Mitochondrial function in CLL cells seemed maintained by co-culture with CD40L fibroblasts. 3 of the 5 CLL cases tested showed consistent increases in mitochondrial indices such as baseline respiration, ATP production, maximal respiration and spare capacity. This is important because a recent study has shown that circulating CLL cells use mitochondrial metabolism and have resulting in the increased production of ROS (Jitschin et al., 2014). Increased levels of ROS are cytotoxic to cells unless they have a mechanism in place to counteract the oxidative stress created by ROS. Induction of glycolysis is one of these mechanisms. Therefore, the results of this chapter provide insight into cytoprotective effects of CD40 ligation on CLL cells. Moreover, increased ROS levels within malignant cells can be harnessed to mediate change in the

surrounding tumour stroma (Martinez-Outschoorn et al., 2011). It is possible that CD40 ligation on CLL cells facilitates the ability of these cells to produce ROS and thereby provide a potential mechanism through which CLL cells influence the metabolism of supportive cells.

That CLL cells can affect supportive cells is demonstrated by Fluidigm array analysis of gene expression in CD40L and parental fibroblasts. Co-culture of CD40L fibroblasts with CLL cells seemed to induce expression of genes involved in glycolysis. In particular, MCT4 expression was induced, and this was confirmed by Western blot analysis. A study by Martinez-Outschoorn et al. (2013) describes a similar result and shows that upregulated MCT4 expression accompanied by an increase in glycolysis is induced in fibroblasts following co-culture with HaCaT cells, a keratinocyte cell line which has a high proliferative capacity. The ability of cancer cells to exert an influence over the metabolism of supportive cells within the microenvironment has been described in other malignancies (Bonuccelli et al., 2010b, Martinez-Outschoorn et al., 2013). Taken together, these data suggest that future experiments are required to examine the mechanisms through which CLL cells can manipulate the metabolism of the adjacent stromal cells.

In addition to the increased expression of genes associated with glycolysis, CD40 activation of CLL cells also had an effect on fatty acid metabolism. ELOVL6 and FASN, and to a lesser degree ACACA, were all upregulated suggesting that fatty acid synthesis (FAS) is stimulated. This is important because it suggests that CLL cells may utilise fatty acids to fuel energy generating processes to support cell division (Cheng et al., 2014). In particular, increased expression of FASN is reported in other malignancies, and has been shown to be correlated with disease progression (Hamada et al., 2014, Long et al., 2014, Menendez and Lupu, 2007). The importance of fatty acid metabolism in CLL has not been fully explored although oxidation of fatty acids in circulating CLL cells has been shown in studies by Tung et al. (2013) and Spaner et al. (2013) showing these cells to be vulnerable to disrupted lipolysis.

The upregulation of other metabolic genes in response to CD40L such as GLS and ME2 may facilitate FAS. For instance, GLS and ME2 are involved in glutaminolysis and the TCA cycle, and have the ability to provide substrates for FAS while increased expression of SLC1A5 and SLC25A11 aids substrate uptake (Hassanein et al., 2013, Catalina-Rodriguez et al., 2012). Alternatively, the upregulation of GLS may be indicative of a "glutamine addiction" whereby the cells rely on glutaminolysis as their primary energy generating process as is the case in cervical cancer (Jose et al., 2011, Vousden, 2010). However, this is unlikely to be the case in CLL because inhibition of glycolysis using lonidamide and 2DG has been shown to induce cell death (Tura et al., 1984, Tidmarsh et al., 2004).

In conclusion, the findings presented in this chapter shows for the first time that the microenvironment modulates the expression of MCT -1 and -4 in CLL cells. Specifically contact of CLL cells with fibroblasts may induce MCT1 expression whereas MCT4 is upregulated in CLL cells following CD40 ligation. The data collected from the Fluidigm Biomark™ array and SeahorseXF24 implies this is likely due to the induction of glycolysis, and that CLL cells may instigate changes in the metabolism of the supportive cells of the microenvironment. This is important because it suggests that CLL cells may become vulnerable to disrupted monocarboxylate transport, specifically MCT4 inhibition. Moreover, because the upregulation of MCT4 is mediated by CD40L this has the potential to overcome CD40L dependent mechanisms of drug resistance. However, further work is needed to truly assess whether the degree of CD40L-mediated glycolysis induction in CLL cells is large enough to sensitise these cells to disrupted monocarboxylate transport.

4 CHAPTER 4: ASSESSING THE SENSITIVITY OF CLL CELLS TO MCT -1 AND -4 INHIBITION

4.1 INTRODUCTION

Recognition of the importance of cell metabolism with respect to cancer biology has lead to an increase in compounds directed against metabolic processes. One of the aims of this study is to examine the effect of disrupting monocarboxylate transport by inhibiting MCT1 function in CLL cells using the specific inhibitor, AZD3965. This compound is a small molecule inhibitor which exerts its effect on MCT1 by binding to the transporter and disrupting glycolytic activity by preventing lactate export (Polanski et al., 2014). It is derived from a similar compound known as AR-C155858, that was originally developed because of its activity as an immunosuppressive agent (Ekberg et al., 2007), and this fits with known upregulation of glycolysis in antigen stimulated B and T cells (Garcia-Manteiga et al., 2011, Michalek and Rathmell, 2010).

MCT1 as a therapeutic target has been investigated in several types of cancer. For instance, MCT1 inhibition has been shown to have anti-tumor effects in lung, breast, colorectal, and prostate cancers, as well as in brain tumors (Guo et al., 2013, Miranda-Goncalves et al., 2013, Doherty et al., 2013, Kim et al., 2012, Shim et al., 2007, Zhang et al., 2002). Moreover, a study by Sonveaux et al. (2008) showed that inhibiting MCT1 function in tumor-adjacent endothelial cells disrupted tumor angiogenesis. In B cell malignancies MCT1 inhibition has been examined in lymphoma, and has been taken forward into phase I/II clinical trials (Doherty et al., 2013, Kumar et al., 2013, Dhup et al., 2012, Cheong et al., 2012).

Following on from the examination of MCT -1 and -4 expression in CLL cells in the previous chapters of this thesis, the aim of this chapter is to examine the potential of MCT1 as a therapeutic target in CLL. This was done by investigating the sensitivity of CLL cell lines to AZD3965, and examining any potential additional role of MCT4.

4.2 MATERIALS AND METHODS

4.2.1 Suspension cell lines

The HG3 cell line, which are Epstein Barr Virus-transformed CD40-stimulated CLL cells, were obtained from Professor Anders Rosén (Linköping University, Sweden) (Rosen et al., 2012). Details of the other cell lines used in this section are detailed in section 2.2.1.3. Prior to use each of the cell lines were tested for the presence of mycoplasma (Appendix 6.3). These analyses were performed using an EZ PCR Mycoplasma test kit (Biological Industries, Salisbury, Cellseco, UK) in accordance with the manufacturer's guidelines.

4.2.2 Cell culture

HG3 cells were maintained in RPMI supplemented with 100 units/mL penicillin-streptomycin, 2mM L-glutamine, and 10% heat inactivated FCS. The other cell lines were maintained as previously described.

4.2.3 Treatment with MCT1 inhibitor AZD3965

The MCT1 inhibitor AZD3965 was provided by AstraZeneca (AstraZeneca, Manchester, UK). A 10mM stock was prepared in DMSO and aliquots were stored at -20°C to avoid repeat freeze thawing. DMSO was used as a diluent to obtain working concentrations of this drug. Assays were normally carried out in a flat bottomed 96 well plate using 100µl of Raji cells (2 x 10^5 cells/mL), MEC-1 cells (2 x 10^5 cells/mL) or HG3 cells (1 x 10^5 cells/mL). Each experiment was run in triplicate. Plates were incubated for 48-72 hours at 37°C and 5% CO_2.

4.2.4 Alamar blue® cell viability assay

Cell viability was assessed using AlamarBlue® Cell viability reagent according to the manufacturer's instructions (Invitrogen, Paisley, UK). For this assay a blacked out 96

well plate with a clear flat bottom was used (BD Biosciences, Oxford, UK). The plate was prepared as in section 4.2.3. The plate was read using the MQX200 µQuant plate reader at 540nm (samples) and 620nm (blank) as per the manufacturer's guidelines.

4.2.5 3,3'-Dihexyloxacarbocyanine Iodide ($DiOC_6$) and Propidium iodide (PI) staining for cell death

Following incubation with AZD3965 50µL of each well was transferred to a FACS tube. To this 50µL of 80nM 3,3'-dihexyloxacarbocyanine Iodide ($DiOC_6$) (Merck KGaA, Middlesex, UK) was added and the samples were incubated for 20 minutes in the dark at 37°C. 100µL of propidium iodide (PI) (Sigma, Gillingham, UK) was then added (1:1 final concentration 0.1µg/mL) and the samples were analysed using the BD™ FACS Calibur™.

4.2.6 Metabolic flux analysis of Raji and MEC-1 cells using the SeahorseXF24 metabolic flux analyser

As detailed in section 3.2.10. Seeding densities of 2 x 10^6 cells/mL was used for the Raji cells while 5 x 10^6 cells/mL was used for the MEC-1 cells. Experiments on MEC-1 cells were carried out using unbuffered DMEM (Sigma, Gillingham, UK) modified with 10mM glucose (Sigma, Gillingham, UK), 2mM L-glutamine and 2mM sodium pyruvate. For injection of the MCT1 inhibitor AZD3965, this was first prepared as in section 4.2.3 using appropriate unbuffered media. The designated concentrations including an untreated (UT) media only and DMSO vehicle control (DMSO) were then added (50µL) into injection port A of the XF24 calibration microplate (Seahorse Bioscience, Saint Marcell, France). Measurements were taken every 6 minutes for 5 hours and values were later normalised to the baseline and DNA content.

4.2.7 Nucleofection

siRNA and plasmid transfections were carried out using nucleofection. A cell suspension of 2 x 10^6 cells/mL of MEC-1 or Raji cells was allowed to recover in the

incubator at 37°C and 5% CO_2 for 1 hour. 1mL aliquots of MEC-1 or Raji cells were then added into a sterile eppendorf tube and centrifuged at 500 rcf for 5 minutes and washed in warm PBS (37ºC). After removing the supernatant the samples were nucleofected using the Amaxa solution V transfection kit according to the manufacturer's instructions (Lonza Biologics, Slough, UK). The nucleofector program used for MEC-1 cells was X-01. The nucleofector program used for Raji cells was M-13.

4.2.8 MCT4 knockdown using siRNA

Cells were treated with either specific MCT4 siRNA (Insight Biotechnology, Wembley, UK) or a scrambled control (Insight Biotechnology, Wembley, UK) at a final concentration of 0.1μM. To assess transfection efficiency a sample was also nucleofected with a GFP plasmid (Lonza Biologics, Slough, UK) and assessed for GFP expression after 24 hours using flow cytometry.

4.2.9 Transient transfection with MCT4 expression vector

4.2.9.1 Plasmid

A pMCT4-EGFP expression vector was kindly provided by Dr Nancy Philp (Thomas Jefferson University, PA, USA). Details relating to the production of this plasmid can obtained from a publication by Castorino et al. (2011).

4.2.9.2 Plasmid preparation

4.2.9.2.1 Transformation of *E coli*

0.5μL of plasmid DNA was added to a sterile eppendorf at 4ºC. Next 25μL of DH5α competent cells (Invitrogen, Paisley, UK) were thawed on ice and added to the plasmid DNA and incubated for a further 20 minutes at 4ºC. The cells were then heat shocked at 42ºC for 50 seconds and then put back on ice for 2 minutes after which an aliquot of

950µL of sterile super optimal broth with catabolite repression (SOC) medium (Sigma, Gillingham, UK) was added at room temperature. This reaction mixture was subsequently incubated at 37ºC for 1.5 hours with constant shaking at 150 rpm. Following the incubation period either 10µL or 100µL of the reaction mixture was added to LB-kanamycin agar plates (Sigma, Gillingham, UK) and incubated overnight at 37ºC for less than 16 hours to ensure the kanamycin (Sigma, Gillingham, UK) maintained its efficacy. The plates were then wrapped in parafilm and stored at 4ºC. Colonies were extracted using a sterile pipette tip which was placed into 5mL of LB-kanamycin broth in a universal and cultured overnight at 37ºC at 150 rpm. The plates were then stored at 4ºC. After 16 hours the cultures were also stored at 4ºC.

4.2.9.2.2 Selection of transformed *E coli*

To select for transformed colonies a LB-kanamycin (0.01mg/mL) selection plate was used. The pEGFP-N1 vector confers kanamycin resistance thus cells successfully transformed with the plasmid are resistant to the drug.

4.2.9.2.3 Isolation of plasmid DNA

Plasmid DNA was isolated using a Zyppy™ plasmid miniprep kit (Zymo research, Cambridge Bioscience, Cambridge, UK) as per the manufacturer's instructions. Quantification of the DNA was performed using a NanoDrop 2000c spectrophotometer. Sample quality was assessed using the measurement of the 260:280 ratio.

4.2.9.3 DNA Sequencing

The pMCT4-EGFP plasmid was sequenced to ensure the plasmid contained MCT4 using four forward primers (Figure 4.1) designed using GenScript Sequencing Primer Design (WWW, genscript.com/cgi-bin/tools/sequencing_primer_design) in addition to in house CMV forward and EGFP-N1 reverse primers from Source Bioscience (Nottingham, UK). Sequencing was performed by Source Bioscience (Nottingham, UK) and then subjected to a Basic Local Alignment Search Tool (BLAST) search for

human MCT4. Figure 4.2 shows the results of the sequencing and the analysis demonstrating the 100% alignment of MCT4.

4.2.10 Western blot analysis

As detailed section in 2.2.8.

4.2.11 Antibodies

As detailed in section 2.2.5. In addition to this mouse monoclonal anti-GFP (sc-9996) (Insight Biotechnology, Wembley, UK) was also used.

Primer	Sequence
1	*TACCATGGTGATGCGGTTTT*
2	atcggctacagcgacacag
3	ctcaactgctgcgtgtgtg
4	cctcgtggtcttctgcatct

Figure 4.1: Primers used for DNA sequencing of the pMCT4-EGFP plasmid. Primer 1 is located in the multiple cloning site (MCS) while primers 2-4 are located within the MCT4 sequence.

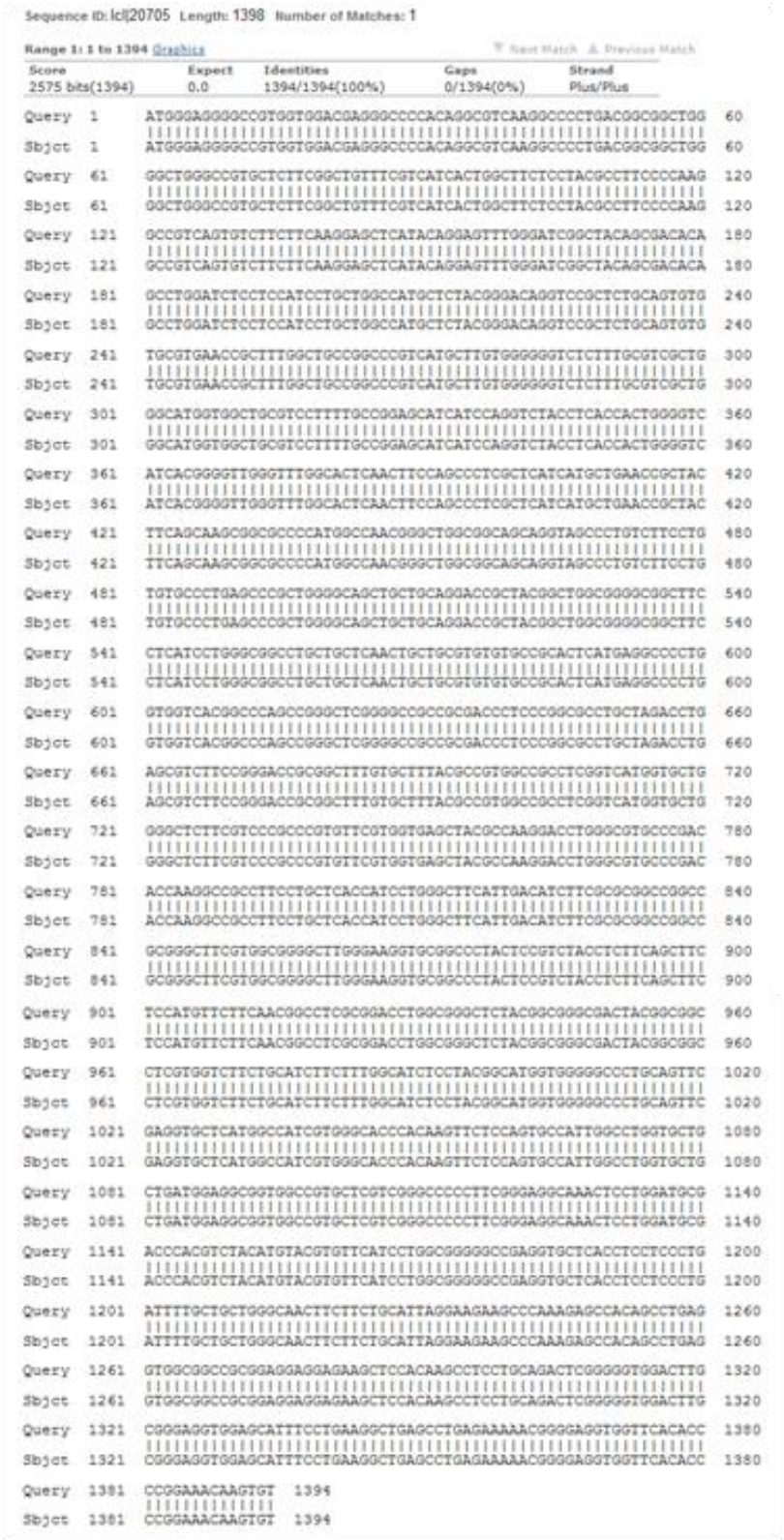

Figure 4.2: BLAST analysis for MCT4 in pMCT4-EGFP plasmid.

4.2.12 Quality assurance

To control for the solvent used to dissolve AZD3965 a vehicle control of 5µL 6% DMSO was added to a 95µL cell suspension (final concentration 0.3%). This was used to control for the toxicity of the DMSO which has been shown to cause cell death at room temperature.

To ensure that the $DiOC_6$ and PI cell death and Alamar blue® cell viability assays were working a death inducing positive control was used. 10nM of staurosporine was used for this purpose as described (Twomey et al., 1990). This was added 4 hours prior to the addition of the AlamarBlue® Cell viability reagent 4 hours prior to analysis by $DiOC_6$ and PI staining. A *P* value of $P = <0.05$ was considered to be statistically significant.

4.2.13 Statistical analysis

Statistical analyses were performed using GraphPad Prism (Version 6.01, GraphPad Software Inc., CA, USA). The statistical tests used are identified when and where they are used within the results section of this chapter. A *P* value of $P = <0.05$ was considered to be statistically significant.

4.3 RESULTS

4.3.1 Pre-clinical evaluation of the MCT1 inhibitor AZD3965 in CLL

4.3.1.1 Inhibition of MCT1 using AZD3965 in a Raji cell line

Raji cells only express MCT1, and are susceptible to AZD3965. Preliminary data obtained from AstraZeneca shows that these cells undergo apoptosis when exposed to nanomolar concentrations [IC_{50} of 10nM (0.01µM)] of this compound. Therefore, they serve as a positive control for subsequent experiments.

Proliferation of Raji cells was first determined so that an optimal seeding density could be obtained. Figure 4.3 shows a cell counting experiment in which the cells were plated out in a 24 well plate at the following densities; 1 x 10^5, 2 x 10^5 and 4 x 10^5 cells/mL. The experiment was run over a period of four days to account for the amount of time the cells would be incubated with the compound. Cell counts were performed in duplicate using the trypan blue exclusion assay as previously described in section 2.2.2. A density of 2 x 10^5 cells/mL was chosen as cells continued to double for the four day time period whereas at 4 x 10^5 cells/mL the count no longer increased after day three. This is in agreement with the seeding density optimised by AstraZeneca who also used 2 x 10^5 cells/mL.

Flow cytometry was used to measure $DiOC_6$ and PI staining and assess cell death in experiments measuring the cytotoxicity of AZD3965. Figure 4.4 illustrates the gating procedure used to distinguish live from dead cells. A typical dotplot of side scatter versus forward scatter shows two distinct populations of the total number of cells to be analysed, and this was designated R3. Live cells are gated within region 2 (R2) and show up as $DiOC_6^{bright}$ PI^{dim} cells (upper left hand quadrant, marked in green) in the quadrant plot of $DiOC_6$ versus PI. Dead or late apoptotic cells are gated with region 1 (R1), and show up as $DiOC_6^{dim}$ PI^{bright} cells (lower right hand quadrant, marked in red) in the quadrant plot of $DiOC_6$ versus PI. Treatment of Raji cells with 0.01µM of

AZD3965 resulted in an increase in the number of cells included within R1 [compare Figure 4.4 (A) with 4.4 (B)].

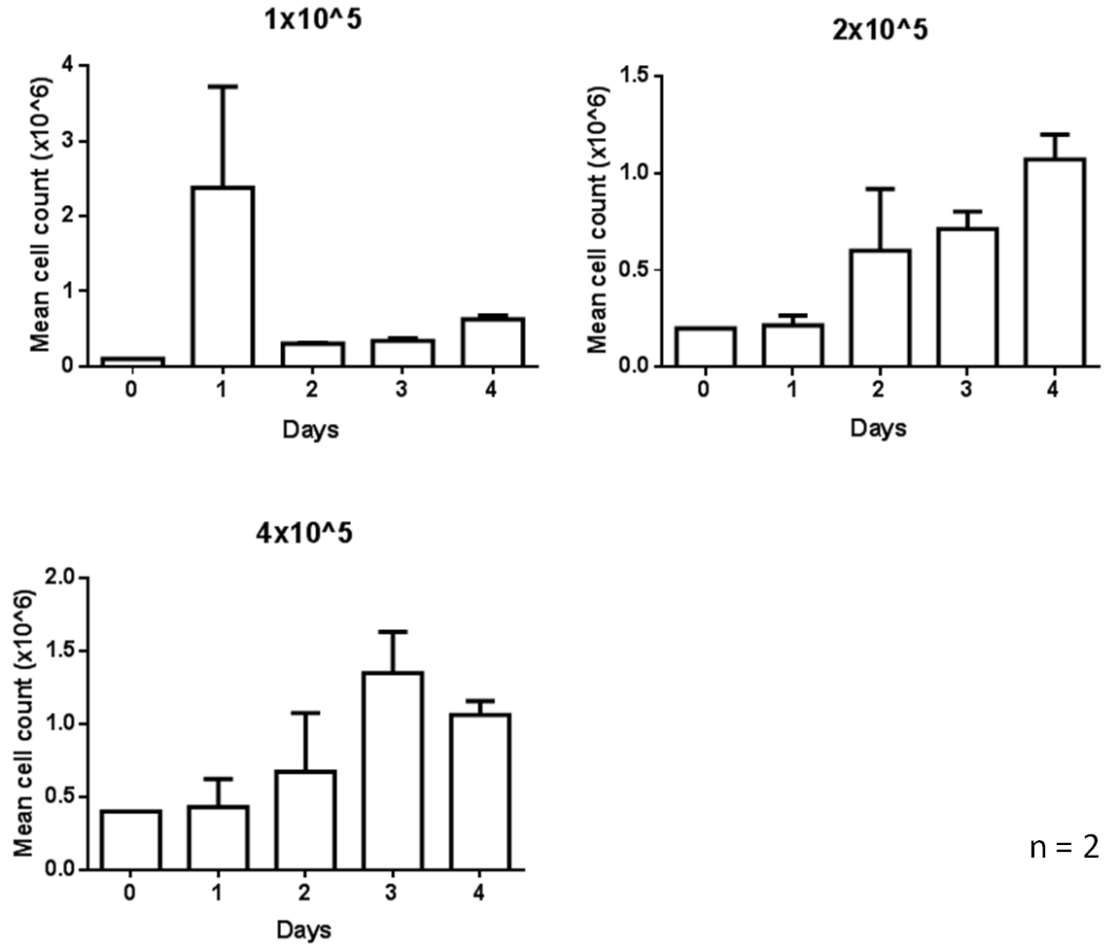

Figure 4.3: Evaluation of seeding density for the Raji cell line. Cells were plated out in a 24 well plate at the following densities; 1 x 10^5, 2 x 10^5 and 4 x 10^5 cells/mL. Cell counts were performed in duplicate using the trypan blue exclusion assay. A density of 2 x 10^5 cells/mL was chosen as cells continued to double for the four day time period whereas at 4 x 10^5 cells/mL the count no longer increased after day three. Error bars are the SEM.

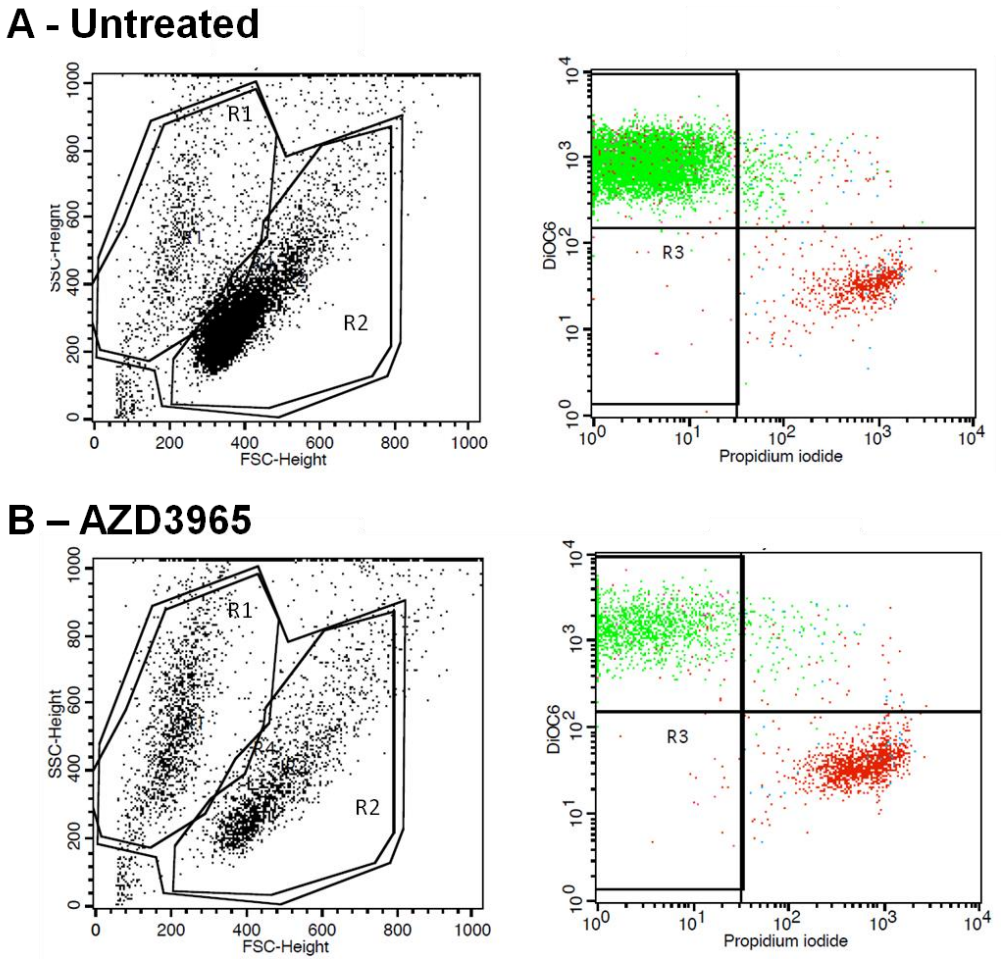

Figure 4.4: 3,3'-Dihexyloxacarbocyanine Iodide ($DiOC_6$) and Propidium iodide (PI) staining for cell death. A representative example of the gating strategy used for analysis by flow cytometry. The two distinct populations of the total number of cells to be analysed shown in the dotplot are designated R3. Live (R2) and dead/late apoptotic (R1) cell populations correspond to the live cells (green) which are $DiOC_6$ positive/PI negative and dead cells (red) which are $DiOC_6$ negative/PI positive respectively. **(A)** Raji cell untreated (UT) control. **(B)** Raji cells treated with 0.01µM of AZD3965.

Figures 4.5 and Figure 4.6 show the killing effect of AZD3965 on Raji cells after 48 hours treatment. The Raji cells were seeded at a density of 2 x 10^5 cells/mL and incubated with 0, 0.001, 0.01, 0.1 and 1μM of AZD3965. There was no significant difference in $DiOC_6$ and PI staining between UT and DMSO vehicle control treated Raji cells ($DiOC_6$; $P = 0.1100$, PI; $P = 0.2143$), providing confirmation for the inert nature of the DMSO solvent used to dissolve AZD3965. Increasing cell death was observed with increasing concentration of AZD3965 over the concentration range tested, and 0.1μM was shown to be the most effective at inducing apoptosis of Raji cells ($DiOC_6$; *** $P = 0.0008$, PI; ** $P = 0.0019$) (n = 3).

Figure 4.6 verifies the results obtained using $DiOC_6$ and PI staining. Here, a AlamarBlue® Cell viability assay showed that 0.1μM of AZD3965 was the most effective concentration at reducing cell viability (** $P = 0.0052$).

In both Figures 4.5 and 4.6 staurosporine was used to induce apoptosis in cells. In each figure the presence of this compound reduced cell viability.

Taken together, these results show that 0.1μM of AZD3965 could be used for future experiments.

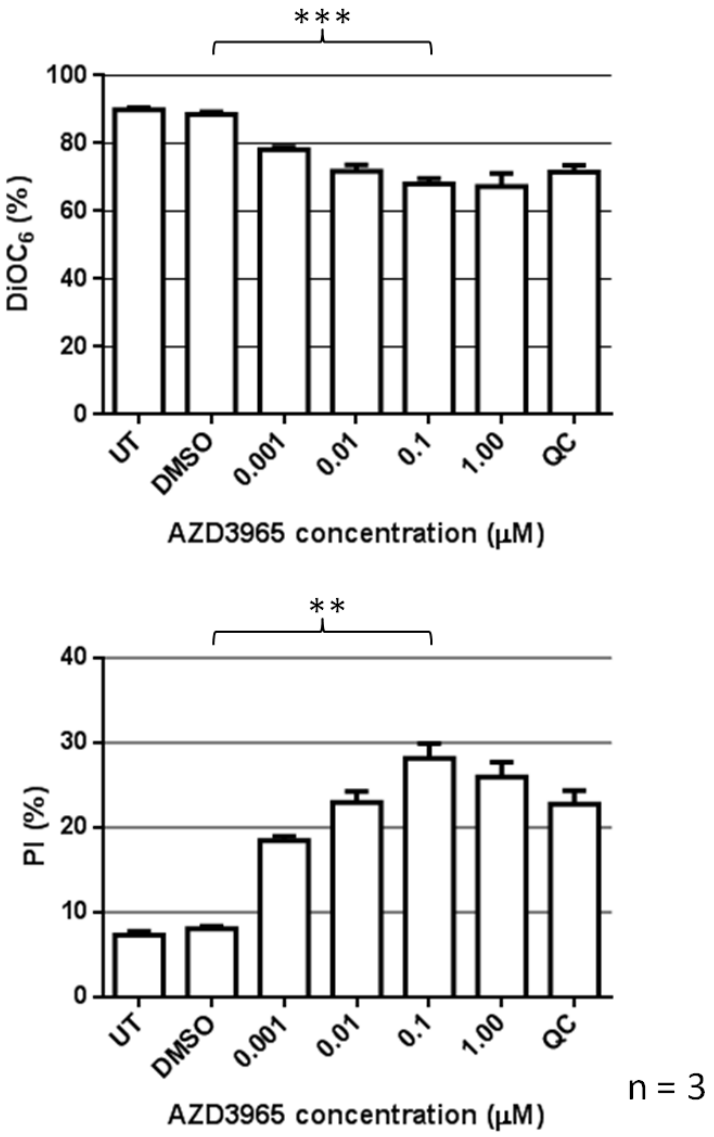

Figure 4.5: Inhibition of MCT1 using increasing concentrations of AZD3965 in a Raji cell line ($DiOC_6$ and PI staining). Raji cells (2×10^4) were incubated with AZD3965 (0-1μM) for 48 hours. A paired t test showed there was no significant difference between the UT and DMSO vehicle control ($DiOC_6$; $P = 0.1100$, PI; $P = 0.2143$). A significant difference was seen between the vehicle control versus each concentration of the drug with 0.1μM of AZD3965 being the most effective ($DiOC_6$; *** $P = 0.0008$, PI; ** $P = 0.0019$). 10nM staurosporine was used as a positive control (QC). Error bars are the SEM.

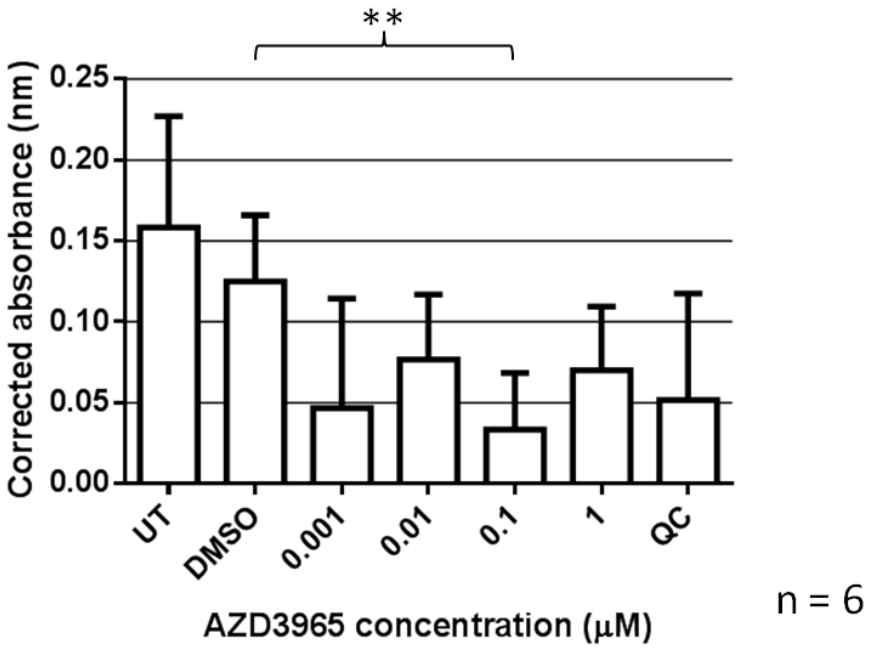

Figure 4.6: Inhibition of MCT1 using increasing concentrations of AZD3965 in a Raji cell line (Alamar blue® cell viability assay). Raji cells (2 x 10^4) were incubated with AZD3965 for 48 hours. A paired t test showed there was no significant difference between the UT and DMSO vehicle control (P = 0.1747). A significant difference was seen between the vehicle control and each concentration of the drug 0.001-1μM (P = <0.05) excluding 0.01μM (P = >0.05). 0.1μM of AZD3965 was shown to be the most effective (** P = 0.0052). 10nM staurosporine was used as a positive control (QC). Error bars represent the SEM.

4.3.1.2 Investigating the effect of proliferation on the sensitivity of the Raji cell line to AZD3965

The effect of AZD3965 on Raji cells cultured under different proliferation conditions was next examined because metabolic activity within cells can be linked to their ability to divide (Garedew et al., 2012). To assess the effect of proliferation on the sensitivity of the Raji cells to AZD3965 the cells were cultured in serum rich (10% FCS) and serum free media (SFM) and incubated with 0.1μM of the drug. Figure 4.7 shows a cell counting experiment which was used to ensure the Raji cells ceased to divide in serum free conditions whilst they continued to proliferate in the presence of FCS (n = 3). Figure 4.8 shows that Raji cells cultured in serum rich conditions are sensitive to MCT1 inhibition with AZD3965, while Raji cells cultured in serum free conditions remained resistant to the drug. Importantly, the presence of staurosporine induced apoptosis of Raji cells regardless of culture conditions. These data suggest that AZD3965 is effective only on proliferating cells.

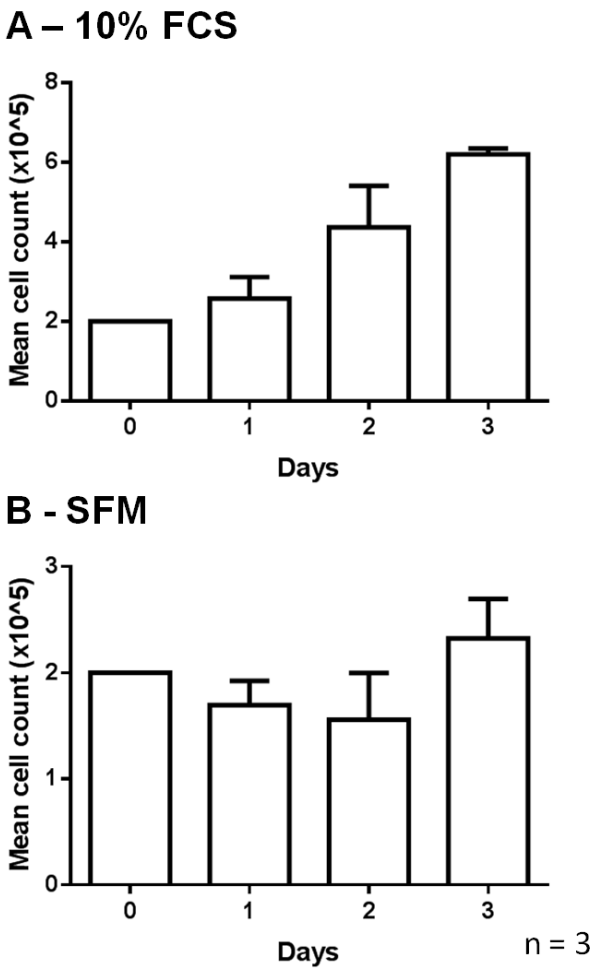

Figure 4.7: Cell counting experiment to show the effect of serum free media on proliferation of Raji cells. Raji cells were seeded at 2 x 10^5 cells/mL and grown over a 3 days period in **(A)** RPMI media supplemented with 100 units/mL penicillin-streptomycin, 2mM L-glutamine and 10% heat inactivated FCS or **(B)** SFM supplemented with 100 units/mL penicillin-streptomycin and 2mM L-glutamine. In serum rich conditions the cell count increased doubling after 2 days while in SFM the cell count did not double. Error bars represent the SEM.

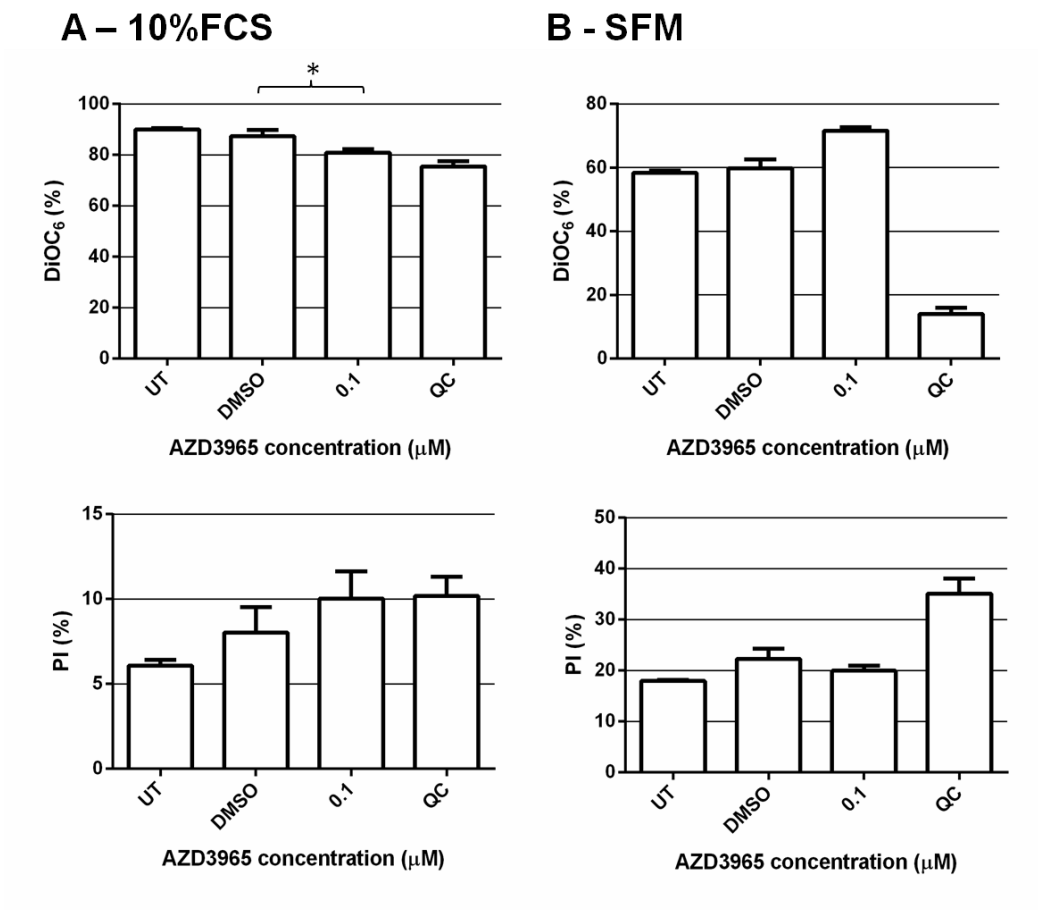

Figure 4.8: Sensitivity to AZD3965 in Raji cells cultured in serum rich and serum free media ($DiOC_6$ and PI staining) (48hrs). Raji cells (2 x 10^4) were incubated for 48 hours with AZD3965 in **(A)** RPMI media modified with 100 units/mL penicillin-streptomycin, 2mM L-glutamine and 10% heat inactivated FCS or **(B)** Raji cells in SFM. In serum rich media a paired t test showed no significant difference between the UT and DMSO vehicle control ($DiOC_6$; $P = 0.3445$, PI; $P = 0.2353$). A significant decrease in the live cell population was observed between the vehicle control and 0.1μM AZD3965 ($DiOC_6$; * $P = 0.0490$, PI; $P = 0.0808$). In serum free conditions a paired t test showed no significant difference between the UT and DMSO vehicle control ($DiOC_6$; $P = 0.6351$, PI; $P = 0.1404$). 10nM staurosporine was used as a positive control (QC). Error bars are the SEM.

4.3.1.3 Inhibition of MCT1 using AZD3965 in a MEC-1 cell line

Following the validation of the Raji cell line as a positive control for AZD3965 the effect of MCT1 inhibition was assessed using the CLL cell line, MEC-1. Both MCT -1 and -4 expression was detected using Western blot analysis (Figures 2.9 and 2.12) and qRT-PCR (Figure 2.15), and this is akin to the expression profile seen in primary CLL cells (Figures 2.10, 2.11, 2.13, 2.14 and 2.16).

Figure 4.9 shows a cell counting experiment to assess the appropriate seeding density for these cells as done previously with the Raji cell line. Cells were plated out in a 24 well plate at the following densities; 1×10^5, 2×10^5 and 4×10^5 cells/mL. Over four days cell counts were performed in duplicate using the trypan blue exclusion assay as previously described in section 2.2.2. A density of 2×10^5 cells/mL was chosen as the cells continued to double at a higher rate than when seeded at the lower density for the four day time period despite the count dropping slightly on the final day. Further to this, use of this seeding density replicated the work with the Raji cell line meaning that the same amount of the compound would be added to the same number of cells.

Figure 4.10 (A) illustrates the effect of MCT1 inhibition in the MEC-1cell line with AZD3965 after 48 hours. Cells were seeded at 2×10^5 cells/mL and incubated with 0, 0.001, 0.01, 0.1, 1μM of AZD3965 for 48 hours. No effect of AZD3965 was observed on MEC-1 cells. In contrast, the presence of staurosporine induced significant cell death as detected using $DiOC_6$/PI staining or Alamar blue ® (Figure 4.11). Similar results were observed even if the cells were cultured for 72 hours (Figures 4.10 and 4.11). This result indicates that AZD3965 has no clear concentration effect on MEC-1 cell viability within the same range that it affects Raji cells. However, when used at 30μM, AZD3965 did reduce MEC-1 cell viability. Considering that at this concentration AZD3965 also inhibits MCT4, it is possible that the reduction in cell viability is due to inhibition of both MCT -1 and -4.

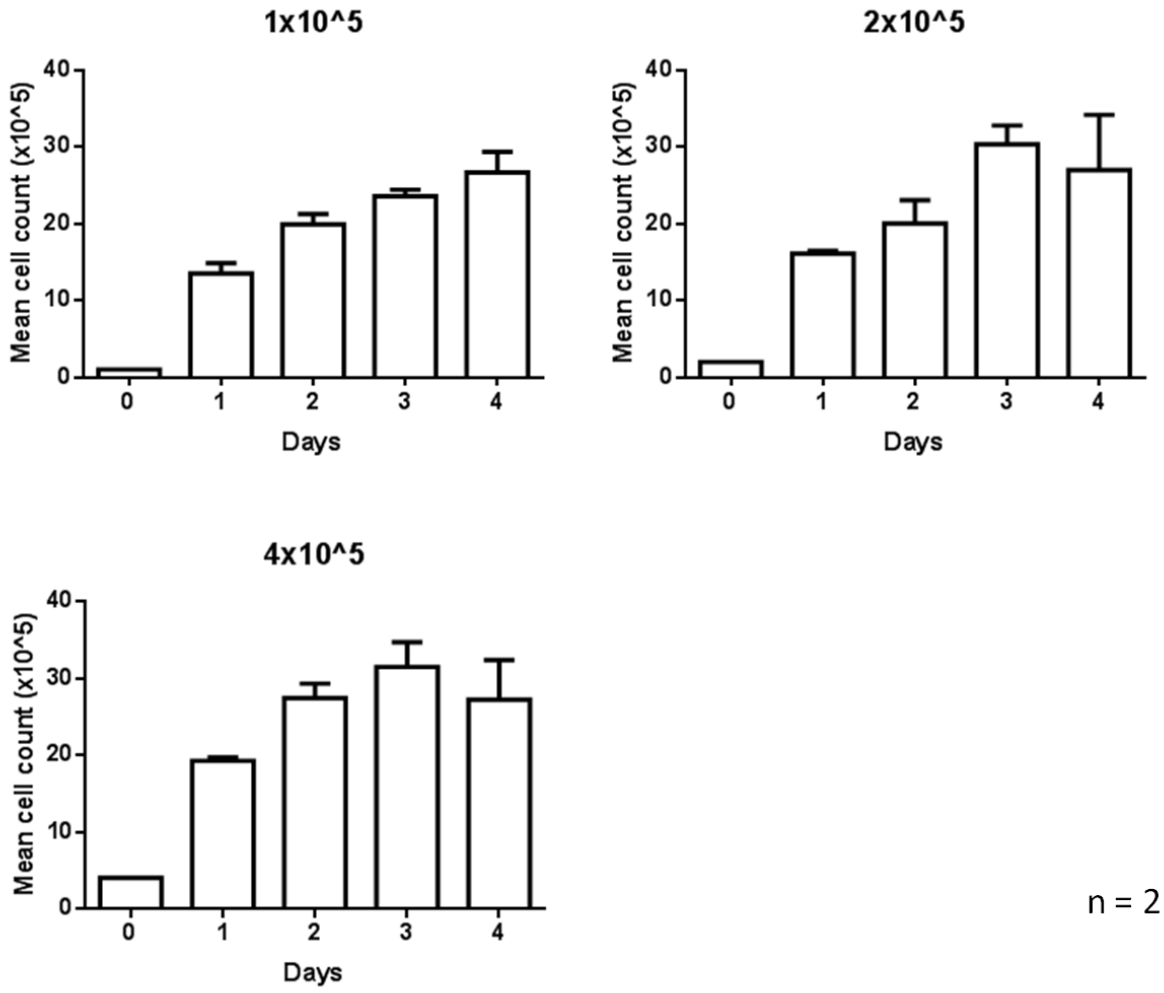

Figure 4.9: Evaluation of seeding density for the MEC-1 cell line. Cells were plated out in a 24 well plate at the following densities; 1 x 10^5, 2 x 10^5 and 4 x 10^5 cells/mL. Cell counts were performed in duplicate using the trypan blue exclusion assay. A density of 2 x 10^5 cells/mL was chosen as the cells continued to double at a higher rate than when seeded at the lower density for the four day time period despite the count dropping slightly on the final day. Further to this, use of this seeding density replicated the work with the Raji cell line meaning that the same amount of the compound would be added to the same number of cells. Error bars represent the SEM.

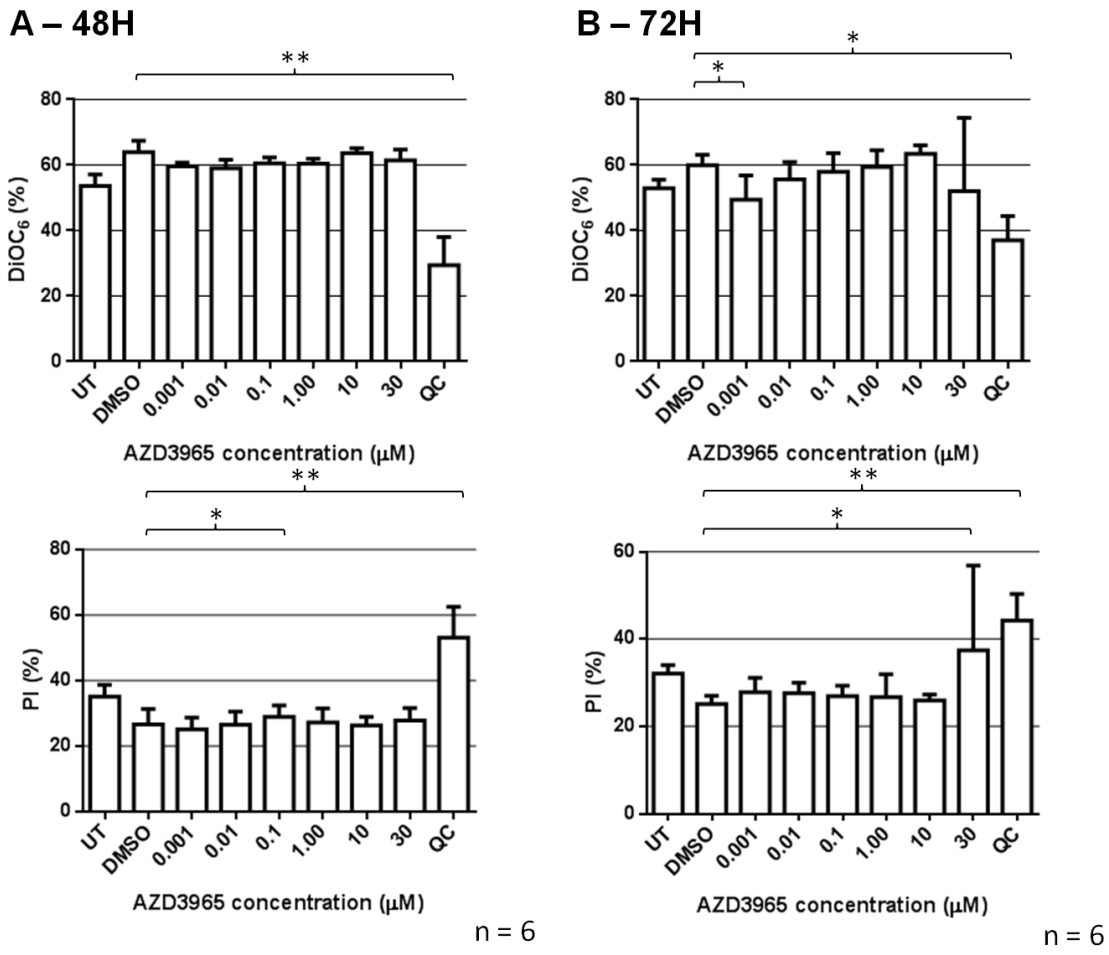

Figure 4.10: Inhibition of MCT1 using increasing concentrations of AZD3965 in a MEC-1 cell line ($DiOC_6$ and PI staining). MEC-1 cells (2×10^4) were incubated with increasing concentrations of AZD3965 (0-30μM) for 48 **(A)** or 72 hours **(B)**. **(A)** A paired t test showed there was no significant difference between the DMSO vehicle control and 0.001-30μM of AZD3965 ($DiOC_6$; $P = > 0.05$, PI; $P = > 0.05$) except for 0.1μM ($DiOC_6$; $P = 0.2050$, PI; * $P = 0.0180$). **(B)** A paired t test showed there was no significant difference between the vehicle control and 0.001-10μM of AZD3965 except for 0.001μM ($DiOC_6$; * $P = 0.0417$, PI; $P = 0.1076$) and 30μM ($DiOC_6$; $P = 0.6111$, PI; * $P = 0.0267$). 10nM staurosporine was used as a positive control (QC). Error bars are the SEM.

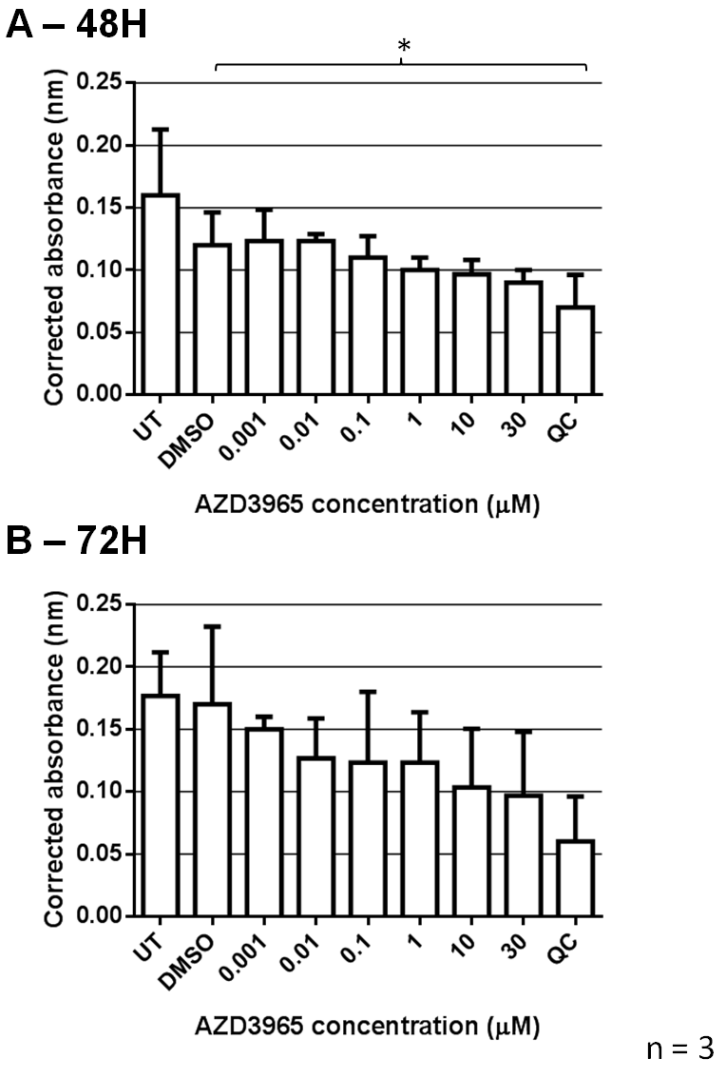

Figure 4.11: Inhibition of MCT1 using increasing concentrations of AZD3965 in a MEC-1 cell line (Alamar blue® cell viability assay). MEC-1 cells (2 x 10^4) were incubated with increasing concentrations of AZD3965 (0-30μM) for either 48 **(A)** or 72 hours **(B)**. **(A)** A paired t test showed there was no significant difference between the DMSO vehicle control and 0-30μM of AZD3965 (P = >0.05). **(B)** A paired t test showed there was no significant difference between the vehicle control and 0-30μM of AZD3965 even at 30μM (P = >0.05). 10nM staurosporine was used as a positive control (QC). Error bars are the SEM.

4.3.1.4 Inhibition of MCT1 using AZD3965 in a HG3 cell line

In addition to investigating the sensitivity of MEC-1 cells to MCT1 inhibition a second CLL cell line was examined. Described by Rosen et al. (2012) the HG3 cell line was established from IgM positive UM-CLL cells cultured on CD40L fibroblasts by *in vitro* infection of Epstein-Barr virus (EBV). These cells express both MCT -1 and -4 as detected by Western blot analysis (Figures 4.12).

Figure 4.13 shows a cell counting experiment to assess optimal seeding density. Cells were plated out in a 24 well plate at the following densities; 1 x 10^5, 2 x 10^5, 4 x 10^5 and 2 x 10^6 cells/mL and counted in duplicate over four days using trypan blue (section 2.2.2). A density of 1 x 10^5 cells/mL was chosen as cells continued to double in comparison to the other seeding densities which began to plateau after two to three days.

The results showing the effect of MCT1 inhibition in HG3cells with AZD3965 are shown in Figure 4.14. Cells were seeded at 1 x 10^5 cells/mL and incubated with 0, 0.001, 0.01, 0.1, 1μM of AZD3965. As observed with MEC-1 cells, there was no effect of AZD3965 on HG3 cell viability, except when the concentration reached 30μM (Figures 4.14 and 4.15).

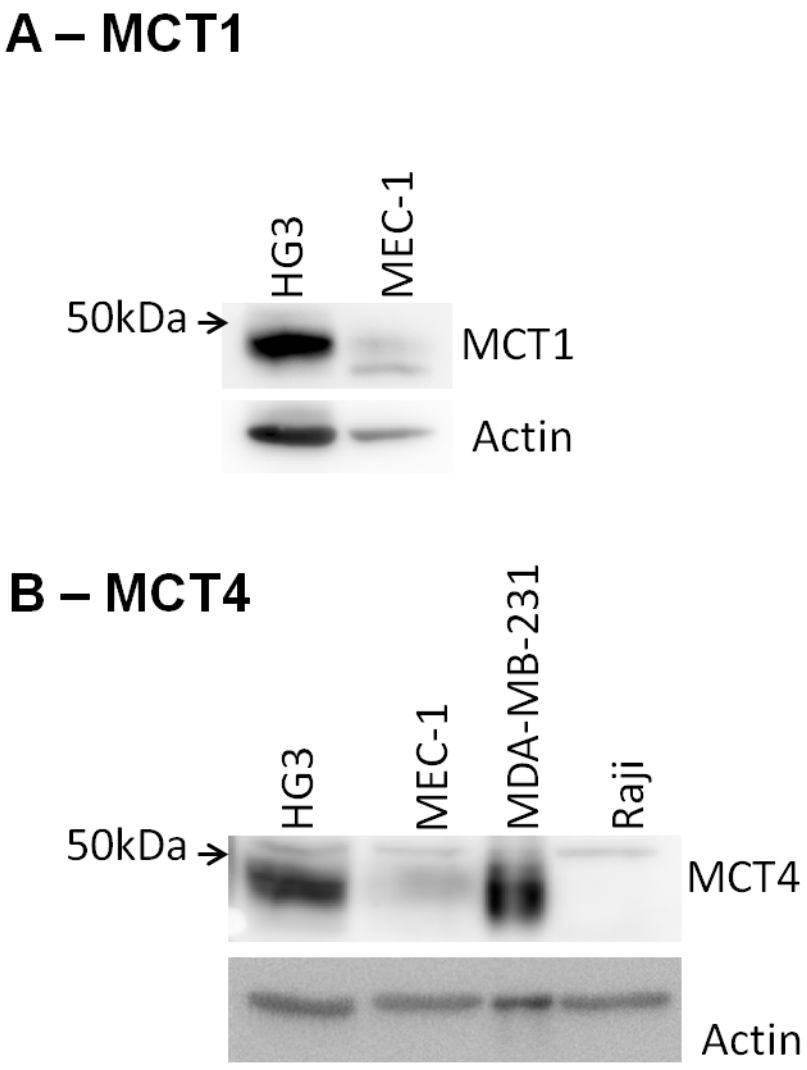

Figure 4.12: MCT -1 and -4 expression in a HG3 cell line. Western blot analysis showing MCT -1 and -4 expression in HG3 cells when treated with **(A)** mouse monoclonal anti-MCT1 (H-1) (sc-365501) (Insight Biotechnology, Wembley, UK) and **(B)** mouse monoclonal anti-MCT4 (sc-376101). Blots were probed with mouse monoclonal anti-β-actin (clone AC-74) as a control to ensure equal protein loading. A MEC-1 cell line was used as a positive control for MCT1 (AstraZeneca, Manchester, UK). A MDA-MB-231cell line and a Raji cell line were used as positive and negative controls for MCT4 expression (Gallagher et al., 2007, Lin et al., 1998b).

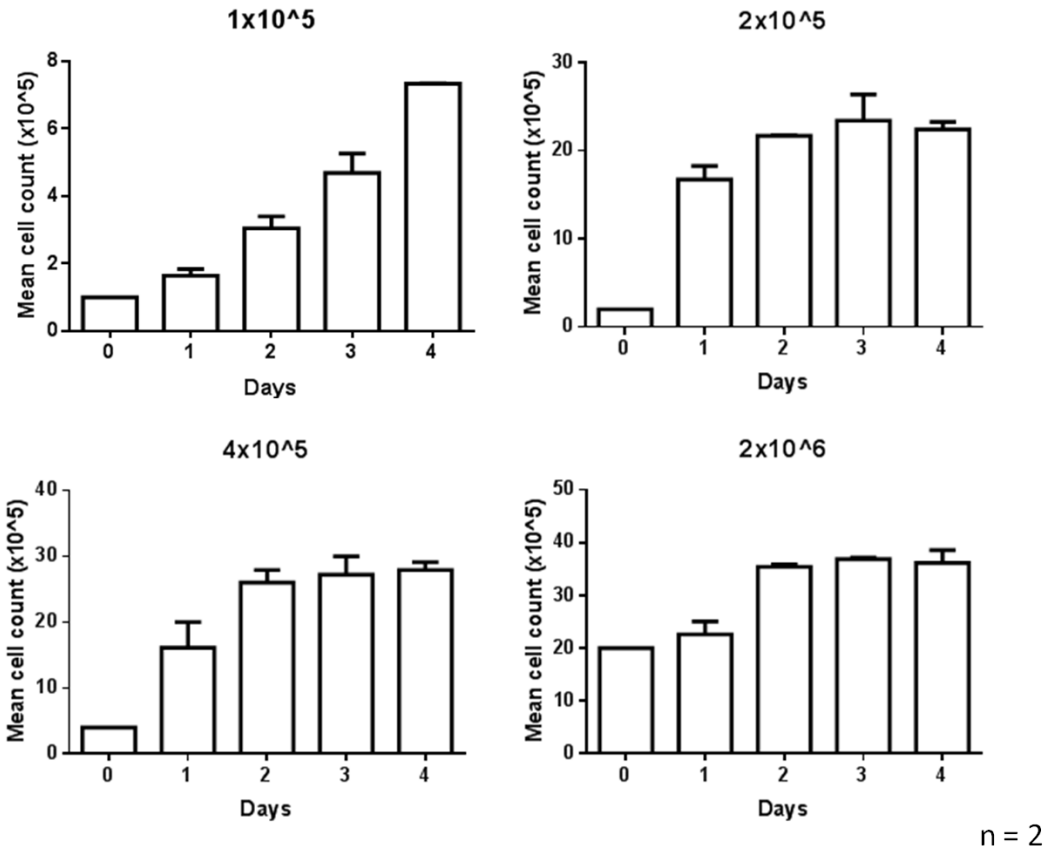

Figure 4.13: Evaluation of seeding density for the HG3 cell line. Cells were plated out in a 24 well plate at the following densities; 1 x 10^5, 2 x 10^5, 4 x 10^5 and 2 x 10^6cells/mL. Cell counts were performed in duplicate using the trypan blue exclusion assay. A density of 1 x 10^5 cells/mL was chosen as cells continued to double in comparison to the other seeding densities which began to plateau after two to three days. Error bars represent the SEM.

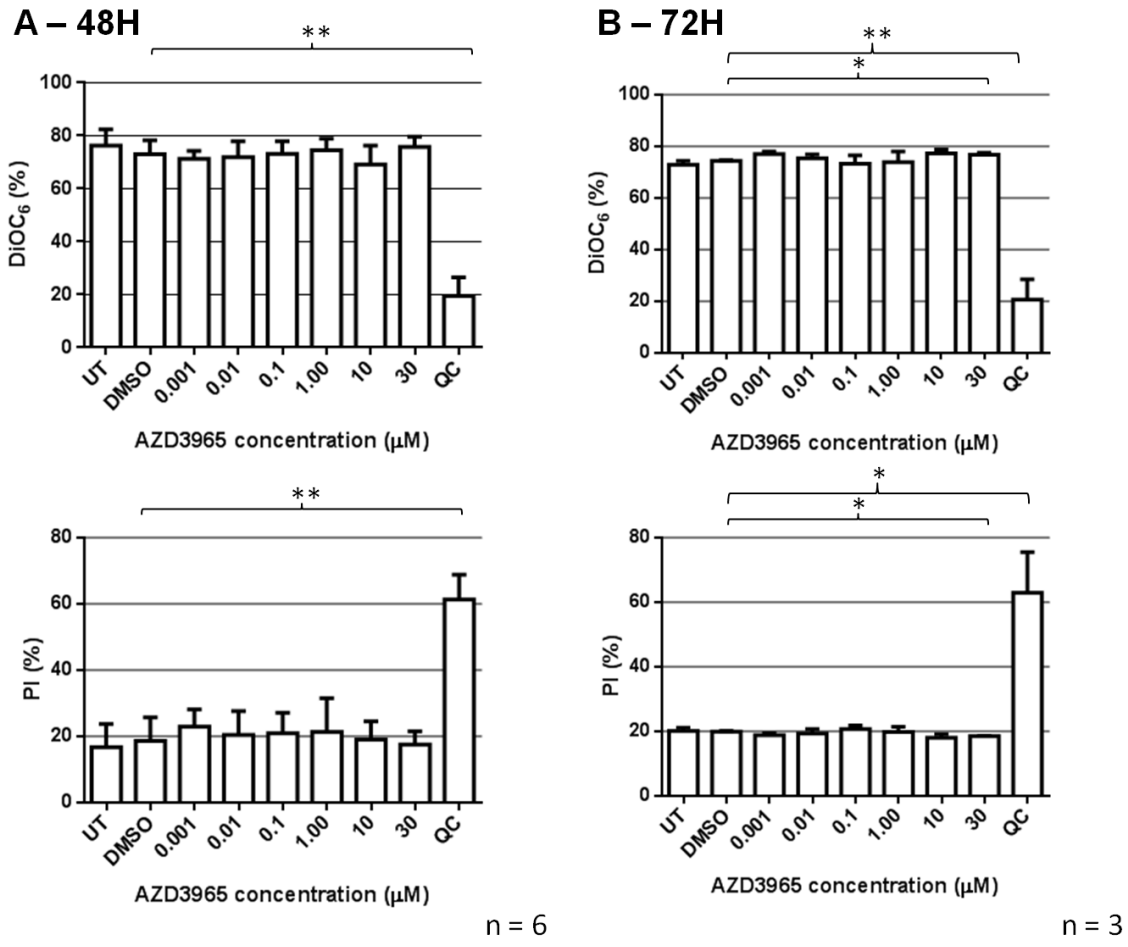

Figure 4.14: Inhibition of MCT1 using increasing concentrations of AZD3965 in a HG3 cell line ($DiOC_6$and PI staining). HG3 cells (1×10^4) were incubated with increasing concentrations of AZD3965 (0-30μM) for 48 **(A)** or 72 hours **(B)**. **(A)** A paired t test showed there was no significant difference between the DMSO vehicle control and 0.001-30μM of AZD3965 ($DiOC_6$; $P = > 0.05$, PI; $P = > 0.05$). **(B)** A paired t test showed there was no significant difference between the vehicle control and 0.001-10μM of AZD3965 ($DiOC_6$; $P = > 0.05$, PI; $P = > 0.05$). 30μM was shown to have a significant effect on cell viability ($DiOC_6$; * $P = 0.0243$, PI; * $P = 0.0120$). 10nM staurosporine was used as a positive control (QC). Error bars are the SEM.

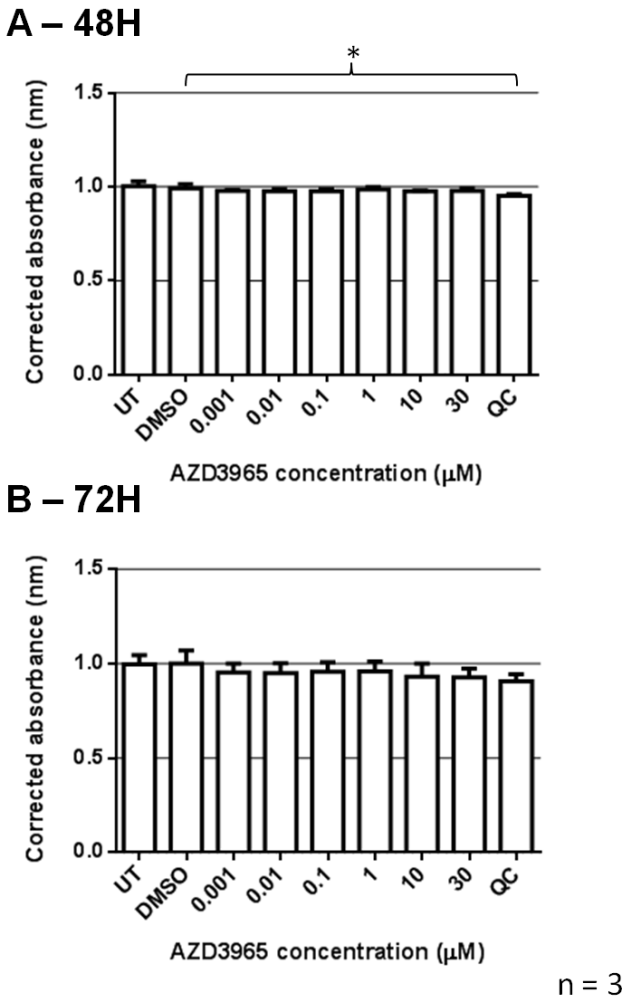

Figure 4.15: Inhibition of MCT1 using increasing concentrations of AZD3965 in a HG31 cell line (Alamar blue® cell viability assay). HG3 cells (1 x 10^4) were incubated with increasing concentrations of AZD3965 (0-30µM) for 48 **(A)** or 72 hours **(B)**. **(A)** A paired t test showed there was no significant difference between the DMSO vehicle control and 0-30µM of AZD3965 (P = >0.05). **(B)** A paired t test showed there was no significant difference between the vehicle control and 0-30µM of AZD3965 (P = >0.05). 10nM staurosporine was used as a positive control (QC). Error bars are the SEM.

4.3.2 Assessment of the effect of MCT4 disruption in CLL

4.3.2.1 siRNA knockdown of MCT4 expression in a MEC-1 cell line

One of the initial aims of this study was to examine the therapeutic potential of inhibiting MCT -1 and -4 in CLL cells using compounds developed by AstraZeneca. However, throughout the course of the project the MCT4 inhibitor remained in development and was unavailable. Therefore, in the absence of a specific inhibitor of MCT4, siRNA was used as an alternative means of investigating the importance of this transporter.

MEC-1 cells were chosen for these experiments because they seemed to have comparatively less MCT4 expression than did HG3 cells (Figure 4.12), and it was thought that MCT4 knockdown would be easier. Figures 4.16 (A) and (B) show Western blot analysis of MCT -1 and -4 expression in MEC1 cells following treatment with MCT4 specific and control siRNA. The presence of the specific siRNA distinctly lowered the expression of MCT4 in treated cells, while MCT1 expression remained constant. However, knockdown was not complete and there remained a residual level of MCT4 expression [Figure 4.16 (C)]. Such reduction in MCT4 expression had no effect on cell viability (Figure 4.17). Subsequent experiments testing the effect of the MCT1 inhibitor on MEC-1 cells where MCT4 expression was reduced showed no effect on cell viability (data not shown).

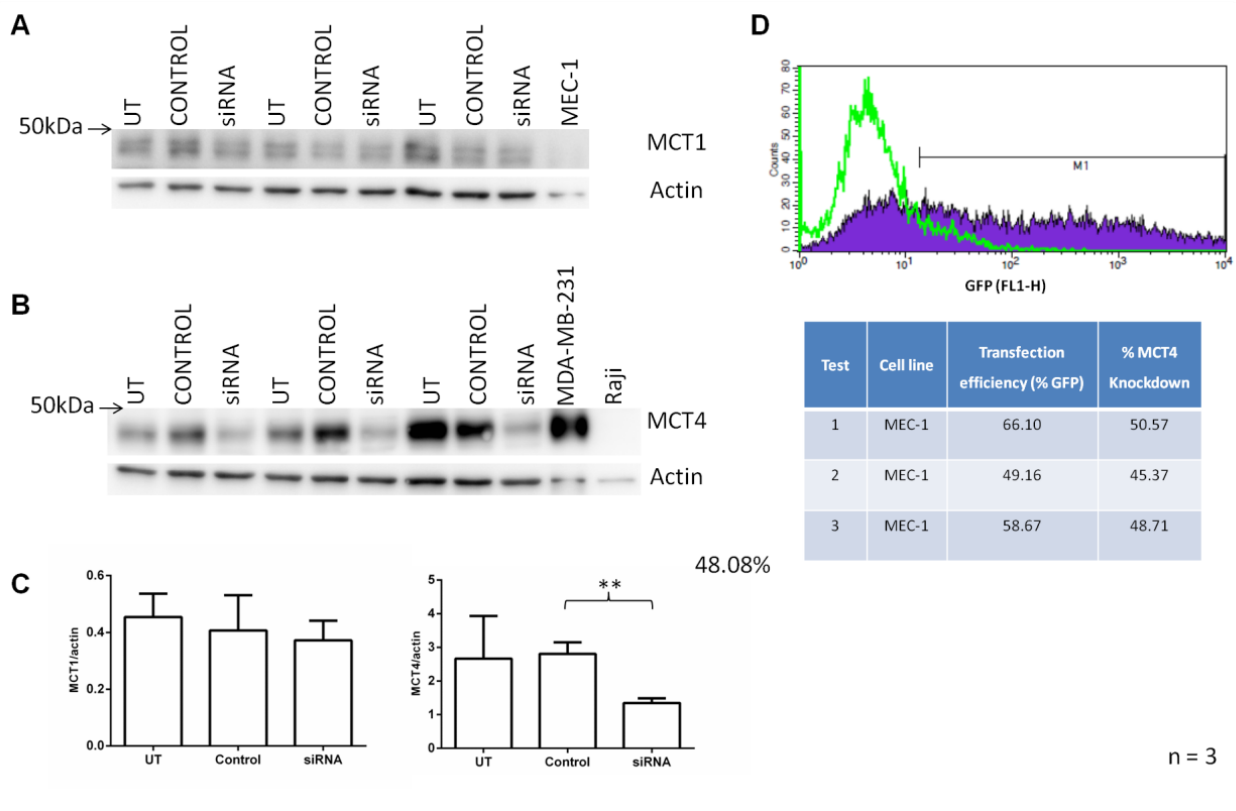

Test	Cell line	Transfection efficiency (% GFP)	% MCT4 Knockdown
1	MEC-1	66.10	50.57
2	MEC-1	49.16	45.37
3	MEC-1	58.67	48.71

Figure 4.16: siRNA knockdown of MCT4 in a MEC-1 cell line. Immunoblot showing MCT -1 and -4 expression following silencing of MCT4 using siRNA in a MEC-1 cell line when treated with either mouse monoclonal anti-MCT1 (sc-365501) (1:1000) (Insight Biotechnology, Wembley, UK) or rabbit polyclonal anti-MCT4 (sc-50329) (1:1000) (Insight Biotechnology, Wembley, UK). **(A)** MCT1 expression remains unchanged. **(B)** MCT4 expression is reduced. **(C)** A paired t test showed MCT1 to be unchanged (P = 0.3902) while MCT4 was significantly down regulated (** P = 0.0081) producing a mean knockdown of 48.08%. **(D)** Transfection efficiency (% GFP) confirmed by flow cytometry after 24 hours and %MCT4 knockdown for all three cases. A MEC-1 lysate used in the previous Western analyses was used as a positive control for MCT1. A MDA-MB-231 was used as a positive control for MCT4 (Gallagher et al., 2007). A Raji cell line was used as a negative control for MCT4 (Lin et al., 1998b). Blots were probed with mouse monoclonal anti-β-actin (clone AC-74) as a control to ensure equal protein loading. Error bars are the SEM.

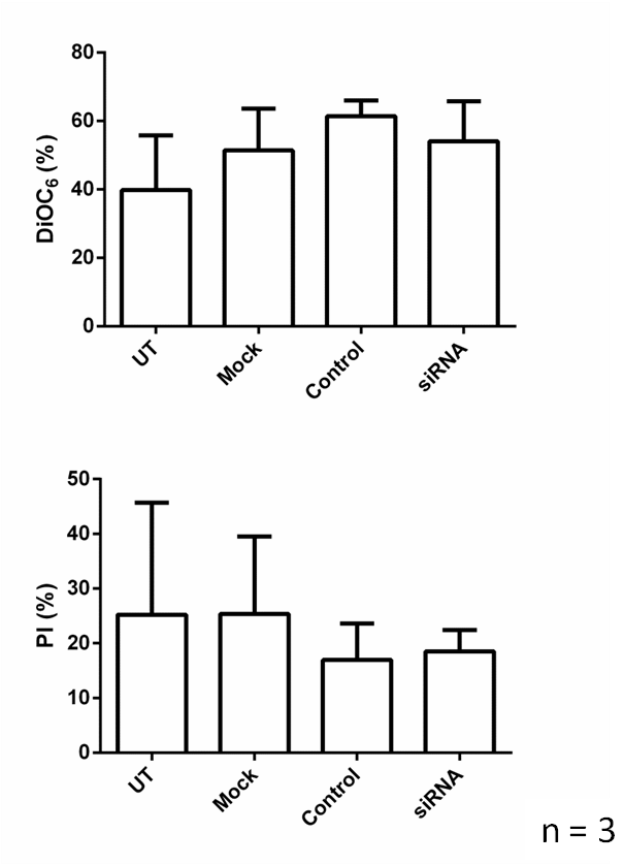

Figure 4.17: Effect of silencing MCT4 on cell death in MEC-1 cells ($DiOC_6$ and PI staining). Knockdown of MCT4 in MEC-1 cells after 48 hours appears to have no effect on cell death as shown by $DiOC_6$ and PI staining. A paired t test showed there was no significant difference between the UT versus the mock transfected sample ($DiOC_6$; P = > 0.05, PI; P = > 0.05). There was also no significant difference between the mock transfected sample versus the control or the control versus MCT4 siRNA respectively ($DiOC_6$; P = > 0.05, PI; P = > 0.05), ($DiOC_6$; P = > 0.05, PI; P = > 0.05). Error bars are the SEM.

4.3.3 Investigating compensatory effects of MCT4 following MCT1 inhibition

To further investigate whether MCT4 compensates for MCT1 inhibition, Raji cells were transiently transfected with an expression plasmid coding for MCT4 which was C-terminally tagged with EGFP. This construct coded for a functional protein as was shown in a recent paper by Castorino et al. (2011), from whom the plasmid was obtained. The plasmids were validated using sequencing as previously discussed in the methods section. As a control Raji cells were transiently transfected with the empty pAc-EGFP1-N1 plasmid.

Figure 4.18 shows the results of the transient transfections. Both MCT4-EGFP and EGFP were detectable in Raji cells 24 hours post nucleofection [Figure 4.18 (A)]. Transfection efficiency was estimated at approximately 22%, and Western blot analysis for MCT4 and GFP expression further validated the plasmid by showing similar MW bands for MCT4-EGFP in transfected cells (Figure 4.18 B and C). These results demonstrate that a recovery period of 24 hours post transfection was sufficient for the Raji cells to take up the pMCT4-EGFP plasmid.

The transfected Raji cells were then treated with AZD3965. Figure 4.19 illustrates the rescue effect of induced MCT4 expression in Raji cells. Thus, the presence of AZD3965 noticeably reduced the number of live cells in mock- and EGFP-transfected Raji cells, whereas in MCT4-EGFP-transfected Raji cells a small population of live cells was preserved. Analysis of this small population of AZD3965-resistant cells showed that they expressed GFP [Figure 4.20 (A)], suggesting that Raji cells able to express MCT4 had gained resistance to the compound. Comparison of the effect of AZD3965 on EGFP- and MCT4-EGFP-transfected Raji cells showed that AZD3965 reduced cell viability of EGFP-transfected Raji cells, but had no effect on MCT4-EGFP-transfected Raji cells which increased in number [Figure 4.20 (B)]. Those cells which did not take up the pMCT4-EGFP plasmid remained sensitive to the killing effects of AZD3965, and this was apparent when the total cell population was analysed [Figure 4.20 (C)]. These results indicate that induced expression of MCT4 in Raji cells confers resistance to AZD3965.

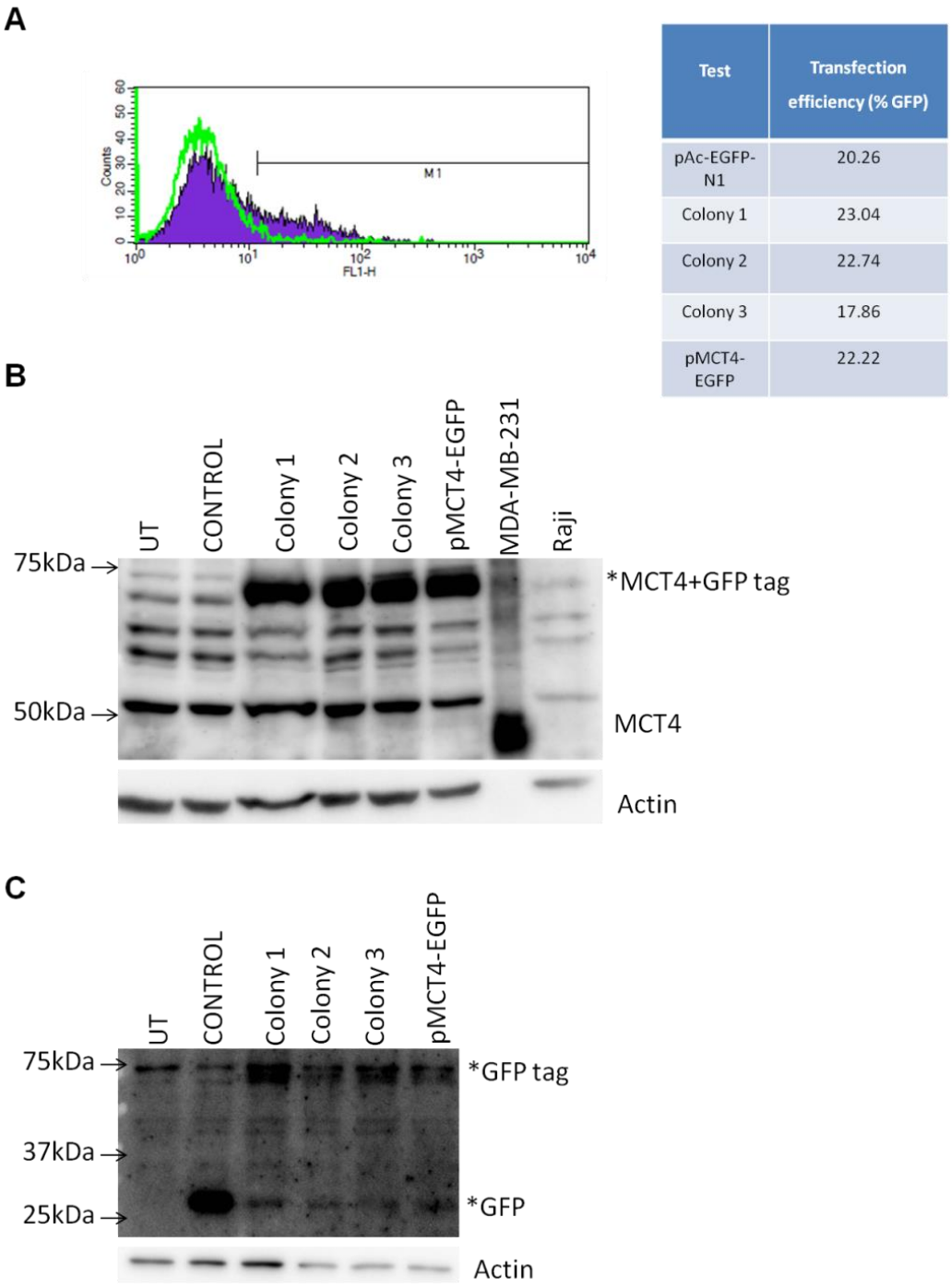

Test	Transfection efficiency (% GFP)
pAc-EGFP-N1	20.26
Colony 1	23.04
Colony 2	22.74
Colony 3	17.86
pMCT4-EGFP	22.22

Figure 4.18: MCT4 and GFP expression following transient transfection of a Raji cell line with pMCT4-EGFP plasmid (24 hours). (A) GFP transfection efficiency (17.86-23.04%) measured using flow cytometry. The green line shows non-specific fluorescence (isotype control FITC (FL1-H)) while the purple section shows the fluorescence associated with the expression of GFP (FL1-H). M1 shows cells selected

as being positive for CD40L expression. **(B)** Immunoblot showing MCT4 expression following incubation with rabbit polyclonal anti-MCT4 (sc-50329) (1:1000) (Insight Biotechnology, Wembley, UK). Blots were probed with mouse monoclonal anti-β-actin (clone AC-74) as a control to ensure equal protein loading. MCT4 is expressed in the Raji cells transiently transfected with the pMCT4-EGFP colonies (~74kDa). 20ug of protein was loaded. MDA-MB-231 and Raji preparation were used as positive and negative controls for MCT4 expression (Lin et al., 1998b) (Gallagher et al., 2007). **(C)** Immunoblot showing GFP expression after incubation with mouse monoclonal anti-GFP (sc-9996) (1:2000) (Insight Biotechnology, Wembley, UK). GFP is expressed in the control plasmid pAc-EGFP1-N1 (~20kDa) and cells transfected with pMCT4-EGFP (~74kDa).

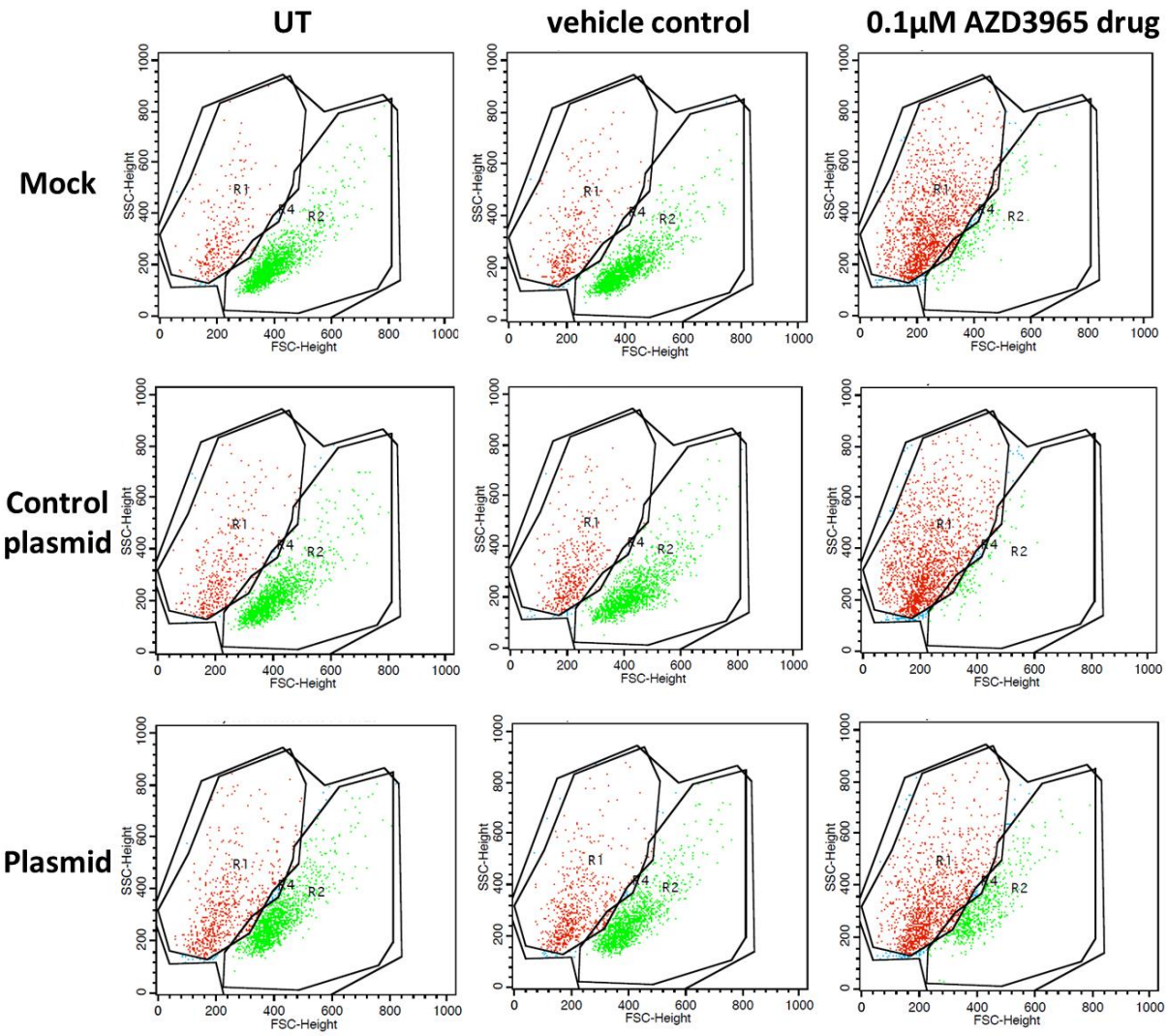

Figure 4.19: Cell death following MCT1 inhibition using AZD3965 in Raji cells transiently transfected with pMCT4-EGFP visualized by side scatter (SSC) and forward scatter (FSC). Representation of the rescue effect of transient MCT4 expression in Raji cells following treatment with AZD3965. Incubation of the mock transfected control (mock) and the Raji cells transfected with the control plasmid pAc-EGFP1-N1 (control) can be seen to result in a reduction in the live cell population (R2 in green) with an increase in the dead cell population (R1 in red) which is absent when incubated with the DMSO vehicle control. Incubation of the Raji cells transfected with pMCT4-EGFP with AZD3965 has little effect on the live (R2) or dead cell populations (R1).

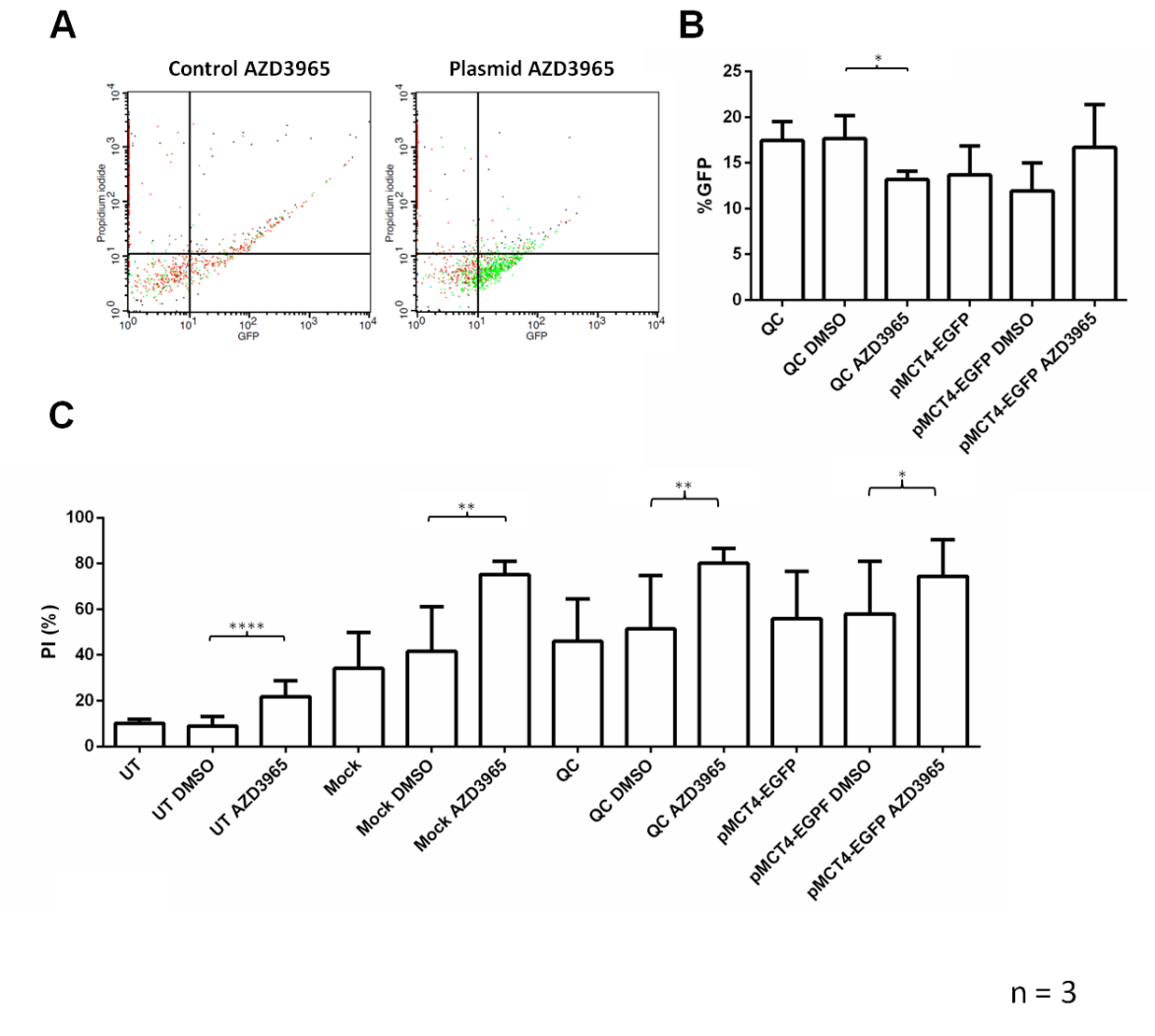

Figure 4.20: Inhibition of MCT1 using AZD3965 in Raji cells transiently transfected with pMCT4-EGFP (PI staining). Raji cells were transiently transfected with either a pAc-EGFP1-N1 (control) or pMCT4-EGFP for 24 hours and then incubated with 0.1µM of AZD3965 for 48 hours. **(A)** Quadrant analysis of the live (green) population of cells in R2 (Figure 4.19) showing them to express GFP whereas the majority of the cell population for the control corresponds to dead cells (red). **(B)** 0.1µM of AZD3965 caused a significant cell death (red) in the % of GFP positive cells (LR quadrant) in the control plasmid pAc-GFP1-N1 (* P = 0.0414) while no significant loss (live cells = green) in the % of GFP positive cells (LR) was seen in the Raji cells transfected with the pMCT4-EGFP (P = >0.05). **(C)** PI showed the untreated (UT), the mock transfected (mock), and the control to be sensitive to AZD3965 (**** P = <0.0001), (** P = 0.0045), (** P = 0.0088) respectively using a paired t test. No

significant cell death was seen with the DMSO vehicle control (P = >0.05) for either the UT, mock or control. For the pMCT4-EGFP plasmid cell death was seen (* P = 0.0403) in comparison to the vehicle control. Error bars are the SEM.

4.3.4 Examining of the effect of the AZD3965 on cell metabolism in CLL cell lines

The previous data investigating the sensitivity of CLL cell lines to the MCT1 inhibitor AZD3965 primarily focused on measuring parameters such as cell death and cell viability to ascertain the functional effects of the compound. Although this is of clinical interest, it is also important to examine metabolic changes which may occur in the cell prior to these events to understand the mechanism through which AZD3965 works. Metabolic flux analyses were performed using the SeahorseXF24 metabolic flux analyser as described in chapter 3. This method was chosen because transport of substrates across the plasma membrane is proton linked and allows a broader question about monocarboxylate transport to be addressed.

Firstly, the protocol was optimised for Raji cells. These cells were plated out at 2 x 10^5/mL, 6 x 10^5/mL, and 2 x 10^6/mL, and subjected to a mitochondrial stress test (Figure 4.21). A seeding density of 2 x 10^6 cells/mL had the highest baseline oxygen consumption rate [OCR (pMoles/min)], and it was determined that the mitochondrial stress test for this density was successful because of the notable changes in OCR that were evident following addition of each of the mitochondrial stressor drugs. Next, the concentration of FCCP was titrated over a concentration range of 0.5-3μM (Figure 4.22). It was determined that maximum respiration measured by OCR (pMoles/min) was obtained using a concentration of 1.5μM FCCP.

The effect of AZD3965 on Raji cell metabolism was tested by measuring the normalised extracellular acidification rate [%ECAR (mpH/min/μgDNA)] and normalised OCR [%OCR (pMoles/min/μgDNA)] against an increasing concentration range of 0.1-30μM of this compound (Figure 4.23). Injection of AZD3965 causes a concentration-dependent drop in %ECAR indicating a slowing of the acidification rate of the extracellular media. This is accompanied by an increase in %OCR indicating a potential greater reliance on aerobic metabolism. Thus, the presence of AZD3965 leads to changes in the energy-generating pathways of Raji cells consistent with a decrease in glycolytic activity and increase in oxidative phosphorylation. For subsequent experiments the lower concentration of 0.1μM AZD3965 was selected because it was effective at reducing cell viability.

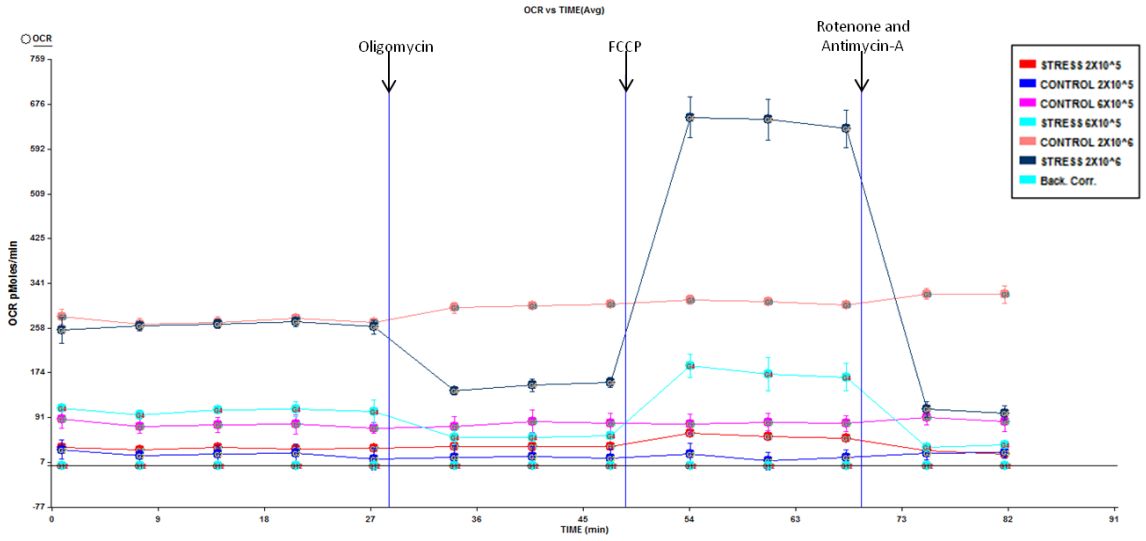

Figure 4.21: **Evaluation of seeding density for the Raji cell line for metabolic flux analyses.** Raji cells were plated out at 2 x 10^5/mL, 6 x 10^5/mL, and 2 x 10^6/mL and subjected to a mitochondrial stress test (oligomycin 1.26µM, FCCP 1.5µM and rotenone and antimycin-A 1µM). OCR (pMoles/min) was measured. A density of 2 x 10^6/mL was selected for future use because of the higher baseline OCR and responsiveness to the mitochondrial stressors.

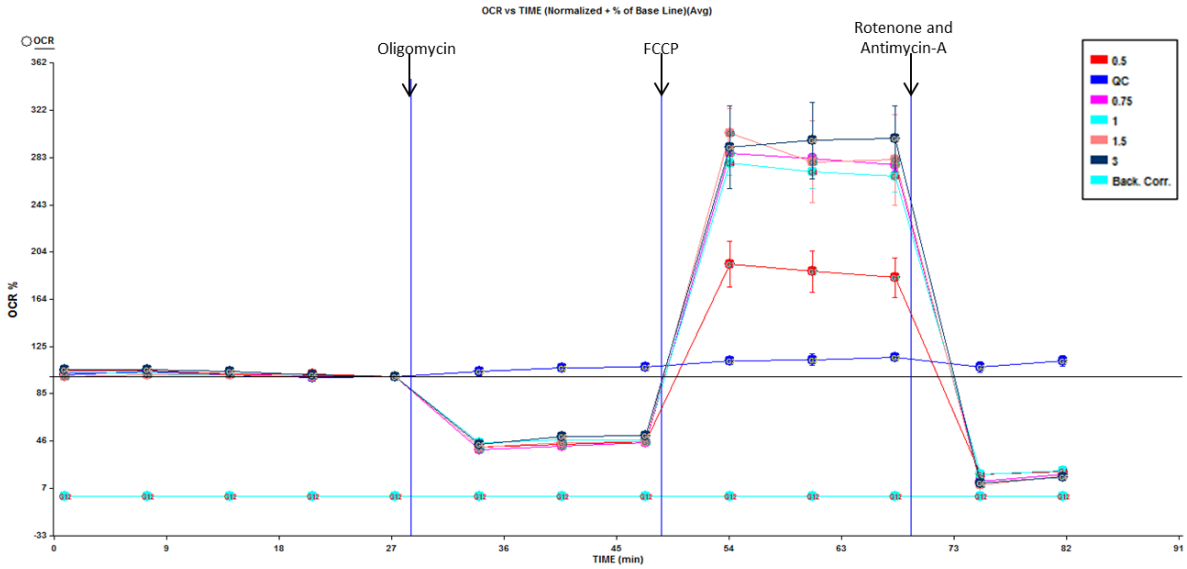

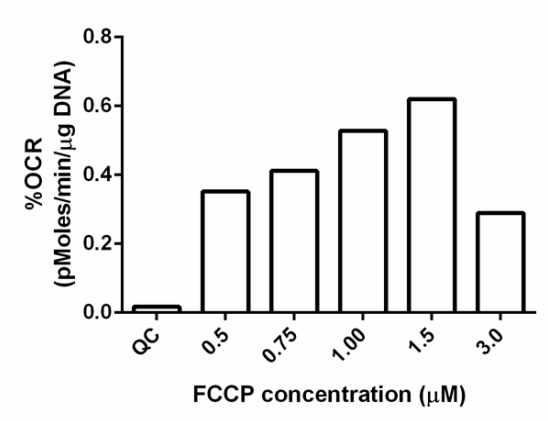

n = 1

Figure 4.22: FCCP titration in a Raji cell line. Raji cells were plated out at 2 x 10^6/mL and subjected to a mitochondrial stress test (oligomycin 1.26µM, FCCP and rotenone and antimycin-A 1µM) with increasing concentrations of FCCP (0, 0.5, 0.75, 1, 1.5, 3µM). %OCR (pMoles/min/µgDNA) was measured. 1.5µM was selected as the optimum concentration to induce maximum respiration.

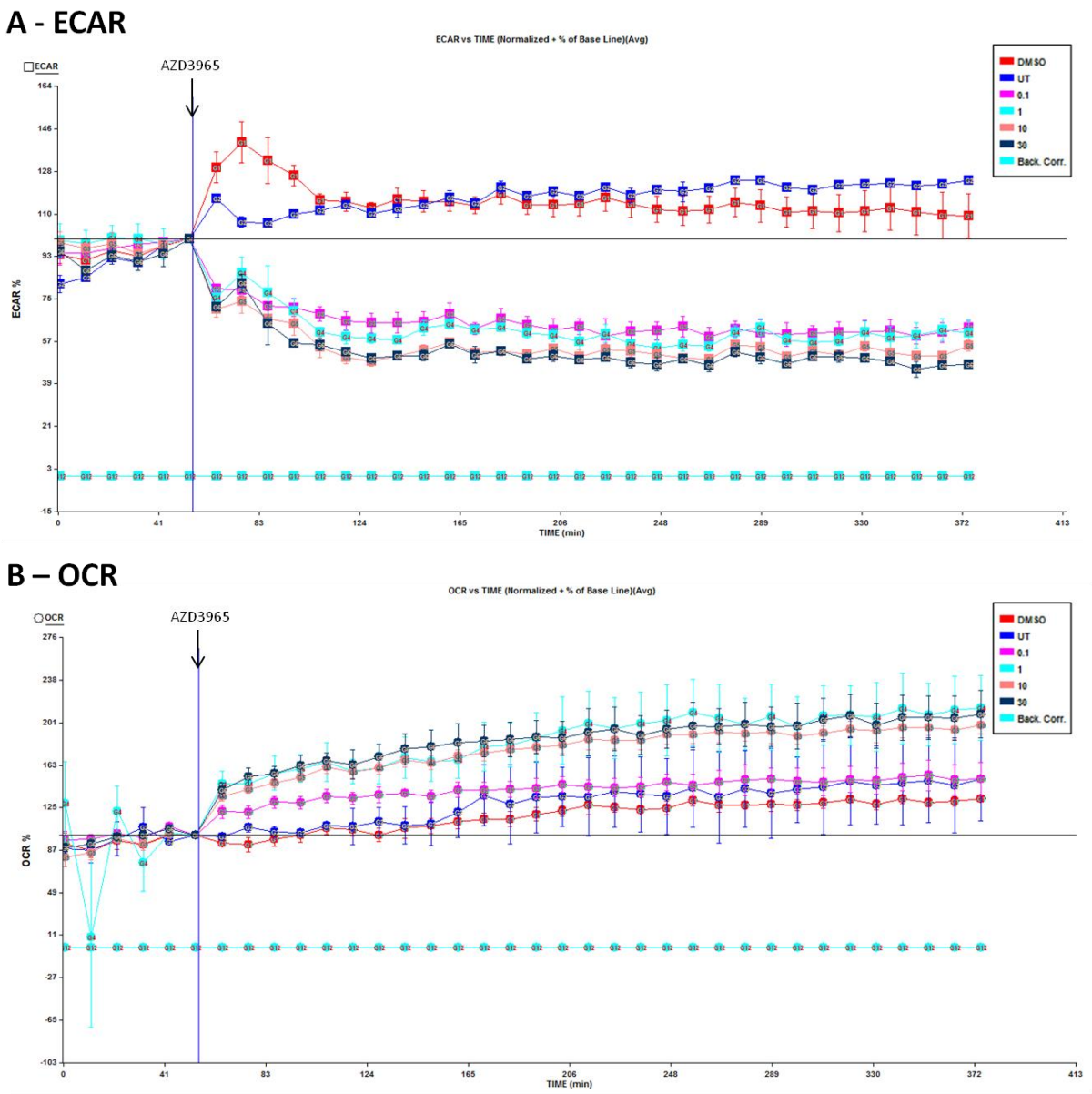

Figure 4.23: Effect of MCT1 inhibition using AZD3965 on ECAR and OCR in the Raji cell line. Raji cells were seeded at a density of 2 x 10^6/mL and treated with increasing concentrations of AZD3965 0.1, 1, 10, 30µM. **(A)** %ECAR (mpH/min/µgDNA) and **(B)** %OCR (pMoles/min/µgDNA) were measured in real time for 5 hours post drug injection.

To confirm that AZD3965 affected glycolytic activity in Raji cells, oligomycin (1.26μM) was used to shut down ATP synthase and force the cells to use glycolysis as an energy-generating pathway (glycolytic capacity). The presence of 0.1μM AZD3965 leads to a significant decrease in the %ECAR of the cultured Raji cells [Figure 4.24 (A) and (B)]. When oligomycin is added, untreated Raji increase the %ECAR consistent with a switch to glycolysis as the preferred metabolic pathway. With AZD3965-treated Raji cells, the addition of oligomycin also induces an increase in %ECAR [Figure 4.24 (A)], but the extent is significantly less than that of the untreated Raji cells [Figure 4.24 (B)]. Thus, this experiment shows that AZD3965-treated Raji cells have significantly reduced glycolytic capacity.

Examination of oxidative phosphorylation in Raji cells was assessed next. Figure 4.25 (A) shows %OCR in untreated and AZD3965-treated Raji cells. The %OCR of AZD3965-treated Raji cells is significantly greater than that of untreated cells [Figure 4.25 (B)]. When oligomycin is added, there is a similar drop in %OCR for both untreated and AZD3965-treated Raji cells, and this indicates that oxidative phosphorylation produces similar levels of ATP under both conditions [Figure 4.25 (C)]. This result suggests that the increased OCR associated with AZD3965-treated Raji cells is not due to increased respiration. The integrity of mitochondrial respiration is shown to be intact when FCCP is added to uncouple the mitochondria. Thus, there is no significant difference in the %OCR between untreated and AZD3965-treated Raji cells when FCCP is added [Figure 4.25 (D)]. Moreover, the final addition of rotenone and antimycin-A to measure proton leak and spare respiratory capacity show that both untreated and AZD3965-treated Raji cells respond in a similar fashion [Figures 4.25 (E) and (F)]. Taken together, these data suggest that increased oxygen consumption by the AZD3965-treated Raji cells is not due to increased respiration because excess ATP is not produced, and that the reason why excess ATP is not produced is not a result of mitochondrial damage.

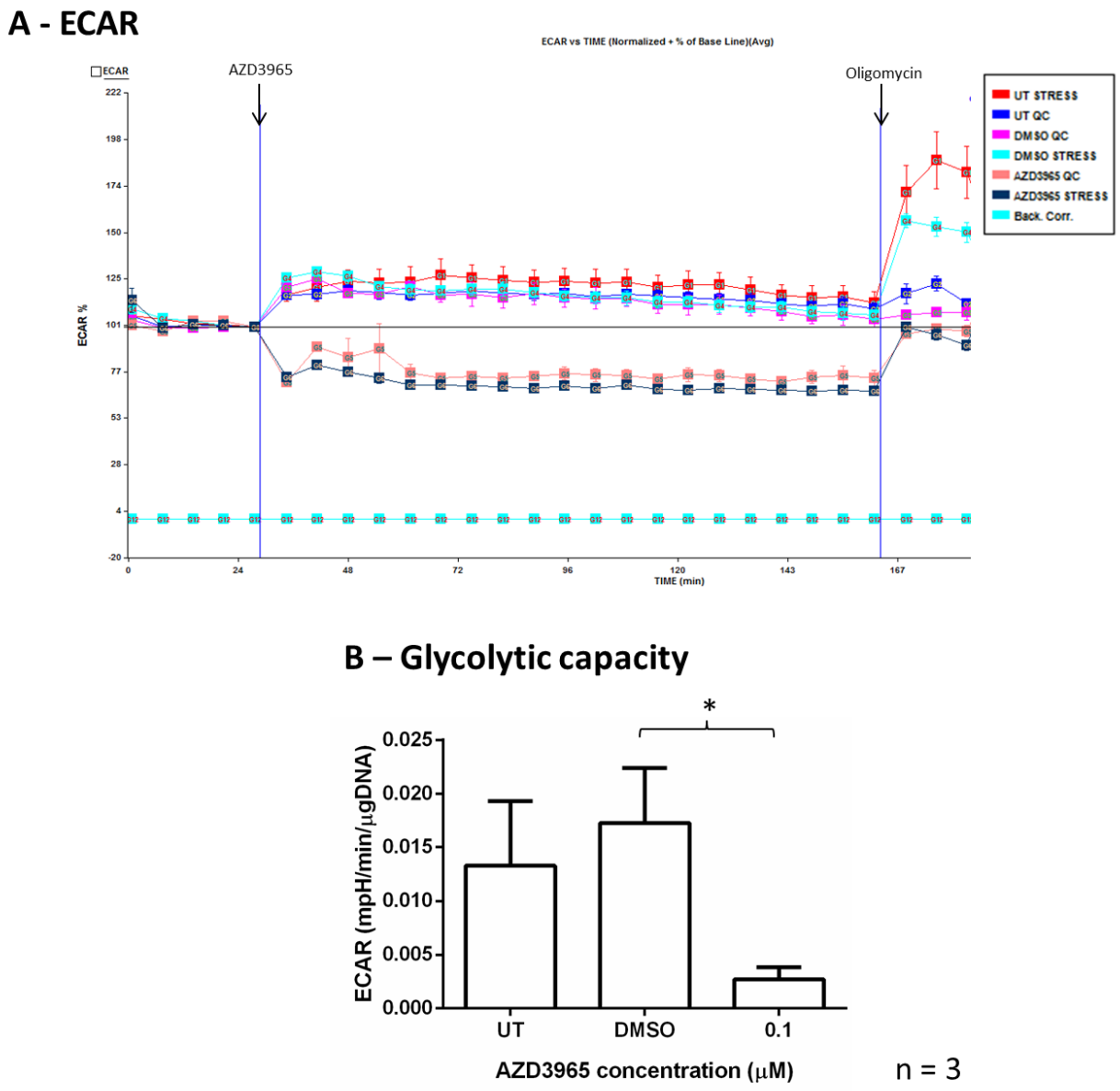

Figure 4.24: Effect of treatment with 0.1µM of AZD3965 in the Raji cell line on glycolytic capacity. Raji cells (2 x 10^6/mL) were treated with 0.1µM of AZD3965 left for 5 hours. Oligomycin 1.26µM was then added. **(A)** %ECAR (mpH/min/µgDNA) and **(B)** glycolytic capacity calculated by subtracting measurement 28 (after oligomycin) from measurement 25 (before oligomycin). A paired t test revealed a significant decrease in glycolytic capacity following treatment with AZD3965 (* P = 0.0504). Error bars are SEM.

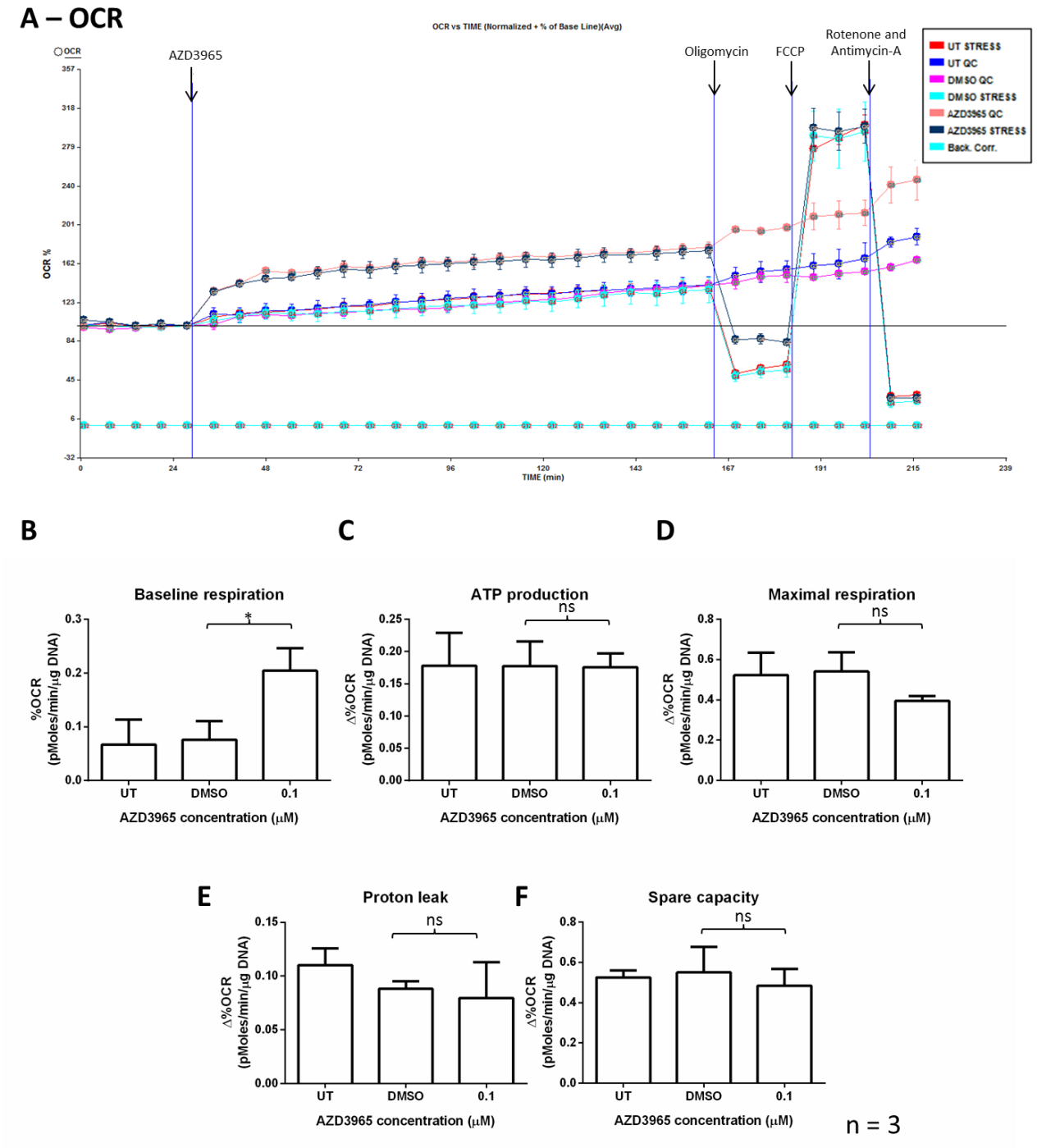

Figure 4.25: Effect of treatment with 0.1µM of AZD3965 in the Raji cell line on responsiveness to mitochondrial stressors. Raji cells (2 x 10^6/mL) were treated with 0.1µM of AZD3965 left for 5 hours. Cells were then subjected to a mitochondrial stress test (oligomycin 1.26µM, FCCP 1.5µM and rotenone and antimycin-A 1µM). **(A)** OCR (pMoles/min/µgDNA). **(B)** Paired t tests revealed there to be a significant change in

baseline OCR in response to AZD3965 (* $P = 0.0451$). No significant difference in response to the mitochondrial stressors was observed ($P = > 0.05$). Error bars are SEM.

To understand why MEC-1 cells are resistant to the cytotoxic effects of AZD3965, they were also subjected to metabolic flux analysis. Seeding density of this cell line was optimised as shown in Figure 4.26. Only seeding densities of 2 x 10^6/mL and 2 x 10^7/mL were responsive to the mitochondrial stressors. However, for the seeding density of 2 x 10^6/mL there was not enough difference in OCR in response to mitochondrial stressors to afford reliable measurement, and a seeding density of 2 x 10^7/mL yielded values at the top of the measurable range. Therefore, a density of 5 x 10^6/mL was selected for future use.

MEC-1 cells were then treated with increasing concentrations of AZD3965 (0.1, 1, 10, 30μM) to assess whether the compound affected %ECAR and %OCR (Figure 4.27). An initial increase in %ECAR was observed following injection from port A, and this was apparent for all injections regardless of treatment. The presence of 30μM AZD3965 increased %ECAR above untreated and DMSO-treated MEC-1 cells, an observation that is inconsistent with those obtained using Raji cells (Figure 4.24). This result suggests that AZD3965 does not shut down monocarboxylate transport in MEC-1 cells, even when used at concentrations which kill MEC-1 cells and also potentially shut down MCT-1 and -4 function. With respect to %OCR, the presence of AZD3965 had the effect of decreasing oxygen consumption by MEC-1 cells. This is in contract to Raji cells where the presence of AZD3965 lead to increased %OCR (Figure 4.25). Taken together, these results indicate that MEC-1 cells are resistant to the effects of AZD3965 and MCT1 inhibition on the metabolism of these cells.

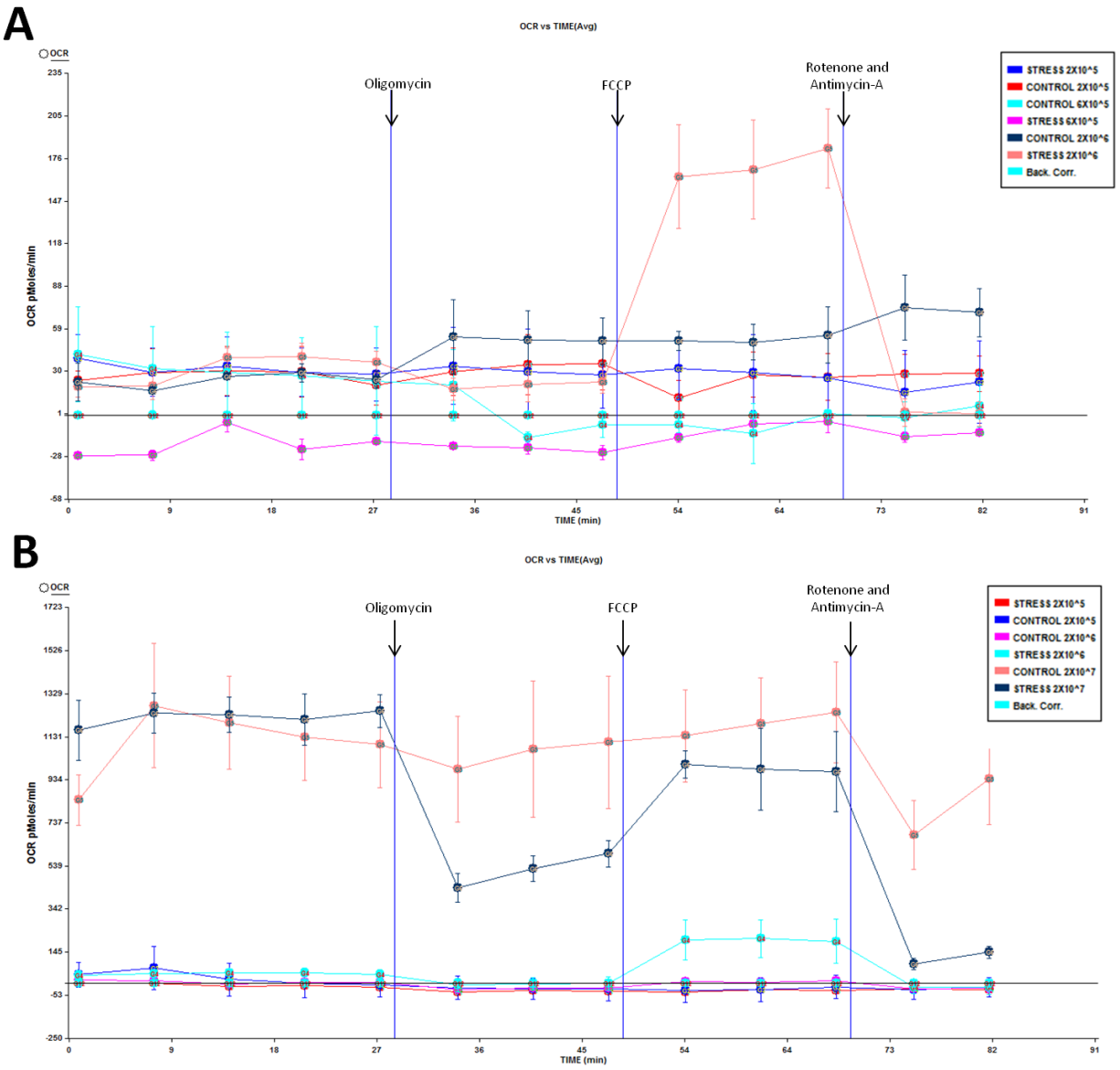

Figure 4.26: Evaluation of seeding density for the MEC-1 cell line for metabolic flux analyses. MEC-1 cells were plated out at **(A)** 2 x 10^5/mL, 6 x 10^5/mL, and 2 x 10^6/mL and **(B)** 2 x 10^5/mL, 2 x 10^6/mL, and 2 x 10^7/mL and subjected to a mitochondrial stress test (oligomycin 1.26µM, FCCP 1.5µM and rotenone and antimycin-A 1µM). OCR (pMoles/min/µgDNA) was measured. **(A)** Shows only 2 x 10^6/mL responds to stressors. **(B)** Suggests 2 x 10^7/mL to be out of range and confirms the data shown in **(A).** Because the baseline value was low for 2 x 10^6/mL and out of range for 2 x 10^7/mL a density of 5 x 10^6/mL was selected.

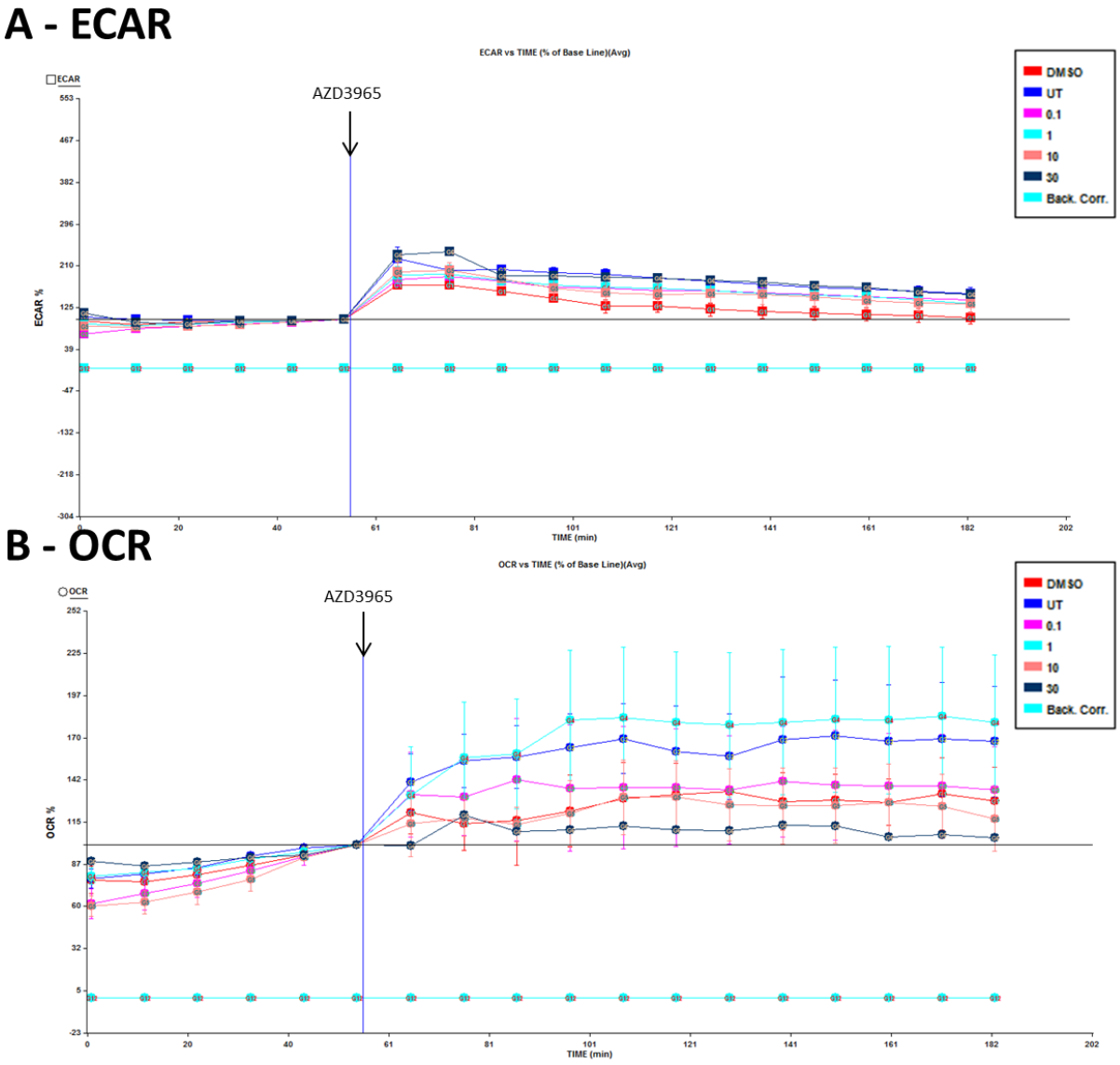

Figure 4.27: Effect of MCT1 inhibition using AZD3965 on ECAR and OCR in the MEC-1 cell line. MEC-1 cells were seeded at a density of 5 x 10^6/mL and treated with increasing concentrations of AZD3965 0.1, 1, 10, 30µM. **(A)** %ECAR (mpH/min/µgDNA) and **(B)** %OCR (pMoles/min/µgDNA) were measured in real time for 5 hours post drug injection.

4.4 DISCUSSION

Inhibitors of MCT-1 and -4 were originally designed to modulate immunosuppression based on an understanding that antigen receptor signalling induces glycolysis (Garcia-Manteiga et al., 2011, Michalek and Rathmell, 2010). The potential of these compounds in the treatment of CLL has not been previously explored, but seemed important because of the role of antigen in progression of this disease. In chapter 2 CLL cells were demonstrated to express both MCT -1 and -4, and chapter 3 demonstrated that CD40-stimulated CLL cells upregulated expression of MCT4. The aim of this chapter was to investigate whether MCT1 could be therapeutically targeted in cells where both MCT -1 and -4 were present.

The experiments in this chapter are primarily based on Raji and MEC-1 cells, the former cell line expressing only MCT1, while the latter expresses both MCT1 and 4. Preliminary data suggested that Raji cells are sensitive to nM concentrations of AZD3965 (Critchlow et al., 2012), and the results presented in this chapter confirm this using $DiOC_6$ and PI staining to assess cell death, and Alamar blue® to assess cell viability. Thus, AZD3965 has a concentration-dependent cytotoxic effect on Raji cells, where 100nM was observed as the optimal concentration. This concentration of AZD3965 was then demonstrated to have effect on the metabolism of Raji cells. Metabolic analyses using the SeahorseXF24 metabolic flux analyser revealed that Raji cells treated with this drug changed their ECAR suggesting that proton-linked transport (i.e. monocarboxylate transport) was inhibited. This finding is in agreement with work recently published by Doherty et al. (2013) where Raji cells were treated with similar MCT1 inhibitors AR-C122982 and AR-C155858. Importantly, AZD3965 is derived from AR-C155858 and is reported to show 10 fold greater affect (Ekberg et al., 2007). The work of this chapter provides greater insight into the mechanism of action of MCT1 inhibition because the change in ECAR following the addition of oligomycin shows that AZD3965-treated Raji cells have lost glycolytic capacity. This, in turn, suggests that glycolysis is being shut down in treated Raji cells most likely because of lowering of optimal pH for the enzymes involved in this pathway (Mansour, 1963). Metabolic measurements also show that the presence of AZD3965 induced increased oxygen

consumption by Raji cells. This is likely not due to increased respiration because the indices of mitochondrial function, ATP production, maximal respiration, proton leak and spare capacity all remained unaffected by the presence of this drug. However, this does not mean that AZD3965 does not lead to mitochondrial damage because the time scale of the experiment may be too short. Maximal respiration was measured 3 hours following the addition of AZD3965, and this may be too short an incubation to observed significantly different rates of maximal respiration between untreated and treated cells. AZD3965-treated Raji cells did seem to have reduced maximal respiration, and further experimentation is necessary to determine the full mechanism through which this drug induces its cytotoxic effect.

In contrast to Raji cells, the presence of AZD3965 had no effect on the metabolism of MEC-1 cells. MEC-1 cells were also largely resistant to the cytotoxic effects of this drug. With respect to monocarboxylate transporter expression, it may be that MCT4 compensates for the function of MCT1 when AZD3965 is present in MEC-1 cell cultures. This notion is tested by ectopic expression of MCT4 in Raji cells, these cells also become resistant to the cytotoxic effects of AZD3965. Attempts were made to knock down expression of MCT1 in MEC-1 cells, however, only a partial knockdown was achieved and this was insufficient for further experiments measuring the effects of AZD3965 to take place. Nevertheless, this approach may be successful in future experiments because studies of this compensation mechanism in small cell lung cancer (SCLC) cell lines show that siRNA knockdown of MCT4 increases sensitivity to MCT1 inhibition (Polanski et al., 2014).

In conclusion the data presented in this chapter suggests that the therapeutic targeting of MCT1 is likely to be ineffective without the inhibition of MCT4 in cells that express both transporters. These data, in combination with the previous data from chapter 3, suggests that inhibition of MCT1 will unlikely be effective in killing CLL cells within the microenvironment because of the upregulation of MCT4 that is induced when these cells come into contact with CD40 ligand.

5 CHAPTER 5: GENERAL DISCUSSION AND FUTURE WORK

The overall aim of this thesis was to examine the potential of targeting the metabolism of chronic lymphocytic leukaemia (CLL) cells through the inhibition of MCT -1 and -4. This was accomplished by investigating the expression profile of these transporters on primary CLL cells from the peripheral circulation, and examining how their expression is affected during contact with the microenvironment where CLL cells encounter proliferative and survival stimuli. Finally, potential sensitivity of CLL cells to MCT-1 inhibition was assessed using AZD3965.

The work presented in this thesis is important because it explores the possibility of therapeutically targeting a fundamental area of cancer cell biology, an area which for CLL is relatively uncharted. Other studies looking at new therapeutic approaches for this disease focus on targeting recurrent/refractory disease. These new therapies take the approach of disrupting; BCR signaling (ibrutinib), the PI3K pathway (idelalisib), modulating the immune system (lenalidomide), or inducing cell death by targeting Bcl-2 (AZD4320) (Tausch et al., 2014).

As previously discussed, early work suggested that the gradual accumulation of malignant B cells in CLL was due to failed apoptosis (Brody et al., 1969, Dameshek, 1967, Gottardi et al., 1995, Zenz et al., 2010, Pepper et al., 1997, Kitada et al., 1998). Thus, within this paradigm CLL cells would likely have low levels of metabolic activity, a notion which was supported by studies examining glucose uptake as well as the expression levels of glycolytic enzymes (Vives Corrons et al., 1989, Ho et al., 1982, Musolino et al., 1992).

However, in the last decade cancer cell metabolism has come into the forefront of cancer research because a hallmark of malignancy is the rapid consumption of glucose coupled with enhanced aerobic glycolysis; the Warburg effect (Warburg et al., 1924). Renewed interest in this field has led to the development of new drugs which target cell metabolism, which, when combined with standard therapies have been shown to have a synergistic effect (Xie et al., 2011, Rosilio et al., 2014, Zhao et al., 2013). The potential

of this approach in the context of CLL has not been realised, although a significant proliferative component of the malignant clone has been identified.

Chapter 2 begins to address the aims of this study by first examining the expression of MCT -1 and -4 as well as their chaperone protein CD147 in CLL and normal B cells. The results shown in this chapter are the first to demonstrate the presence of MCT -1, -4 and CD147 on CLL cells, as well as confirm the expression of these transporters in their healthy counterparts (Merezhinskaya et al., 2004). Typically, the levels of MCT -1, -4 and CD147 are higher on malignant cells compared to normal cells, however, on CLL cells they show reduced expression in comparison to normal B cells (Arendt et al., 2012, de Vries et al., 2010, Liu et al., 2009, Thorns et al., 2002, Nabeshima et al., 2004, Shi et al., 2003). This may be because other lymphoid cancers are known to experience a much higher rate of cell turnover in comparison to CLL, which require microenvironmental stimuli for cell proliferation to occur. In other lymphoid cancers a consequence of proliferative activity is greater energy demand and an increased need for monocarboxylate transport, hence the need for increased MCT -1 and -4 expression. That expression of these transporters is low on CLL cells suggests that these cells have a decreased level of metabolic activity which reflects their non-dividing state, or that their primary energy source is not glycolysis.

The former notion that metabolism is slowed in circulating CLL cells is a feature seen in other malignancies whereby a quiescent phenotype is adopted to enhance cell survival and protect against metabolic stress (Leontieva et al., 2012, Valcourt et al., 2012). This is of interest with respect to disease pathology because the longer a CLL cell can survive in circulation, the better chance it will have of re-entering secondary tissues and encountering proliferative and survival signals (van Gent et al., 2008). Ricciardi et al. (2001) have shown quiescence to be correlated to progressive disease. This study compared cells from patients with stable and progressive disease using RNA content and $p27^{kip1}$ to measure the ability of the cell to cycle. In the cells obtained from patient's with progressive disease RNA content was reduced and $p27^{kip1}$ expression was increased, both features associated with a quiescent state. Moreover, 'progressive' cells were shown to be less susceptible to apoptotic stimuli suggesting that by becoming

quiescent cell survival is enhanced. Whether the adoption of a quiescent state by circulating CLL cells is therapeutically targetable has value not only in the context of CLL, but may have relevance in other malignancies where circulating tumour cells are present within peripheral blood.

That glycolysis is likely not the primary means of energy generation by CLL cells is supported by a recent paper by Jitschin et al. (2014), who show that peripheral blood CLL cells rely on oxidative phosphorylation. This study shows that CLL cells have increased levels of mitochondrial respiration in comparison to normal B cells, and this is in keeping with a previous report describing high levels of oxidative stress in CLL cells (Moran et al., 2002). These findings are important for understanding CLL cell bioenergetics because they suggest that circulating CLL cells utilise the same metabolic pathway as naïve and memory B cells, and prefer oxidative phosphorylation (Garcia-Manteiga et al., 2011). Thus, it is likely that following contact with microenvironmental stimuli CLL cells adopt a more glycolytic phenotype to support proliferation as is seen with normal B cells. Induction of glycolysis implies that expression of MCT -1 and/or -4 is likely to increase in order to mediate lactate efflux.

Chapter 3 of this thesis examines whether the levels of MCT -1 and -4 change when CLL cells come into contact with the microenvironment; modelled using CD40L-expressing fibroblasts. The initial aims of this project were based on the assumption that circulating CLL cells would be vulnerable to MCT1 inhibition, either alone or in combination with MCT4 inhibition. Because of the protective role microenvironment has in mediating resistance to traditional therapies such as fludarabine (Hallaert et al., 2008, Hayden et al., 2010), it was hypothesised that such contact may also effect CLL cell response to MCT inhibition. The data presented in this chapter demonstrate that contact with fibroblasts appears to stimulate expression of MCT1 expression on CLL cells, and contact with CD40L-expressing fibroblasts strongly stimulates the expression of MCT4. This indicates that CLL cells are unlikely to become vulnerable to the MCT1 inhibitor, AZD3965, either in circulation or when the cells are within the microenvironment. However, what is evident is that MCT4 may be a viable target, particularly when CLL cells are within so-called proliferation centres where they receive

stimulation to proliferate through engagement of CD40. This is important not only because it provides an avenue by which cells which are resistant to fludarabine may be killed, but also because activation through CD40 is a potential mechanism by which resistance may arise to the newly available compounds which target BCR signalling. Furthermore, the cell-specific distribution of MCT4 in glycolytic cells in comparison to the more ubiquitous expression of MCT1 may be a more desirable target owing to the limited degree of non-specific toxicity to normal cells (Halestrap and Wilson, 2012).

The mechanism by which AZD3965 is thought to induce cell death is by preventing the MCT1-mediated export of lactic acid out of cells resulting in intracellular acidification. It can be assumed that inhibition of MCT4 would likely cause cell death via the same mechanism; cell death would result from an increase in intracellular acidification from lactate accumulation that results from glycolytic activity. The data collected from the Fluidigm Biomark™ chip array indicates that CD40 ligation on CLL cells induces expression of genes involved in glycolysis by showing the expression of genes involved in glycolysis to be upregulated, namely; HK1 and HK2.

To complement this work measurement of real time metabolic flux were attempted using the SeahorseXF24. CLL cells either cultured alone or co-cultured with parental and CD40L expressing fibroblasts were analysed. However, no differences in the ability of the cells to utilise either oxidative phosphorylation or glycolysis were seen. Reproducibility was an issue due to the lack of freshly obtained cells and it was felt that injection of a soluble CD40L was a better approach however preliminary experiments using the soluble ligand from previous experiments yielded no results, possibly because of the strength of the stimulation was too weak. Further experiments would be desirable with a stronger immobilised CD40L, but this was not commercially available and remained unobtainable throughout the course of the project.

The array data also revealed changes in the microenvironmental cells following CD40-CD40L interaction. For these experiments CD40L was brought into contact with CLL cells using a co-culture system whereby human CD40L was engineered to be expressed on a mouse fibroblast cell line. Upregulation of MCT4 in these cells was accompanied

by an increase in glycolytic activity and slowing of other metabolic processes which may utilise the same substrates such as the pentose phosphate pathway, fatty acid synthesis, and the TCA cycle. This is important because it suggests that a symbiotic relationship may be occurring between the CLL cells and the tumour microenvironment. Evidence of this reciprocal metabolic activity has been described as being important in cancer biology (Bonuccelli et al., 2010, Feron, 2009). Thus, the therapeutic targeting of MCT4 may also promote cell death by disrupting the metabolism of neighboring supportive cells. However, further work is required to understand the interactions which occur between CLL cells and the microenvironment and how these interactions influence the metabolism of both cell types.

The work presented in the first two results chapters suggests that MCT4 inhibition is a more promising therapeutic target than MCT1 for the treatment of CLL. Chapter 2 shows how both transporters are downregulated in circulating CLL cells in comparison to healthy counterparts, while chapter 3 shows a meager increase in MCT1 following contact with fibroblasts cells and a stark increase in MCT4 expression following CD40L stimulation. Chapter 4 demonstrates that targeting of MCT1 is likely to be ineffective in CLL as well as providing evidence that inhibition of MCT4 alone is also likely to have limited efficacy.

Assessment of the sensitivity of the CLL cell lines, MEC-1 and HG3, to AZD3965 a specific inhibitor of MCT1 revealed that treatment with this compound had no death inducing effects in either cell type up to a concentration of 10μM. Increasing the concentration of the drug to 30μM did induce an apoptotic effect, however at this concentration AZD3965 is reported to lose specificity for MCT1 and can additionally target MCT4, suggesting that MCT4 may compensate for MCT1 function (Critchlow et al., 2012). However, metabolic flux analyses within the present study indicated that the cytotoxicity of 30μM AZD3965 in MEC-1 cells is likely due to non-specific effects rather than to a change in cell metabolism. The presence of 30μM AZD3965 did not affect ECAR by MEC-1 cells, which would suggest that proton-linked transport was not inhibited by this compound. In contrast, Raji cells, which only express MCT1, showed a dose dependent change in ECAR that was accompanied by an increase in OCR when

exposed to AZD3965 even at nM concentrations. Cell death analyses showed these cells to be sensitive to AZD3965, the apoptotic effects likely being caused by intracellular acidification and reduced glycolysis because the glycolytic capacity of AZD3965-treated Raji cells was shown to be significantly reduced.

To explore the notion that the presence of MCT4 in the MEC-1 cells may account for AZD3965 resistance, the effect of transiently expressing MCT4 in the Raji cell line was examined. This experiment showed that Raji cells induced to express MCT4 became resistant to the inhibition of MCT1 using AZD3965 suggesting that MCT4 can compensate for disrupted MCT1 function, a finding that is in keeping with recent studies in small cell lung cancer (SCLC) (Polanski et al., 2014). In an attempt to investigate whether it would be possible to target MCT1 in cells which express both MCT -1 and -4 siRNA was used to examine the effect of silencing MCT4 expression in MEC-1 cells because no specific inhibitor was available. While no significant cell death was seen in MEC-1 cells treated with MCT4 specific siRNA only a partial knockdown of MCT4 expression was achieved making this technique unsuitable for further experiments in the primary cells. Preliminary attempts to silence MCT4 in CLL cells co-cultured with CD40L fibroblasts were unsuccessful. As previously mentioned the use of an alternative immobilised CD40L would have simplified the experiment giving it a greater chance of success. Taken together, these data provide evidence that further work is needed to investigate the potential of targeting MCT -1 and -4 in cell types such as CLL which express both transporters.

In the absence of specific inhibitors for MCT4 alternative techniques may be used in future work to attenuate MCT4 expression such as lentiviral transfection and CRISPR® genome editing as well as the generation of a stable cells. However, this approach may not be sufficient to demonstrate sensitivity to MCT1 inhibition if the cells are not fully stimulated to divide. As CD40L stimulation is the basis for other models simulating the influence of the microenvironment, the addition of other factors such as IL-4 and IL-21 would also be an avenue by which this work may be progressed. Further to this other end points in addition to the measurement of cell death could be more closely examined. For instance, the levels of substrates transported by MCT -1 and -4 could be directly

measured using NMR or mass spectrometry to better understand the metabolic characteristics of these cells and understand the mechanism by which MCT inhibition causes cytoxicity. In addition to this strategy further work could also be completed using the SeahorseXF24 metabolic flux analyser which was optimised for this study. Preliminary experiments within this investigation were unable to sufficiently demonstrate whether CD40L stimulation of CLL cells induces a change in metabolic flux. The use of a soluble ligand did not induce a significant change in MCT4 expression by which to adequately control a metabolic flux experiment and the co-culture with CD40L expressing fibroblasts failed to show any real time changes in ECAR or OCR. As previously mentioned the use of an alternative immobilised CD40L would allow real time measurements. Moreover, the addition of further stimuli such as IL-4 and IL-21 as previously described would allow the assessment of how each stimuli contributes to the induction of metabolic activity as well as allowing a drug injection port for the addition of a inhibitor such as AZD3965 (Ahearne et al., 2013). Combination of a CD40L, IL-4 and IL-21 into one port would also allow for the addition of multiple compounds plus AZD3965 such as metformin, an approach that is becoming popular with users of the SeahorseXF24 because its use in the treatment of diabetes and the effect it has on glucose metabolism (Doherty et al., 2013).

In conclusion, this thesis aimed to assess the potential of therapeutically targeting the metabolism of CLL cells by inhibiting monocarboxylate transporters. The data presented addressed this aim by testing three hypotheses. The findings in chapter 2 proved that MCT -1 and -4 are expressed by CLL cells. However, this data indicates that the inhibition of MCT1 is unlikely to be effective because levels of this transporter are reduced in CLL cells in comparison to normal B cells. Chapter 3 showed that the need for monocarboxylate transport is increased when CLL cells are induced to proliferate. Although similarly to MCT1, MCT4 levels are seen to be reduced in circulating CLL cells, when stimulated with CD40L MCT4 is increased likely due to an increased demand for monocarboxylate transport as a consequence of enhanced glycolytic activity. Thus, MCT4 may be a viable target. Chapter 4 examines the third hypothesis. This chapter is unable to prove that CLL cells are sensitive to MCT -1 and/or -4 inhibition however; work in cell lines in this chapter does show that MCT4 is

able to compensate for disrupted MCT1 function mediating resistance to AZD3965. Whether or not MCT1 can compensate for MCT4 remains unanswered therefore inhibition of MCT -1 and -4 may be required to induce cell death. This work provides a foundation for future research concentrating on targeting CLL cell metabolism therapeutically as well as supporting recent publications examining MCTs in other cell types describing the relationship between MCT -1 and -4.

6 APPENDIX

6.1 Buffers

SDS-PAGE clear lysis buffer:

1% Sodium dodecyl sulfate (SDS) (1mL of 10% stock) (Fischer Scientific, Leicestershire, UK).
50mM Tris pH 6.8 (1mL 0.5M Tris) (Fischer Scientific Chemicals, Leicestershire, UK).
5mM EDTA (1mL of 50mM EDTA) (Sigma, Gillingham, UK).
10% glycerol (1mL) (Sigma, Gillingham, UK).
6mL dH_2O.

5 x Sample buffer:

1M Tris pH 6.8.
50% glycerol.
15% SDS.
25% β-metacaptoethanol (Sigma, Gillingham, UK).
Bromophenol blue (Fischer Scientific, Leicestershire, UK).

1 x Sample buffer:

5 x Sample buffer diluted 1:5 in dH_2O.

SDS-PAGE running buffer:

10X:
0.1% SDS.
192mM glycine (Fischer Scientific, Leicestershire, UK).
25M Tris.

Diluted 1:10 with dH_2O to produce 1X.

Transfer buffer:

10X:
0.25M Tris (pH 6.8).
1.92M glycine.

Diluted 1:10 with dH_2O to produce 1X.

TBS:

10X
10mM Tris (pH 7.4)
150mM Sodium chloride (NaCl) (Fischer Scientific, Leicestershire, UK).

TBS-T:

1X TBS
0.075% Tween20 (Acros organics, Thermo Fischer Scientific, Leicestershire, UK).

Blocking buffer:

1g powdered milk / 20mL TBS-T.

6.2 Sample purity

Case no.	UT (% CD19)	CD40L (% CD19)	Par (% CD19)
1725	-	-	-
1819	-	-	-
2205	92.63	82.08	80.36
2764	-	89.01	93.7
2918	73	84.44	83.33
2979	-	83.41	82.95
3078	66.02	78.71	71.58

Table 6.1: Sample purity following co-culture. CD19 was measured using flow cytometry to assess sample purity following the removal of CLL cells from the fibroblast monolayer for 6 cases assessed for MCT -1 and -4 protein levels.

6.3 Mycoplasma analysis

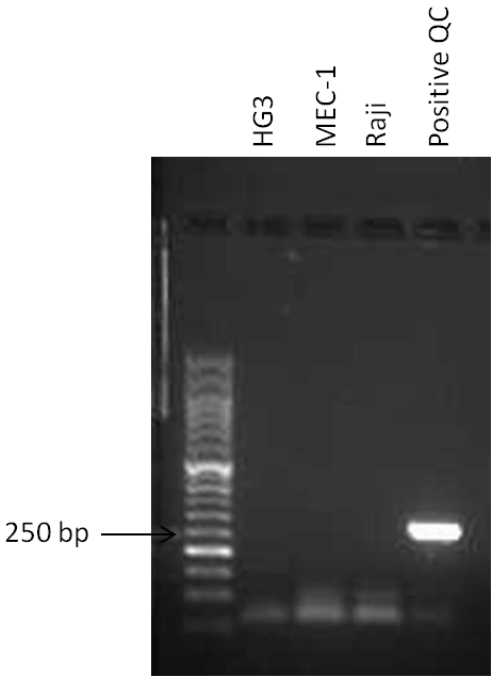

Figure 6.1: Mycoplasma analysis. Example of the mycoplasma analysis in HG3 and MEC-1 (CLL) cell lines and the Raji (B cell lymphoma) cell line. Cell lines were shown to be negative for Mycoplasma, the presence of which can slow proliferation.

6.4 Fluidigm Biomark™ chip array

6.4.1 Sample loading

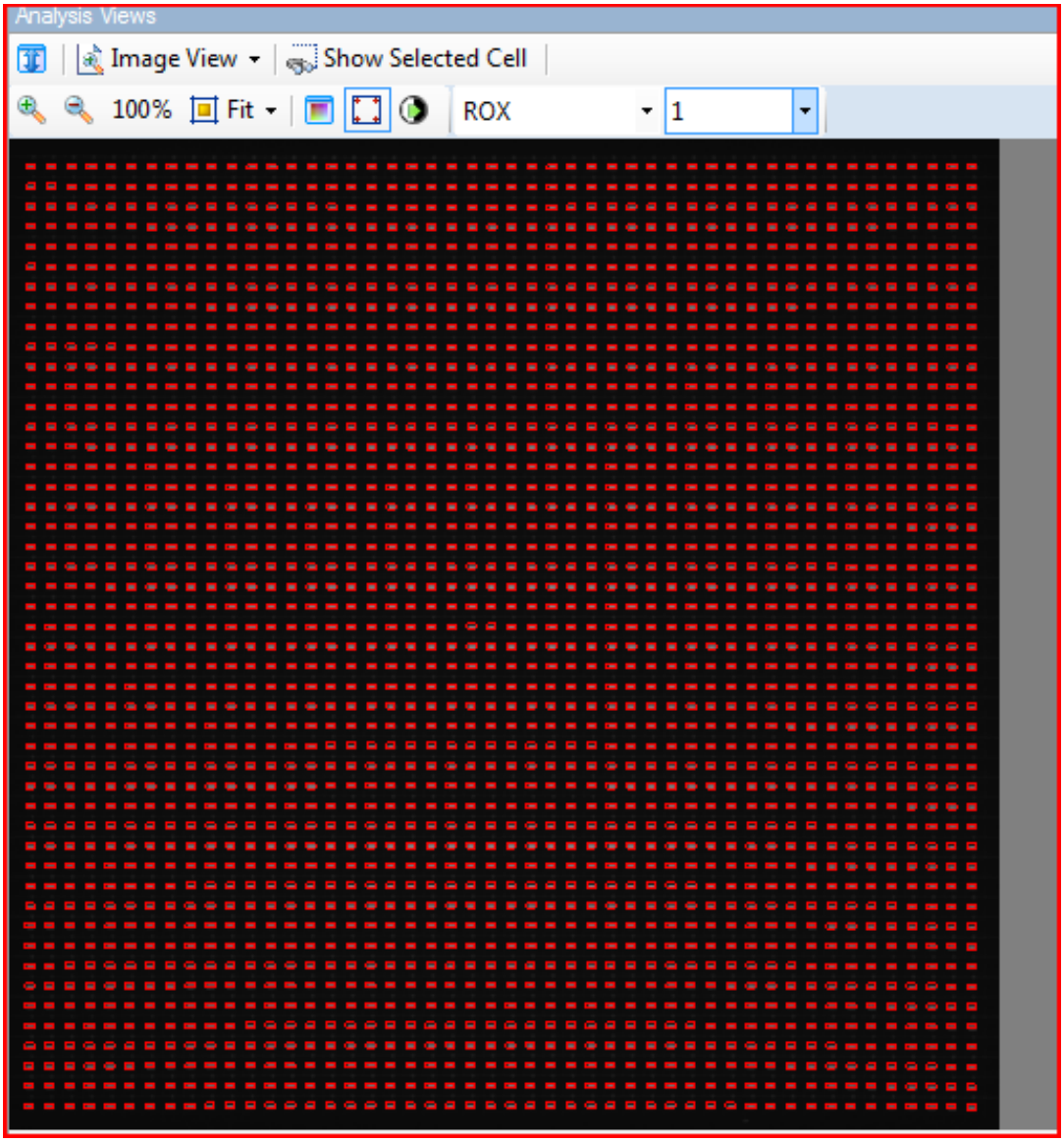

Figure 6.2: ROX™ expression. ROX™ expression was measured at cycle 1 as a passive reference control to normalise non-PCR-related fluctuations in fluorescence. The Fluidigm Biomark™ Real Time PCR Analysis Software (Version 3.1.3) draws a red square round each well which is within range.

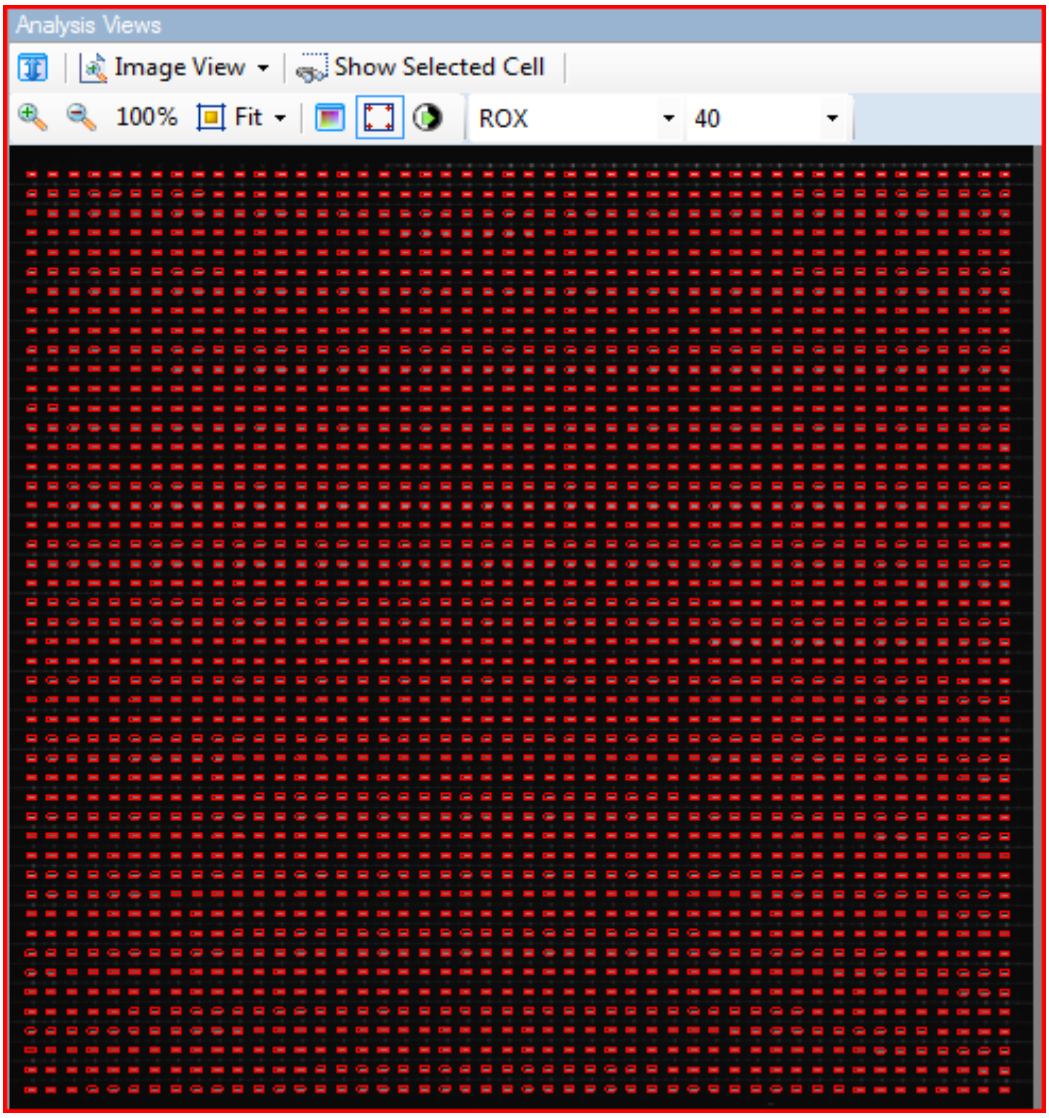

Figure 6.3: ROX™ expression. ROX™ expression was measured at cycle 40 as a passive reference control to normalise non-PCR-related fluctuations in fluorescence. The Fluidigm Biomark™ Real Time PCR Analysis Software (Version 3.1.3) draws a red square round each well which is within range.

7 REFERENCES

AHEARNE, M. J., WILLIMOTT, S., PINON, L., KENNEDY, D. B., MIALL, F., DYER, M. J. S. & WAGNER, S. D. 2013. Enhancement of CD154/IL4 proliferation by the T follicular helper (Tfh) cytokine, IL21 and increased numbers of circulating cells resembling Tfh cells in chronic lymphocytic leukaemia. *British Journal of Haematology,* 162**,** 360-370.

ALDUAIJ, W. & ILLIDGE, T. M. 2011. The future of anti-CD20 monoclonal antibodies: are we making progress? *Blood,* 117**,** 2993-3001.

ALTMAN, S. A., RANDERS, L. & RAO, G. 1993. Comparison of trypan blue dye exclusion and fluorometric assays for mammalian cell viability determinations. *Biotechnology Progress,* 9**,** 671-674.

ARENDT, B. K., WALTERS, D. K., WU, X., TSCHUMPER, R. C., HUDDLESTON, P. M., HENDERSON, K. J., DISPENZIERI, A. & JELINEK, D. F. 2012. Increased expression of extracellular matrix metalloproteinase inducer (CD147) in multiple myeloma: role in regulation of myeloma cell proliferation. *Leukemia,* 26**,** 2286-2296.

ARSHAM, A. M., HOWELL, J. J. & SIMON, M. C. 2003. A novel hypoxia-inducible factor-independent hypoxic response regulating mammalian target of rapamycin and its targets. *Journal of Biological Chemistry,* 278**,** 29655-29660.

BENNETT, J. M., CATOVSKY, D., DANIEL, M. T., FLANDRIN, G., GALTON, D. A., GRALNICK, H. R. & SULTAN, C. 1989. Proposals for the classification of chronic (mature) B and T lymphoid leukaemias. French-American-British (FAB) Cooperative Group. *J Clin Pathol,* 42**,** 567-84.

BENSAAD, K. & VOUSDEN, K. H. 2007. p53: new roles in metabolism. *Trends in Cell Biology,* 17**,** 286-291.

BINET, J. L., AUQUIER, A., DIGHIERO, G., CHASTANG, C., PIGUET, H., GOASGUEN, J., VAUGIER, G., POTRON, G., COLONA, P., OBERLING, F., THOMAS, M., TCHERNIA, G., JACQUILLAT, C., BOIVIN, P., LESTY, C., DUAULT, M. T., MONCONDUIT, M., BELABBES, S. & GREMY, F. 1981. A new prognostic classification of chronic lymphocytic leukemia derived from a multivariate survival analysis. *Cancer,* 48**,** 198-206.

BONUCCELLI, G., TSIRIGOS, A., WHITAKER-MENEZES, D., PAVLIDES, S., PESTELL, R. G., CHIAVARINA, B., FRANK, P. G., FLOMENBERG, N., HOWELL, A., MARTINEZ-OUTSCHOORN, U. E., SOTGIA, F. & LISANTI, M. P. 2010a. Ketones and lactate "fuel" tumor growth and metastasis evidence that epithelial cancer cells use oxidative mitochondrial metabolism. *Cell Cycle,* 9**,** 3506-3514.

BONUCCELLI, G., WHITAKER-MENEZES, D., CASTELLO-CROS, R., PAVLIDES, S., PESTELL, R. G., FATATIS, A., WITKIEWICZ, A. K., VANDER HEIDEN, M. G., MIGNECO, G., CHIAVARINA, B., FRANK, P. G., CAPOZZA, F., FLOMENBERG, N., MARTINEZ-OUTSCHOORN, U. E., SOTGIA, F. & LISANTI, M. P. 2010b. The reverse Warburg effect glycolysis inhibitors prevent the tumor promoting effects of caveolin-1 deficient cancer associated fibroblasts. *Cell Cycle,* 9**,** 1960-1971.

BRODY, J. I., OSKI, F. A. & SINGER, D. E. 1969. Impaired pentose phosphate shunt and decreased glycolytic activity in lymphocytes of chronic lymphocytic leukemia metabolic pathway. *Blood-the Journal of Hematology,* 34**,** 421-&.

BURGER, J. A. & CHIORAZZI, N. 2013. B cell receptor signaling in chronic lymphocytic leukemia. *Trends in Immunology,* 34**,** 592-601.

CALIGARIS-CAPPIO, F. 2009. Chronic lymphocytic leukemia: "Cinderella" is becoming a star. *Mol Med,* 15**,** 67-9.

CAMBIER, J. C., GAULD, S. B., MERRELL, K. T. & VILEN, B. J. 2007. B-cell anergy: from transgenic models to naturally occurring anergic B cells? *Nature Reviews Immunology,* 7**,** 633-643.

CAPASSO, M., BHAMRAH, M. K., HENLEY, T., BOYD, R. S., LANGLAIS, C., CAIN, K., DINSDALE, D., PULFORD, K., KHAN, M., MUSSET, B., CHERNY, V. V., MORGAN, D., GASCOYNE, R. D., VIGORITO, E., DECOURSEY, T. E., MACLENNAN, I. C. M. & DYER, M. J. S. 2010. HVCN1 modulates BCR signal strength via regulation of BCR-dependent generation of reactive oxygen species. *Nature Immunology,* 11**,** 265-U12.

CAPORASO, N., GOLDIN, L., PLASS, C., CALIN, G., MARTI, G., BAUER, S., RAVECHE, E., MCMASTER, M. L., NG, D., LANDGREN, O. & SLAGER, S. 2007. Chronic lymphocytic leukaemia genetics overview. *British Journal of Haematology,* 139**,** 630-634.

CASTORINO, J. J., DEBORDE, S., DEORA, A., SCHREINER, R., GALLAGHER-COLOMBO, S. M., RODRIGUEZ-BOULAN, E. & PHILP, N. J. 2011. Basolateral Sorting Signals Regulating Tissue-Specific Polarity of Heteromeric Monocarboxylate Transporters in Epithelia. *Traffic,* 12**,** 483-498.

CATALINA-RODRIGUEZ, O., KOLUKULA, V. K., TOMITA, Y., PREET, A., PALMIERI, F., WELLSTEIN, A., BYERS, S., GIACCIA, A. J., GLASGOW, E., ALBANESE, C. & AVANTAGGIATI, M. L. 2012. The mitochondrial citrate transporter, CIC, is essential for mitochondrial homeostasis. *Oncotarget,* 3**,** 1220-35.

CHACKO, B. K., KRAMER, PHILIP A., RAVI, SARANYA., JOHNSON, MICHELLE S., HARDY, ROBERT W., BALLINGER, SCOTT W., AND DARLEY-USMAR, VICTOR M. 2013. Methods for defining distinct bioenergetic profiles in platelets, lymphocytes, monocytes, and neutrophils, and the oxidative burst from human blood. *Laboratory Investigation,* 00**,** 1-11.

CHEN, C. I. 2013. Lenalidomide Alone and in Combination for Chronic Lymphocytic Leukemia. *Current hematologic malignancy reports,* 8**,** 7-13.

CHENG, C., CHEN, Z. Q. & SHI, X. T. 2014. MicroRNA-320 inhibits osteosarcoma cells proliferation by directly targeting fatty acid synthase. *Tumour Biol,* 35**,** 4177-83.

CHEONG, H., LU, C., LINDSTEN, T. & THOMPSON, C. B. 2012. Therapeutic targets in cancer cell metabolism and autophagy. *Nature Biotechnology,* 30**,** 671-678.

CHEUNG, E. C. & VOUSDEN, K. H. 2010. The role of p53 in glucose metabolism. *Current Opinion in Cell Biology,* 22**,** 186-191.

CHIORAZZI, N. & FERRARINI, M. 2003. B cell chronic lymphocytic leukemia: lessons learned from studies of the B cell antigen receptor. *Annual Review of Immunology,* 21**,** 841-894.

CHIORAZZI, N. & FERRARINI, M. 2011. Cellular origin(s) of chronic lymphocytic leukemia: cautionary notes and additional considerations and possibilities. *Blood,* 117**,** 1781-91.

CITORES, M. J., CASTEJON, R., VILLARREAL, M., ROSADO, S., GARCIA-MARCO, J. A. & VARGAS, J. A. 2010. CD154 expression triggered by purine analogues in vitro: Correlation with treatment response and autoimmune events in chronic lymphocytic leukemia. *Experimental Hematology,* 38**,** 165-173.

CLARK, M. R., MANDAL, M., OCHIAI, K. & SINGH, H. 2014. Orchestrating B cell lymphopoiesis through interplay of IL-7 receptor and pre-B cell receptor signalling. *Nat Rev Immunol,* 14**,** 69-80.

COSTANTINI, A., MANCINI, S., GIULIODORO, S., BUTINI, L., REGNERY, C. M., SILVESTRI, G. & MONTRONI, M. 2003. Effects of cryopreservation on lymphocyte immunophenotype and function. *Journal of Immunological Methods,* 278**,** 145-55.

CRESPO, M., BOSCH, F., VILLAMOR, N., BELLOSILLO, B., COLOMER, D., ROZMAN, M., MARCE, S., LOPEZ-GUILLERMO, A., CAMPO, E. & MONTSERRAT, E. 2003. ZAP-70 expression as a surrogate for immunoglobulin-variable-region mutations in chronic lymphocytic leukemia. *New England Journal of Medicine,* 348**,** 1764-1775.

CRITCHLOW, S., HOPCROFT, L., MOONEY, L., CURTIS, N., WHALLEY, N., ZHONG, H., LOGIE, A., REVILL, M., XIE, L., ZHANG, J., YU, D., MURRAY, C. & SMITH, P. D. Pre-clinical targeting of the metabolic phenotype of lymphoma by AZD3965, a selective inhibitor of monocarboxylate transporter 1 (MCT1). American Association for Cancer Research, April 15, 2012 2012 Chicago, IL.

CROWTHER-SWANEPOEL, D. & HOULSTON, R. S. 2009. The molecular basis of familial chronic lymphocytic leukemia. *Haematologica-the Hematology Journal,* 94**,** 606-609.

DAMESHEK, W. 1967. Chronic lymphocytic leukemia-an accumulative disease of immunolgically incompetent lymphocytes. *Blood,* 29**,** Suppl:566-84.

DAMLE, R. N., GHIOTTO, F., VALETTO, A., ALBASIANO, E., FAIS, F., YAN, X. J., SISON, C. P., ALLEN, S. L., KOLITZ, J., SCHULMAN, P., VINCIGUERRA, V. P., BUDDE, P., FREY, J., RAI, K. R., FERRARINI, M. & CHIORAZZI, N. 2002. B-cell chronic lymphocytic leukemia cells express a surface membrane phenotype of activated, antigen-experienced B lymphocytes. *Blood,* 99**,** 4087-4093.

DAMLE, R. N., WASIL, T., FAIS, F., GHIOTTO, F., VALETTO, A., ALLEN, S. L., BUCHBINDER, A., BUDMAN, D., DITTMAR, K., KOLITZ, J., LICHTMAN, S. M., SCHULMAN, P., VINCIGUERRA, V. P., RAI, K. R., FERRARINI, M. & CHIORAZZI, N. 1999. Ig V gene mutation status and CD38 expression as novel prognostic indicators in chronic lymphocytic leukemia. *Blood,* 94**,** 1840-1847.

DANG, C. V. 2012. Links between metabolism and cancer. *Genes & Development,* 26**,** 877-890.

DANILOV, A. V., DANILOVA, O. V., BROWN, J. R., RABINOWITZ, A., KLEIN, A. K. & HUBER, B. T. 2010. Dipeptidyl peptidase 2 apoptosis assay determines the

B-cell activation stage and predicts prognosis in chronic lymphocytic leukemia. *Experimental Hematology,* 38**,** 1167-1177.

DASANU, C. A. 2008. Intrinsic and treatment-related immune alterations in chronic lymphocytic leukaemia and their impact for clinical practice. *Expert Opin Pharmacother,* 9**,** 1481-94.

DE VRIES, J. F., MARVELDE, J. G. T., WIND, H. K., VAN DONGEN, J. J. M. & VAN DER VELDEN, V. H. J. 2010. The potential use of basigin (CD147) as a prognostic marker in B-cell precursor acute lymphoblastic leukaemia. *British Journal of Haematology,* 150**,** 624-626.

DEEG, H. J., BLAZAR, B. R., BOLWELL, B. J., LONG, G. D., SCHUENING, F., CUNNINGHAM, J., RIFKIN, R. M., ABHYANKAR, S., BRIGGS, A. D., BURT, R., LIPANI, J., ROSKOS, L. K., WHITE, J. M., HAVRILLA, N., SCHWAB, G. & HESLOP, H. E. 2001. Treatment of steroid-refractory acute graft-versus-host disease with anti-CD147 monoclonal antibody ABX-CBL. *Blood,* 98**,** 2052-2058.

DEFOICHE, J., DEBACQ, C., ASQUITH, B., ZHANG, Y., BURNY, A., BRON, D., LAGNEAUX, L., MACALLAN, D. & WILLEMS, L. 2008. Reduction of B cell turnover in chronic lymphocytic leukaemia. *British Journal of Haematology,* 143**,** 240-247.

DENEYS, V., THIRY, V., HOUGARDY, N., MAZZON, A. M., LEVEUGLE, P. & DE BRUYERE, M. 1999. Impact of cryopreservation on B cell chronic lymphocytic leukaemia phenotype. *Journal of Immunological Methods,* 228**,** 13-21.

DHUP, S., DADHICH, R. K., PORPORATO, P. E. & SONVEAUX, P. 2012. Multiple biological activities of lactic acid in cancer: influences on tumor growth, angiogenesis and metastasis. *Current Pharmaceutical Design,* 18**,** 1319-1330.

DIGHIERO, G. & HAMBLIN, T. J. 2008. Chronic lymphocytic leukaemia. *Lancet,* 371**,** 1017-1029.

DOHERTY, J. R., YANG, C., SCOTT, K. E., CAMERON, M. D., FALLAHI, M., LI, W., HALL, M. A., AMELIO, A. L., MISHRA, J. K., LI, F., TORTOSA, M., GENAU, H. M., ROUNBEHLER, R. J., LU, Y., DANG, C. V., KUMAR, K. G., BUTLER, A. A., BANNISTER, T. D., HOOPER, A. T., UNSAL-KACMAZ, K., ROUSH, W. R. & CLEVELAND, J. L. 2013. Blocking Lactate Export by Inhibiting the Myc Target MCT1 Disables Glycolysis and Glutathione Synthesis. *Cancer Res*.

DOHNER, H., FISCHER, K., BENTZ, M., HANSEN, K., BENNER, A., CABOT, G., DIEHL, D., SCHLENK, R., COY, J., STILGENBAUER, S., VOLKMANN, M., GALLE, P. R., POUSTKA, A., HUNSTEIN, W. & LICHTER, P. 1995. P53 gene deletion predicts for poor survival and non-response to therapy with purine analogs in chronic B cell leukemias. *Blood,* 85**,** 1580-1589.

DONO, M., BURGIO, V. L., TACCHETTI, C., FAVRE, A., AUGLIERA, A., ZUPO, S., TABORELLI, G., CHIORAZZI, N., GROSSI, C. E. & FERRARINI, M. 1996a. Subepithelial B cells in the human palatine tonsil. I. Morphologic, cytochemical and phenotypic characterization. *Eur J Immunol,* 26**,** 2035-42.

DONO, M., ZUPO, S., AUGLIERA, A., BURGIO, V. L., MASSARA, R., MELAGRANA, A., COSTA, M., GROSSI, C. E., CHIORAZZI, N. &

FERRARINI, M. 1996b. Subepithelial B cells in the human palatine tonsil. II. Functional characterization. *Eur J Immunol,* 26**,** 2043-9.
DORSHKIND, K. & MONTECINO-RODRIGUEZ, E. 2007. Fetal B-cell lymphopoiesis and the emergence of B-1-cell potential. *Nat Rev Immunol,* 7**,** 213-9.
DOUGHTY, C. A., BLEIMAN, B. F., WAGNER, D. J., DUFORT, F. J., MATARAZA, J. M., ROBERTS, M. F. & CHILES, T. C. 2006. Antigen receptor-mediated changes in glucose metabolism in B lymphocytes: role of phosphatidylinositol 3-kinase signaling in the glycolytic control of growth. *Blood,* 107**,** 4458-4465.
EKBERG, H., QI, Z., PAHLMAN, C., VERESS, B., BUNDICK, R. V., CRAGGS, R. I., HOLNESS, E., EDWARDS, S., MURRAY, C. M., FERGUSON, D., KERRY, P. J., WILSON, E. & DONALD, D. K. 2007. The specific monocarboxylate transporter-1 (MCT-1) inhibitor, AR-C117977, induces donor-specific suppression, reducing acute and chronic allograft rejection in the rat. *Transplantation,* 84**,** 1191-9.
EL-MABHOUH, A. A., AYRES, M. L., SHPALL, E. J., BALADANDAYUTHAPANI, V., KEATING, M. J., WIERDA, W. G. & GANDHI, V. 2014. Evaluation of bendamustine in combination with fludarabine in primary chronic lymphocytic leukemia cells. *Blood*.
FAINT, J. M., TUNCER, C., GARG, A., ADAMS, D. H. & LALOR, P. F. 2011. Functional consequences of human lymphocyte cryopreservation: implications for subsequent interactions of cells with endothelium. *J Immunother,* 34**,** 588-96.
FARAHANI, M., TREWEEKE, A. T., TOH, C. H., TILL, K. J., HARRIS, R. J., CAWLEY, J. C., ZUZEL, M. & CHEN, H. 2005. Autocrine VEGF mediates the antiapoptotic effect of CD154 on CLL cells. *Leukemia,* 19**,** 524-530.
FERON, O. 2009. Pyruvate into lactate and back: from the Warburg effect to symbiotic energy fuel exchange in cancer cells. *Radiotherapy and Oncology,* 92**,** 329-333.
FERRARINI, M. 2009. The continuing search for the cell of origin of chronic lymphocytic leukemia. *7th Meeting New Insights in Hematology,* 3**,** 81-85.
FU, Y. C., MAIANU, L., MELBERT, B. R. & GARVEY, W. T. 2004. Facilitative glucose transporter gene expression in human lymphocytes, monocytes, and macrophages: a role for GLUT isoforms 1, 3, and 5 in the immune response and foam cell formation. *Blood Cells Molecules and Diseases,* 32**,** 182-190.
GALLAGHER, S. M., CASTORINO, J. J., WANG, D. & PHILP, N. J. 2007. Monocarboxylate transporter 4 regulates maturation and trafficking of CD147 to the plasma membrane in the metastatic breast cancer cell line MDA-MB-231. *Cancer Research,* 67**,** 4182-4189.
GARCIA-MANTEIGA, J. M., MARI, S., GODEJOHANN, M., SPRAUL, M., NAPOLI, C., CENCI, S., MUSCO, G. & SITIA, R. 2011. Metabolomics of B to plasma cell differentiation. *Journal of Proteome Research,* 10**,** 4165-4176.
GAREDEW, A., ANDREASSI, C. & MONCADA, S. 2012. Mitochondrial dynamics, biogenesis, and function are coordinated with the cell cycle by APC/C-CDH1. *Cell Metabolism,* 15**,** 466-479.
GHIA, P., CIRCOSTA, P., SCIELZO, C., VALLARIO, A., CAMPOREALE, A., GRANZIERO, L. & CALIGARIS-CAPPIO, F. 2005. Differential effects on

CLL cell survival exerted by different microenvironmental elements. *Chronic Lymphocytic Leukemia,* 294**,** 135-145.
GOLDIN, L. R. & CAPORASO, N. E. 2007. Family studies in chronic lymphocytic leukaemia and other lymphoproliferative tumours. *British Journal of Haematology,* 139**,** 774-779.
GONZALEZ, D., MARTINEZ, P., WADE, R., HOCKLEY, S., OSCIER, D., MATUTES, E., DEARDEN, C. E., RICHARDS, S. M., CATOVSKY, D. & MORGAN, G. J. 2011. Mutational status of the TP53 gene as a predictor of response and survival in patients with chronic lymphocytic leukemia: results from the LRF CLL4 trial. *Journal of Clinical Oncology,* 29**,** 2223-2229.
GOTTARDI, D., ALFARANO, A., DE LEO, A. M., STACCHINI, A., BERGUI, L. & CALIGARIS-CAPPIO, F. 1995. Defective apoptosis due to bcl-2 overexpression may explain why B-CLL cells accumulate in G0. *Current topics in microbiology and immunology,* 194**,** 307-12.
GRICKS, C. S., ZAHRIEH, D., ZAULS, A. J., GORGUN, G., DRANDI, D., MAUERER, K., NEUBERG, D. & GRIBBEN, J. G. 2004. Differential regulation of gene expression following CD40 activation of leukemic compared to healthy B cells. *Blood,* 104**,** 4002-9.
GRIFFIN, D. O., HOLODICK, N. E. & ROTHSTEIN, T. L. 2011. Human B1 cells in umbilical cord and adult peripheral blood express the novel phenotype CD20+ CD27+ CD43+ CD70. *J Exp Med,* 208**,** 67-80.
GUO, F.-C., WANG, L.-Q., ZHANG, J. & WANG, Y.-S. 2013. Study on the anti-Lewis lung carcinoma effect of metformin combined with MCT1 inhibitor CHC. *Sichuan da xue xue bao. Yi xue ban = Journal of Sichuan University. Medical science edition,* 44**,** 375-8.
HALESTRAP, A. P. & MEREDITH, D. 2004. The SLC16 gene family - from monocarboxylate transporters (MCTs) to aromatic amino acid transporters and beyond. *Pflugers Archiv-European Journal of Physiology,* 447**,** 619-628.
HALESTRAP, A. P. & PRICE, N. T. 1999. The proton-linked monocarboxylate transporter (MCT) family: structure, function and regulation. *Biochemical Journal,* 343**,** 281-299.
HALESTRAP, A. P. & WILSON, M. C. 2012. The monocarboxylate transporter family role and regulation. *Iubmb Life,* 64**,** 109-119.
HALINA, A., ARTUR, P., BARBARA, M. K., JOANNA, S. & ANNA, D. 2010. Alterations in TP53, cyclin D2, c-Myc, p21WAF1/CIP1 and p27KIP1 expression associated with progression in B-CLL. *Folia Histochem Cytobiol,* 48**,** 534-41.
HALLAERT, D. Y., JASPERS, A., VAN NOESEL, C. J., VAN OERS, M. H., KATER, A. P. & ELDERING, E. 2008. c-Abl kinase inhibitors overcome CD40-mediated drug resistance in CLL: implications for therapeutic targeting of chemoresistant niches. *Blood,* 112**,** 5141-9.
HALLEK, M. & EICHHORST, B. F. 2004. Chemotherapy combination treatment regimens with fludarabine in chronic lymphocytic leukemia. *Hematology Journal,* 5**,** S20-S30.
HAMADA, S., HORIGUCHI, A., ASANO, T., KURODA, K., ASAKUMA, J., ITO, K., MIYAI, K. & IWAYA, K. 2014. Prognostic impact of fatty acid synthase

expression in upper urinary tract urothelial carcinoma. *Jpn J Clin Oncol,* 44**,** 486-92.

HAMBLIN, T. J. 2001. Achieving optimal outcomes in chronic lymphocytic leukaemia. *Drugs,* 61**,** 593-611.

HAMILTON, E., PEARCE, L., MORGAN, L., ROBINSON, S., WARE, V., BRENNAN, P., THOMAS, N. S., YALLOP, D., DEVEREUX, S., FEGAN, C., BUGGINS, A. G. & PEPPER, C. 2012. Mimicking the tumour microenvironment: three different co-culture systems induce a similar phenotype but distinct proliferative signals in primary chronic lymphocytic leukaemia cells. *Br J Haematol,* 158**,** 589-99.

HAN, S., HATHCOCK, K., ZHENG, B., KELPER, T.B., HODES, R., & KELSOE, G. 1995. Cellular interaction in germinal centers. Roles of CD40 ligand and B7-2 in established germinal centers. *J Immunol,* 155, 556-567.

HARTMANN, S., AGOSTINELLI, C., DIENER, J., DOERING, C., FANTI, S., ZINZANI, P. L., GALLAMINI, A., BERGMANN, L., PILERI, S. & HANSMANN, M.-L. 2012. GLUT1 expression patterns in different Hodgkin lymphoma subtypes and progressively transformed germinal centers. *Bmc Cancer,* 12.

HASHIMOTO, T., HUSSIEN, R., OOMMEN, S., GOHIL, K. & BROOKS, G. A. 2007. Lactate sensitive transcription factor network in L6 cells: activation of MCT1 and mitochondrial biogenesis. *Faseb Journal,* 21**,** 2602-2612.

HASSANEIN, M., HOEKSEMA, M. D., SHIOTA, M., QIAN, J., HARRIS, B. K., CHEN, H., CLARK, J. E., ALBORN, W. E., EISENBERG, R. & MASSION, P. P. 2013. SLC1A5 mediates glutamine transport required for lung cancer cell growth and survival. *Clin Cancer Res,* 19**,** 560-70.

HAYDEN, R. E., PRATT, G., DAVIES, N. J., KHANIM, F. L., BIRTWISTLE, J., DELGADO, J., PEARCE, C., SANT, T., DRAYSON, M. T. & BUNCE, C. M. 2009. Treatment of primary CLL cells with bezafibrate and medroxyprogesterone acetate induces apoptosis and represses the pro-proliferative signal of CD40-ligand, in part through increased 15d Delta(12,14,)PGJ(2). *Leukemia,* 23**,** 292-304.

HAYDEN, R. E., PRATT, G., DRAYSON, M. T. & BUNCE, C. M. 2010. Lycorine sensitizes CD40 ligand-protected chronic lymphocytic leukemia cells to bezafibrate- and medroxyprogesterone acetate-induced apoptosis but dasatanib does not overcome reported CD40-mediated drug resistance. *Haematologica,* 95**,** 1889-96.

HE, Y., JIANG, X. & CHEN, J. 2013. The role of miR-150 in normal and malignant hematopoiesis. *Oncogene***,** 1-7.

HENDRIKS, R. W., YUVARAJ, S. & KIL, L. P. 2014. Targeting Bruton's tyrosine kinase in B cell malignancies. *Nature Reviews Cancer,* 14**,** 219-232.

HILLMEN, P. 2004. Advancing therapy for chronic lymphocytic leukemia - The role of rituximab. *Seminars in Oncology,* 31**,** 22-26.

HO, A. D., FIEHN, W. & HUNSTEIN, W. 1982. Intracellular lactic dehydrogenase and phosphohexose isomerase activity in leukemia and malignant lymphoma. *British Journal of Haematology,* 50**,** 637-645.

HOWLADER, N., NOONE, A., KRAPCHO, M., GARSHELL, J., NEYMAN, N., ALTEKRUSE, S., KOSARY, C., YU, M., RUHL, J., TATALOVICH, Z., CHO, H., MARIOTTO, A., LEWIS, D., CHEN, H., FEUER, E. & CRONIN, K. E. 2012. *SEER Cancer Statistics Review 1975-2010* [Online]. Bethesda, MD. [Accessed 12.9.13 2013].

JIANG, S., ZHANG, L.-F., ZHANG, H.-W., HU, S., LU, M.-H., LIANG, S., LI, B., LI, Y., LI, D., WANG, E.-D. & LIU, M.-F. 2012. A novel miR-155/miR-143 cascade controls glycolysis by regulating hexokinase 2 in breast cancer cells. *Embo Journal,* 31**,** 1985-1998.

JITSCHIN, R., HOFMANN, A. D., BRUNS, H., GIESSL, A., BRICKS, J., BERGER, J., SAUL, D., ECKART, M. J., MACKENSEN, A. & MOUGIAKAKOS, D. 2014. Mitochondrial metabolism contributes to oxidative stress and reveals therapeutic targets in chronic lymphocytic leukemia. *Blood,* 123**,** 2663-72.

JONES, R. V., GOFFI, G. P. & HUTT, M. S. 1962. Lymphocyte glycogen content in various diseases. *Journal of Clinical Pathology,* 15**,** 36-9.

JOSE, C., BELLANCE, N. & ROSSIGNOL, R. 2011. Choosing between glycolysis and oxidative phosphorylation: a tumor's dilemma? *Biochimica Et Biophysica Acta-Bioenergetics,* 1807**,** 552-561.

KARAM, M., NOVAK, L., CYRIAC, J., ALI, A., NAZEER, T. & NUGENT, F. 2006. Role of fluorine-18 fluoro-deoxyglucose positron emission tomography scan in the evaluation and follow-up of patients with low-grade lymphomas. *Cancer,* 107**,** 175-183.

KASINRERK, W., PENG-IN, P., KHUNKAEWLA, P. & CHIAMPANICHAYAKUL, S. 2006. CD147 contains different bioactive epitopes involving the regulation of cell adhesion and lymphocyte activation. *Journal of Immunology,* 176**,** S210-S211.

KENNEDY, K. M. & DEWHIRST, M. W. 2010a. Tumor metabolism of lactate: the influence and therapeutic potential for MCT and CD147 regulation. *Future Oncol,* 6**,** 127-48.

KENNEDY, K. M. & DEWHIRST, M. W. 2010b. Tumor metabolism of lactate: the influence and therapeutic potential for MCT and CD147 regulation. *Future Oncology,* 6**,** 127-148.

KIM, H. S., MASKO, E. M., POULTON, S. L., KENNEDY, K. M., PIZZO, S. V., DEWHIRST, M. W. & FREEDLAND, S. J. 2012. Carbohydrate restriction and lactate transporter inhibition in a mouse xenograft model of human prostate cancer. *BJU Int,* 110**,** 1062-9.

KIRK, P., WILSON, M. C., HEDDLE, C., BROWN, M. H., BARCLAY, A. N. & HALESTRAP, A. P. 2000. CD147 is tightly associated with lactate transporters MCT1 and MCT4 and facilitates their cell surface expression. *Embo Journal,* 19**,** 3896-3904.

KITADA, S., ANDERSEN, J., AKAR, S., ZAPATA, J. M., TAKAYAMA, S., KRAJEWSKI, S., WANG, H. G., ZHANG, X., BULLRICH, F., CROCE, C. M., RAI, K., HINES, J. & REED, J. C. 1998. Expression of apoptosis-regulating proteins in chronic lymphocytic leukemia: correlations with in vitro and in vivo chemoresponses. *Blood,* 91**,** 3379-3389.

KLEIN, U., TU, Y., STOLOVITZKY, G. A., MATTIOLI, M., CATTORETTI, G., HUSSON, H., FREEDMAN, A., INGHIRAMI, G., CRO, L., BALDINI, L., NERI, A., CALIFANO, A. & DALLA-FAVERA, R. 2001. Gene expression profiling of B cell chronic lymphocytic leukemia reveals a homogeneous phenotype related to memory B cells. *J Exp Med,* 194**,** 1625-38.

KOCH, C., STAFFLER, G., HUTTINGER, R., HILGERT, I., PRAGER, E., CERNY, J., STEINLEIN, P., MAJDIC, O., HOREJSI, V. & STOCKINGER, H. 1999. T cell activation-associated epitopes of CD147 in regulation of the T cell response, and their definition by antibody affinity and antigen density. *International Immunology,* 11**,** 777-786.

KOMINSKY, D. J., CAMPBELL, E. L. & COLGAN, S. P. 2010. Metabolic shifts in immunity and inflammation. *Journal of Immunology,* 184**,** 4062-4068.

KRYSOV, S., POTTER, K. N., MOCKRIDGE, C. I., COELHO, V., WHEATLEY, I., PACKHAM, G. & STEVENSON, F. K. 2010. Surface IgM of CLL cells displays unusual glycans indicative of engagement of antigen in vivo. *Blood,* 115**,** 4198-4205.

KUMAR, A., KANT, S. & SINGH, S. M. 2013. alpha-Cyano-4-hydroxycinnamate induces apoptosis in Dalton's lymphoma cells: role of altered cell survival-regulatory mechanisms. *Anticancer Drugs,* 24**,** 158-71.

LAMBERT, D. W., WOOD, I. S., ELLIS, A. & SHIRAZI-BEECHEY, S. P. 2002. Molecular changes in the expression of human colonic nutrient transporters during the transition from normality to malignancy. *British Journal of Cancer,* 86**,** 1262-1269.

LANDGREN, O., RAPKIN, J. S., CAPORASO, N. E., MELLEMKJAER, L., GRIDLEY, G., GOLDIN, L. R. & ENGELS, E. A. 2007. Respiratory tract infections and subsequent risk of chronic lymphocytic leukemia. *Blood,* 109**,** 2198-2201.

LARSEN, S., WRIGHT-PARADIS, C., GNAIGER, E., HELGE, J. W. & BOUSHEL, R. 2012. Cryopreservation of human skeletal muscle impairs mitochondrial function. *Cryo Letters,* 33**,** 170-6.

LEBIEN, T. W. & TEDDER, T. F. 2008. B lymphocytes: how they develop and function. *Blood,* 112**,** 1570-1580.

LEONTIEVA, O. V., NATARAJAN, V., DEMIDENKO, Z. N., BURDELYA, L. G., GUDKOV, A. V. & BLAGOSKLONNY, M. V. 2012. Hypoxia suppresses conversion from proliferative arrest to cellular senescence. *Proceedings of the National Academy of Sciences of the United States of America,* 109**,** 13314-13318.

LIN, R. Y., VERA, J. C., CHAGANTI, R. S. & GOLDE, D. W. 1998a. Human monocarboxylate transporter 2 (MCT2) is a high affinity pyruvate transporter. *J Biol Chem,* 273**,** 28959-65.

LIN, R. Y., VERA, J. C., CHAGANTI, R. S. K. & GOLDE, D. W. 1998b. Human monocarboxylate transporter 2 (MCT2) is a high affinity pyruvate transporter. *Journal of Biological Chemistry,* 273**,** 28959-28965.

LINET, M. S., SCHUBAUER-BERIGAN, M. K., WEISENBURGER, D. D., RICHARDSON, D. B., LANDGREN, O., BLAIR, A., SILVER, S., FIELD, R. W., CALDWELL, G., HATCH, M. & DORES, G. M. 2007. Chronic

lymphocytic leukaemia: an overview of aetiology in light of recent developments in classification and pathogenesis. *British Journal of Haematology,* 139**,** 672-686.

LIU, A. G., HU, Q., TAO, H. F., LIU, S. Y., ZHANG, L. Q. & HU, Y. 2009. [Expression of CD147 and matrix metalloproteinase-9 in children with non-Hodgkin's lymphoma and its correlation with prognosis]. *Zhonghua Er Ke Za Zhi,* 47**,** 785-8.

LONG, Q. Q., YI, Y. X., QIU, J., XU, C. J. & HUANG, P. L. 2014. Fatty acid synthase (FASN) levels in serum of colorectal cancer patients: correlation with clinical outcomes. *Tumour Biol,* 35**,** 3855-9.

MACINTYRE, D. A., JIMÉNEZ, B., LEWINTRE, E. J., MARTÍN, C. R., SCHÄFER, H., BALLESTEROS, C. G., MAYANS, J. R., SPRAUL, M., GARCÍA-CONDE, J. & PINEDA-LUCENA, A. 2010. Serum metabolome analysis by 1H-NMR reveals differences between chronic lymphocytic leukaemia molecular subgroups. *Leukemia,* 24**,** 788-797.

MANSOUR, T. E. 1963. Studies on heart phosphofructokinase purification, inhibition and activation. *Journal of Biological Chemistry,* 238**,** 2285-&.

MARTINEZ-OUTSCHOORN, U. E., CURRY, J. M., KO, Y. H., LIN, Z., TULUC, M., COGNETTI, D., BIRBE, R. C., PRIBITKIN, E., BOMBONATI, A., PESTELL, R. G., HOWELL, A., SOTGIA, F. & LISANTI, M. P. 2013. Oncogenes and inflammation rewire host energy metabolism in the tumor microenvironment: RAS and NFkappaB target stromal MCT4. *Cell Cycle,* 12**,** 2580-97.

MARTINEZ-OUTSCHOORN, U. E., LIN, Z., TRIMMER, C., FLOMENBERG, N., WANG, C., PAVLIDES, S., PESTELL, R. G., HOWELL, A., SOTGIA, F. & LISANTI, M. P. 2011. Cancer cells metabolically "fertilize" the tumor microenvironment with hydrogen peroxide, driving the Warburg effect Implications for PET imaging of human tumors. *Cell Cycle,* 10**,** 2504-2520.

MELCHERS, F. 2005. B cell development and its deregulation to transformed states at the pre-B cell receptor-expressing pre-BII cell stage. *Curr Top Microbiol Immunol,* 294**,** 1-17.

MELLMAN, I. & NELSON, W. J. 2008. Coordinated protein sorting, targeting and distribution in polarized cells. *Nature Reviews Molecular Cell Biology,* 9**,** 833-845.

MENENDEZ, J. A. & LUPU, R. 2007. Fatty acid synthase and the lipogenic phenotype in cancer pathogenesis. *Nat Rev Cancer,* 7**,** 763-77.

MEREZHINSKAYA, N., OGUNWUYI, S. A., MULLICK, F. G. & FISHBEIN, W. N. 2004. Presence and localization of three lactic acid transporters (MCT1, -2, and -4) in separated human granulocytes, lymphocytes, and monocytes. *Journal of Histochemistry & Cytochemistry,* 52**,** 1483-1493.

MESSMER, B. T., ALBESIANO, E., EFREMOV, D. G., GHIOTTO, F., ALLEN, S. L., KOLITZ, J., FOA, R., DAMLE, R. N., FAIS, F., MESSMER, D., RAI, K. R., FERRARINI, M. & CHIORAZZI, N. 2004. Multiple distinct sets of stereotyped antigen receptors indicate a role for antigen in promoting chronic lymphocytic leukemia. *Journal of Experimental Medicine,* 200**,** 519-525.

MESSMER, B. T., MESSMER, D., ALLEN, S. L., KOLITZ, J. E., KUDALKAR, P., CESAR, D., MURPHY, E. J., KODURU, P., FERRARINI, M., ZUPO, S.,

CUTRONA, G., DAMLE, R. N., WASIL, T., RAI, K. R., HELLERSTEIN, M. K. & CHIORAZZI, N. 2005. In vivo measurements document the dynamic cellular kinetics of chronic lymphocytic leukemia B cells. *Journal of Clinical Investigation,* 115**,** 755-764.

MICHALEK, R. D. & RATHMELL, J. C. 2010. The metabolic life and times of a T-cell. *Immunological Reviews,* 236**,** 190-202.

MIRANDA-GONCALVES, V., HONAVAR, M., PINHEIRO, C., MARTINHO, O., PIRES, M. M., PINHEIRO, C., CORDEIRO, M., BEBIANO, G., COSTA, P., PALMEIRIM, I., REIS, R. M. & BALTAZAR, F. 2013. Monocarboxylate transporters (MCTs) in gliomas: expression and exploitation as therapeutic targets. *Neuro-Oncology,* 15**,** 172-188.

MITUS, W. J., BERGNA, L. J., MEDNICOFF, I. B. & DAMESHEK, W. 1958. Cytochemical studies of glycogen content of lymphocytes in lymphocytic proliferations. *Blood,* 13**,** 748-756.

MOLICA, S. & ALBERTI, A. 1987. Prognostic value of the lymphocyte doubling time in chronic lymphocytic leukemia. *Cancer,* 60**,** 2712-2716.

MONTSERRAT, E., SANCHEZ-BISONO, J., VINOLAS, N. & ROZMAN, C. 1986. Lymphocyte doubling time in chronic lymphocytic leukaemia: analysis of its prognostic significance. *Br J Haematol,* 62**,** 567-75.

MORAN, E. C., KAMIGUTI, A. S., CAWLEY, J. C. & PETTITT, A. R. 2002. Cytoprotective antioxidant activity of serum albumin and autocrine catalase in chronic lymphocytic leukaemia. *British Journal of Haematology,* 116**,** 316-328.

MOREAU, E. J., MATUTES, E., A'HERN, R. P., MORILLA, A. M., MORILLA, R. M., OWUSU-ANKOMAH, K. A., SEON, B. K. & CATOVSKY, D. 1997. Improvement of the chronic lymphocytic leukemia scoring system with the monoclonal antibody SN8 (CD79b). *Am J Clin Pathol,* 108**,** 378-82.

MORRIS, M. E. & FELMLEE, M. A. 2008. Overview of the proton-coupled MCT (SLC16A) family of transporters: characterization, function and role in the transport of the drug of abuse gamma-hydroxybutyric acid. *Aaps Journal,* 10**,** 311-321.

MORRISON, V. A. 2010. Infectious complications of chronic lymphocytic leukaemia: pathogenesis, spectrum of infection, preventive approaches. *Best Pract Res Clin Haematol,* 23**,** 145-53.

MURRAY, C. M., HUTCHINSON, R., BANTICK, J. R., BELFIELD, G. P., BENJAMIN, A. D., BRAZMA, D., BUNDICK, R. V., COOK, I. D., CRAGGS, R. I., EDWARDS, S., EVANS, L. R., HARRISON, R., HOLNESS, E., JACKSON, A. P., JACKSON, C. G., KINGSTON, L. P., PERRY, M. W. D., ROSS, A. R. J., RUGMAN, P. A., SIDHU, S. S., SULLIVAN, M., TAYLOR-FISHWICK, D. A., WALKER, P. C., WHITEHEAD, Y. M., WILKINSON, D. J., WRIGHT, A. & DONALD, D. K. 2005. Monocarboxylate transporter MCT1 is a target for immunosuppression. *Nature Chemical Biology,* 1**,** 371-376.

MUSOLINO, C., ALONCI, A., ALLEGRA, A., DICESARE, E., ORLANDO, A., GROSSO, P., BUDA, G. & SQUADRITO, G. 1992. Intracellular and serum levels of aldolase activity in B chronic lymphocytic leukemia. *International Journal of Hematology,* 56**,** 213-217.

NABESHIMA, K., SUZUMIYA, J., NAGANO, M., OHSHIMA, K., TOOLE, B. P., TAMURA, K., IWASAKI, H. & KIKUCHI, M. 2004. Emmprin, a cell surface inducer of matrix metalloproteinases (MMPs), is expressed in T-cell lymphomas. *J Pathol,* 202**,** 341-51.

NAGASAWA, T. 2006. Microenvironmental niches in the bone marrow required for B-cell development. *Nat Rev Immunol,* 6**,** 107-16.

NOWAKOWSKI, G. S., HOYER, J. D., SHANAFELT, T. D., GEYER, S. M., LAPLANT, B. R., CALL, T. G., JELINEK, D. F., ZENT, C. S. & KAY, N. E. 2007. Using smudge cells on routine blood smears to predict clinical outcome in chronic lymphocytic leukemia: a universally available prognostic test. *Mayo Clin Proc,* 82**,** 449-53.

NUTT, S. L. & KEE, B. L. 2007. The transcriptional regulation of B cell lineage commitment. *Immunity,* 26**,** 715-725.

O'BRIEN, S. M., KANTARJIAN, A. M., CORTES, J., BERAN, M., KOLLER, C. A., GILES, F. J., LERNER, S. & KEATING, M. 2001. Results of the fludarabine and cyclophosphamide combination regimen in chronic lymphocytic leukemia. *Journal of Clinical Oncology,* 19**,** 1414-1420.

OKKENHAUG, K. & VANHAESEBROECK, B. 2003. PI3K in lymphocyte development, differentiation and activation. *Nat Rev Immunol,* 3**,** 317-30.

OSCIER, D., DEARDEN, C., EREM, E., FEGAN, C., FOLLOWS, G., HILLMEN, P., ILLIDGE, T., MATUTES, E., MILLIGAN, D. W., PETTITT, A., SCHUH, A., WIMPERIS, J. & BRITISH COMM STAND, H. 2012. Guidelines on the diagnosis, investigation and management of chronic lymphocytic leukaemia. *British Journal of Haematology,* 159**,** 541-564.

OSCIER, D., FEGAN, C., HILLMEN, P., ILLIDGE, T., JOHNSON, S., MAGUIRE, P., MATUTES, E. & MILLIGAN, D. 2004. Guidelines on the diagnosis and management of chronic lymphocytic leukaemia. *British Journal of Haematology,* 125**,** 294-317.

PASCUTTI, M. F., JAK, M., TROMP, J. M., DERKS, I. A. M., REMMERSWAAL, E. B. M., THIJSSEN, R., VAN ATTEKUM, M. H. A., VAN BOCHOVE, G. G., LUIJKS, D. M., PALS, S. T., VAN LIER, R. A. W., KATER, A. P., VAN OERS, M. H. J. & ELDERING, E. 2013. IL-21 and CD40L signals from autologous T cells can induce antigen-independent proliferation of CLL cells. *Blood,* 122**,** 3010-3019.

PATTEN, P. E. M., BUGGINS, A. G. S., RICHARDS, J., WOTHERSPOON, A., SALISBURY, J., MUFTI, G. J., HAMBLIN, T. J. & DEVEREUX, S. 2008. CD38 expression in chronic lymphocytic leukemia is regulated by the tumor microenvironment. *Blood,* 111**,** 5173-5181.

PEPPER, C., HOY, T. & BENTLEY, D. P. 1997. Bcl-2/Bax ratios in chronic lymphocytic leukaemia and their correlation with in vitro apoptosis and clinical resistance. *British Journal of Cancer,* 76**,** 935-938.

PEREZ-VERA, P., REYES-LEON, A. & FUENTES-PANANA, E. M. 2011. Signaling proteins and transcription factors in normal and malignant early B cell development. *Bone marrow research,* 2011**,** 502751-502751.

PERTEGA-GOMES, N., VIZCAINO, J. R., MIRANDA-GONCALVES, V., PINHEIRO, C., SILVA, J., PEREIRA, H., MONTEIRO, P., HENRIQUE, R.

M., REIS, R. M., LOPES, C. & BALTAZAR, F. 2011. Monocarboxylate transporter 4 (MCT4) and CD147 overexpression is associated with poor prognosis in prostate cancer. *Bmc Cancer,* 11.

PETTITT, A. R., SHERRINGTON, P. D. & CAWLEY, J. C. 1999. The effect of p53 dysfunction on purine analogue cytotoxicity in chronic lymphocytic leukaemia. *British Journal of Haematology,* 106**,** 1049-1051.

PINHEIRO, C., ALBERGARIA, A., PAREDES, J., SOUSA, B., DUFLOTH, R., VIEIRA, D., SCHMITT, F. & BALTAZAR, F. 2010. Monocarboxylate transporter 1 is up-regulated in basal-like breast carcinoma. *Histopathology,* 56**,** 860-867.

PINHEIRO, C., LONGATTO-FILHO, A., AZEVEDO-SILVA, J., CASAL, M., SCHMITT, F. C. & BALTAZAR, F. 2012. Role of monocarboxylate transporters in human cancers: state of the art. *Journal of Bioenergetics and Biomembranes,* 44**,** 127-139.

PINHEIRO, C., LONGATTO-FILHO, A., SIMOES, K., JACOB, C. E., CALDAS BRESCIANI, C. J., ZILBERSTEIN, B., CECCONELLO, I., FERREIRA ALVES, V. A., SCHMITT, F. & BALTAZAR, F. 2009. The prognostic value of CD147/EMMPRIN is associated with monocarboxylate transporter 1 co-expression in gastric cancer. *European Journal of Cancer,* 45**,** 2418-2424.

PLEYER, L., EGLE, A., HARTMANN, T. N. & GREIL, R. 2009. Molecular and cellular mechanisms of CLL: novel therapeutic approaches. *Nature Reviews Clinical Oncology,* 6**,** 405-418.

POLANSKI, R., HODGKINSON, C. L., FUSI, A., NONAKA, D., PRIEST, L., KELLY, P., TRAPANI, F., BISHOP, P. W., WHITE, A., CRITCHLOW, S. E., SMITH, P. D., BLACKHALL, F., DIVE, C. & MORROW, C. J. 2014. Activity of the Monocarboxylate Transporter 1 Inhibitor AZD3965 in Small Cell Lung Cancer. *Clin Cancer Res,* 20**,** 926-37.

PUT, N., VAN ROOSBROECK, K., KONINGS, P., MEEUS, P., BRUSSELMANS, C., RACK, K., GERVAIS, C., NGUYEN-KHAC, F., CHAPIRO, E., RADFORD-WEISS, I., STRUSKI, S., DASTUGUE, N., GACHARD, N., LEFEBVRE, C., BARIN, C., ECLACHE, V., FERT-FERRER, S., LAIBE, S., MOZZICONACCI, M. J., QUILICHINI, B., POIREL, H. A., WLODARSKA, I., HAGEMEIJER, A., MOREAU, Y., VANDENBERGHE, P. & MICHAUX, L. 2012. Chronic lymphocytic leukemia and prolymphocytic leukemia with MYC translocations: a subgroup with an aggressive disease course. *Ann Hematol,* 91**,** 863-73.

RAHMAN, B., SCHNEIDER, H. P., BROER, A., DEITMER, J. W. & BROER, S. 1999. Helix 8 and helix 10 are involved in substrate recognition in the rat monocarboxylate transporter MCT1. *Biochemistry,* 38**,** 11577-11584.

RAI, K. R., SAWITSKY, A., CRONKITE, E. P., CHANANA, A. D., LEVY, R. N. & PASTERNACK, B. S. 1975. Clinical staging of chronic lymphocytic leukemia. *Blood,* 46**,** 219-34.

RAMPAZZO, E., BONALDI, L., TRENTIN, L., VISCO, C., KEPPEL, S., GIUNCO, S., FREZZATO, F., FACCO, M., NOVELLA, E., GIARETTA, I., DEL BIANCO, P., SEMENZATO, G. & DE ROSSI, A. 2012. Telomere length and telomerase levels delineate subgroups of B-cell chronic lymphocytic leukemia

with different biological characteristics and clinical outcomes. *Haematologica-the Hematology Journal,* 97**,** 56-63.

RAMSAY, A. D. & RODRIGUEZ-JUSTO, M. 2013. Chronic lymphocytic leukaemia - the role of the microenvironment pathogenesis and therapy. *British Journal of Haematology,* 162**,** 15-24.

REFAELI, Y., YOUNG, R. M., TURNER, B. C., DUDA, J., FIELD, K. A. & BISHOP, J. M. 2008. The B cell antigen receptor and overexpression of MYC can cooperate in the genesis of B cell lymphomas. *PLoS Biol,* 6**,** e152.

REGO, N., BIANCHI, S., MORENO, P., PERSSON, H., KVIST, A., PENA, A., OPPEZZO, P., NAYA, H., ROVIRA, C., DIGHIERO, G. & PRITSCH, O. 2012. Search for an aetiological virus candidate in chronic lymphocytic leukaemia by extensive transcriptome analysis. *Br J Haematol,* 157**,** 709-17.

REITZER, L. J., WICE, B. M. & KENNELL, D. 1979. Evidence that glutamine, not sugar, is the major energy source for cultured HELA cells. *Journal of Biological Chemistry,* 254**,** 2669-2676.

RICCIARDI, M. R., PETRUCCI, M. T., GREGORJ, C., ARIOLA, C., LEMOLI, R. M., FOGLI, M., MAURO, F. R., CERRETTI, R., FOA, R., MANDELLI, F. & TAFURI, A. 2001. Reduced susceptibility to apoptosis correlates with kinetic quiescence in disease progression of chronic lymphocytic leukaemia. *British Journal of Haematology,* 113**,** 391-399.

RODRIGUEZ, D., RAMSAY, A. J., QUESADA, V., GARABAYA, C., CAMPO, E., FREIJE, J. M. P. & LOPEZ-OTIN, C. 2013. Functional analysis of sucrase-isomaltase mutations from chronic lymphocytic leukemia patients. *Human Molecular Genetics,* 22**,** 2273-2282.

ROSEN, A., BERGH, A. C., GOGOK, P., EVALDSSON, C., MYHRINDER, A. L., HELLQVIST, E., RASUL, A., BJORKHOLM, M., JANSSON, M., MANSOURI, L., LIU, A., TEH, B. T., ROSENQUIST, R. & KLEIN, E. 2012. Lymphoblastoid cell line with B1 cell characteristics established from a chronic lymphocytic leukemia clone by in vitro EBV infection. *Oncoimmunology,* 1**,** 18-27.

ROSILIO, C., BEN-SAHRA, I., BOST, F. & PEYRON, J. F. 2014. Metformin: A metabolic disruptor and anti-diabetic drug to target human leukemia. *Cancer Lett,* 346**,** 188-96.

ROSSI, D. & GAIDANO, G. 2010. Biological and clinical significance of stereotyped B-cell receptors in chronic lymphocytic leukemia. *Haematologica,* 95**,** 1992-5.

SCIELZO, C., APOLLONIO, B., SCARFO, L., JANUS, A., MUZIO, M., TEN HACKEN, E., GHIA, P. & CALIGARIS-CAPPIO, F. 2011. The functional in vitro response to CD40 ligation reflects a different clinical outcome in patients with chronic lymphocytic leukemia. *Leukemia,* 25**,** 1760-1767.

SEIFERT, M., SELLMANN, L., BLOEHDORN, J., WEIN, F., STILGENBAUER, S., DUERIG, J. & KUEPPERS, R. 2012. Cellular origin and pathophysiology of chronic lymphocytic leukemia. *Journal of Experimental Medicine,* 209**,** 2183-2198.

SHACHAR, I., COHEN, S., MAROM, A. & BECKER-HERMAN, S. 2012. Regulation of CLL survival by hypoxia-inducible factor and its target genes. *FEBS Lett,* 586**,** 2906-10.

SHERBORNE, A. L. & HOULSTON, R. S. 2010. What are genome-wide association studies telling us about B-cell tumor development? *Oncotarget,* 1**,** 367-372.
SHI, B., HSU, H. L., EVENS, A. M., GORDON, L. I. & GARTENHAUS, R. B. 2003. Expression of the candidate MCT-1 oncogene in B- and T-cell lymphoid malignancies. *Blood,* 102**,** 297-302.
SHIM, C. K., CHEON, E. P., KANG, K. W., SEO, K. S. & HAN, H. K. 2007. Inhibition effect of flavonoids on monocarboxylate transporter 1 (MCT1) in Caco-2 cells. *J Pharm Pharmacol,* 59**,** 1515-9.
SLOAN, E. J. & AYER, D. E. 2010. Myc, mondo, and metabolism. *Genes & cancer,* 1**,** 587-96.
SMOLEJ, L., DOUBEK, M., PANOVSKA, A., SIMKOVIC, M., BRYCHTOVA, Y., BELADA, D., MOTYCKOVA, M. & MAYER, J. 2012. Rituximab in combination with high-dose dexamethasone for the treatment of relapsed/refractory chronic lymphocytic leukemia. *Leuk Res,* 36**,** 1278-82.
SONVEAUX, P., VEGRAN, F., SCHROEDER, T., WERGIN, M. C., VERRAX, J., RABBANI, Z. N., DE SAEDELEER, C. J., KENNEDY, K. M., DIEPART, C., JORDAN, B. F., KELLEY, M. J., GALLEZ, B., WAHL, M. L., FERON, O. & DEWHIRST, M. W. 2008. Targeting lactate-fueled respiration selectively kills hypoxic tumor cells in mice. *Journal of Clinical Investigation,* 118**,** 3930-3942.
SPANER, D. E., LEE, E., SHI, Y., WEN, F., LI, Y., TUNG, S., MCCAW, L., WONG, K., GARY-GOUY, H., DALLOUL, A., CEDDIA, R. & GORZCYNSKI, R. 2013. PPAR-alpha is a therapeutic target for chronic lymphocytic leukemia. *Leukemia,* 27**,** 1090-1099.
SU, J., CHEN, X. & KANEKURA, T. 2009. A CD147-targeting siRNA inhibits the proliferation, invasiveness and VEGF production of human malignant melanoma cells by down-regulating glycolysis. *Cancer Letters,* 273**,** 140-147.
TAUSCH, E., MERTENS, D., & STILGENBAUER, S. 2014. Advances in treating chronic lymphocytic leukaemia. *F1000Prime Rep,* 6, 65.
TEMBHARE, P. R., MARTI, G., WIESTNER, A., DEGHEIDY, H., FAROOQUI, M., KREITMAN, R. J., JASPER, G. A., YUAN, C. M., LIEWEHR, D., VENZON, D. & STETLER-STEVENSON, M. 2013. Quantification of expression of antigens targeted by antibody-based therapy in chronic lymphocytic leukemia. *Am J Clin Pathol,* 140**,** 813-8.
THORNS, C., FELLER, A. C. & MERZ, H. 2002. EMMPRIN (CD 174) is expressed in Hodgkin's lymphoma and anaplastic large cell lymphoma. An immunohistochemical study of 60 cases. *Anticancer Res,* 22**,** 1983-6.
TIDMARSH, G. F., TANNER, L. I., O'CONNOR, J., ENG, C. & MORDEC, K. 2004. Effect of 2-deoxyglucose, a glycolytic Inhibitor, on the ATP levels and viability of B lymphocytes from subjects with chronic lymphocytic leukemia (CLL). *ASH Annual Meeting Abstracts,* 104**,** 4810-.
TILI, E., MICHAILLE, J.-J., LUO, Z., VOLINIA, S., RASSENTI, L. Z., KIPPS, T. J. & CROCE, C. M. 2012. The down-regulation of miR-125b in chronic lymphocytic leukemias leads to metabolic adaptation of cells to a transformed state. *Blood,* 120**,** 2631-2638.
TORRES DE OLIVEIRA, A. T., PINHEIRO, C., LONGATTO-FILHO, A., BRITO, M. J., MARTINHO, O., MATOS, D., CARVALHO, A. L., VAZQUEZ, V. L.,

SILVA, T. B., SCAPULATEMPO, C., SAAD, S. S., REIS, R. M. & BALTAZAR, F. 2012. Co-expression of monocarboxylate transporter 1 (MCT1) and its chaperone (CD147) is associated with low survival in patients with gastrointestinal stromal tumors (GISTs). *Journal of Bioenergetics and Biomembranes,* 44**,** 171-178.

TRUSAL, L. R., GUZMAN, A. W. & BAKER, C. J. 1984. Characterization of Freeze-Thaw Induced Ultrastructural Damage to Endothelial Cells in vitro. *In Vitro,* 20**,** 353-364.

TSUTSAEVA, A. A. & GORDIENKO, A. D. 1982. [Respiration activity of frozen-thawed lymphoid cells]. *Ukr Biokhim Zh,* 54**,** 89-92.

TUNG, S., SHI, Y., WONG, K., ZHU, F., GORCZYNSKI, R., LAISTER, R. C., MINDEN, M., BLECHERT, A. K., GENZEL, Y., REICHL, U. & SPANER, D. E. 2013. PPARalpha and fatty acid oxidation mediate glucocorticoid resistance in chronic lymphocytic leukemia. *Blood,* 122**,** 969-80.

TURA, S., CAVO, M., GOBBI, M. & FRANCHI, P. 1984. Lonidamine in the treatment of chronic lymphocytic leukemia. *Oncology,* 41**,** 90-93.

TWOMEY, B., MUID, R. E. & DALE, M. M. 1990. The effect of putative protein kinase C inhibitors, K252A and staurosporine, on the human neutrophil respiratiory burst activated by both receptor stimulation and post-receptor mechanisms. *British Journal of Pharmacology,* 100**,** 819-825.

ULLAH, M. S., DAVIES, A. J. & HALESTRAP, A. P. 2006. The plasma membrane lactate transporter MCT4, but not MCT1, is up-regulated by hypoxia through a HIF-1 alpha-dependent mechanism. *Journal of Biological Chemistry,* 281**,** 9030-9037.

VALCOURT, J. R., LEMONS, J. M. S., HALEY, E. M., KOJIMA, M., DEMUREN, O. O. & COLLER, H. A. 2012. Staying alive: metabolic adaptations to quiescence. *Cell Cycle,* 11**,** 1680-1696.

VAN GENT, R., KATER, A. P., OTTO, S. A., JASPERS, A., BORGHANS, J. A. M., VRISEKOOP, N., ACKERMANS, M. A. T., RUITER, A. F. C., WITTEBOL, S., ELDERING, E., VAN OERS, M. H. J., TESSELAAR, K., KERSTEN, M. J. & MIEDEMA, F. 2008. In vivo dynamics of stable chronic lymphocytic leukemia inversely correlate with somatic hypermutation levels and suggest no major leukemic turnover in bone marrow. *Cancer Research,* 68**,** 10137-10144.

VANDER HEIDEN, M. G., CANTLEY, L. C. & THOMPSON, C. B. 2009. Understanding the Warburg effect: the metabolic requirements of cell proliferation. *Science (New York, N.Y.),* 324**,** 1029-33.

VANGEEPURAM, N., ONG, G. L. & MATTES, M. J. 1997. Processing of antibodies bound to B-cell lymphomas and lymphoblastoid cell lines. *Cancer,* 80**,** 2425-2430.

VILPO, J., TOBIN, G., HULKKONEN, J., HURME, M., THUNBERG, U., SUNDSTROM, C., VILPO, L. & ROSENQUIST, R. 2005. Mitogen induced activation, proliferation and surface antigen expression patterns in unmutated and hypermutated chronic lymphocytic leukemia cells. *European Journal of Haematology,* 75**,** 34-40.

VISSER, W. E., FRIESEMA, E. C. H., JANSEN, J. & VISSER, T. J. 2007. Thyroid hormone transport by monocarboxylate transporters. *Best Practice & Research Clinical Endocrinology & Metabolism,* 21**,** 223-236.

VIVES CORRONS, J. L., COLOMER, D., PUJADES, A., MATUTES, E., PASTOR, C. & AYMERICH, M. 1989. Relationship between lymphocyte size and enzyme activities in two morphological variants of B chronic lymphocytic leukemia. *Acta Haematologica (Basel),* 82**,** 22-26.

VOUSDEN, K. H. 2010. Alternative fuel-another role for p53 in the regulation of metabolism. *Proceedings of the National Academy of Sciences of the United States of America,* 107**,** 7117-7118.

VOUSDEN, K. H. & RYAN, K. M. 2009. p53 and metabolism. *Nature Reviews Cancer,* 9**,** 691-700.

WARBURG, O., POSENER, K. & NEGELEIN, E. 1924. On the metabolism of carcinoma cells. *Biochemische Zeitschrift,* 152**,** 309-344.

WILLIMOTT, S., BAOU, M., NARESH, K. & WAGNER, S. D. 2007. CD154 induces a switch in pro-survival Bcl-2 family members in chronic lymphocytic leukaemia. *British Journal of Haematology,* 138**,** 721-732.

WILLIMOTT, S. & WAGNER, S. D. 2012. Stromal cells and CD40 ligand (CD154) alter the miRNome and induce miRNA clusters including, miR-125b/miR-99a/let-7c and miR-17-92 in chronic lymphocytic leukaemia. *Leukemia,* 26**,** 1113-1116.

WOODS, B., HAWKINS, N., DUNLOP, W., O'TOOLE, A. & BRAMHAM-JONES, S. 2012. Bendamustine versus chlorambucil for the first-line treatment of chronic lymphocytic leukemia in England and Wales: a cost-utility analysis. *Value Health,* 15**,** 759-70.

XIE, J., WANG, B. S., YU, D. H., LU, Q., MA, J., QI, H., FANG, C. & CHEN, H. Z. 2011. Dichloroacetate shifts the metabolism from glycolysis to glucose oxidation and exhibits synergistic growth inhibition with cisplatin in HeLa cells. *Int J Oncol,* 38**,** 409-17.

YE, M. & GRAF, T. 2007. Early decisions in lymphoid development. *Curr Opin Immunol,* 19**,** 123-8.

ZAJA, F., MIAN, M., VOLPETTI, S., VISCO, C., SISSA, C., NICHELE, I., CASTELLI, M., AMBROSETTI, A., PUGLISI, S., FANIN, R., CORTELAZZO, S., PIZZOLO, G., TRENTIN, L., RODEGHIERO, F., PAOLINI, R., VIVALDI, P., SANCETTA, R., ISOLA, M. & SEMENZATO, G. 2013. Bendamustine in chronic lymphocytic leukemia: Outcome according to different clinical and biological prognostic factors in the everyday clinical practice. *American journal of hematology,* 88**,** 955-960.

ZENZ, T., MERTENS, D., KUEPPERS, R., DOEHNER, H. & STILGENBAUER, S. 2010. From pathogenesis to treatment of chronic lymphocytic leukaemia. *Nature Reviews Cancer,* 10**,** 37-50.

ZHANG, G. Z., HUANG, G. J., LI, W. L., WU, G. M. & QIAN, G. S. 2002. [Effect of co-inhibition of MCT1 gene and NHE1 gene on proliferation and growth of human lung adenocarcinoma cells]. *Ai Zheng,* 21**,** 719-23.

ZHANG, Q., IIDA, R., YOKOTA, T. & KINCADE, P. W. 2013. Early events in lymphopoiesis: an update. *Current opinion in hematology,* 20**,** 265-72.

ZHAO, Y., BUTLER, E. B. & TAN, M. 2013a. Targeting cellular metabolism to improve cancer therapeutics. *Cell Death Dis,* 4**,** e532.
ZHAO, Y., BUTLER, E. B. & TAN, M. 2013b. Targeting cellular metabolism to improve cancer therapeutics. *Cell Death & Disease,* 4.
ZHAO, Z., WU, M.-S., ZOU, C., TANG, Q., LU, J., LIU, D., WU, Y., YIN, J., XIE, X., SHEN, J., KANG, T. & WANG, J. 2014. Downregulation of MCT1 inhibits tumor growth, metastasis and enhances chemotherapeutic efficacy in osteosarcoma through regulation of the NF-κB pathway. *Cancer Letters,* 342**,** 150-158.
ZHU, X., SONG, Z., ZHANG, S., NANDA, A. & LI, G. 2013. CD147: a Novel Modulator of Inflammatory and Immune Disorders. *Curr Med Chem*.